

Letter from the Editors

Dear readers of *Acta Naturae*, We would like to bring to your attention the 21st issue of the journal (as you can see, the number of issues is now over twenty!). As always, the scientific section of the issue is rather diverse. We offer you two reviews. The first one is a review by V.K. Il'in and N.V. Kiryukhin. It focuses on the fundamental medical aspects of habitability in artificial environments. Taking into account the current progress in space research (in particular, in preparing for interplanetary missions), such problems should be considered as highly relevant. This material will undoubtedly be interesting to ecologists. Looking ahead, it should be noted that the review is very concordant with the theme of the Forum section in this issue. The second review (B.B. Vartapetyan et al.) focuses on breeding plants that are tolerant to anaerobic stress. The authors of the review mainly generalize the results of their own research in this field. Genetic and cellular engineering of plants is a fascinating subject which generates lively debate. In our opinion, the review is of fundamental importance and will be interesting to our readers.

Experimental publications cover a wide range of disciplines and approaches, including structural and functional genomics (articles by A.V. Nedoluzhko et al., O.V. Arkova et al., E.A. Nikitina et al.) and various aspects of fundamental medicine (publications by E.A. Trifonova et al., S.S. Popov et al.). This issue includes numerous articles focusing on new methods in molecular and cellular biology, as well as biotechnological techniques for manufacturing target products and biopharmaceutical issues. We suspect that the works related to the design of models for studying human diseases (articles by Nikitina et al. and Syrkina et al.) will be of great interest. The study dealing with the targeted delivery of drugs (Garas et al.) and the study of the expression of HER2 tumor antigen (Dolgikh et al.) are noteworthy. Our readers have also shown continuous interest in telomerase research (Evfratov et al.).

The ceremonial presentation of the Russian Federation State Prizes took place on

June 12, 2014, the Russia Day, in the Kremlin. Academician Anatoliy Ivanovich Grigor'ev, the Vice-President of the Russian Academy of Sciences and the Chairman of the Editorial Board of *Acta Naturae*, was among the winners this year. On this occasion, we congratulate Anatoliy Ivanovich on being chosen for this prestigious award. We wish him good health and success in his efforts in science. We are grateful for his hard work on the establishment and regular support of our journal. Our readers can find an interview with the winner in the Forum section. We find it an interesting and fascinating story about the problems of space medicine, Russia being among the leaders in this field.

In conclusion, we would like to briefly mention the potential role of our journal in demonstrating the results of Russian life science. In connection with competitions of the Russian Science Foundation and several programs of the Ministry of Education and Science that require very high publication scores, a considerable number of articles are currently being submitted to the Editorial Board. There are also articles from abroad. Our journal is currently indexed in all databases (PubMed with open access to the full-text version, Scopus, Web of Science, e.library), which makes it an attractive platform for publishing the results of works under grants. Hence, we would like to avoid publishing duplicating elements and non-essential material. The editorial staff and Editorial Board adhere to the strict requirement of peer-review and use the opinions of two independent reviews for decision making. In some cases, we send the material to a third reviewer. We have also introduced the practice of rejecting articles at the stage prior to sending it to reviewers. This decision can be made by the members of the Editorial Board if the article clearly does not comply with the methodological level of modern studies or is highly technical.

Enjoy your reading and see you again in our next issue! ●

Editorial Board

15-17 october 2014
**SAINT-PETERSBURG
EXPOFORUM**



ST. PETERSBURG INTERNATIONAL HEALTH FORUM



**MEDIZ
SAINT-PETERSBURG**
Medicine and Health
www.mediz-spb.ru



PHARMACY
www.pharma.primexpo.ru



BIOINDUSTRY
www.bio.expoforum.ru



HEALTHCARE TOURISM
www.healthtourism.primexpo.ru



VISUS-EXPO
www.kmc-med.com



AESTHETIC MEDICINE
www.primexpo.ru



www.pmfz.expoforum.ru

+7 812 240 40 40

EXPOFORUM



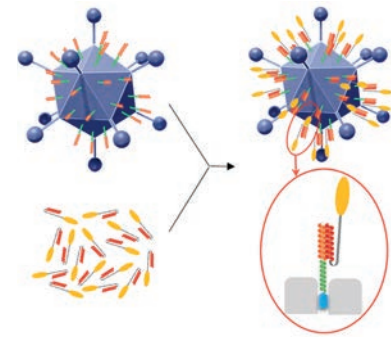
0+



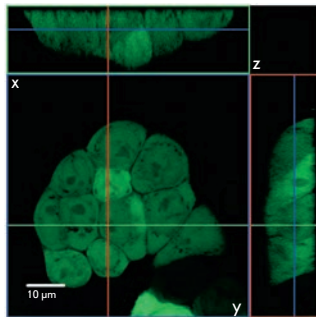
Lipid-Protein Nanodiscs Offer New Perspectives for Structural and Functional Studies of Water-Soluble Membrane-Active Peptides

M. N. Garas, S. V. Tillib, O. V. Zubkova, V. N. Rogozhin, T. I. Ivanova, L. A. Vasilev, D. Yu. Logunov, M. M. Shmarov, I. L. Tutykhina, I. B. Esmagambetov, I. Yu. Gribova, A. S. Bandelyuk, B. S. Naroditsky, A. L. Gintsburg

A new approach to creating targeted vectors using recombinant pseudoadenoviral nanoparticles (RPANs) based on the genome of human adenovirus serotype 5 carrying the modified gene of the capsid protein pIX is proposed. The resulting Ad5-EGFP-pIX-ER is a universal platform that specifically binds nano-antibodies against a certain surface antigen on the RPAN surface, thus delivering the target gene to the desired cells.



Schematic representation of the formation of the Ad5-EGFP-pIX-ER complex



Localization of the fluorescence of EGFP in steadily transfected HT-29 cells

Cell Models for the Investigation of the Role of the Mucin MUC1 Extracellular Domain in Metastasizing

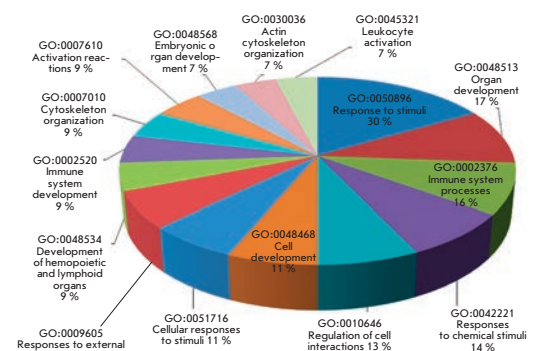
M. S. Syrkina, M. A. Rubtsov, D. M. Potashnikova, Yu. D. Kondratenko, A. A. Dokunova, V. P. Veiko

Genetic constructs encoding various combinations of the functional moieties of human mucin MUC1 and markers for identifying the synthesized fusion proteins were designed based on the pEGFP-N3 expression vector. These constructs were used to transfect HT-29 cells. The resulting cells can be used as a model of the MUC1-expressing cancer and to study the role of various functional moieties of mucin MUC1 in the metastatic disease.

Analysis of the Placental Tissue Transcriptome of Normal and Preeclampsia Complicated Pregnancies

E.A. Trifonova, T.V. Gabdulina, N.I. Ershov, V.N. Serebrova, A.Yu. Vorozhishcheva, V.A. Stepanov

Preeclampsia is one of the most severe gestational complications which holds a leading position among the causes of maternal and perinatal morbidity and mortality. This work is the first Russian genome-wide association study of differential gene expression in placental tissues in females with normal and complicated pregnancies. Sixty-three genes, whose expression is significantly different in the placental tissue of females with preeclampsia and with physiological pregnancies, were identified.



Main biological processes involving the differentially expressed genes which are associated with preeclampsia

Founders

Ministry of Education and
Science of the Russian Federation,
Lomonosov Moscow State University,
Park Media Ltd

Editorial Council

Chairman: A.I. Grigoriev
Editors-in-Chief: A.G. Gabibov, S.N. Kochetkov

V.V. Vlassov, P.G. Georgiev, M.P. Kirpichnikov,
A.A. Makarov, A.I. Miroshnikov, V.A. Tkachuk,
M.V. Ugryumov

Editorial Board

Managing Editor: V.D. Knorre
Publisher: K.V. Kiselev

K.V. Anokhin (Moscow, Russia)
I. Bezprozvanny (Dallas, Texas, USA)
I.P. Bilenkina (Moscow, Russia)
M. Blackburn (Sheffield, England)
S.M. Deyev (Moscow, Russia)
V.M. Govorun (Moscow, Russia)
O.A. Dontsova (Moscow, Russia)
K. Drauz (Hanau-Wolfgang, Germany)
A. Friboulet (Paris, France)
M. Issagouliants (Stockholm, Sweden)
A.L. Konov (Moscow, Russia)
M. Lukic (Abu Dhabi, United Arab Emirates)
P. Masson (La Tronche, France)
K. Nierhaus (Berlin, Germany)
V.O. Popov (Moscow, Russia)
I.A. Tikhonovich (Moscow, Russia)
A. Tramontano (Davis, California, USA)
V.K. Švedas (Moscow, Russia)
J.-R. Wu (Shanghai, China)
N.K. Yankovsky (Moscow, Russia)
M. Zouali (Paris, France)

Project Head: S.B. Nevskaya
Editor: N.Yu. Deeva

Strategic Development Director: E.L. Pustovalova

Designer: K.K. Oparin

Photo Editor: I.A. Solovey

Art and Layout: K. Shnaider

Copy Chief: Daniel M. Medjo

Address: 119234 Moscow, Russia, Leninskiye Gory, Nauchny
Park MGU, vlad.1, stroeniye 75G.
Phone/Fax: +7 (495) 930 88 50
E-mail: vera.knorre@gmail.com, mmorozova@strf.ru,
actanaturae@gmail.com

Reprinting is by permission only.

© ACTA NATURAE, 2014

Номер подписан в печать 4 июня 2014 г.

Тираж 200 экз. Цена свободная.

Отпечатано в типографии «МЕДИА-ГРАНД»

CONTENTS

Letter from the Editors 1

FORUM

Space medicine: past, present and future 6

REVIEWS

V. K. Ilyin, N. V. Kiryukhina

**Disruption of the Colonization Resistance
Syndrome in Humans in Altered Habitats and Its
Prevention 10**

B. B. Vartapetian, Y. I. Dolgikh, L. I. Polyakova,
N. V. Chichkova, A. B. Vartapetian

**Biotechnological approaches to creation
of hypoxia and anoxia tolerant plants 19**

RESEARCH ARTICLES

A. V. Nedoluzhko, E. S. Boulygina, A. S. Sokolov,
S. V. Tsygankova, N. M. Gruzdeva, A. D.
Rezepkin, E. B. Prokhortchouk

**Analysis of the Mitochondrial Genome
of a Novosvobodnaya Culture Representative
using Next-Generation Sequencing and Its
Relation to the Funnel Beaker Culture 31**

O. V. Arkova, N. A. Kuznetsov, O. S. Fedorova,
N. A. Kolchanov, L. K. Savinkova

**Real-Time Interaction between TBP
and the TATA Box of the Human
Triosephosphate Isomerase Gene Promoter
in the Norm and Pathology 36**

CONTENTS

- S. A. Evfratov, E. M. Smekalova, A. V. Golovin,
N. A. Logvina, M. I. Zvereva, O. A. Dontsova
**Structural Features of the Telomerase
RNA Gene in the Naked Mole
Rat *Heterocephalus glaber*41**
- D. V. Kapustin, A. I. Prostyakova,
Ya. I. Alexeev, D. A. Varlamov, V. P. Zubov,
S. K. Zavriev
**High-throughput Method of One-Step DNA
Isolation for PCR Diagnostics
of *Mycobacterium tuberculosis*.48**
- E. A. Nikitina, A. V. Medvedeva,
G. A. Zakharov, E. V. Savvateeva-Popova
**The *Drosophila agnostic* Locus: Involvement
in the Formation of Cognitive Defects
in Williams Syndrome.53**
- M. S. Syrkina, M. A. Rubtsov,
D. M. Potashnikova, Y. D. Kondratenko,
A. A. Dokrunova, V. P. Veiko
**Cell Models for the Investigation
of the Role of the Mucin MUC1 Extracellular
Domain in Metastasizing62**
- E. A. Trifonova, T. V. Gabidulina, N. I. Ershov,
V. N. Serebrova, A. Yu. Vorozhishcheva,
V. A. Stepanov
**Analysis of the Placental Tissue Transcriptome
of Normal and Preeclampsia Complicated
Pregnancies71**
- Z. O. Shenkarev, E. N. Lyukmanova,
A. S. Paramonov, P. V. Panteleev,
S. V. Balandin, M. A. Shulepko, K. S. Mineev,
T. V. Ovchinnikova, M. P. Kirpichnikov,
A. S. Arseniev
**Lipid-Protein Nanodiscs Offer
New Perspectives for Structural
and Functional Studies of Water-Soluble
Membrane-Active Peptides84**
- M. N. Garas, S. V. Tillib, O. V. Zubkova,
V. N. Rogozhin, T. I. Ivanova, L. A. Vasilev,
D. Yu. Logunov, M. M. Shmarov,
I. L. Tutykhina, I. B. Esmagambetov,
I. Yu. Gribova, A. S. Bandelyuk,
B. S. Naroditsky, A. L. Gintsburg
**Construction of a pIX-modified
Adenovirus Vector Able to Effectively
Bind to Nanoantibodies for Targeting.95**
- V. V. Dolgikh, I. V. Senderskiy, G. V. Tetz,
V. V. Tetz
**Optimization of the Protocol for the Isolation
and Refolding of the Extracellular Domain
of HER2 Expressed in *Escherichia coli*106**
- S. S. Popov, K. K. Shulgin, A. N. Pashkov,
A. A. Agarkov
**The Effect of Melaxen on the Activity
of Caspases and the Glutathione
Antioxidant System in Toxic Liver Injury110**
- Guidelines for Authors.119**

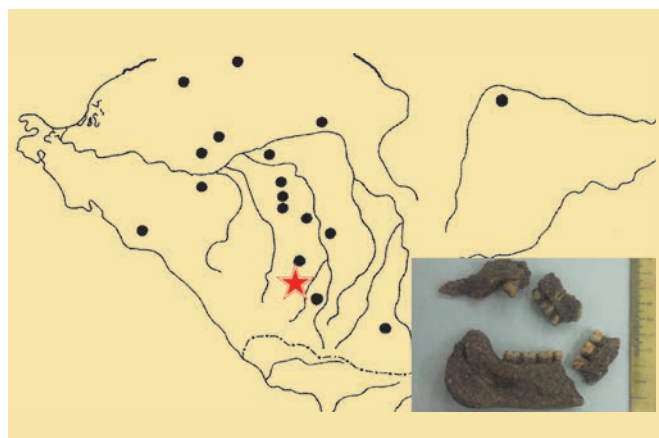


IMAGE ON THE COVER PAGE
See the article by Nedoluzhko et al.

Space medicine: past, present and future

Interview with Academician Anatoly I. Grigor'ev, laureate of the State Prize of the Russian Federation in the field of science and technology, 2014

Anatoliy Ivanovich Grigor'ev is an outstanding scientist who has made a notable contribution to solving the fundamental and applied problems of space physiology and medicine. He is the force behind the new scientific discipline known as gravitational physiology. He has helped shed light on a number of important principles of the functioning of the vestibular, cardiovascular, and endocrine systems, water and electrolytes, as well as mineral metabolism under altered gravity conditions. Grigor'ev's experimental research and theoretical studies are widely used in the search for solutions to the problems of protecting astronauts' health during long flights. A system for the medical support of crews during year-long or longer flights has been proven, developed, and implemented under his supervision. The research done by A.I. Grigor'ev, his numerous scientific works, active practical efforts to support manned spaceflight, and participation in international cooperation have earned him a well-deserved recognition both in Russia and abroad.



The first orbital space flights (SF) presented the tasks of studying the effect of space flight factors on the human body, identifying the main patterns of human body adaptation to space environment, and using these findings to develop and implement a scientifically grounded medical health care system for astronauts.

The problem of medical support is multifaceted and includes several interrelated directions. Academician Anatoliy Ivanovich Grigor'ev talks about these problems in his interview with a correspondent of *Acta Naturae*.

Acta Naturae (AN) correspondent: What scientific studies focus on the justification of the system of medical support of astronauts' health in your opinion?

A.I. Grigor'ev: Throughout manned space flights, the creation and modernization of the medical health care system for astronauts have been based on the results of fundamental research in space

physiology, biology, biochemistry, biophysics, and other scientific disciplines, carried out in ground-based simulation experiments, at biological satellites, and in space missions. This has made it possible to better understand the effect of space flight factors on different functional structures of the body, to explore the patterns of body adaptation in response to their action, and to provide a rationale for approaches to developing a health support system for astronauts during long missions.

In the early years of space exploration, the short-term manned missions were carried out using the Vostok, Voskhod and Soyuz spacecrafts with a relatively "simple" medical support and health control system.

Today, manned astronautics is tasked with the problem of increasing flight duration and the number of crew members. This has required the development of a reliable medical support system for expeditions lasting for several months. The experimental ground-based models

simulating the effects of zero gravity were developed at the Institute of Biomedical Problems (IBMP) to solve this problem. They were clinostatic and antiorthostatic hypokinesia (bed rest) and "dry immersion" (immersion of a test subject into a special water bath).

Numerous experiments on clinostatic hypokinesia lasting 15 to 120 days were carried out in 1966–1976. These experiments examined the status of various systems of the body under these conditions in combination with the use of preventive measures (exercises and the use of pharmacological agents). A series of experiments with clinostatic hypokinesia lasting 3–120 days were carried out at IBMP in the 1980s to study the cardiovascular system, metabolism, and features of their regulation. This has made it possible to develop and test a scheme for applying water plus electrolyte additives in combination with negative pressure on the lower part of the body (NPLB), which have be-

come an integral component of the prevention system at the final stage of long SFs.

AN correspondent: Which study can be distinguished among the overall series of projects carried out during previous years?

A.I. Grigor'ev: The unprecedented for its duration, 370-day-long experiment, with antiorthostatic hypokinesia was carried out in 1988. This experiment studied the dynamics of changes in major body systems, including water-electrolyte and mineral metabolism. The experiment showed that it is possible to use alternative technologies of prevention, which allow one to purposefully enhance the physiological capabilities of an astronaut's body; in particular to improve the tolerance to g-loads during disorbiting. In a continuous 56-day-long experiment with "dry" immersion, we thoroughly studied the state of the cardiovascular system, water-electrolyte metabolism, and renal function and tested the preventive measures, including exercises and artificial gravity generated by a small-radius centrifuge.

AN correspondent: Anatoliy Ivanovich, you are the originator of the new branch of science known as gravitational physiology. Could you please tell us about the main achievements in the field?

A.I. Grigor'ev: Gravitational physiology studies the principles of regulation of bodily functions under altered gravity conditions. Important scientific data were obtained in studies conducted at 11 biological satellites, which were carried out with the participation of experts from Russian and foreign scientific centers (coordinated by E.A. Il'in). The research was conducted in many biomedical disciplines using a broad evolutionary range of biological objects (from microorganisms to primates). These studies, in cooperation with Yu.V. Natochin, have provided important data for understanding the mechanisms of

metabolism adaptation in living organisms exposed to altered gravity. These results significantly contribute to the theory of space biology.

The following general theoretical achievements are considered to be important ones: the discovery of changes in the sensitivity of end organs to biologically active substances in humans during long SFs; defining the role of shifts in water-electrolyte metabolism in the development of vestibular disorders, orthostatic instability and reduced tolerability to accelerations; identification of the mechanisms of restructuring water and ion transportation systems in the kidney; and establishing ways to minimize physiological functions under these conditions. We have implemented programs studying the cardiovascular system and metabolism during long flights and uncovered previously unknown mechanisms of endocrine regulation of metabolism in zero gravity. When studying the effects of microgravity on human multipotent stromal cells (MSCs), in cooperation with L.B. Buravkova, structural and molecular-genetic changes in the MSCs of human bone marrow were detected. These results are indicative of the presence of gravity-dependent intracellular mechanisms that lead to both early and late responses of progenitor cells to the simulation of the effects of microgravity, thus indicating the specific role of the actin cytoskeleton, being the basic cell structure (including stem cells), as a gravitationally sensitive cell structure. Studies focused on the molecular mechanisms of the changes detected in MSCs under these conditions have shown transient changes in the level of expression of the structural and regulatory genes associated with the actin cytoskeleton. It has been established for the first time that this effect significantly changes the expression pattern of the genes, being "stem cell markers," including the genes encoding the proteins

involved in intracellular signaling, cell adhesion, and the regulation of proliferation and differentiation of stem cells.

The simulation experiments and flight studies performed allowed us to justify, and later to develop and put into flight practice, methods for the medical control, prediction and management of the human status, to create a complex of technologies to mitigate the adverse effects of zero gravity, and this contributed to the launching of long-term missions at the Mir orbital station (OS) and allowed our country to assume a leading position in manned astronautics.

AN correspondent: In 1996–2008, you were the head of the medical support service of the missions at the Mir orbital stations and International Space Station (ISS). Could you please tell us more about that?

A.I. Grigor'ev: Our team has developed a system for rendering medical support to crews during long-term orbital flights, which includes the following components:

- medical selection, periodic and preflight medical examination of astronauts, medical certification;
- biomedical crew training;
- maintaining the health and performance of astronauts during an orbital flight: health monitoring, medical diagnosis, a system of preventive measures, functional state management, psychological support, medical assistance (if necessary), radiation monitoring and environment control;
- post-flight medical rehabilitation to restore the health of space crews;
- healthcare support for the development of manned spacecraft; and
- medical and technical support for the development of satellite-borne biomedical support measures.

AN Correspondent: Anatoliy Ivanovich, we know that you were the chairman of the Chief Medical Commission of the Russian Space Agency for the certification of as-

tronauts and candidates for astronauts from 1990–2008. Could you please tell us about the medical selection and training of astronauts?

AI Grigor'ev: The system of medical selection of astronauts developed in cooperation with the experts of the Yu.A. Gagarin Cosmonaut Training Center includes a comprehensive medical examination of astronauts to assess their physical and mental health, to determine the functional capacities of the body according to results related to tolerance to special stress tests. The latest advances in medical science and technologies are being used when upgrading the selection system. The parameters of the astronauts' genotype are studied, along with extensive physiological and biochemical research, in order to predict tolerance to extreme conditions. Increasingly more attention will apparently be focused on the "genetic predisposition" of a person to tolerance to g-force associated with the pre-training and directly with long-term stays in space.

AN correspondent: How is the medical control of a crew's health conducted during flights?

A.I. Grigor'ev: The medical control during SFs is based on integrated monitoring aimed at assessing the current state of astronauts' health, dynamic monitoring of the basic functions of their bodies and the habitat, and controlling regulation and adaptation to the living environment. The structure of the medical monitoring allows us to identify the adverse conditions that may develop during flight and, if necessary, to conduct emergency surveys according to predictions. The system for minimizing health risks in case of potential failures of the life support system and technical problems during flight operations was developed and functions effectively now. Modes, measures and methods of prevention have also been developed, tested in ground-based experiments, and implemented in

flights. The system of preventive measures has been developed and successfully implemented at all stages of long-term missions in collaboration with O.G. Gazenko, A.S. Barer, L.I. Kakurin, I.B. Kozlovskiy, I.D. Pestov, B.V. Morukov and other IBMP staff. The onboard prevention system includes physical exercises using treadmill, cycle ergometer, and press machines, muscle loading along the longitudinal axis of the body using the Penguin suit, low-frequency electrical stimulation of the muscles, the effect of negative pressure on the lower part of the body using the Chibis pneumatic-vacuum suit, drugs and other measures to prevent potential disorders of the functional state during a space flight. The important purposes of the system at the initial phase of the flight include prevention and relief of manifestations of the adaptation syndrome, while the purposes of the final stage include measures to prevent post-flight orthostatic instability (NPLB and water plus electrolytes additives).

The studies conducted during and after SFs have shown that the Russian preventive system is effective in preventing or reducing the adverse effects of exposure to zero gravity and other adverse factors of long-term SFs. It has become the basis for the medical support of crews at the International Space Station.

AN correspondent: Could you please describe the structure of the health care system?

A.I. Grigor'ev: The onboard health care system is based on the principle of nosology. It was developed on the basis of the most recent achievements in clinical medicine, taking into account the specific conditions of space flights. The Russian system of medical aid includes an onboard medical kit and a set of specialized medical packages for emergency care, packages with cardiovascular agents, gastrointestinal agents, antiseptic and other drugs. In some

cases the medical care kit at the Mir and ISS orbital stations has made it possible to conduct curative measures in acute and emergency conditions and injuries, which have made it possible to diagnose and monitor the targeted treatment. The studies carried out in cooperation with I.P. Neumyvakin, L.L. Stazhadze, V.V. Bogomolov, I.B. Goncharov, A.D. Egorov and the staff of a number of clinics in Moscow and St. Petersburg have significantly contributed to the formation of the health care system at orbital stations.

AN correspondent: Anatoliy Ivanovich, what about the implementation of new remote-action technologies in the medical monitoring of astronauts?

A.I. Grigor'ev: Space telemedicine has been in constant improvement and implemented since the 1990s. This has allowed us to significantly improve medical care during SFs and at landing sites. The practical use of telemedicine in SFs significantly complements the capabilities of diagnosis and analysis of the effectiveness of health care.

AN correspondent: And how do you control the environment and radiation?

A.I. Grigor'ev: Much attention is given to the monitoring of the OS habitat, including the assessment of air quality and monitoring of the concentrations of toxic substances. A classification of pollution levels has been developed, and personal protective equipment has been designed. Assessment of onboard water quality and the level of microbial contamination are regularly conducted during flights. The level of noise in the living compartments of OSs is regularly assessed and otprotection methods are being elaborated when it is exceeded. Scientific and methodological materials related to the radiation safety of orbital station crews have been developed, and a permanent Radiation Safety Service for Space Flights has been

formed. It is equipped with facilities for continuous monitoring of the radiation environment along the flight path and in the living compartments, including the assessment of radiation doses and radiation risk to crew members, development and implementation of recommendations for minimizing the radiation hazard to the crew. With the prospect of interplanetary missions, we have been paying a great deal of attention to research into the effect of heavy ions on living systems.

AN correspondent: Is post-flight medical rehabilitation equally topical at present?

A.I. Grigor'ev: IBMP staff have thoroughly analyzed the changes in the state of many systems of the body of astronauts which occur after long-term flights and require special health rehabilitation measures for their recovery during the post-flight period. They have improved some measures and methods of post-flight rehabilitation; designed a medical-evacuation complex and medical equipment for examination and medical assistance to astronauts at the landing site; and developed methods of medical care after a flight. These studies were further developed in connection with flights to the ISS. IBMP staff (B.M. Fedorov, T.D. Vasil'eva, V.V. Bogomolov) and Yu.A. Gagarin CTC staff (V.V. Morgun, V.I. Pochuev, O.V. Kotov) have conducted a series of studies aimed at developing a set of methods and measures for restoring astronauts' health after long-term flights which uses individual schemes and regimens of interventions during rehabilitation.

The main result of the medical support system that we have developed for the crews flying to the Mir and ISS OSs is the maintenance of health and the ability of crew members to perform, which are sufficient for effective implementation of flight programs, as well as a favorable course of rehabili-

tation given adequate restorative and therapeutic measures. It is important to mention the active role of astronauts, especially physician astronauts, in the implementation of this system. The effectiveness of the Russian system of medical selection, medical monitoring of the health of crews during long-term flights, and the system of onboard prevention and post-flight rehabilitation has been proved. This was also demonstrated by the successful extra-long-term missions, including the uniquely complex flights of V.V. Polyakov (a 438-day flight) and S.K. Krikalev (803 days in 6 flights).

AN correspondent: Anatoliy Ivanovich, what is the ground that space medicine has covered from orbital stations to interplanetary flights?

A.I. Grigor'ev: The achievements in the creation and successful use of the Russian medical health care system for astronauts during long-term space missions underlie the development of the concept of biomedical support during interplanetary missions. The research and developments in this field are being conducted at IBMP. The international 520-day-long interplanetary flight modeling experiment (Mars-500 project) that was carried out in 2010–2011 was the most significant one. The system of medical support for crews' health was worked out during this experiment, the technological operations of "landing" on Mars have been modeled, and important data on the dynamics of the status of the main body systems during prolonged isolation have been obtained. The experiment has been praised by the international scientific community.

AN correspondent: Can the achievements of space medicine be used in clinical practice?

A.I. Grigor'ev: We actively suggest using our achievements in public health care practice. In collaboration with clinicians at some medical

institutions we have managed numerous unique achievements during SFs and in simulations of vital functions of the body under ground-based conditions in the Russian health care system. In particular, we have designed a number of measures for preventing and correcting motor disorders (special loading suits, neuromuscular stimulation facilities, etc.) in cooperation with I.B. Kozlovskiy and E.P. Tikhomirov. During tests, these facilities were adapted to the needs of the clinic for children with cerebral palsy (K.A. Semenova) and persons who have suffered traumatic brain injury and strokes (A.B. Geht, L.A. Chernikova, V.M. Shklovskiy et al.). Now these facilities are successfully "running" at the manufacturing venture at IBMP (I.V. Saenko).

New experimental data for the analysis of the destructive and adaptive processes taking place in human bone structures and changes in the mineral metabolism under conditions of reduced gravity load were obtained, and a system for the correction of musculoskeletal system disorders in zero gravity and hypokinesia has been developed in cooperation with V.S. Oganov.

AN correspondent: Anatoliy Ivanovich, let me congratulate you on the important government award and thank you for this interview. We would like to wish you success in the area of knowledge, where our country has been at the forefront for many years, and, judging from what you have told us, is not giving up its position today.

A.I. Grigor'ev: Thank you for your congratulations. I would like to mention that this research is work made by a large team, including not only IBMP staff, but also all staff at institutes and industrial organizations – our "cooperation" that I was lucky to head for many years. I would like to thank all my colleagues and congratulate them on our shared success! ●

Disruption of the Colonization Resistance Syndrome in Humans in Altered Habitats and Its Prevention

V. K. Ilyin, N. V. Kiryukhina*

Institute of Biomedical Problems, Russian Academy of Sciences, Khoroshevskoe shosse, 76A, Moscow, Russia, 123007

*E-mail: kiryukhina_nataliya@hotmail.com

Received 07.08.2013

Revised manuscript received 12.03.2014

Copyright © 2014 Park-media, Ltd. This is an open access article distributed under the Creative Commons Attribution License, which permits unrestricted use, distribution, and reproduction in any medium, provided the original work is properly cited.

ABSTRACT Exposure of human subjects to environments with modified parameters is associated with reduced colonization resistance of the intestine and epithelial tissue, which leads to dysbiotic changes. Probiotics – preparations based on protective microflora – are used to correct dysbacteriosis of different etiologies and localizations. However, the effectiveness of probiotics largely depends on the adhesive ability of a probiotic strain and lack of competitive relations with the indigenous microflora, which can be achieved by individual selection of a preparation. We propose to use autochthonous microflora as a probiotic drug to optimize the prevention and treatment results. A personalized approach to probiotic selection will improve therapy efficiency and reduce the risk of adverse effects in each individual patient.

KEYWORDS autostrains; autoprobiotics; dysbacteriosis; altered habitat; disruption of colonization resistance.

INTRODUCTION

Human exploration of space, oceans, and the Earth's core leads to the creation of bio-isolated artificial human ecosystems with modified habitat parameters [1]. It substantially alters the phylogenetically established relationships between commensals of the human–microflora ecosystem. In humans, this manifests itself as the disruption of the colonization resistance syndrome. It is, therefore, evident that in order to develop a strategy of environmental approaches to disease prevention in humans in extreme habitats we need to study the state of natural colonization barriers against infectious agents in the human body.

Van der Waaij [2] defined “colonization resistance” as “resistance which a potentially pathogenic microorganism encounters when it tries to colonize a ‘landing site’ on the mucosa in one of the three tracts that have an open communication with the outside world: respiratory, urinary and digestive.” van der Waaij identifies two main barriers responsible for resistance to infections in humans: the barrier formed by commensal microflora and the barrier provided by factors of cell-mediated and humoral immunity. V.M. Bondarenko [3] additionally mentions the epithelium of mucous membranes as a natural barrier, as its physiological state largely defines its permeability to causative agents. Studies by Noble [4] allow us to add skin tissue to the list of colonization barriers.

The first and main barrier against colonization, the barrier formed by microbial associations of commensals in a human body, deserves a more detailed analysis. The system of relationships both within such associations and between associations and the host is quite complex. When a person is infected, a causative agent enters the host organism as a population of genetically heterogeneous cells through food, water, particles of drop or dust aerosols, etc. The primary focus of infection is formed as a causative agent displaces normal host microflora and colonizes the new habitat. Adhesion, colonization, and subsequent propagation of the agent that synthesizes toxic compounds leads to pathomorphological changes in the host; in the case of opportunistic microorganisms, it is characterized by a lack of specificity and mosaic disorders in various organs and tissues. Impairment of the overall resistance of the organism and lower levels of protective microflora results in an increased population of opportunistic microorganisms, which can translocate to other biotopes [5]. Endogenous infections etiologically caused by autochthonous microflora develop along a similar pathway.

According to modern beliefs, the natural microflora of any biotope can be divided into permanent (resident) and accidental (transient) based on its origin. Resident microflora includes microorganisms specific to a certain biotope, whereas the transient one consists of exogenic microorganisms. The composition of the resident mi-

croflora of a biotope is relatively stable; however, the physiological importance of its microorganisms differs substantially. Therefore, resident microflora is further subdivided into an obligatory and a opportunistic one.

Obligatory microflora is the main component of any microbiocenosis; it prevents colonization of the biotope by random microorganisms and is involved in fermentation and immunity stimulation processes. Thus, obligatory microflora in the large intestine includes bifidobacteria, lactobacilli, typical collibacilli, peptostreptococci, eubacteria, and most bacteroid and enterococci species [6]. The natural microflora of the digestive tract has important physiological functions: it enables colonization resistance of the mucosa; stimulates the formation of the immune system in newborns; maintains the immune status in adults via muramyl peptides of bacterial cell walls and other adjuvant-active macromolecules; participates in metabolic processes (secretion of the enzymes involved in the protein, lipid, nucleic and bile acid metabolism); maintains the electrolyte balance and synthesis of vitamins B, K and D; regulates the gaseous environment in the intestine; is involved in the biochemical processes of digestion (fermentation of food substrates, regulation of the motor-evacuation function of the intestine); and it inactivates toxic exogenous and endogenous products by biotransformation and biodegradation.

A sufficient number of resident microorganisms attached to the intestinal walls prevent the propagation of pathogenic agents, their invasion of enterocytes and passage through the intestinal wall; this is achieved by the formation of an environment with pH values adverse to extraneous microflora in the biotope, as well as by the production of bacteriocins (antibiotic substances) and the deprivation of competing microorganisms of nutrients and adhesion sites. Beneficent metabolic activity also includes the production of vitamin K, biotin, niacin, pyridoxine and folic acid; the hydrolysis of bile salts and cholesterol; regulation of its levels; and hormone re-circulation. The lack of a favorable microflora in the intestinal microbiocenosis leads to a disruption in the recirculation of the estrogens secreted in the gastrointestinal tract (GIT) with bile and the development of corresponding pathological disorders in the female reproductive system. Normally, functioning resident microflora controls the toxin production in the intestine, as well as prevents their over-expression and penetration into the bloodstream. Resident microflora has detoxifying and proteolytic properties, which allow it to metabolize endotoxins, allergens, and antigens in the intestine by proteolysis. It also involves absorption of partially digested proteins in the intestine, including those associated with the development of food intolerance and accompanying skin disorders. A disruption in

the microbiocenosis allows these substances to enter the bloodstream.

The detoxifying and protective role of indigenous microflora in preventing the adverse effects of radiation, chemical impurities in food, carcinogenic factors, toxic exogenous substrates, unfamiliar and exotic food, and contaminated water is also noteworthy. This occurs by the stimulation of the immune response and improvement of non-specific immune resistance: potentiation of the production of interferons, interleukins and enhancing the phagocytic abilities of macrophages.

Let us describe the main groups of protective microflora used to produce popular modern probiotic preparations.

Bifidobacteria constitute the main group of intestinal bacteria; they amount to 25% of the entire intestinal microbial population in adults and 95% in newborns. Bifidobacteria produce acetic and lactic acids. Subsequent development of an acidic environment induces an antibacterial effect. Bifidobacteria are capable of releasing metabolic products that can directly inhibit the development of opportunistic Gram-positive and Gram-negative pathogens. Bifidobacteria convert potentially toxic ammonia (or amines) into NH_4 ions that are unable to penetrate through mucosa and reach the bloodstream. Furthermore, these bacteria do not form aliphatic amines, hydrogen sulfides, or nitrites. Bifidobacteria produce vitamins (mostly group B ones), as well as digestive enzymes, such as casein phosphatase and lysozyme. Bifidobacteria restore the normal intestine microflora after antibiotic therapy [6].

Enterococci, previously classified as group D streptococci, are a large group of bacteria belonging to the genus *Enterococcus*, which includes the *E. faecalis*, *E. faecium*, *E. avium*, *E. casseliflavus*, *E. durans*, *E. gallinarum*, *E. raffinosus*, *E. irae*, *E. malodoratus* and *E. mundtii* species. *E. faecalis*, *E. faecium*, *E. gilvus* and *E. pallens* were identified in human clinical isolates. Enterococci are detected in newborns as early as in the first days of their lives; in breastfed babies under 1 year, their levels vary between 10^6 and 10^7 CFU/g. In formula-fed babies enterococci levels can reach 10^8 – 10^9 CFU/g. The enterococci levels in the intestine of a healthy human remain consistent and reach 10^7 – 10^8 CFU/g of feces. Enterococci are present in almost every intestine section. The main properties of enterococci include involvement in the synthesis of vitamins and metabolism of sugars (lactose); immunostimulation (maintenance of the level of broad-spectrum cytokines); high antagonistic activity against staphylococci, listeria and collibacilli via the production of bacteriocins; anti-inflammatory activity; and high resistance to environmental factors (temperature, pH).

Normally, the levels of enterococci in the intestine do not exceed the overall level of colibacilli [6].

Lactobacilli also constitute a substantial part of protective microorganisms' population in most human biotopes. Lactobacilli are Gram-positive rod-shaped bacteria, opportunistic anaerobes. Lactobacilli differ in their requirements for nutrients and growth factors. Lactobacilli exhibit proteolytic activity mediated by the activity of the proteases and peptidases they produce; their lipolytic properties allow them to digest milk fat and some triglycerides; they also synthesize DNase and/or RNase and pseudocatalase through exonuclease activity; and they produce enzymes that ferment hexoses, disaccharides and polysaccharides. The antagonistic activity of Lactobacilli is mediated by their extensive ability to produce an acidic environment as well as by the production of antibiotic compounds (such as acidophilin – *Lactobacillus acidophilus*, lactolin – *L. plantarum*, brevin – *L. brevis*), hydrogen peroxide, and lysozyme [6].

The mechanisms of colonization resistance can be divided into a direct and indirect activity. The direct mechanisms include the production of inhibitors that interrupt the metabolism of pathogenic and opportunistic bacteria by bacterial strains, competitive relationships with pathogenic bacteria for nutritious substrates and adhesion sites, direct degradation of toxins, anti-endotoxic activity, and the prevention of microorganism translocation to other parts of the body. The indirect effects include stimulation of the immune system, stimulation of mononucleocytes, induction of interferon, inhibition of bile acid conjugation, etc. The observed variety of colonization resistance mechanisms naturally implies a large number of variants, particular combinations under certain circumstances, which define the state of colonization resistance that most likely depends on the microflora amount and quality and its habitat.

The aforementioned functions, beneficial to human health, are stable if both a quantitative and qualitative consistency of microflora is maintained. It is also natural that not all the beneficial functions of microflora are exhibited in all biotopes or are exhibited to an equal extent. They depend on the anatomical, physiological, and biochemical features of a biotope (i.e., gastrointestinal, urological tracts, skin or respiratory tract, etc).

DISRUPTION OF COLONIZATION RESISTANCE UNDER THE INFLUENCE OF EXTREME FACTORS

Extreme conditions disrupt the barrier functions of the body associated with normal functioning of the skin, intestine, and mucous membranes, which come in direct contact with the environment [7]. Stress (psycho-emotional or physical) has been shown to cause the

activation of endogenous microflora in the intestine, penetration of bacteria into the bloodstream, and subsequent excretion through the urinary tract [8]. If the intensity of the factors affecting either directly or indirectly the fixation, survival, and functioning of normal microflora exceeds the capacity of the compensatory mechanisms of the host-microflora ecosystem, this will induce microenvironmental disruptions; their type, degree of manifestation, and duration will depend on impact dose and length. The ability to resist noxi-influence depends on many factors, which characterize the state of the organism. Studies involving astronauts, divers, and athletes have revealed symptoms of secondary immunodeficiency and impairment of the regulatory mechanisms. The response of each individual depends on his genetic and immunological potential, as well as on the state of his microbiocenosis [9, 10].

Nowadays, the disruption of colonization resistance is considered to be a pathological condition that manifests in people holding "extreme jobs": astronauts, scuba divers, submariners, compressed air workers, etc. Dysbacteriosis is one of the most important manifestations of the disruption of colonization resistance, which is characterized by a loss or reduction in the levels of some obligatory representatives of normal microflora, increased incidence of the concentration of representatives of opportunistic microflora, and possible appearance of bacterial strains atypical of a certain biotope.

The entire combination of factors affecting humans or animals during a space flight or prolonged exposure to hyperbaric conditions is quite unique; therefore, no adaptive measures against it have been developed through evolution [11]. In addition, the data suggest that such factors as nervous and functional stress, hypokinesia, extreme exercise load, prolonged stay in isolated conditions with modified parameters of the gaseous environment and microclimate also contribute to the development of dysbacteriosis [12]. The same study shows that nervous and functional stress results in a reduced number of bifidobacteria and lactobacilli, in some cases up to their complete eradication. Changes in aerobic microflora leading to increased concentration of some representatives also occur in the case of extreme exercise load. Pronounced changes in microflora also occur in people after they stay in a diving chamber with an altered gaseous environment and microclimate. These are common changes in the intestinal microflora resulting from exposure to extreme situations. The development of dysbacteriosis is triggered by a reduced concentration of bifidobacteria and lactobacilli. The degree of manifestation of dysbiotic rearrangement of microflora largely depends on the initial state of the microenvironmental status.

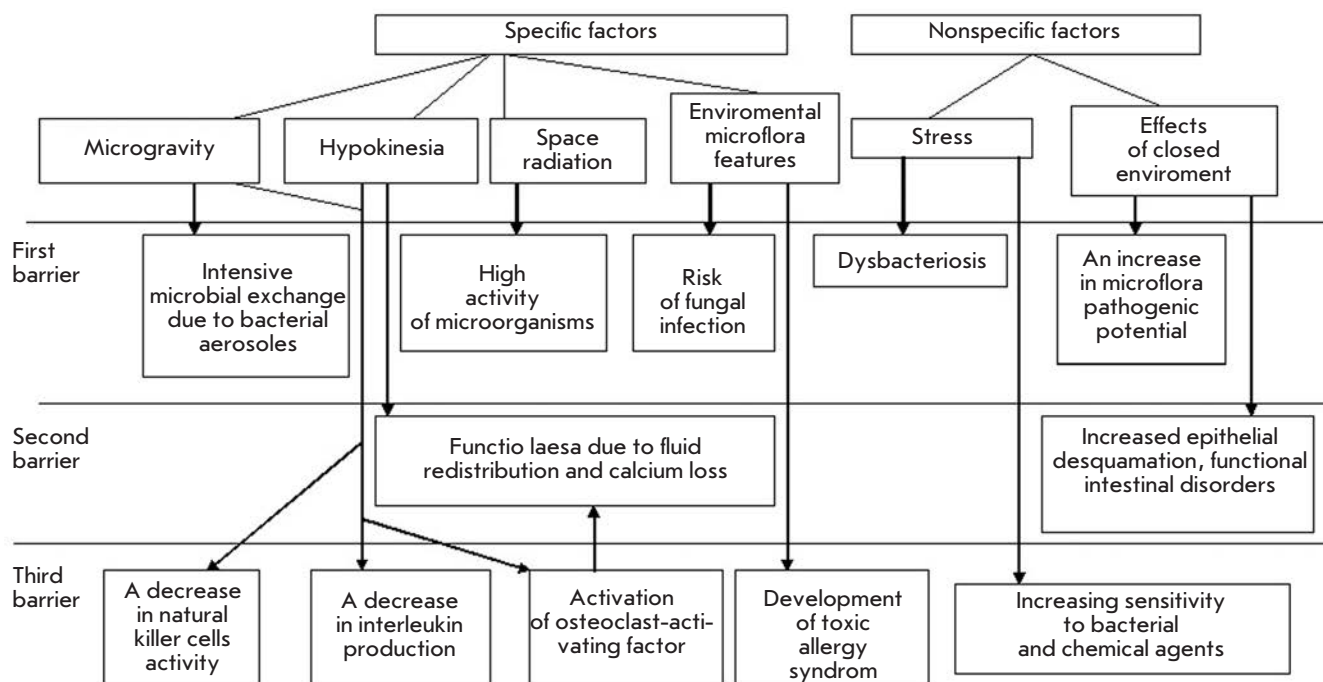


Fig. 1. Scheme showing the development of the colonization resistance disruption syndrome in space flights

N.N. Lizko's discussed the type of stress-induced changes in his review [13]. Stressful situations establish the conditions for modification of the adhesive properties of bacteria and cell adhesiveness of a host. For example, the physical and chemical state of intestinal mucin may be disrupted by bile acids, proteolytic enzymes, and pH changes. An abrupt reduction in the mucosal component (mucin) and a decreased level of acidic mucopolysaccharides on the surface of the mucosal layer and mucosal lining cells are considered to be indicators of reaction to stress. Direct evidence support the existence of a certain predilection for changes in adhesion during stress-induced shifts in the digestive process. Notable changes in immune reactivity were observed in response to stress-induced activation of the hypothalamic-pituitary-adrenal axis. Reduced immune resistance can affect the topographic distribution of some microbial populations in the GIT. This may result in endogenous contamination and metabolic consequences of enhanced bacterial growth in the small intestine.

Thereby, disruption of the colonization resistance syndrome develops in almost all cases of humans living in artificially modified habitats. However, development of this syndrome depends on both specific factors, e.g. altered habitat factors (space radiation, micro-gravity, hypokinesia for space flights; a combination of an al-

tered gaseous environment and changes in the pressure for hyperbaric conditions, etc), and non-specific factors, primarily stress-induced factors, and factors related to an enclosed space. They affect almost all colonization barriers.

Thus, during a space flight (Fig. 1), a combination of specific (microgravity, hypokinesia, space radiation, colonization of environmental elements by bacterial-fungal associations) and non-specific factors (stress, closed environment factors) affect the conditions of all three colonization barriers. Intensive microbial exchange, exogenous contamination, stress-induced dysbacteriosis, and increased pathogenic potential in the human-microorganism system lead to a weakening of the first barrier formed by protective microflora. The second barrier (epithelial tissue and mucosa) also experiences a weakening of its protective properties due to several pathophysiological processes (redistribution of fluids, disruption of calcium homeostasis, increased desquamation of epithelium, and disruption of the physiological function of the intestine). The third barrier (factors of cell-mediated and humoral immunity) is also impaired, thus leading to changes in phagocytosis, serum bactericidal activity, reduced activity of killer cells and decreased production of interleukins, activation of the osteoclast-activating factor, and development of toxic and allergic conditions.

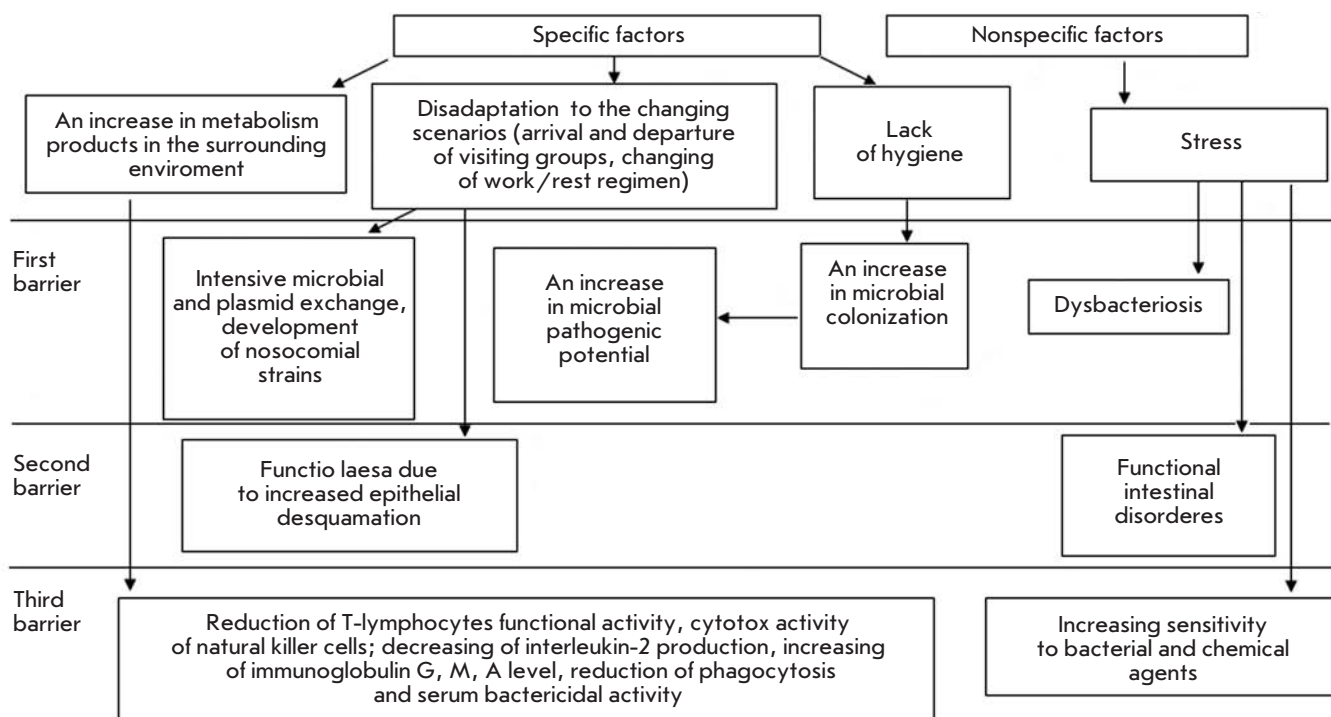


Fig. 2. Scheme showing the development of the colonization resistance disruption syndrome in ground-based closed-chamber studies

In inhabited ground-based closed-chambers (Fig. 2), specific environmental factors (elevated concentration of metabolic products, deadaptation, limits on hygienic procedures) and stress promote an increased intensity of both microbial and plasmid exchanges, which results in the spontaneous formation of nosocomial-like strains as early as during the first days of isolation, as well as an increased size of microbial foci, replacement of less virulent strains with more virulent strains of the same species, systemic dysbacteriosis, etc. The physiological status of epithelial tissue is also affected. The disrupted immunity manifests itself in a reduced functional activity of T lymphocytes and cytotoxic activity of natural killer T cells; a decreased production of interleukin 2; increased levels of immunoglobulins A, M, G; weakened phagocytosis and blood serum bactericidal activity; and increased sensitivity to bacterial and chemical agents.

Disruption of the colonization resistance syndrome caused by a prolonged exposure to hyperbaric conditions is the most pronounced and most dangerous one (Fig. 3). Under such conditions, a combination of specific factors (a combination of the influences of a hyperbaric environment and altered gaseous environment) leads to pronounced activation of opportunistic microflora and suppression of the protective microflora. As a result, a manifestation of the disruption of the colonization

resistance syndrome develops linearly with intensive colonization of the habitat with sapronose infectious agents, mainly *Pseudomonas aeruginosa*. The severity of the syndrome depends on the length of stay in hyperbaric conditions and the pressure. The barrier functions of epithelial tissue are additionally impaired by micro-barotraumas, maceration of epithelium, a decreased activity of ceruminal glands in external auditory canals, which become *locus minoris resistentiae* for infections. Infection caused by prolonged diving often manifests itself as external otitis, which results in premature decompression of the affected divers for medical reasons (Table 1) [7].

METHODS FOR PREVENTING THE DISRUPTION OF THE COLONIZATION RESISTANCE SYNDROME

Various commercial probiotic preparations based on collection strains are widely used to prevent and treat dysbacterioses of different origins. However, it is well known that probiotics introduced into the body may create an imbalance in the host's autoflora as a result of antagonism between the indigenous and industrial strains [14]. Some researchers have shown that probiotics based on industrial strains fail due to biological incompatibility [15]. The number of reports on the adverse effects of probiotic therapy with preparations containing industrial strains is on the rise. Most pa-

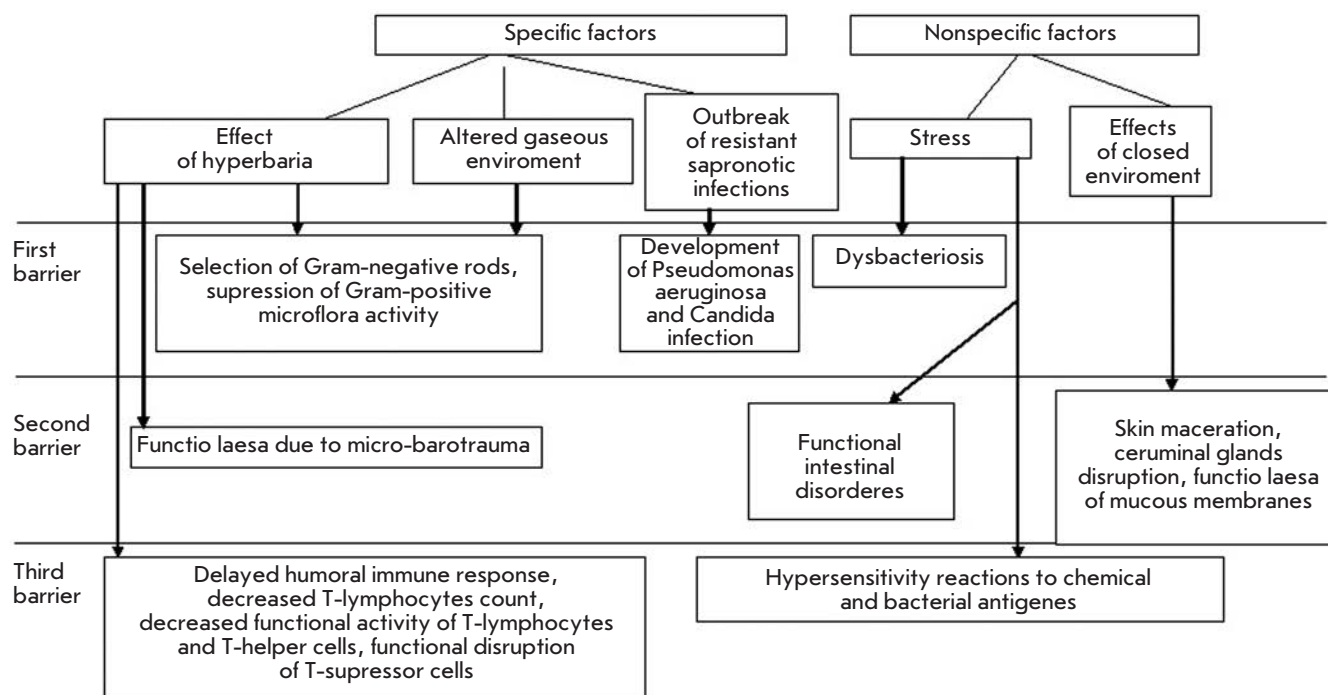


Fig. 3. Scheme showing the development of the colonization resistance disruption syndrome under hyperbaric conditions

pers report infectious complications associated with the use of commercial probiotics. Such adverse effects are likely to develop in weakened, elderly or immune-compromised patients. This fact should always be taken into account when using probiotic correction measures.

Detailed data on the complications associated with probiotic therapy of both bacterial and fungal etiology is presented in review [16] and partially summarized in *Table 2*.

In addition to meeting the standards of genetic safety and resistance to antibacterial agents, the efficiency of a probiotic is also determined by its adhesive activity, lack of competitive relationships with the indigenous microflora, as well as by its antagonistic properties against opportunistic pathogens, which can be, to an extent, achieved through personalized selection of probiotic preparations [26]. The highest degree of preparation customization can evidently be reached by using autostrains of microorganisms selected from the microbiocenosis of the subject.

According to B.A. Shenderov, a fetus develops immunological tolerance to the normal microflora of the mother already during intrauterine growth [27]. According to the published data, the differences in the ability of industrial and autostrains to adhere to epithelium cells depend on the compatibility between a

strain’s receptors and cell receptors [28–30]. Thus, it has been shown that vaginal lactobacilli adhere to cells of vaginal epithelium better than strains isolated from other sources [28, 29].

B.A. Berdichevsky studied the protective role of autobacteria under stress conditions [8]. Activation of the autochthonous microflora in response to surgical stress, which included translocation of autobacteria into extraintestinal biotopes followed by elimination through the urinary tract, was demonstrated experimentally.

Some authors have proposed to use full human microbiocenosis as preparations [31–33]. To ensure infinite preservation of microflora it is recommended to store the biological material in cryobanks and subsequently use it to construct autoprobiotics and products of functional nutrition [31, 32]. The patent “Method for establishing a bank of autochthonous strains of microorganisms for the restoration of human intestine microbiocenosis” describes a method for producing a preparation of autologous intestine microorganisms [33]. The method includes collecting stool samples from the same subject during clinically healthy periods, starting with days 7–15 after birth and subsequently at least once a year over his entire life. Autostrains of the normal intestine microflora are isolated from the samples and identified. The biomass

REVIEWS

Table 1. Development of the disruption of colonization resistance under hyperbaric conditions, presented as a change in ratios between the protective and opportunistic microflora in epithelial tissue and the intestine

Stage	Day of study	Group of microorganisms, %		
		Protective Gram-positive	Opportunistic Gram-negative	<i>Pseudomonas aeruginosa</i>
Baseline	0	90.3	4.8	0
The isopression phase	1–3	67.3	11.5	9.6
	5–8	62.5	32.8	25.0
	11–13	39.6	31.0	20.6
Decompression	18–22	25.0	31.0	25.8
	24–28	38.7	40.3	29.0
Yield	30–34	68.5	28.5	22.8

Table 2. Cases of bacterial and fungal sepsis chronologically associated with the use of probiotics *

Form of sepsis	Patient's age (years)	Risk factors	Probiotic	Identification method	Reference
Hepatic abscess	74	Diabetes	LGG**	API 50 CH***, PFGE	[17]
Endocarditis	67	Mitral insufficiency, tooth extraction	<i>Lactobacillus rhamnosus</i> , 3 × 10 ⁹ CFU/day	API 50 CH, mass spectrometry	[18]
Bacteraemia	11 months	Prematurity, gastrostomy, short bowel syndrome, CVC, intravenous feeding, rotavirus-induced diarrhea	LGG, 1/4 capsule/day	rRNA sequencing	[19]
Endocarditis	4 months	Cardiac surgery, antibiotics-associated diarrhea	LGG, 10 ¹⁰ CFU/day	DNA dactylography	[20]
Bacteraemia	47	Not given	<i>Bacillus subtilis</i> , 8 × 10 ⁹ spores/day	Antibiotics sensitivity	[21]
Bacteraemia	73	Chronic lymphatic leukemia	<i>B. subtilis</i> , 8 × 10 ⁹ spores/day	16S rRNA sequencing	[22]
Fungaemia	3 months	CVC, diarrhea, intravenous feeding	<i>Saccharomyces boulardii</i> , 100 mg/day****	PFGE of mitochondrial DNA	[23]
Fungaemia	51	Chronic lymphatic leukemia	<i>S. boulardii</i> , 1 g/day	PFGE	[24]
Fungaemia	42	Kidney and pancreas transplantation, immunosuppression, diarrhea associated with <i>Clostridium difficile</i>	<i>S. boulardii</i> , 1 g/day	PFGE	[25]

Notes. CVC – central venous catheter, rRNA – ribosome RNA, PFGE – pulsed field gel electrophoresis, LGG – *Lactobacillus rhamnosus* GG, CFU – colony-forming unit.

*Ref. [16].

**If the dosage is not listed in the table, the exact dosage was not provided in the original paper.

***A kit for identifying *Lactobacillus* spp., BioMerieux.

****250 mg of *S. boulardii* = 5.425 × 10¹³ living cells.

of each bacterial species is grown on selective media up to at least 10³–10⁹ cells/ml. The resulting bio-masses are joined and supplemented with a stabilizing solution. The mixture is divided into samples. Each sample is preserved during the entire lifetime of the subject with the biotiter being occasionally inspected.

In infants less than 1 year old, the normal intestinal microflora predominantly consists of bifidobacteria *Bifidobacterium bifidum*, *B. brevis*, *B. infantis* and lactobacilli *Lactobacillus acidophilus*, *L. fermenti*. The normal intestinal microflora of individuals older than 1 year predominantly consists of bifidobacteria

B. longum, *B. adolescentis*, lactobacilli *L. acidophilus*, *L. fermenti*, *L. plantarum*, strains of *Escherichia coli* and lactic streptococci *Streptococcus faecium*, *Str. faecalis*, *Str. avium*, *Str. salivarius* and *Str. bovis*. During the storage, equal amounts of autostrains samples isolated during different stages of a person's life are further combined after biotiters are inspected. The introduction of a sample from the bank of autostrain microorganisms into the intestine makes it possible to simultaneously affect different components of the disrupted intestine biocenosis due to the use of the entire range of normal intestinal microflora [33].

The method for obtaining an autoprobiotic culture based on enterococci was described in patent "Method for obtaining autoprobiotic based on *Enterococcus faecium*, a representative of the indigenous microflora of a host intestine" [34]. The novelty of the proposed method for preparing lactic culture lies in the fact that the product is prepared from one's own (autoprobiotic) *E. faecium* strain isolated from his gastrointestinal tract. This method proposed for the first time to use the polymerase chain reaction (PCR) after the selection of colonies with a characteristic morphology and directly before preparing the product in order to determine the enterococcus species and genetic determinants of pathogenicity. This approach guarantees absolute safety of the end product for the subject. The method is also characterized by fast production of a mature culture (4–6 days following the day the material is collected). Isolation of indigenous enterococci from feces to produce autoprobiotic lactic acid cultures requires implementation of the following algorithm: to plate bacteria from the individual's feces on a selective medium, to identify the genus to which the strain belongs, to run PCR to determine the enterococcus species and potential pathogenicity factors, to select clones that satisfy genetic safety and physiological functionality criteria, to store individual enterococcus strains in a cryobank, and finally to produce the lactic culture [34].

In 2006, Van Likui comprehensively studied the treatment of bacterial vaginosis with autochthonous microorganisms [35]. The use of a commercial lactobacterin preparation in the form of a vaginal suppository improved the content of the vaginal microflora; however, it did not result in full recovery of lactic microflora due to the low survival rate of lactobacilli from the intestine in the vagina. It was proposed to use autochthonous lactobacilli isolated from female patients' vaginas to correct microbiocenosis impairment. Suppositories containing lactobacilli autostrains were topically applied after a course of antibacterial therapy, which ensured successful implantation of probiotics and significantly reduced the risk of recurrent

bacterial vaginosis. A similar method was successfully employed to restore the disrupted microbiocenosis of vaginas in pregnant women after treating pyelonephritis with antibiotics [36].

It was demonstrated [37] that the commercial bacterial preparation Acylact is quickly eliminated from the vaginal environment. A 12-month-long randomized double-blind trial of commercial and autologous lactobacilli was carried out. A total of 165 women with bacterial vaginosis were involved in the study. One hundred and thirty-two patients underwent control examination: 70 patients from the group that received autochthonous lactobacilli (group I) and 62 patients from the group that received the Acylact preparation (group II). The therapeutic efficiency was measured using the criteria of clinical response, recovery of vaginal microbiocenosis and disappearance of the objective symptoms accompanying the disease. Prevention efficiency was measured by the number of relapses over the entire follow-up period. The dynamics of vaginal biocenosis recovery to its normal state was significantly different between the two treatment methods. When using autochthonous lactobacilli, biocenosis in most women (82.2%) recovered its normal state as early as after 3 months, while the maximum values (88.7%) were observed after 6 months; at the end of the study, the improvement was only 1.5%. When using Acylact preparations, the recovery to the normal state after 3 months was observed only in 61.7% of patients; after 6 months, in 71.4% of patients; and after 12 months, in 78% of patients. The rate and percentage of recovery in group II were significantly different from the values observed for group I ($p \leq 0.05$). The results of these studies show that lactobacilli exhibit genetic heterogeneity, which defines its specificity towards the host [37].

CONCLUSIONS

The use of indigenous strains of protective microorganisms to correct dysbiosis has been studied by several authors [31–43]. The application of autostrains to prevent and treat dysbacteriosis in people holding extreme jobs (astronauts, pilots, divers, athletes, rescue workers) is particularly relevant. The lack of infectious complications, biological incompatibility and low acceptability make it possible to suggest that these preparations can be used to treat newborns, elderly people, and patients with a suppressed immune system. The concept of creating cryobanks of human microbiocenosis and autoprobiotics can be considered at the moment as a separate branch of personalized medicine. A customized approach to drug selection allows one to improve the efficiency of both prevention and treatment, as well as to reduce the risk of adverse drug reactions in each patient. ●

REFERENCES

1. Grigoriev A.I., Gazenko O.G. // Herald of the Russian Academy of Sciences. 1980. № 2. P. 71–75.
2. Van der Waaij D. // Nahrung. 1987. V. 31. № 5–6. P. 507–17.
3. Bondarenko V.M., Jalko-Titarenko V.P. // Journal of Microbiology Epidemiology and Immunobiology. 1991. №8. P. 23–27.
4. Noble W.C. // Curr. Probl. Dermatol. 1989. V. 18. P. 37–41.
5. Berg, R.D. // Jikken Dobutsu. 1985. V. 34. № 1. P. 1–16.
6. Borisov L.B. Medical Microbiology, Virology, Immunology. M: MIA, 2002, 736 p.
7. Ilyin V.K., Volozhin A. I., Viha G.V. Colonization resistance of the organism in the changed conditions of life. M.: Nauka, 2005, 280 p.
8. Berdichevsky B.A. Autobacteria, stress and human (anthology of one of the observations). M: Medical Book, 2001. 207 p.
9. Grigoriev A.I., Tonevickii A.G. // Molecular Medicine. 2008. № 3. P. 29–40.
10. Lizko N.N. // Abstracts of the 6th all-Russian Congress of microbiologists, epidemiologists and parasitologists in Niznii Novgorod. 1991. V. 2. P. 107.
11. Grigoriev A.I. // I.M. Sechenov Physiological Journal. 2007. V. 93. № 5. P. 473–484.
12. Lizko N.N. // Annals of the Russian Academy of Medical Sciences. 1996. №8. P. 31–34.
13. Lizko N.N. // Antibiotics and Medical Biotechnology. 1987. V. 32. № 3. P. 184–186.
14. Glushanova N.A., Shenderov B.A. // Journal of Microbiology, Epidemiology and Immunology. 2005. № 2. P. 56–61.
15. Boirivant M., Strober W. // Curr. Opin. Gastroenterol. 2007. V. 23. № 6. P. 679–92.
16. Boyle R.J., Robins-R. Browne, and Tang M.L.K. // Am. J. Clin. Nutr. 2006. V. 83. № 6. P. 1256–1264.
17. Rautio M., Jousimies-Somer H., Kauma H., Pietarinen I., Saxelin M., Tynkkynen S., Koskela M. // Clin. Infect. Dis. 1999. V. 28. № 5. P. 1159–1160.
18. Mackay A.D., Taylor M.B., Kibbler C.C., Hamilton-Miller J.M. // Clin. Microbiol. Infec. 1999. V. 5. № 5. P. 290–292.
19. DeGroot M.A., Frank D.N., Dowell E., Glode M.P., Pace N.R. // Pediatr. Infect. Dis. J. 2005. V. 24. № 3. P. 278–280.
20. Land M.H., Rouster-Stevens K., Woods C.R., Cannon M.L., Cnota J., Shetty A.K. // Pediatrics. 2005. V. 115. №1. P. 178–181.
21. Richard V., Van der Auwera P., Snoeck R., Daneau D., Meunier F. // Eur. J. Clin. Microbiol. Infect. Dis. 1988. V. 7. № 6. P. 783–785.
22. Oggioni M.R., Pozzi G., Valensin P.E., Galieni P., Bigazzi C. // J. Clin. Microbiol. 1998. V. 36. № 1. P. 325–326.
23. Perapoch J., Planes A.M., Querol A., Lopez V., Martínez-Bendayan I., Tormo R., Fernandez F., Peguero G., Salcedo S. // Eur. J. Clin. Microbiol. Infect. Dis. 2000. V. 19. № 6. P. 468–470.
24. Bassetti S., Frei R., Zimmerli W. // Am. J. Med. 1998. V. 105. № 1. P. 71–72.
25. Riquelme A.J., Calvo M.A., Guzman A.M., Depix M.S., Garcia P., Perez C., Arrese M., Labarca J.A. // J. Clin. Gastroenterol. 2003. V. 36. № 1. P. 41–43.
26. Orishak E.A., Boitsov A.G., Nilova L.Yu. // Patent № 2428468. RF. C12N1/20, A61K35/74. 2010.
27. Shenderov B. A. // Russian Journal of Gastroenterology, Hepatology, Coloproctology. 1998. V. 8. № 1. P. 61–65.
28. Kirjavainen P. V., Ouwehand A. C., Isolauri E., Salminen S. J. // FEMS Microbiol. Lett. 1998. V. 167. № 2. P. 185–189.
29. Boris S., Suraz J.E., Vazquez F., Barbes, C. // Infect. Immun. 1998. V. 66. № 5. P. 1985–1989.
30. Boitsov A.G., Rischuk S.V., Ilyasov Yu.Yu., Grechaninova T.A. // Bulletin of St. I.I. Mechnikov Petersburg Medical Academy. 2004. V.4. № 5. P. 191–193.
31. Shenderov V.A., Manvelova M.A. // Patent № 2139070. RF. A61K35/00. 1999.
32. Shenderov B.A. // Journal of Rehabilitation Medicine. 2003. №1. C. 29–31.
33. Khachatryan A.P., Khachatryan P.G. // Patent № 2126043. RF. C12N1/00. 1999.
34. Suvorov A.N., Simanenkov V.I., Sundukova Z.R., Ermolenko E.I., Tsapieva A.N., Donets V.N., Soloviev V.I. // Patent № 2460778. RF. C12N1/20. 2012.
35. Van Likui // Use of probiotics and lactobacilli autostrains in the complex treatment of bacterial vaginosis. M.: RN-RMU, 2006.
36. Wisotskyh T.S., Bekkieva M.H., Tikina A.P. // Proceedings of IX all-Russian scientific forum «Mother and child». 2007. P. 43.
37. Melnikov V.A., Stulova S.V., Tyumina O.V., Denisova N. G., Schukin V. Yu. // Fundamental research. 2012. № 1. P. 64–67.
38. Korshunov V.M., Smejanov V.V., Efimov B.A. // Annals of the Russian Academy of Medical Sciences. 1996. № 2. C. 60–65.
39. Simanenkov V.I., Suvorov A.N., Donets V.N., Ermolenko E.I., Sundukova Z.R. // Proceedings of all-Russian conference of gastroenterologists of South-Western region, Rostov - Na -Donu. 2009. P. 83–87.
40. Sundukova Z.R., Donets V.I. // Actual problems of clinical and experimental medicine: abstracts of the scientific-practical conference of young scientists. St. Petersburg, 2009. P. 62.
41. Ilyin V.K., Suvorov A.N., Kiryukhina N.V., Usanova N.A., Starkova L.V., Bojarintsev V.V., Karaseva A.B. // Annals of the Russian Academy of Medical Sciences. 2013. № 2. P. 56–62.
42. Kiryukhina N.V. Use of probiotics in order to correct upper respiratory tract microflora. M.: MSPCO, 2009.
43. Ilyin V.K., Kiryukhina N.V., Usanova N.A., Tiurina D.A. // Proceedings of the 3rd International Probiotic Conference. Slovakia. 2008. P. 17.

Biotechnological approaches to creation of hypoxia and anoxia tolerant plants

B. B. Vartapetian^{1*}, Y. I. Dolgikh¹, L. I. Polyakova¹, N. V. Chichkova², A. B. Vartapetian²

¹ Timiryazev Institute of Plant Physiology, Russian Academy of Sciences, Botanicheskaya Str., 35, Moscow, Russia, 127276

² A.N.Belozersky Institute of Physico-Chemical Biology Moscow State University

*E-mail: borisvartapet@ippras.ru

Received: 06.08.2013

Revised manuscript received 19.03.2014

Copyright © 2014 Park-media, Ltd. This is an open access article distributed under the Creative Commons Attribution License, which permits unrestricted use, distribution, and reproduction in any medium, provided the original work is properly cited.

ABSTRACT The present work provides results of a number of biotechnological studies aimed at creating cell lines and entire plants resistant to anaerobic stress. Developed biotechnological approaches were based on earlier fundamental researches into anaerobic stress in plants, so “Introduction” briefly covers the importance of the problem and focuses on works considering two main strategies of plants adaptation to anaerobic stress. Those are adaptation at molecular level where key factor is anaerobic metabolism of energy (true tolerance) and adaptation of the entire plant via formation of aerenchyma and facilitated transportation of oxygen (apparent tolerance). Thus, sugarcane and wheat cells resistant to anaerobic stress were obtained through consecutive *in vitro* selection under conditions of anoxia and absence of exogenous carbohydrates. Tolerant wheat cells were used to regenerate entire plants of higher resistance to root anaerobiosis. It has been demonstrated that cells tolerance to anoxia is significantly supported by their ability to utilize exogenous nitrate. Cells tolerance established itself at the genetic level and was inherited by further generations. Apart from that, other successful attempts to increase tolerance of plants to anaerobic stress by means of stimulation of glycolysis and overexpression of genes responsible for cytokinin synthesis and programmed cell death are also discussed. The presented data proved the notion of two main strategies of plants adaptation to anaerobic stress proposed earlier on the base of fundamental studies.

KEYWORDS anaerobic stress, growth index, *in vitro* cell selection, programmed cell death, transgenic plants, mitochondrial ultrastructure.

ABBREVIATIONS PDC – pyruvate decarboxylase; ADH – alcohol dehydrogenase; ISPA- International Society for Plant Anaerobiosis.

INTRODUCTION

As plants are obligate aerobes, oxygen deficiency (hypoxia) and especially its total absence (anoxia) cause dramatic ecological stress. Meanwhile plants often suffer from sudden molecular oxygen deprivation both under natural condition and as a result of human activity. Most often plants are subject to oxygen deprivation on hydromorphic and flooded soils for the oxygen's poor solubility and low diffusion rate in the water [1, 2]. Nowadays, there are vast areas of hydromorphic soils in many countries [3–5]. It is believed that melting of permafrost and polar ice, together with ensuing rise of the world ocean level, may lead to a flooding of numerous regions of the planet. Oxygen scarcity is also observed in firm soils [6]. In this respect, roots and seeds of plants are the most vulnerable. In northern countries and countries with a moderate climate winter cereals and perennials can be damaged by ice crust, impermeable to gas, that appears on the surface of soil in au-

tumn and winter [7]. Anaerobic stress may damage and even lead to a total failure of crop and wildings thus causing considerable ecologic and economic losses.

Problem of hypoxia and anoxia is also important in regard to long-term storage of agricultural commodities like fruits, grain, vegetables [8].

In last decades anaerobic stress in plants has become a topical subject of study not only among physiologists and biochemists, but molecular biologists and geneticists as well. Number of publications and ISPA conferences devoted to study of hypoxia and anoxia in plants is constantly rising. Anaerobic stress has been discussed in numerous special issues of international journals (see *Annals of Botany* (special section). 1994. V. 74. No 3. Ed. Jackson M.B.; *Annals of Botany* (special Issue). 1997. V. 79. Ed. Jackson M.B.; *Annals of Botany* (special section). 2002. V. 90. No 4. Ed. Smirnov N.; *Annals of Botany* (special Issue). 2003. V. 91. Eds Visser E., Voesenek L.A.C.J., Jackson M.B.; *Russian J. of Plant Physiology* (Special

Issue). 2003. T. 50. No. 6. Ed. by Vartapetyan B. B. ; Annals of Botany (special Issue). 2005. V. 96. Ed. Jackson M.B.; Annals of Botany (special Issue). 2009. Eds Jackson M.B., Ishizawa K., Ito O.; New Phytologist (special Issue). 2011. V. 190. № 2. Eds Perata P., Armstrong W., Voesenek L.A.C.J.) Along with that a number of monographs [9–14] issued by ISPA members have had a significant impact on further development of this scientific trend.

Commonly admitted notion of two main strategies of plants adaptation to anaerobic stress has been actively elaborated. The first one is molecular adaptation which takes place at the absence or lack of oxygen through fundamental rearrangement of the entire cell metabolism. The second is adaptation of the plant as an entire body due to transportation of oxygen from aerial parts to parts localized in anoxic environment (roots), that is escape strategy to avoid anaerobiosis. It becomes more and more clear that cell energy metabolism is a key factor in both metabolic adaptation and plant damage under anaerobic stress.

High sensitivity of plants to the lack of oxygen, especially its total absence, can be explained by the fact that higher plants, being obligate aerobes, demand constantly available molecular oxygen in the environment to maintain itself.

However, many species, mainly wildings, in the course of evolution acquired the ability to inhabit temporarily or constantly hydromorphic and even flooded anaerobic soils [15, 16]. The only exception among cultivated plants is rice – *Oryza sativa* L. – that is known to be grown mostly on flooded soils [17–19]. Nevertheless, it is often that even rice plants suffer from anaerobic stress when sprouts get entirely submerged as it happens in monsoon season in East and South-East Asia [20].

The fact that numerous plants in the course of natural evolution or due to man-made selection acquired an ability to inhabit temporarily or constantly flooded anaerobic soils makes it important and viable to carry out both fundamental studies having their aim in finding out molecular mechanisms of plants adaptation and applied ones in particular biotechnological approaches (gene and cell engineering) to creation of plants tolerant to anaerobic stress. However, researches in this field were mostly fundamental and they prepared serious base for more active studies of applied problems of anaerobiosis, in particular development of biotechnological methods of creation plants tolerant to hypoxia and anoxia, which was the main objective of this review.

The present review discusses biotechnological approaches elaborated on the base of earlier fundamental studies in this field, in particular on the notion of two strategies of plants adaptation to anaerobic stress

[15–17, 21, 22]. One of these approaches was devised from results of studies that demonstrated key role of anaerobic metabolism (glycolysis and fermentation) and carbohydrates metabolism in adaptation of plants to anaerobic stress [21–24]. This knowledge allowed to create cell lines of *Saccharum officinarum* L. [22, 25] and *Triticum aestivum* L. [26, 27] via *in vitro* selection in the absence of exogenous carbohydrates, that were more resistant to anoxia than original callus cells. More resistant cells of *T. aestivum* L. were further used to regenerate entire plants that occurred to be more tolerant to the soil anaerobiosis as their cultivation in ample water conditions proved.

Experimental results on *in vitro* selection of plant cells showing protective function of exogenous nitrate as potential alternative acceptor of electrons in severe conditions of anoxia have been also reviewed [28].

Taking into account the role of energy metabolism in adaptation of plants to anaerobic stress the possibility of increasing plants resistance via super expression of PDC and ADH genes were considered [29–32].

Another biotechnological approach, also successfully applied to obtain plants resistant to hydromorphic soils [33], was absolutely different from already mentioned. In this case another widely-known fact was used, namely the reaction of majority plants sensitive to hypoxia and anoxia to anaerobic stress: flooding at an early stages lead to withering and aging of aboveground organs and only after that to death. On the other hand, it is well known that aging of plants is subject to hormonal regulation. Thus, cytokinines make substantially rejuvenate aging aerial organs [34, 35]. Considering these circumstances, there was an attempt to enhance capability of plants to synthesize cytokinin and thus to boost their resistance to anaerobic stress by means of transformation of the plant with *ipt* gene responsible for the synthesis of this hormone [26, 33].

Possibility to increase plants resistance to anaerobic stress was also studied in transgenic tobacco *N. tabacum* Samsun NN characterized by high activity of recently discovered enzyme phytaspase [36–38] mediating programmed cell death. An interest to transgenic tobacco derives from earlier studies [15, 17, 22] that demonstrated not the molecular metabolic adaptation but crucially different pattern of plant adaptation to anaerobic environment expressing itself in formation of aerenchyma and avoidance of anaerobiosis due to long-distance transportation of oxygen that is the adaptation on the level of the entire plant body.

IN VITRO SELECTION OF SACCHARUM OFFICINARUM CELLS TOLERANT TO ANAEROBIC STRESS

As it has already been mentioned the basis for this biotechnological approach was experimental results

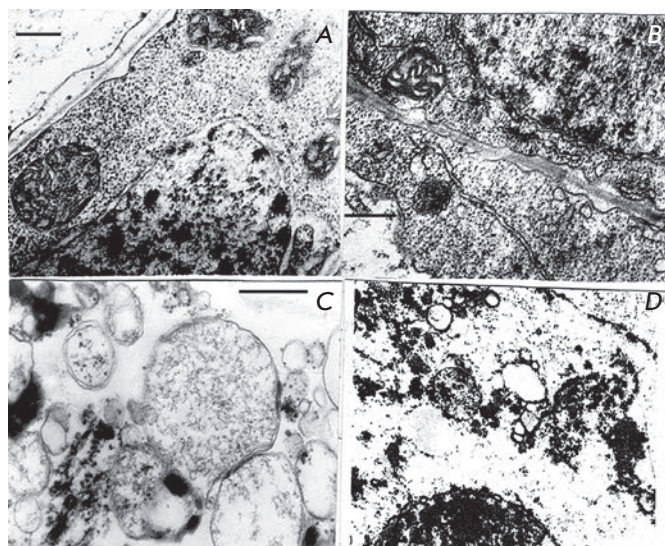


Fig. 1. Ultrastructure of *Saccharum officinarum* L callus cells sensitive to anaerobic stress. Under anoxia and in the absence of exogenous glucose. a – control; b – 24 h anaerobic incubation; c – 48 h anaerobic incubation; d – 72 h anaerobic incubation. M – mitochondria Bars = 0.5µm

proving the key role of anaerobic metabolism in resistance of various organs of plants to hypoxia and anoxia [15–17, 21–24]. Key role of anaerobic metabolism in resistance to anoxia and hypoxia is also confirmed by presented electron micrographs of ultrastructure of mitochondria from sugarcane callus cells that was transferred from aerobic medium to anaerobic in the absence and the presence of exogenous glucose (Fig. 1 and 2). The strength of cells resistance to anaerobic stress was assessed through electron-microscopic study of ultrastructure of mitochondria that are highly sensitive to the lack of oxygen. Oxygen deprived mitochondria membranes demonstrate certain change pattern of ultrastructure.

In the absence of exogenous carbohydrates in the medium, ultrastructure of mitochondria and other organelles of cells, kept for 24 hours under anoxia (Fig. 1B), did not significantly differ from aerobic control (Fig. 1A). At the longer anaerobiosis (48 hours) more distinct features of destruction in mitochondria and other organelles were detected (Fig. 1C). Anoxia of 72 hour length caused total degradation of mitochondria and other cell organelles (Fig. 1D).

On the contrary, addition of glucose in concentration of 3% to a medium demonstrated no destructive changes of mitochondria and organelles even at anaerobiosis of 96 hours (Fig. 2B).

Alongside the electron microscopy observations the ability of callus to restore its growth after anaerobic

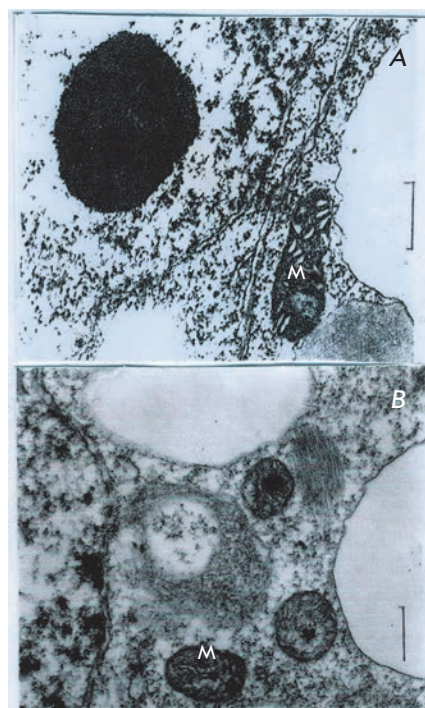


Fig. 2. Ultrastructure of *Saccharum officinarum* L of callus cells sensitive to anaerobic stress. Under condition of anoxia and in the presence of 3% glucose. a – control; b – 96 h anaerobic incubation. M – mitochondria Bars = 0.5µm

period in conditions close to normal aeration was also assessed. To do this, we defined callus growth index (the difference between the final and the initial masses divided by the initial) following one month of cultivating in normal conditions.

Results of these experiments indicated the decrease of post-anaerobic growth index for cells in the absence of exogenous carbohydrates as the duration of anaerobiosis increases; at 96-hour anaerobiosis this index tends to zero (Table 1).

Cells demonstrated substantially better resistance to anoxia at administration of exogenous glucose (Table 2).

Since the experiments with cells of sugarcane callus confirmed the key role of anaerobic energy metabolism in formation of cells resistance to anoxia, further selection of tolerant callus cells [25–28] and anaerobic exposure were carried out in the absence of exogenous carbohydrates (glucose) in the medium. Only in those conditions when cells resistance was defined by parameters of anaerobic energy metabolism of endogenous carbohydrates one could hope to obtain cells genuinely tolerant to anoxia.

From the results of trial experiments a consecutive *in vitro* selection of anoxia-tolerant cells in carbohydrate-free medium was derived. After 48-hour incubation 13% of cells remained capable of growing further in aerobic conditions. Calluses were incubated without oxygen for 48 hours and kept under normal aeration.

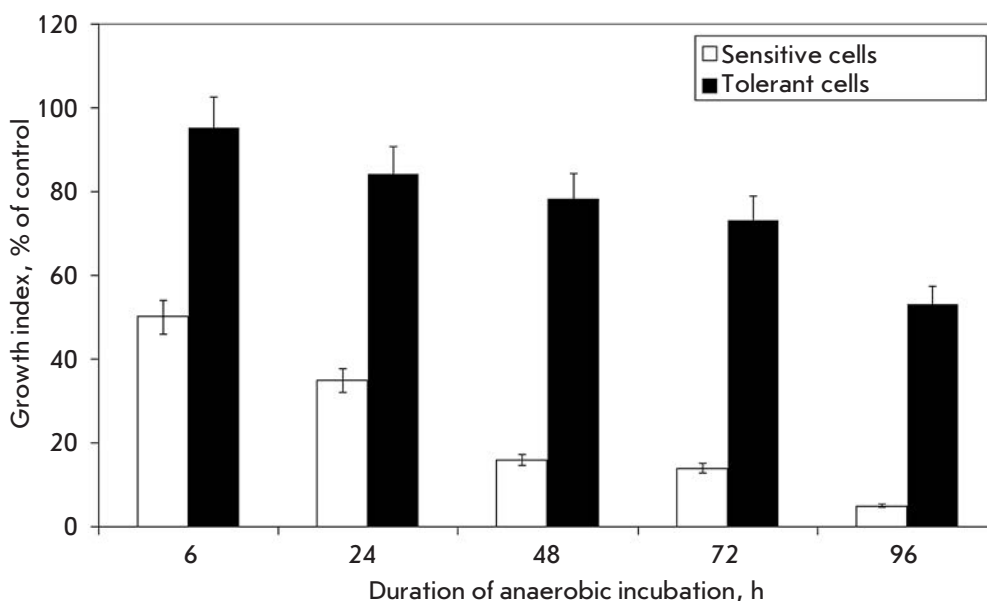
Table 1. Growth index of *Saccharinum officinarum* L exposed to varying in length anaerobic incubation on glucose-free medium after cultivation under normal aeration conditions for 1 month

Anaerobic incubation, h	Growth index	% of control
0	4.63 ± 0.50	100
6	2.35 ± 0.25	50.7 ± 5.4
24	1.47 ± 0.15	31.7 ± 3.2
48	0.60 ± 0.09	13.0 ± 2.0
72	0.55 ± 0.10	11.8 ± 2.2
96	0.16 ± 0.01	3.5 ± 0.32

Table 2. Growth index of *Saccharinum officinarum* L exposed to anaerobic incubation anaerobic incubation on medium containing 3% glucose after cultivation under normal aeration conditions for 1 month

Anaerobic incubation, days	Growth index	% of control
0	5.7 ± 0.51	100
3	3.0 ± 0.29	52.0 ± 5.0
5	2.9 ± 0.31	50.8 ± 5.4
7	2.5 ± 0.27	43.8 ± 4.7
9	1.5 ± 0.14	26.3 ± 2.4
14	0.2 ± 0.06	3.3 ± 1.1

Fig. 3. Growth index of *Saccharum officinarum* L sensitive and tolerant cells, that were, after anaerobic incubation, cultivated during one month under condition of normal aeration. White column – callus cells before *in vitro* selection. Shaded column – callus cells after *in vitro* selection



Clones, formed under anaerobic incubation (48 hours), were then exposed to anoxia for 72 hours. From cells that survived the second stage of selection and underwent subsequent anaerobiosis for 96 hours aerobically growing clones were picked. Thus after three stages of selection we obtained a cell line of sugarcane that grew in post-anaerobic period under conditions of normal aeration more actively than original callus. Even after exposure to anoxia for 96 hours half of such cells remained capable of dividing, whereas the original callus showed such capability only after 6-hour anaerobiosis (Fig. 3).

IN VITRO SELECTION OF ANOXIA-TOLERANT WHEAT CELLS AND REGENERATION OF ENTIRE PLANTS RESISTANT TO FLOODING OF ROOTS

Similar experiments on selection of tolerant cells in the absence of exogenous carbohydrates were carried out with *T. aestivum* L. callus in order to regenerate the entire plant, resistant to flooding of roots [27]. In the course of selection cells exposed to anoxia were gradually losing the ability either to grow further in aerobic conditions or to regenerate into new plants, so we selected cells under conditions of 32 hour anaerobiosis. In this case cell growth index comprised 45%, whereas the

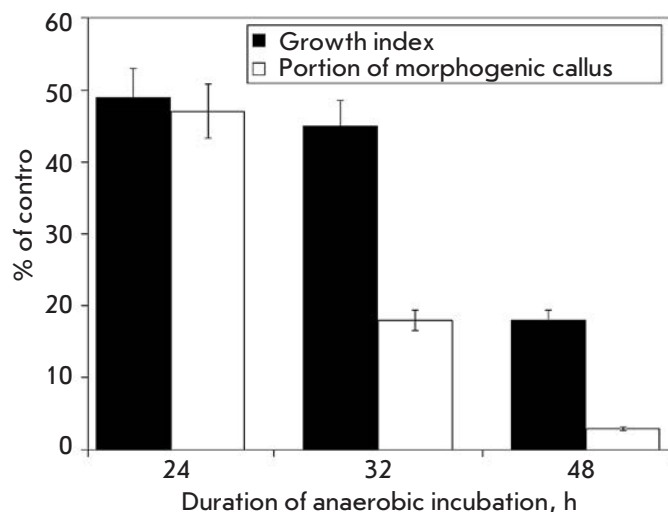


Fig. 4. Growth index and percent of morphogenic calli of *Triticum aestivum* L. after anaerobic incubation in the absence of exogenous glucose. Control – under aerobic condition



Fig. 5. Wheat plants after 8-days flooding. Control (A) and tolerant (B) plants

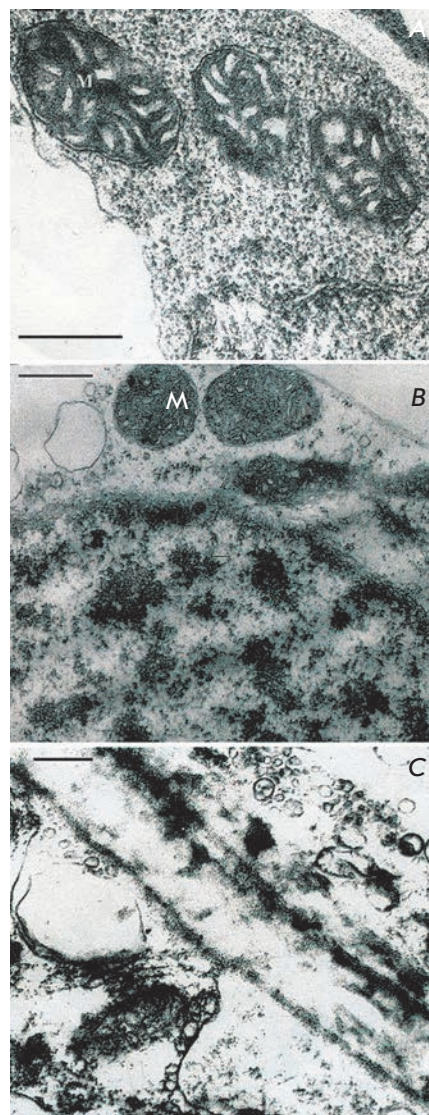


Fig. 6. Ultrastructure of *Saccharum officinarum* L. sensitive callus cells under conditions of anoxia and in the absence of exogenous nitrate. a – control; b – 6 h anaerobic incubation in the absence of exogenous nitrate; c - 24 h anaerobic incubation in the absence of nitrate. M – mitochondria Bars = 0.5μm

Table 3. Survival of *Triticum aestivum* L plants R₁ and R₂ under conditions of root anaerobiosis at different temperature regimens

Experimental conditions	Plants	Total number of plants	Survived plants	
			N	Rate, %
8 day flooding, 32°C	Control	20	0	0
	R ₁	22	7	32
10 day flooding, 22°C	Control	32	18	56
	R ₁	36	36	100
8 day flooding, 32°C	Control	24	11	46
	R ₂	32	32	100

Fig.7. Ultrastructure of *Saccharum officinarum* L. t sensitive callus cells under conditions of anoxia and in the presence of exogenous nitrate. a – control; b – 6 h anaerobic incubation; c – 24 h anaerobic incubation. M – mitochondria Bars = 0.5µm

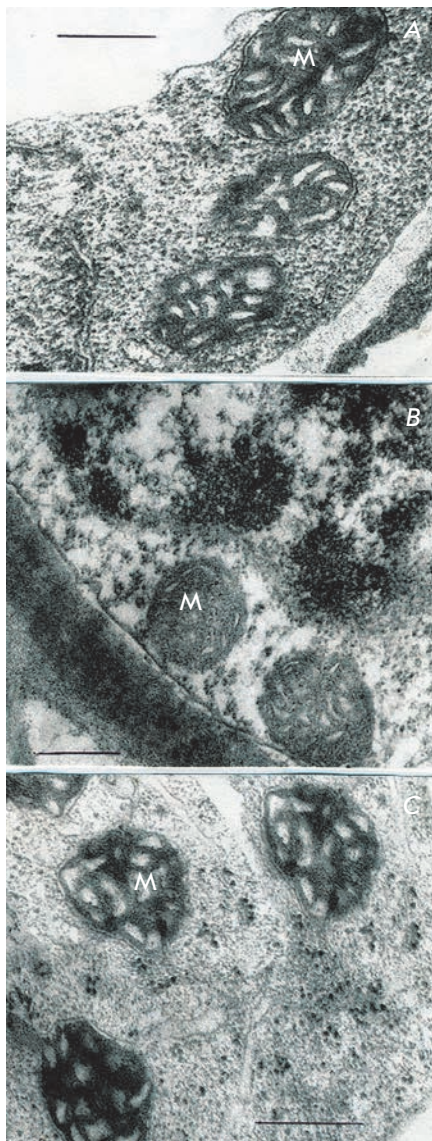
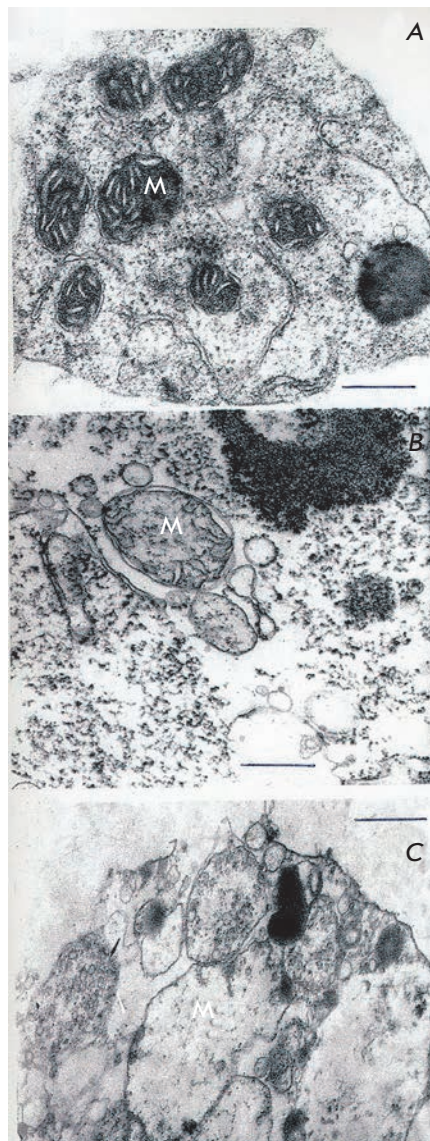


Fig.8. Ultrastructure of *Saccharum officinarum* L. tolerant callus cells under conditions of anoxia and in the absence of exogenous nitrate a – control; b – 24 h anaerobic incubation; c – 48 h anaerobic incubation M – mitochondria Bars = 0.5µm



capability of regenerating a whole plants from tolerant cells – 18% (Fig. 4).

Plants obtained from tolerant cells after selection under anoxia were tested together with controls for flooding of roots during 16 days at the temperature of 26°C. Among controls only 30% of plants survived, whereas among regenerants – about 73%.

In order to find out the genetic aspects of tolerance to soil anaerobiosis we sowed seeds acquired from regenerated tolerant plants of the first generation and then assessed tolerance of new plants to root anaerobiosis. R₁ plants obtained as a result of self-pollination of regenerant plants were examined for root flooding in soil experiment at the average temperature of 32 and 22°C (Table 3). At all used temperatures survival rate

among descendants of regenerated plants was higher than that among controls.

In the soil experiment R₂ plants remained tolerant to the root flooding (Table 3, Fig. 5). Thus it was confirmed that regenerant plants inherit increased tolerance to flooding.

PROTECTIVE ROLE OF NITRATE IN ANOXIA TOLERANCE OF *S. OFFICINARUM* CELLS OBTAINED THROUGH *IN VITRO* SELECTION

Further experiments on anoxia tolerant cells of *S. officinarum*, isolated in the course of selection, and callus cells as control were an attempt to find out possible role of exogenous nitrate (NO₃⁻) as protective factor at anaerobic incubation of cells [28]. Previous studies car-

ried out on whole plants and separate organs showed mobilization and utilization of exogenous nitrate to play significant role in plants tolerance at the absence of molecular oxygen [39–44].

Electron microscopic examination of cells of original sugarcane callus (control) showed their high sensitivity to anoxia in the absence of nitrate in the medium (Fig. 6). Although 6-hour anaerobic incubation did not cause any serious damage to mitochondria membranes, following 24-hours of anaerobiosis we observed not only damaged membranes, but entirely degraded both mitochondria and other cell structures (Fig. 6C).

In the presence of exogenous nitrate callus cells of the control intolerant line were demonstrated to have increased anoxia tolerance. Even at the 24-hour anaerobiosis were detected no obvious signs of membrane degradation in mitochondria and other organelles (Fig. 7C). Substantial destruction of mitochondria membranes close to degradation was observed at longer anaerobiosis (48 hours).

Cells of tolerant line obtained through *in vitro* selection even in the absence of nitrate in the medium were significantly more resistant to anoxia than original cells (Fig. 8). Anaerobic incubation of cells during 24 hours did not cause destruction of membranes (Fig. 8B). Only after 48 hours of anaerobiosis evident signs of mitochondrial destruction were recorded (Fig. 8C) and only

after 72 hours when the cells ultrastructure completely degenerated.

The most serious distinctions between callus lines were revealed at the anaerobic incubation of tolerant cells isolated through *in vitro* selection in the presence of nitrates in the medium. Mitochondria ultrastructure of such cells remained intact even after 48–72 hours of anaerobiosis (Fig. 9B, C, D) except for small non-pathological morphologic changes. However, these changes in ultrastructure and morphology were not destructive even after 72 hour exposure (Fig. 9D).

Along with the monitoring of the cells ultrastructure under conditions of anaerobiosis in the presence and in the absence of nitrate we also monitored growth of cells from the sensitive and the resistant lines of callus in post anaerobic period. In the mentioned period growth of the sensitive cells in the nitrate-free medium was considerably suppressed. Supplement of nitrate did not make callus of the sensitive line to grow much better. For instance, following 48-hour of anoxia accretion comprised only 10% of the control level for nitrate-free medium and 16% for the full medium. Adding nitrate to the medium significantly favors growth of tolerant cells. Thus, after 48 hours of anaerobiosis callus mass grew 18% bigger in the nitrate-containing media than in the nitrate-free medium (Fig. 10). In the presence of nitrates tolerant cells remained able to grow even after 72 hours of anoxia, whereas in the nitrate-free medium such growth was not detected.

As far as calluses of the sensitive line are concerned, their exposure to anoxia stipulated considerable decrease of the growth index and compared to resistant line protective role of nitrate was expressed significantly weaker.

Thus, the gained results clearly indicate that under conditions of anoxia, exogenous nitrate serves a protective factor both in control cells and in cells obtained via *in vitro* selection in the absence of molecular oxygen. However, in cells acquired through *in vitro* selection protective function of exogenous nitrate was considerably stronger than that in original (control) cells.

Recent publications confirming positive influence of nitrate on plants exposed to hypoxia and anoxia showed similar results in the absence of nitrate, but in the presence of trace amount of nitrite in the medium [45–47]. These results let us assume that protective action of nitrate in the absence of oxygen is stipulated by electron-acceptor function of not nitrate, but, more likely, that of nitrite or by signal function of NO_2^- that is formed from nitrate under anaerobiosis. On the other hand, as it was demonstrated in Hill laboratory [47] under conditions of hypoxia, as a result of NO_2^- reduction, mitochondria synthesize ATP, likely one of the most important protective factors of both nitrite and nitrate,

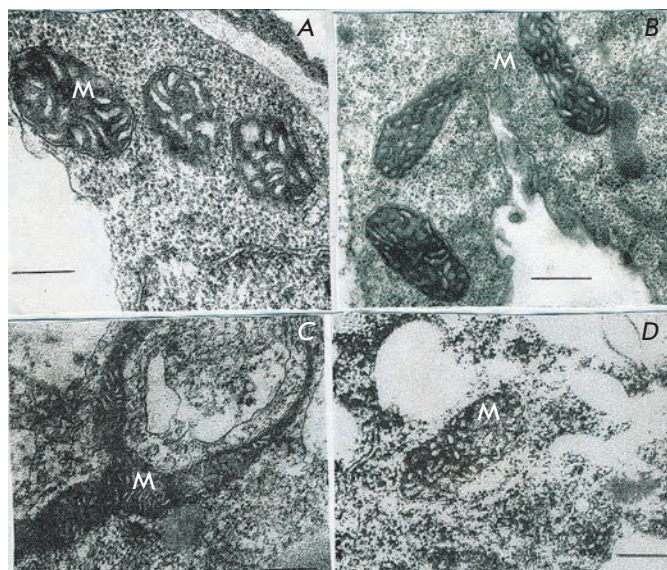


Fig. 9. Ultrastructure of *Saccharum officinarum* L. tolerant callus cells under conditions of anoxia and in the presence of exogenous nitrate. a – 24 h anaerobic incubation; b, c – 48 h anaerobic incubation; d – 72 h anaerobic incubation. M – mitochondria Bars = 0.5 μm

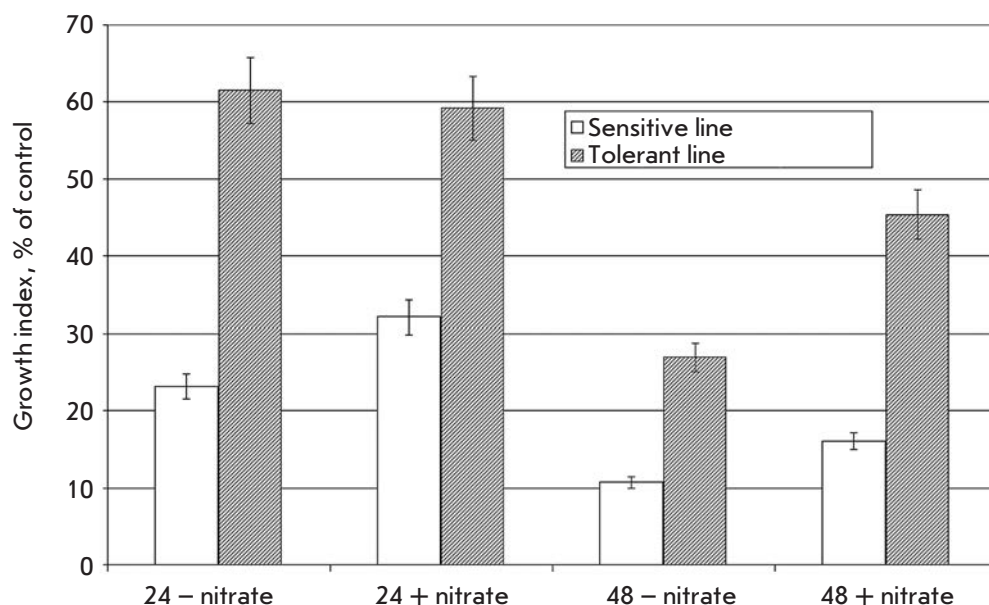


Fig. 10. Growth index of *Saccharum officinarum* L. tolerant and sensitive cells after anaerobic incubation. The figures indicate the duration (h) of anaerobic incubation of callus cells in the presence and in the absence of nitrate Control – aerobic condition

the latter being a source of nitrite under conditions of hypoxia and anoxia.

One should pay attention to the following trait of tolerant cells obtained through consecutive *in vitro* selection under anoxia stress: in the presence of nitrate anoxia tolerance of selected cells is significantly higher than that of original cells used for selection [28]. This observation entitles us to assume that anoxia tolerance of *S. officinarum* cells substantially rose in the course of selection defined by glycolytic reactions along with processes of nitrate and, probably, nitrite utilization, under such harsh conditions.

It appears viable to devote further attempts to finding out physiological function of nitrite formed from nitrate as potential alternative electron acceptor or signal factor in the course of anaerobic incubation of callus cells.

ATTEMPTS TO BOOST THE RESISTANCE OF TRANSGENIC PLANTS TO ANAEROBIC STRESS BY MEANS OF STIMULATING THE ACTIVITY OF GLYCOLYTIC ENZYMES (PDC AND ADH)

On the assumption that anaerobic energy metabolism is a key factor in metabolic acclimation of plants to anaerobic stress [15, 21, 22, 48–53], there were numerous attempts to raise plants tolerance to hypoxia and anoxia by enhancing alcoholic fermentation with overexpression of genes of glycolytic enzymes in transgenic plants [29–32]. The results of the first experiments were somewhat controversial [29–31]. Experiments on the activity of alcoholic fermentation enzymes (PDC and ADH) in transgenic *Arabidopsis*

[32] appeared especially interesting. Compared to tobacco roots [30], transgenic *Arabidopsis* with introduced PDC construct exhibited not only higher speed of alcoholic fermentation, but also greater resistance to hypoxia than control plants [32]. Unlike PDC transgenic *Arabidopsis*, plants with ADH transgene and, respectively, higher ADH activity, did not demonstrate the increase in tolerance, although mutation in *adh1* gene substantially enhanced accumulation of acetaldehyde and dramatically reduced the resistance to the hypoxic stress. High sensitivity and vulnerability of ADH mutant of *Arabidopsis* under hypoxia stress could be stipulated by accumulation of acetaldehyde, amount of which sharply rose in ADH deprived cells, and, consequently, by possibility of reduction of acetaldehyde to ethanol and thus protection of cells of its toxic effect. Along with that one cannot totally neglect the accumulation of pyruvic acid in these conditions that may to some extent lead to LDH-mediated accumulation of lactate in toxic concentrations. By administration of 3% sucrose authors demonstrated that the increase of resistance requires plants to be provided with substrate. This conclusion correlates the results of our earlier experiments [21] and works of other authors [48–57]. On the base of mentioned studies [32] it was concluded that PDC activity closely associated with the intensity of carbon flow in alcoholic fermentation and defines tolerance to hypoxia stress, i.e. PDC directly regulate alcoholic fermentation. Thus, results of *Arabidopsis* experiments [32] also confirm the idea that energy metabolism is a key factor to the true resistance of plant cells to anaerobic stress.

Table 4. Change of linear dimensions and yield of *ipt*-transgenic and control wheat plants exposed to 14 day root flooding (in relation to unflooded plants)

Parameters, % of control	Control plants	Transgenic plants
Average plant height increment over 14 days of root flooding	37	51
Portion of heads with seeds	33	89
Average seed weight	26	46
Yield	2	36

ROOT FLOODING RESISTANCE OF TRANSGENIC PLANTS EXPRESSING THE AGROBACTERIUM *ipt* GENE

Alongside finding means to increase the tolerance of wheat to anaerobic stress by *in vitro* cell selection in the absence of exogenous sugars and oxygen there was an attempt to obtain wheat plants more tolerant to root flooding by introducing isopentenyltransferase gene (*ipt*), coding key enzyme of cytokinin biosynthesis pathway [26]. The interest to stimulation of cytokinin synthesis under anaerobic stress was dictated by the fact that cytokinin significantly contributes to preventing plants aging [34, 35]. It is commonly known that above-ground organs of oxygen-deprived plants on flooded soils are characterized by signs of premature aging like chlorosis, leaf fall and lesions [58, 59]. That is why there were attempts to slow down aging of transgenic *Arabidopsis* and wheat by stimulating cytokinin synthesis and thus to improve tolerance to anaerobic stress [26, 33, 60]. Level of isopenteniladenin recorded in transgenic wheat obtained in our experiments in conditions of flooding of roots was 30 times higher than that in untransformed plants. The impact of hormonal balance under anaerobic stress in transgenic and control plants was observed during the entire ontogenesis [26, 33].

In wheat experiments tolerant criteria were growth of the above-ground mass of transgenic and control plants and grain harvest under conditions when the root zone of plants had been flooded for 14 days (Table 4). As it can be seen from the presented data, growth of the above-ground organs in control plants was considerably slower than that in transgenic plants with introduced *ipt* gene. Difference between the crop yield in experimental and control plants was even more

striking. Yield was defined as the weight of crop (in grams) harvested from 1 m² of soil (g/m²).

Alongside the mentioned we also monitored the activity of antioxidant enzymes (superoxide dismutase and catalase) and accumulation of malondialdehyde in control plants and in plants with introduced *Agrobacterium ipt* gene. By the end of the flooding period the amount of malondialdehyde found in transgenic plants was 32% lower than that in controls. On the contrary, activity of superoxide dismutase and catalase in transgenic wheat remained high during the entire hypoxic period, whereas in controls it was falling from the sixth day of the root flooding. These data is evidence that transgenic plants under hypoxia suffered less stress than controls.

Similar to results of *Arabidopsis* experiments [60], provided data indicate the positive effect of stimulation of cytokinin synthesis under anaerobic stress.

ON THE POSSIBLE ROLE OF APOPTOTIC PROTEASE (PHYTASPASE) IN THE INCREASE OF TOBACCO PLANTS TOLERANCE TO ANAEROBIC STRESS

Programmed cell death play a critical role both in development of plants and their reaction to stress including defense against pathogenic agents [61–67]. As it has been mentioned earlier, one of the main strategies

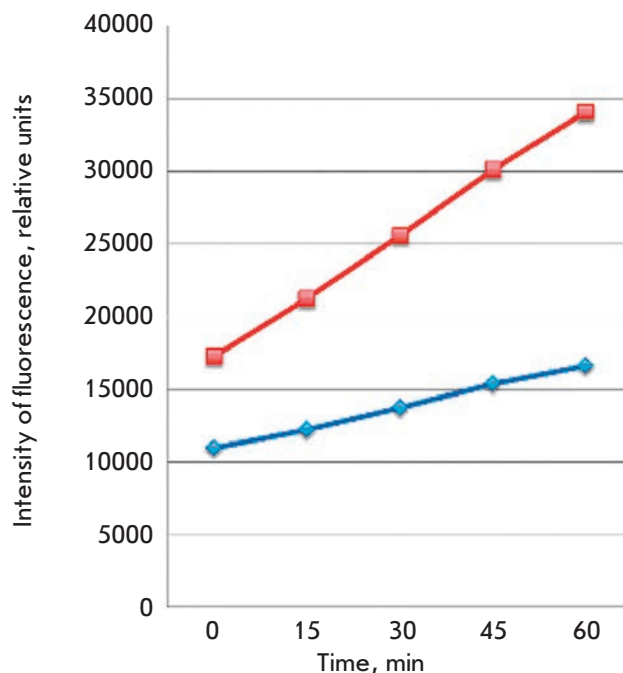


Fig. 11. The rate of hydrolysis of phytaspase fluorescent substrate (Ac-VEID – AFG) in tobacco leaves extracts. Transgenic (red) and wild (blue) plant tips

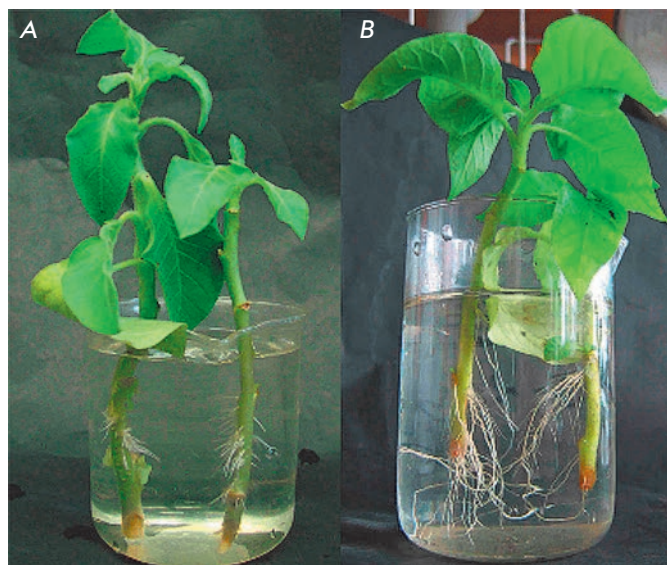


Fig. 12. Rhizogenesis of tobacco cuttings after 17 days of experiment starting. Wild (A) and transgenic (B) plants

of plants adaptation to hypoxia and anoxia is to avoid anaerobiosis by formation of spaces in roots (aerenchyma) as a result of apoptosis of a certain part of cells. Aerenchyma substantially alleviates long-distance transportation of oxygen from above-ground organs of plant to roots and rootstocks resting in anaerobic environment. Thus, it allows plants to survive even on the flooded soils.

However, aerenchyma forms mainly in wild species inhabiting flooded anaerobic soils. As cultivated plants do not possess such advanced ability to form aerenchyma, anaerobiosis often damages and kills them. Hence, of particular interest is recently discovered apoptotic protease phytaspase [36, 68–70], involved into programmed cell death in plants, the very same process during which aerenchyma forms. That is why in present work we tried to find out with the help of plants transformed with phytaspase gene whether it is possible to use this enzyme for formation of aerenchyma and thus to increase tolerance to hypoxia and anoxia in those cultivated species that do not possess such ability or possess a weakly developed one.

In order to do this we used transformed plants of *Nicotianum tabacum* expressing phytaspase gene and wild tobacco plants as control to compare their phenotypical and anatomical traits. Phytaspase activity in transgenic plants was 3 times higher than that in wild plants (Fig. 11).

Results of trial experiments performed while transgenic and control plants were developing evidenced

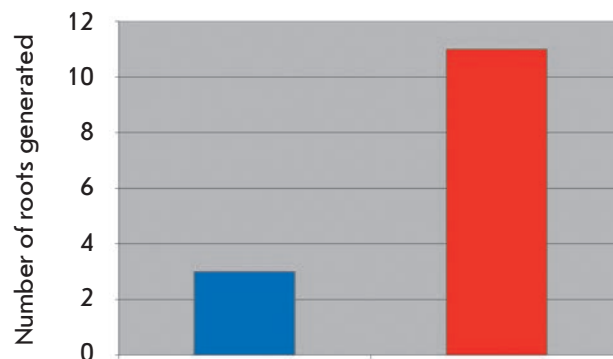


Fig. 13. Rhizogenesis of tobacco cuttings after 17 days of experiment starting. Wild (blue) and transgenic (red) plants

Table 5. Intercellular space area in the roots of transgenic and control plants under normal aeration and under root anaerobiosis

Experimental conditions	Intercellular space area / Total area of root core parenchyma	
	Control plants (wild type)	Transgenic plants
Normal aeration	3.53 ± 0.28	2.92 ± 0.68
Root anaerobiosis, 48h*	4.07 ± 1.1	11.45 ± 2.35

* The roots were flooded 5 cm above the soil surface

considerable differences even in conditions of normal aeration of the root zone and especially during rhizogenesis when shoots were put in water for 17 days (Fig. 12, 13). In transgenic plants the mentioned process went considerably active. The same concerned seed sprouting, growth of leaves and stems of young tobacco plants. All mentioned processes were twice active in transgenic plants.

Another question of our special interest was comparative analysis of anatomy of roots of transgenic and control plants as the enhanced activity of phytaspase, responsible for the programmed cell death was expected to contribute to formation of aerenchyma in roots of transgenic plants and to increase tolerance to the root anaerobiosis.

However, quantitative evaluation of intercellular spaces in the cross sections of roots of both transgenic plants and controls under normal aeration did not reveal significant differences.

As far as soil flooding is concerned, when roots suffer from anaerobic stress, intercellular spaces in transgenic plants were proved to be greater than those in controls by results of trial experiments (Table 5).

Consequently, results of trial experiments that require more thorough consideration and confirmation indicate that increased activity of phytaspase, involved into the programmed cell death, is favorable for formation of intercellular spaces (aerenchyma) in roots of transgenic plants under hypoxia.

CONCLUSION

The present review is devoted to results of a number of experimental works in the course of which authors elaborated biotechnological approaches, including genetic engineering and methods of cell selection *in vitro*, to create plants tolerant to anaerobic stress. These ap-

proaches are based on earlier fundamental studies, in particular a notion on two main strategies of plants adaptation to hypoxia and anoxia: molecular acclimation where anaerobic energy metabolism of cells play major role (true tolerance) and adaptation of the whole plant by formation of aerenchyma and facilitated long-distance transportation of oxygen (apparent tolerance).

The notable contribution that was made into the creation of cells and plants tolerant to anaerobic stress in the considered works lets one hope that these results will serve a foundation of the new avenue of research in biotechnology and help the development of applied studies along with classical approaches to selection and hybridization.

It also should be mentioned that results of considered studies confirmed the idea of two main strategies of plants acclimation to hypoxia and anoxia and on key role of anaerobic energy metabolism in metabolic adaptation of plants to anaerobic stress that were previously suggested on basing on fundamental study of plants life under conditions of anaerobiosis. ●

REFERENCES

- Jackson M.B., Ishizawa K., Ito O. // *Ann. Bot.* 2009.V. 103. P. 137–142.
- Visser E.J.W., Voesebec L.A.C.J., Vartapetian B.B., Jackson M.B. // *Ann. Bot.* 2003. V. 91. P. 107–109.
- Maltby E. // *Plant life under oxygen deprivation: ecology, physiology and biochemistry* / Eds Jackson M.B., Davies D.D., Lambers H. The Hague: SPB Academic, 1991. P. 3–21.
- Setter T.L., Waters I., Sharma S.K., Sing K.N., Kulshreshtha N., Yaduvanshi N.P.S., Ram P.C., Singh B.N., Rane J., McDonald G., et al. // *Ann. Bot.* 2009. V. 103. P. 221–235.
- Perata P., Armstrong W., Voesebec L.A.C.J. // *New Phytol.* 2011. V. 190. № 2. P. 269–273.
- Smucker A.L.M., Allmaras R.R. // *Internat. Crop Sci. I.* / Eds Buxton D.R., Shibles R., Forsberg R.A., Blad B.L., Asay K.H., Paulsen G.M., Wilson R.F. Madison, Wisconsin: Crop Sci. Soc. America, 1993. P. 727–731.
- Andrews C.J.A. // *Ann. Bot.* 1997. V. 79. Suppl. A. P. 87–92.
- Knee M. // *Plant life under oxygen deprivation: ecology, physiology and biochemistry.* / Eds Jackson M.B., Davies D.D., Lambers H. The Hague: SPB Academic, 1991. P. 229–243.
- Plant life in anaerobic environments* / Eds Hook D.D., Crawford R.M.M. Ann Arbor, Michigan: Ann Arbor Science, 1st and 2nd eds 1978, 1980.
- Plant life in aquatic and amphibious habitats* / Ed. Crawford R.M.M. Oxford: Blackwell, 1987.
- The ecology and management of wetlands* / Eds Hook D.D., McKee W.H., Smith Jr. H.K., Gregory J., Burrell V.G., DeVoe Jr. M.R., Solka R.E., Gilbert S., Banks R., Stolzy L.H., Brooks C., Matthews T.D., Shear T.H. London: Croom Helm, 1988.
- Plant life under oxygen deprivation* / Eds Jackson M.B., Davies D.D., Lambers H. The Hague: SPB Academic, 1991.
- Interacting stresses on plants in a changing climate.* NATO ASI Ser. / Eds Jackson M.B., Black C.R. Berlin: Springer-Verlag, 1993.
- Oxygen and environmental stress in plants* / Eds Crawford R.M.M., Hendry G.A.F., Goodman B.A. Edinburgh: Proc. Royal Soc. Edinburgh Ser. B. 1994. V. 102.
- Vartapetian B.B. // *Plant life in anaerobic environments* / Eds Hook D.D., Crawford R.M.M. Ann Arbor, Michigan: Ann Arbor Science, 1980. P. 1–12.
- Vartapetian B.B., Andreeva I.N., Kursanov A.L. // *Nature (London)*. 1974. V. 248. № 445. P. 258–259. (See also Erratum V. 250. № 461. P. 84).
- Vartapetian B.B., Sachs M.M., Fagerstedt K. // *Plant Stress*. 2008. V. 2. № 1. P. 1–19.
- Magneschi L., Perata P. // *Ann. Bot.* 2009. V. 103. P. 181–196.
- Steffens B., Gesrt T., Sauter M. // *New Phyt.* 2011. V. 190. № 2. P. 369–378.
- Jackson M.B., Ram P.C. // *Ann. Bot.* 2003. V. 91. Spec. Issue. P. 227–241.
- Vartapetian B.B., Andreeva I.N., Kozlova G.I., Agapova L.P. // *Protoplasma*. 1977. V. 93. P. 243–256.
- Vartapetian B.B., Andreeva I.N., Generozova I.P., Polyakova L.I., Maslova I.P., Dolgikh Y.I., Stepanova A.Y. // *Ann. Bot.* 2003. V. 91. P. 155–172.
- Zhang Q., Greenway H. // *J. Exp. Bot.* 1994. V. 45. P. 567–575.
- Perata P., Guglielminetti L., Alpi A. // *Ann. Bot.* 1997. V. 79. P. 49–56.
- Stepanova A.Yu., Polyakova L.I., Dolgikh Yu.I., Vartapetian B.B. // *Russ. J. Plant Physiol.* 2002. V. 49. P. 406–412.
- Tereshonok D., Stepanova A., Dolgikh Yu.I., Osipova E., Belyaev D., Vartapetian B. B. // *Plant Stress*. 2010. V. 4. № 1. P. 79–82.
- Stepanova A.Yu., Dolgikh Yu.I., Vartapetian B.B. // *Biotechnology (Russ.)*. 2010. N 3. P. 1–6.
- Vartapetian B. B., Polyakova L.I., Stepanova A.Yu., Dolgikh Yu.I. // *Russ. J. Plant Physiol.* 2012. V. 59. P. 741–747.
- Bucher M., Brändle R., Kuhlemeier C. // *EMBO J.* 1994. V. 13. P. 2755–2763.

30. Tadege M., Brändle R., Kuhlemeier C. // *Plant J.* 1998. V. 14. P. 327–335.
31. Quimio C.A., Torrizo L.B., Setter T.L., Ellis M., Grover A., Abrigo E.M., Oliva N.P., Ella E.S., Carpena A.L., Ito O., et al. // *Plant Phys.* 2000. V. 156. P. 516–521.
32. Ismond K.P., Dolferus R., Pauw M.D., Dennis E.S., Good A.G. // *J. Plant Phys.* 2003. V. 132. P. 1292–1302.
33. Tereshonok D.V., Stepanova A.Yu., Dolgikh Yu.I., Osipova E.S., Belyaev D.V., Kudoyarova G.R., Vysotskaya L.B., Vartapetian B.B. // *Russ. J. Plant Physiol.* 2011. V. 58. P. 799–807.
34. Romanov G.A. // *Russ. J. Plant Physiol.* 2009. V. 56. P. 268–290.
35. Lomin S.N., Krivosheev D.M., Steklov M.Yu., Osolodkin D.I., Romanov G.A. // *Acta Naturae.* 2012. V. 4. № 3(14). P. 31–45.
36. Chichkova N.V., Kim S.H., Titova E.S., Kalkum M., Morozov V.S., Rubtsov Y.P., Kalinina N.O., Taliansky M.E., Vartapetian A.B. // *Plant Cell.* 2004. V. 16. P. 157–171.
37. Chichkova N.V., Shaw J., Galiullina R.A., Drury G.E., Tuzhikov A.I., Kim S.H., Kalkum M., Hong T.B., Gorshkova E.N., Torrance L., Vartapetian A.B., Taliansky M. // *EMBO J.* 2010. V. 29. № 6. P. 1149–1161.
38. Vartapetian A.B., Tuzhikov A.I., Chichkova N.V., Taliansky M., Wolpert T.J. // *Cell Death Differ.* 2011. V. 18. P. 1289–1297.
39. Reggiani R., Brambilla I., Bertani A. // *J. Exp. Bot.* 1985. V. 36. P. 1193–1199.
40. Botrel A., Magne C., Kaiser W. // *Plant Phys. Biochem.* 1996. V. 34. P. 645–652.
41. Fan T.W.M., Higashi R.M., Frenkiel T., Lane A.N. // *J. Exp. Bot.* 1997. V. 48. P. 1655–1666.
42. Botrel A., Kaiser W. // *Planta.* 1997. V. 201. P. 496–501.
43. Oberson I., Pavelic D., Braendle R., Rawlyer A. // *Plant Phys.* 1999. V. 155. P. 792–794.
44. Vartapetian B.B., Polyakova L.I. // *Mitochondria: Structure, Functions and Dysfunctions* / Ed. Svensson O.L. USA: Nova Publ., 2010. P. 955–966.
45. Igamberdiev A.U., Hill R.D. // *J. Exp. Bot.* 2004. V. 55. P. 2473–2482.
46. Igamberdiev A.U., Hill R.D. // *Ann. Bot.* 2009. V. 103. P. 259–268.
47. Stoimenova M., Igamberdiev A.I., Gupta K.J., Hill R.D. // *Planta.* 2007. V. 226. P. 465–474.
48. Xia J.-H., Saglio P. // *Plant Phys.* 1990. V. 93. P. 453–459.
49. Waters I., Kuiper P.J.C., Watkin E., Greenway H. // *J. Exp. Bot.* 1991a. V. 42. P. 1427–1435.
50. Waters I., Morell S., Greenway H., Colmer T.D. // *J. Exp. Bot.* 1991b. V. 42. P. 1437–1447.
51. Hole D.J., Cobb B.G., Hole P., Drew M.C. // *J. Plant Phys.* 1992. V. 99. P. 213–218.
52. Xia J.-H., Saglio P.H., Roberts J.K.M. // *J. Plant Phys.* 1995. V. 108. P. 589–595.
53. Ricard B., van Toai T., Chourey P., Saglio P.H. // *J. Plant Phys.* 1998. V. 116. P. 1323–1331.
54. Sato T., Harada T., Ischizawa K. // *J. Exp. Bot.* 2002. V. 53. P. 1847–1856.
55. Loreti E., Alpi A., Perata P. // *Plant Phys.* 2003. V. 50. P. 737–742.
56. Voeselek L.A.C.J., Benschop J.J., Bou J., Cox M.C.H., Groeneveld H.W., Millenaar F.F., Vreburg R.A.M., Peeters A.J.M. // *Ann. Bot.* 2003. V. 91. P. 205–211.
57. Magneschi L., Perata P. // *Ann. Bot.* 2009. V. 103. P. 181–196.
58. Trought M.C.T., Drew M.C. // *Plant Soil.* 1980. V. 54. P. 77–94.
59. Singh S., Letham D.S., Palni L.M.S. // *Phys. Plant.* 1992. V. 86. P. 388–397.
60. Zhang J., van Toai T., Huynh L., Preiszner J. // *Mol. Breed.* 2000. V. 6. P. 135–144.
61. Hoerberichts F.A., Woltering E.J. // *BioEssays.* 2003. V. 25. № 1. P. 47–57.
62. Williams B., Dickman M. // *Mol. Plant Pathol.* 2008. V. 9. № 4. P. 531–544.
63. Reape T.J., McCabe P.F. // *New Phytol.* 2008. V. 180. № 1. P. 13–26.
64. Reape T.J., McCabe P.F. // *Apoptosis.* 2010. V. 15. № 3. P. 249–256.
65. Zhang J., Teng C., Liang Y. // *Protein Cell.* 2011. V. 2. № 10. P. 837–844.
66. Van Doorn W.G., Beers E.P., Daugl J.L., Franklin-Tong V.E., Gallois P., Hara-Nishimura I., Jones A.M., Kawai-Yamada M., Lam E., Mundy J., et al. // *Cell Death Differ.* 2011. V. 18. № 8. P. 1241–1246.
67. Fomicheva A.S., Tuzhikov A.I., Beloshistov R.E., Trusova S.V., Galiullina R.A., Mochalova L.V., Chichkova N.V., Vartapetian A.B. // *Biochemistry (Moscow).* 2012. V. 77. № 13. P. 1452–1464.
68. Chichkova N.V., Galiullina R.A., Taliansky M.E., Vartapetian A.B. // *Plant Stress.* 2008. V. 2. P. 89–95.
69. Tuzhikov A.I., Vartapetian B.B., Vartapetian A.B., Chichkova N.V. // *Abiotic stress response in plants physiological, biochemical and genetic perspectives* / Eds Venkateswarla B., Shanker A., Rijeka: Intech-Open Access Publ., 2011. P. 183–195.
70. Chichkova N.V., Tuzhikov A.I., Taliansky M., Vartapetian A.B. // *Phys. Plant.* 2012. V. 145. P. 77–84.

Analysis of the Mitochondrial Genome of a Novosvobodnaya Culture Representative using Next-Generation Sequencing and Its Relation to the Funnel Beaker Culture

A. V. Nedoluzhko^{1*}, E. S. Boulygina¹, A. S. Sokolov¹, S. V. Tsygankova¹, N. M. Gruzdeva¹, A. D. Rezepkin³, E. B. Prokhortchouk^{1,2*}

¹ National Research Center "Kurchatov Institute", Kurchatov sq. 1, 123182, Moscow, Russia

² Center of Bioengineering, Russian Academy of Sciences, 60-letiya Oktyabrya Av., 7-1, 117312, Moscow, Russia

³ Institute for the History of Material Culture, Russian Academy of Sciences, Dvortsovaya Naberezhnaya, 18, 191186, St. Petersburg, Russia

*E-mail: nedoluzhko@gmail.com, prokhortchouk@biengi.ac.ru

Received 25.12.2013

Revised manuscript received 20.03.2014

Copyright © 2014 Park-media, Ltd. This is an open access article distributed under the Creative Commons Attribution License, which permits unrestricted use, distribution, and reproduction in any medium, provided the original work is properly cited.

ABSTRACT The Novosvobodnaya culture is known as a Bronze Age archaeological culture in the North Caucasus region of Southern Russia. It dates back to the middle of the 4th millennium B.C. and seems to have occurred during the time of the Maikop culture. There are now two hypotheses about the emergence of the Novosvobodnaya culture. One hypothesis suggests that the Novosvobodnaya culture was a phase of the Maikop culture, whereas the other one classifies it as an independent event based on the material culture items found in graves. Comparison between Novosvobodnaya pottery and Funnelbeaker (TRB) pottery from Germany has allowed researchers to suggest that the Novosvobodnaya culture developed under the influence of Indo-European culture. Nevertheless, the origin of the Novosvobodnaya culture remains a matter of debate.

WE applied next-generation sequencing to study ~5000-year-old human remains from the Klady kurgan grave in Novosvobodnaya stanitsa (now the Republic of Adygea, Russia). A total of 58,771,105 reads were generated using Illumina GAIIx with a coverage depth of 13.4x over the mitochondrial (mt) DNA genome. The mtDNA haplogroup affiliation was determined as V7, suggesting a role of the TRB culture in the development of the Novosvobodnaya culture and supporting the model of sharing between Novosvobodnaya and early Indo-European cultures.

KEYWORDS Novosvobodnaya culture; Maikop culture; haplogroup, mitochondrial DNA; sequencing; genomics.

ABBREVIATIONS mtDNA – mitochondrial DNA; SNP – single-nucleotide polymorphism.

INTRODUCTION

Since the late 1970s, as archaeological evidence has accumulated, two points of view have emerged pertaining to the emergence of cultural artifacts in the Early Bronze Age in the North Caucasus. One hypothesizes the existence of a single Maikop culture with two developmental phases [1–3], including finds discovered in Novosvobodnaya stanitsa (former Tsarskaya). The other hypothesis suggests that the archaeological collections assembled in Novosvobodnaya stanitsa should be treated individually, as independent artifacts (as a distinct culture). During the archaeological excavations

of the kurgan grave “Klady” near Novosvobodnaya stanitsa in 1979–1991, which were supervised by A.D. Rezepkin, a total of 22 kurgans were uncovered with 93 well-stratified burial sites. These records allow one not only to establish the absolute chronology of the artifacts, but also to contribute to a better understanding of the origin of the Novosvobodnaya culture [4, 5].

Since recently, state-of-the-art tools for genomic analysis have been widely used to solve archaeological [6–10] and paleontological riddles [11–15]. Such studies usually analyze mitochondrial DNA (mtDNA) that possesses characteristics essential for the study

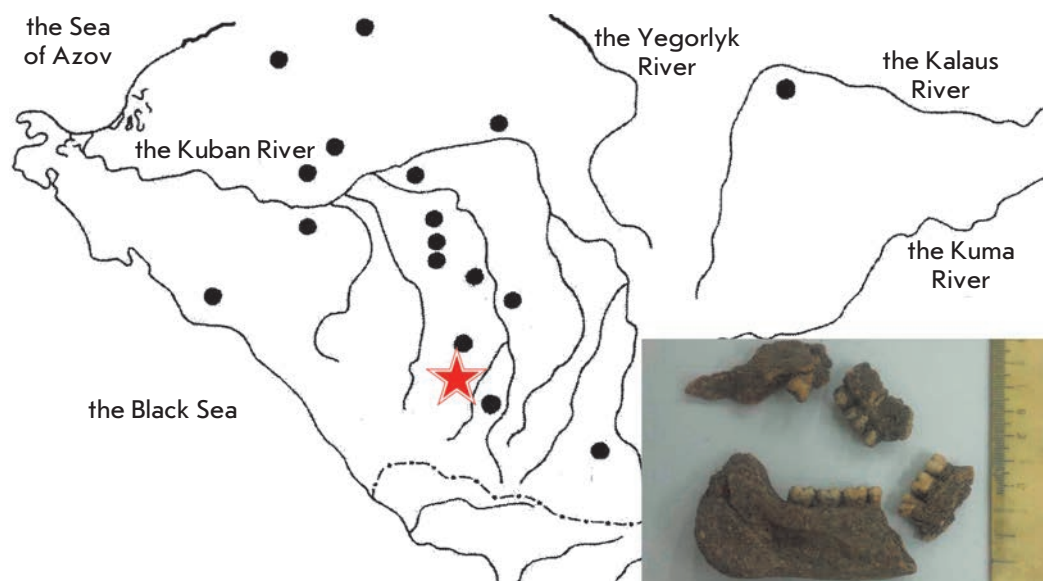


Fig. 1. The range covered by the Novosvobodnaya culture in the North Caucasus (marked with black dots). The site of archaeological excavations of the Klady kurgan near Novosvobodnaya stanitsa in Adygeya (marked with an asterisk) and the bone remains used for the DNA analysis

of human evolution: maternal inheritance; multiple copies of the mitochondrial genome; accelerated accumulation of mutations relative to the nuclear genome; no genetic recombination; a relatively high integrity of mtDNA in ancient human bone remains, since nuclear DNA breaks down twice as fast as mtDNA does [16, 17].

In this work, we report on the complete mitochondrial genome sequence of a representative of the Novosvobodnaya culture. Our findings suggest that this culture should be related to the Funnel Beaker culture. DNA testing has shown that the human sample from the Novosvobodnaya archaeological site belongs to mtDNA haplogroup V7.

EXPERIMENTAL

DNA was extracted from tooth remains discovered during excavations of the kurgan grave “Klady” near Novosvobodnaya stanitsa (The Republic of Adygea) as part of the expedition organized by the Institute for the History of Material Culture, Russian Academy of Sciences (St. Petersburg). The remains date back to approximately Middle to Late 4000 BC (Fig. 1).

DNA extraction, preparation of DNA libraries, and sequencing

Ancient DNA was recovered from bone powder under carefully controlled laboratory conditions to avoid contamination with modern human DNA. Proteinase K (New England Biolabs, USA) and silica beads (Sigma-Aldrich, USA) were used as previously described by Orlando *et al.* [18]. DNA libraries were prepared using a NEBNext Quick DNA Library Prep Master Mix set for 454 (New England Biolabs) with adapter primers on an Illumina Sequencing Platform following the manufac-

turer’s instructions. The purity and amount of DNA libraries were evaluated using a 2100 Bioanalyser (Agilent, USA) and HS Quibit (Invitrogen, USA). For the enrichment of mtDNA, a FleXselect Mitochondrial DNA enrichment kit was utilized (Flexgen, Netherlands) with probes overlapping by 10 to 40% (a detailed list of the oligonucleotide probes for mtDNA enrichment is available upon request). The DNA libraries were sequenced using 50 bp paired-end reads on an Illumina GAIIX instrument.

Bioinformatics analysis

The reads were mapped against the mitochondrial reference sequence (NC_012920.1) using Bowtie2 version 2.1.0 with the *very-sensitive* option [19]. Ancient DNA sequences were authenticated with mapDamage 2.0 [20]. According to the model of post-mortem damage inferred using this software, the quality score was adjusted to allow for nucleotide mismatches. Alternatively, nucleotides that may have arisen from C → T or G → A substitutions were given the lowest quality scores than in the original reads and removed from the analysis of the single nucleotide polymorphisms (SNPs) exhibited by the sample. SNPs were searched for using the VarScan software (v 2.2.3) and selected at $p < 0.01$ [21]. The mtDNA haplogroup affiliation was determined based on the SNPs with the HaploGrep webtool [22]. *De novo* assembly of the mitochondrial genome of a representative of the Novosvobodnaya culture was conducted using AbySS version 1.3.6. at a k-mer of 22 nucleotides [23].

RESULTS AND DISCUSSION

Mitochondrial DNA sequences were retrieved from the libraries of ancient human DNA. A total of 58,771,105

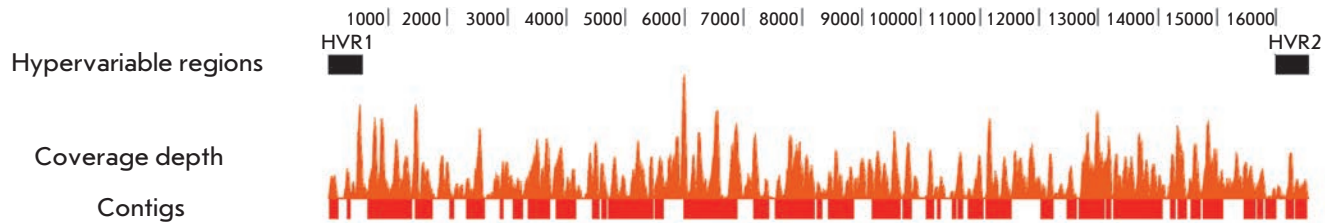


Fig. 2. The results of mitochondrial genome sequencing and *de novo* assembly

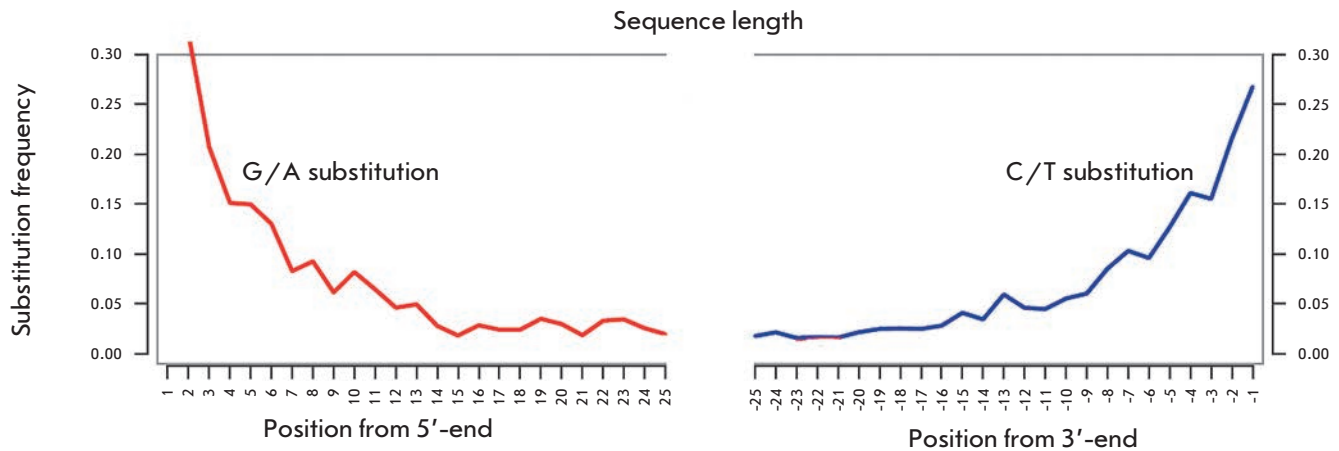


Fig. 3. Nucleotide misincorporation patterns and contamination test

reads were produced from enriched libraries, most part of which (99.994%) consisted of environmental DNA sequences (bacterial), which commonly occurs in an ancient DNA analysis [24], or could be explained by the relatedness between bacterial and eukaryotic mitochondrial genes. Read mapping against the reference mitochondrial genome sequence (hg19) allowed us to achieve a coverage depth of 13.4X: a total of 3,422 reads were uniquely mapped (0.006%) (Fig 2).

Ancient DNA is known to degrade into short fragments over time; cytosine residues (C) located at the ends deaminate to uracil (U) and turn into thymine (T) during sample preparation (PCR). The frequency of terminal C → T substitutions in samples dated older than 300 thousand years could be up to 60% and higher [15, 26]. At the same time, sequencing of modern DNA demonstrates less than 0.5% terminal nucleotide substitutions (data not shown). The substitution frequency was calculated using MapDamage 2.0. The frequency of C → T substitutions at the 3'- and 5'-ends of the DNA libraries exceeded 30% in the sample from Novosvobodnaya stanitsa (Fig. 3). This finding argues for the fact that the total mtDNA is of ancient origin.

When compared with the consensus mitochondrial genome sequence (in light of lowering quality scores for terminal substitutions, see the Experimental section),

individual reads from the sample of an ancient human of Novosvobodnaya stanitsa yielded SNPs, indicating an affiliation within Haplogroup V7 (Fig. 4, Table).

The assembly of the mitochondrial genome of a human from the Novosvobodnaya culture performed with a minimum contig length of 100 nucleotides produced a N50 contig length of 203 nucleotides (N50 is the maximum contig length in *de novo* assembly, such that 50% of the entire assembly is contained in contigs equal to or longer than the N50 length).

The total *de novo* assembly of mtDNA generated 11,063 nucleotides (Fig. 2). Because of ancient DNA degradation, asymmetric PCR amplification and enriched mtDNA (FlexSelect Mitochondrial DNA enrichment kit), most contigs were short and did not overlap, which prevented the assembly of the contigs into a complete mtDNA sequence despite the coverage depth of 13.4X.

Recently, archaeological evidence has emerged to argue against the opinion that the Novosvobodnaya culture shares links with the West Asian Maikop culture. The discovered artifacts support the hypothesis that the Baalberg phase of early periods of the Indo-European Funnel-Beaker culture played a significant role in the Novosvobodnaya archaeological culture, rather than the West Asian Maikop culture [5]. To prove or

Table. SNPs ($p < 0.01$) discovered in the Novosvobodnaya mitochondrial genome

mtDNA SNP position	mt DNA reference sequence (hg19)	A substitution in the sample	Gene
72*	T	C	-
93*	A	G	-
2515	C	T	TVAS5
9378	G	A	JA760602; JA760600
9541	C	T	JA760602; JA760600
11018	C	T	JA760602; JA760600; STRF6; JA760615
11720	A	G	JA760602; JA760600; STRF6; JA760615
11723	C	T	JA760602; JA760600; STRF6; JA760615
12851	G	A	JA760602; JA760600; JA760615
14906	A	G	JA760602; cytochrome b
15302	A	G	JA760602; cytochrome b
15477	C	T	JA760602; cytochrome b

* – SNPs used for haplogroup V7 assignment

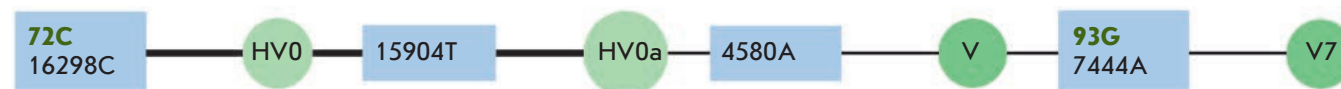


Fig. 4. Mitochondrial haplogroup assignment. The tree branch generated by HaploGrep service is shown. SNPs in green and blue rectangles (72C and 93G) were used for haplogroup determination

rule out this hypothesis, a DNA analysis is required as one of the definitive tools.

Genetic studies devoted to ancient human migrations across Europe have been extensive in the past decades as reviewed by B. Sykes [27]. Thus, in Europe the major mtDNA haplogroups were U, H, V, I, W, T, and K, which appeared and spread 11–14 thousand years ago during de-glaciation. Haplogroup J may have arrived from the Middle East during an influx of farmers [27]. Sequencing of the mtDNA of representatives of the Linear Pottery culture (the ancestor of the Funnel Beaker culture) allowed one to identify the dominant haplogroups as H, V, and T [28]. In addition, some studies have demonstrated that during the time of the Linear Pottery and related cultures, the haplogroups U, H, and V predominantly occurred in Europe [29–32]. Our findings, obtained using current genetic analysis techniques, are in agreement with the hypothesis of the origin of the Novosvobodnaya culture proposed by A.D. Rezepkin [5].

CONCLUSIONS

We have reported on the sequencing of the mtDNA genome of an ancient human of the Novosvobodnaya archaeological culture dated to about 3,500 years before our era. The SNPs revealed during the analysis indi-

cate that the mtDNA belongs to haplogroup V7, which is widely spread in modern Europeans and occurs in cultures that used to exist in Central Europe. The current findings are consistent with the hypothesis that the Novosvobodnaya culture derived from early archaeological cultures of Northern and Central Europe and is now classified as an independent archaeological culture. However, this conclusion requires a thorough genetic analysis of samples from both the Novosvobodnaya and Maikop archaeological cultures. To date, there have been no available data on the status of the mtDNA haplogroup for the Maikop culture and, presumably, the ancestral Late Anatolian Eastern Chalcolithic period of phases III–IV (Amuk F). ●

The authors would like to thank M.V.Koval'chuk (National Research Centre "Kurchatov Institute") for his steadfast support and K.G. Skryabin (Center "Bioengineering", Russian Academy of Sciences) for valuable comments throughout the preparation of the manuscript.

This work was supported by the Russian Fund for Basic Research (grant № 13-06-12025 ofi_m) and a scholarship of the President of the Russian Federation (SP-2056.2012.5).

REFERENCES

1. Yessen A.A. The chronology of “huge Kuban burial mounds”. M.: Soviet Archaeology, 1950. V. 12.
2. Munchaev P.M. The Caucasus in early Bronze Age. M.: Nauka, 1975. 416 p.
3. Munchaev P.M. Maykop culture. Archaeology: Bronze Age of Caucasus and Central Asia. Early and middle Bronze Age of Caucasus. M.: Nauka, 1994. P. 158–225.
4. Rezapkin A.D. Das frühbronzezeitliche Gräberfeld von Klady und die Majkop-Kultur in Nordwestkaukasien. Archäologie in Eurasien. M.: Leidorf, 2000. V. 10. P. 74.
5. Rezapkin A.D. Novosvobodnenskaya culture (on basis of “Klady” excavations). St.-Peterburg, 2012. 343 p.
6. Paabo S. // Nature. 1985. V. 314. № 6012. P. 644–645.
7. Haak W., Balanovsky O., Sanchez J., Koshelev S., Zaporozhchenko V., Adler C., der Sarkissian C., Brandt G., Schwarz C., Nicklisch N., et al. // PLoS Biol. 2010. V. 8. № 11. e1000536.
8. Green R.E., Krause J., Briggs A.W., Maricic T., Stenzel U., Kircher M., Patterson N., Li H., Zhai W., Fritz M.H., et al. // Science. 2010. V. 328. № 5979. P. 710–722.
9. Lorenzen E.D., Nogueira-Bravo D., Orlando L., Weinstock J., Binladen J., Marske K.A., Ugan A., Borregaard M.K., Gilbert M.T., Nielsen R., et al. // Nature. 2011. V. 479. № 7373. P. 359–364.
10. Rasmussen M., Guo X., Wang Y., Lohmueller K.E., Rasmussen S., Albrechtsen A., Skotte L., Lindgreen S., Metspalu M., Jombart T., et al. // Science. 2011. V. 334. № 6052. P. 94–98.
11. Ozawa T., Hayashi S., Mikhelson V.M. // J. Mol. Evol. 1997. V. 44. № 4. P. 406–413.
12. Poinar H., Kuch M., McDonald G., Martin P., Paabo S. // Curr. Biol. 2003. V. 13. № 13. P. 1150–1152.
13. Barnes I., Shapiro B., Lister A., Kuznetsova T., Sher A., Guthrie D., Thomas M.G. // Curr. Biol. 2007. V. 17. № 12. P. 1072–1075.
14. Vilstrup J.T., Seguin-Orlando A., Stiller M., Ginolhac A., Raghavan M., Nielsen S.C., Weinstock J., Froese D., Vasiliev S.K., Ovodov N.D., et al. // PLoS One. 2013. V. 8. № 2. e55950.
15. Orlando L., Ginolhac A., Zhang G., Froese D., Albrechtsen A., Stiller M., Schubert M., Cappellini E., Petersen B., Moltke I., et al. // Nature. 2013. V. 499. № 7456. P. 74–78.
16. Pakendorf B., Stoneking M. // Annu. Rev. Genomics Hum. Genet. 2005. V. 6. P. 165–183.
17. Allentoft M.E., Collins M., Harker D., Haile J., Oskam C.L., Hale M.L., Campos P.F., Samaniego J.A., Gilbert M.T., Willerslev E., et al. // Proc. Biol. Sci. 2012. V. 279. № 1748. P. 4724–4733.
18. Orlando L., Metcalf J.L., Alberdi M.T., Telles-Antunes M., Bonjean D., Otte M., Martin F., Eisenmann V., Mashkour M., Morello F., et al. // Proc. Natl. Acad. Sci. USA. 2009. V. 106. № 51. P. 21754–21759.
19. Langmead B., Salzberg S.L. // Nat. Methods. 2012. V. 9. № 4. P. 357–359.
20. Jonsson H., Ginolhac A., Schubert M., Johnson P.L., Orlando L. // Bioinformatics. 2013. V. 29. № 13. P. 1682–1684.
21. Koboldt D.C., Larson D.E., Chen K., Ding L., Wilson R.K. // Genome Res. 2012. V. 22. № 3. P. 568–576.
22. Kloss-Brandstatter A., Pacher D., Schonherr S., Weissensteiner H., Binna R., Specht G., Kronenberg F., et al. // Hum. Mutat. 2011. V. 32. № 1. P. 25–32.
23. Simpson J.T., Wong K., Jackman S.D., Schein J.E., Jones S.J., Birol I. // Genome Res. 2009. V. 19. № 6. P. 1117–1123.
24. Garcia-Garcera M., Gigli E., Sanchez-Quinto F., Ramirez O., Calafell F., Civit S., Lalueza-Fox C. // PLoS One. 2011. V. 6. № 8. e24161.
25. Hofreiter M., Jaenicke V., Serre D., Haeseler A., Paabo S. // Nucl. Acids Res. 2001. V. 29. № 23. P. 4793–4799.
26. Dabney J., Knapp M., Glocke I., Gansauge M.T., Weihmann A., Nickel B., Valdiosera C., Garcia N., Paabo S., Arsuaga J.L., et al. // Proc. Natl. Acad. Sci. USA. 2013. V. 110. № 39. P. 15758–15763.
27. Sykes B. // Philos. Trans. R. Soc. Lond. B Biol. Sci. 1999. V. 354. № 1379. P. 131–139.
28. Haak W., Forster P., Bramanti B., Matsumura S., Brandt G., Tanzer M., Villems R., Renfrew C., Gronenborn D., Alt K.W., et al. // Science. 2005. V. 310. № 5750. P. 1016–1018.
29. Kittles R. A., Bergen A. W., Urbanek M., Virkkunen M., Linnoila M., Goldman D., Long J.C. // Am. J. Phys. Anthropol. 1999. V. 108. № 4. P. 381–399.
30. Achilli A., Rengo C., Magri C., Battaglia V., Olivieri A., Scozzari R., Cruciani F., Zeviani M., Briem E., Carelli V., et al. // Am. J. Hum. Genet. 2004. V. 75. № 5. P. 910–918.
31. Malmstrom H., Gilbert M.T., Thomas M.G., Brandstrom M., Stora J., Molnar P., Andersen P.K., Bendixen C., Holmlund G., Gotherstrom A., et al. // Curr. Biol. 2009. V. 19. № 20. P. 1758–1762.
32. Skoglund P., Malmstrom H., Raghavan M., Stora J., Hall P., Willerslev E., Gilbert M.T., Gotherstrom A., Jakobsson M. // Science. 2012. V. 336. № 6080. P. 466–469.

Real-Time Interaction between TBP and the TATA Box of the Human Triosephosphate Isomerase Gene Promoter in the Norm and Pathology

O. V. Arkova¹, N. A. Kuznetsov^{2,3}, O. S. Fedorova^{2,3}, N. A. Kolchanov^{1,3}, L. K. Savinkova^{1*}

¹Institute of Cytology and Genetics, Siberian Branch of the Russian Academy of Sciences, Lavrentyev Ave., 10, 630090, Novosibirsk, Russia

²Institute of Chemical Biology and Fundamental Medicine, Siberian Branch of the Russian Academy of Sciences, Lavrentyev Ave., 8, 630090, Novosibirsk, Russia

³Novosibirsk State University, Pirogov Str., 2, 630090, Novosibirsk, Russia

E-mail: savinkl@mail.ru

Received 27.11.2013

Revised manuscript received 21.02.2014

Copyright © 2014 Park-media, Ltd. This is an open access article distributed under the Creative Commons Attribution License, which permits unrestricted use, distribution, and reproduction in any medium, provided the original work is properly cited.

ABSTRACT The TATA-binding protein (TBP) is a key part of the transcription complex of RNA polymerase II. Alone or as a part of the basal transcription factor TFIID, TBP binds the TATA box located in the core region of the TATA-containing promoters of class II genes. Previously, we studied the effects of single nucleotide polymorphisms (SNPs) on TBP/TATA-box interactions using gel retardation assay. It was demonstrated that most SNPs in the TATA boxes of some human gene promoters cause a 2- to 4-fold decrease in TBP/TATA affinity, which is associated with an increased risk of hereditary diseases, such as β thalassemias of diverse severity, hemophilia B Leyden, myocardial infarction, thrombophlebitis, lung cancer, etc. In this work, the process of TBP/TATA complex formation has been studied in real time by a stopped-flow technique using recombinant human TBP and duplexes, which were identical to the TATA box of the wild-type and a SNP-containing triosephosphate isomerase gene promoter and were fluorescently labeled by the Cy3/Cy5 FRET pair. It has been demonstrated for the first time that real-time binding of TBP to the TATA box of the *TPI* gene promoter is complete within 10 s and is described by a single-stage kinetic model. The complex formation of TBP with the wild-type TATA box occurs 5.5 times faster and the complex dissociation occurs 31 times slower compared with the SNP-containing TATA box. Within the first seconds of the interaction, TBP binds to and simultaneously bends the TATA box. Importantly, the TATA box of the wild-type *TPI* gene promoter requires lower TBP concentrations compared to the TATA box containing the -24T \rightarrow G SNP, which is associated with neurological and muscular disorders, cardiomyopathy, and other diseases.

KEYWORDS TATA box; TBP; polymorphism; TBP/TATA-box interaction; stopped flow.

ABBREVIATIONS TBP – TATA-binding protein; TBP/TATA – complex of TBP with an oligonucleotide identical to the TATA box with flanking nucleotides.

INTRODUCTION

The specific nucleotide sequences of a promoter and around it serve as a code that determines when, where, and how efficiently certain genes are transcribed. This code consists of sequences of three types: the core promoter, the proximal promoter region, and distal sequences more remote from the promoter. The core promoter is a region situated at a distance of about 100 nucleotides upstream (in the 5'-region) and downstream (in the 3'-region) of the transcription start site, which comprises such regulatory elements as the TATA box, TFIIB-recognition element (BRE), initia-

tor (Inr), motif ten element (MTE), downstream promoter element (DPE), downstream core element (DCE), X core promoter element 1 (XCPE1), and others; their amounts may vary [1].

The TATA box, located at a distance of ~ 30 bps from the transcription start site, is the best-studied core-promoter element. Interaction between TBP (TATA-binding protein) and the TATA box initiates the assembly of the basal transcription complex of RNA polymerase II and determines the precision of the transcription machine location relative to the start nucleotide [1, 2]. The TATA box nucleotide sequence and the context in

which it occurs determine its affinity for TBP, a subunit of the basal transcription factor, TFIID, which affects the promoter activity [3, 4].

Comparison of the TBP amino acid sequences of human, mouse, fruit flies, yeast, and other organisms has demonstrated that TBP is composed of the highly conserved C-terminal domain of 180 amino acid residues and a variable N-terminal domain [5]. The identity of the TBP C-terminal domain in different species is over 80% [5]. The X-ray analysis, footprinting analysis, and analysis of the location of the C-terminal domain tryptic peptides [6] revealed that TBP is composed of two subdomains, H2 and H2', which form a continuous, slightly bent, antiparallel β -sheet, forming a concave DNA binding saddle, and of four α -helices that lie on the upper side of the molecule. The C-terminal domain of the TATA binding protein contacts the double-stranded DNA along the minor groove primarily through nonpolar and hydrophobic interactions and causes its local unwinding and helix bending. This creates a unique conformation that is crucial for the pre-initiation complex assembly and efficient transcription both *in vitro* and *in vivo* [7]. Various regulatory proteins interact with the top, convex side of TBP [8].

Single nucleotide polymorphisms (SNPs) in TATA boxes and the surrounding nucleotides, which affect their affinity for TBP, can contribute to a variety of complex human diseases, such as hypertension, arthritis, cancer, cardiovascular and immune diseases. They can also cause monogenic diseases, such as β -thalassemias of varying severity, Coppock-like cataract, etc. [9].

The triosephosphate isomerase (*TPI*) gene is expressed in all cell types. It belongs to the housekeeping genes [10]. Multiple forms of *TPI* have been found in human tissues, which are encoded by a single gene and are formed as a result of posttranslational modifications [10]. *TPI* catalyzes the conversion of dihydroxyacetone phosphate to *D*-glyceraldehyde-3-phosphate, which completes the first step of glycolysis. A lack of the enzyme results in the accumulation of dihydroxyacetone phosphate and fructose diphosphate in the cell.

The -24T \rightarrow G SNP in the TATA-box of the *TPI* gene promoter, reported in [11], leads to the synthesis of an insufficient amount of mRNA (hereinafter, under SNP is understood the G allele of the TATA box). The enzyme activity in erythrocytes of the allele carriers decreases and amounts to 3–10% of that in the cells of healthy donors [8, 11, 12]. They develop neurodegenerative disorders, cardiomyopathy, muscle disorders, and, less often, hemolytic anemia [11]. Furthermore, triosephosphate isomerase is capable of converting drug-resistant stomach cancer cells to sensitive ones [13], which improves the chemotherapy efficacy and makes the enzyme a potential target for new antitumor drugs.

Experimental and computational studies of the effect of SNPs within TATA boxes, which are in the context of the DNA of human gene promoters [14, 15], on the interaction with TBP has allowed us to determine the thermodynamic (K_D) and kinetic (k_{on} and k_{off}) parameters for the complex formation of TBP with the “normal” and SNP-containing TATA box of the *TPI* gene promoter.

Thus, it was demonstrated [14] that the -24T \rightarrow G SNP in the TATA box of this gene strongly reduces the TBP/TATA affinity. The equilibrium dissociation constant of the complexes, K_D , increases by 25 times, which correlates with the low gene expression [11]. In the presence of SNP, the rate constant of the TBP/TATA complex formation (k_{on}) decreases by 35 times and the dissociation rate constant (k_{off}) reduces by 30%.

The objective of the present work was to measure and analyze the kinetic parameters of the real-time TBP/TATA interaction. The EMSA classical method, which was used to explore the thermodynamic and kinetic parameters of TBP/TATA complexes, does not allow for studying the interaction dynamics of TBP molecules and the TATA-box of the *TPI* gene promoter in the millisecond and second ranges. Therefore, binding of TBP to the TATA-box of the *TPI* gene promoter was studied using the “stopped-flow” method. The method is based on fast, within ~ 1 ms, mixing of the reactants and registration of the FRET (Förster Resonance Energy Transfer) signal. Recombinant full-length human TBP and 15 bp oligonucleotides identical to the TATA box with flanking nucleotides of the wild-type *TPI* promoter and the SNP-containing TATA box promoter and labeled with fluorescent Cy3 and Cy5 dyes were used in the study. This method enables one to determine the rate constant for the recognition of the wild-type TATA box by the TATA-binding protein and to reveal the structural features of the TBP/TATA complex in real time, under both normal and pathological conditions.

EXPERIMENTAL

Only recombinant full-length human TBP containing the naturally occurring amino acid sequences was used in the study. TBP was expressed in BL21 (DE3) *Escherichia coli* cells transformed with the pAR3038-hTBP plasmid (kindly provided by Prof. B. Puhg, Center for Gene Regulation, Department of Biochemistry and Molecular Biology, Pennsylvania State University, University Park, PA, USA). BL21 (DE3) *E. coli* transformation was performed according to [16]. Expression and purification of TBP were performed according to the procedure described in [17] using the 0.1 mM IPTG concentration. The induction time was 3 h. A TBP concentration in a protein sample was determined by the Bradford method [18].



Fig. 1. The DNA duplexes used were identical to the sequence of the TATA box of the wild-type (T/A) and the -24T → G SNP-containing *TPI* gene promoter and were labeled by the Cy3/Cy5 FRET pair

15 bp oligodeoxynucleotides (ODNs) labeled at the 5'-ends of the chains with cyanine fluorophores Cy3 and Cy5 were synthesized and purified at "NanoTekh-S", Novosibirsk, Russia.

TBP binding to the DNA duplex, which corresponds to the wild-type TATA box of the *TPI* gene promoter (gctcTATATAAagtgg, T allele, and gctcTATAGAAgtgg, G allele), was analyzed by the "stopped-flow" method on an SX20 spectrometer (Applied Photophysics, UK). The fluorescence excitation wavelength of the Cy3 dye was 550 nm; the voltage on the detector was 575 V. Cy5 fluorescence was recorded at wavelengths longer than 645 nm using the RG-645 filter (Scott, Germany). Binding to the DNA duplexes was studied using the following TBP concentrations: the T allele – 1×10^{-7} , 2×10^{-7} , 4×10^{-7} , 6×10^{-7} , 8×10^{-7} , 10×10^{-7} , and 20×10^{-7} M; the G allele – 4×10^{-7} , 6×10^{-7} , 8×10^{-7} , 10×10^{-7} , 20×10^{-7} , 30×10^{-7} , and 40×10^{-7} M. The DNA duplex concentration was 1×10^{-7} M in all cases, the measurement time was 50 s; the total number of points per curve was 6000. Experiments were conducted at 25°C.

To determine a kinetic model for the interaction of TBP with the DNA duplexes and to calculate the rate constants of all elementary reaction steps, the Dynafit software (Biokin, USA) [19] was used.

RESULTS AND DISCUSSION

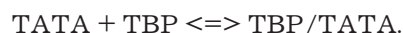
Studying pre-steady-state kinetics allows one to conduct a detailed analysis of the reaction mechanism. The advantage of the "stopped-flow" method is the opportunity it affords to observe transient reactions and to record the conformational transitions of a protein and DNA during a real-time interaction. Although this approach is technically more complex and its use requires a more labor-intensive mathematical analysis, studying the binding of the TATA binding protein to TATA boxes under pre-steady-state conditions enables one to deepen greatly knowledge about the mechanism of their interaction.

In this study, FRET substrates (*Fig. 1*) were used which contained a donor (Cy3)–acceptor (Cy5) pair at the duplex ends, while the central part of the duplex

was the TATA box of the wild-type *TPI* gene promoter or that comprising the SNP.

The kinetics of the binding of the DNA duplexes to TBP, presented in *Figs. 2* and *3*, indicate that the TBP/TATA complex formation leads to an increase in Cy5 fluorescence intensity. The increase in FRET signal intensity is caused by the bending of the DNA duplex in complex with TBP, which makes Cy3 and Cy5 fluorophore moieties approach one another. An analysis of the DNA duplex kinetic curves has revealed that the bending of the duplex containing the wild-type TATA box occurs at lower TBP concentrations than in the case of the G allele of the TATA box (*Figs. 2* and *3*).

Based on these data, we have suggested a kinetic mechanism for TBP binding to the wild-type TATA box of the *TPI* gene and to the SNP-containing TATA box, which is described by a one-step *Scheme*:



The rate constants for the forward and reverse reactions are given in *Table*. It is seen that the complex formation of TBP with the wild-type TATA box occurs 5.5 times faster ($1.1 \times 10^6 \text{ M}^{-1}\text{s}^{-1}$) than with the G allele ($0.2 \times 10^6 \text{ M}^{-1}\text{s}^{-1}$) and the dissociation of TBP/TATA complexes occurs 31 times slower ($2.8 \times 10^{-3} \text{ s}^{-1}$ for the wild-type and $8.9 \times 10^{-2} \text{ s}^{-1}$ for the G allele). It should be noted that this difference in the rate constants of the TBP/TATA complex formation and decomposition leads to a difference in the values of the equilibrium dissociation constants by 150 times ($2.7 \times 10^{-9} \text{ M}$ in the norm and $0.4 \times 10^{-6} \text{ M}$ in the presence of the mutation). The difference in the dissociation constant (K_D) values between the wild-type and SNP-containing TATA box means a sharp decrease in the TBP affinity for oligonucleotides with an altered TATA box.

The obtained data indicate that the G/C-pair occurring in the TATA box makes the DNA structure more rigid, which complicates the TATA box binding to TBP and the formation of a functional complex possessing the optimal conformation. It implies that the triosephosphate isomerase gene containing the -24T → G SNP in the TATA

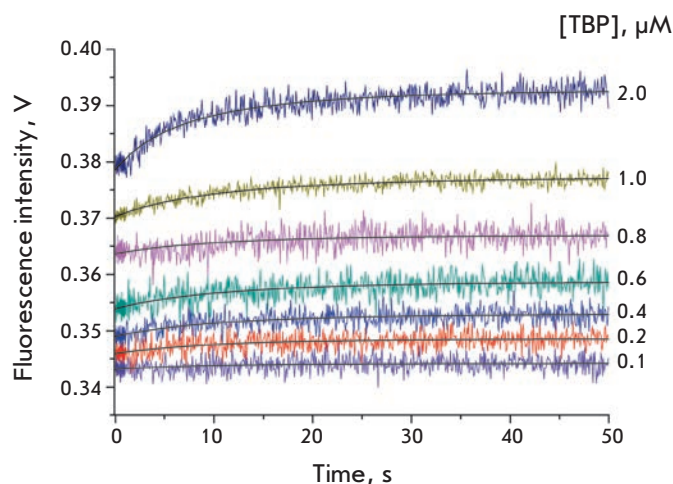


Fig. 2. The kinetics of binding to and bending of the DNA duplex identical to the sequence of the TATA box of the wild-type *TPI* gene

box is *in vivo* transcribed and expressed less efficiently. These results have been confirmed clinically [11].

Comparison of our data and published ones [11, 20] demonstrates that the 150-fold decrease in the TBP affinity for the SNP-containing TATA box of the *TPI* promoter increases the risk of development of some diseases associated with the lack of triosephosphate isomerase. The lack of TPI may be compensated in other ways (e.g., in the pentose phosphate cycle), which follows from differences in the response of patients to TPI deficiency in the body [11, 21]. Despite the fact that TBP affinity for the SNP-containing TATA box of the *TPI* gene promoter is reduced 150-fold, TPI activity in the erythrocytes of some patients falls to 3–10% of the norm [21], and a moderate (26–50% of the norm) decrease in the TPI activity is observed in some heterozygous carriers of this polymorphic allele [11].

The kinetics of interactions between TBP and the normal and the SNP-containing *TPI* TATA box

Constant	Normal TATA box	TATA box with -24T→G SNP
$k_{on}, M^{-1} \times s^{-1}$	$(1.1 \pm 0.1) \times 10^6$	$(0.2 \pm 0.1) \times 10^6$
k_{off}, s^{-1}	$(2.8 \pm 0.1) \times 10^{-3}$	$(8.9 \pm 1.2) \times 10^{-2}$
K_A, M^{-1}	3.7×10^8	2.3×10^6
K_D, M	$2.7 \times 10^{-9} = 2.7 \text{ nM}$	$0.4 \times 10^{-6} = 400 \text{ nM}$

Note. k_{on} is the forward reaction rate constant for TBP / TATA; k_{off} is the reverse reaction rate constant for TBP / TATA; K_A is the equilibrium association constant inferred from kinetic values (k_{on} / k_{off}); K_D is the equilibrium dissociation constant inferred from kinetic values (k_{off} / k_{on}).

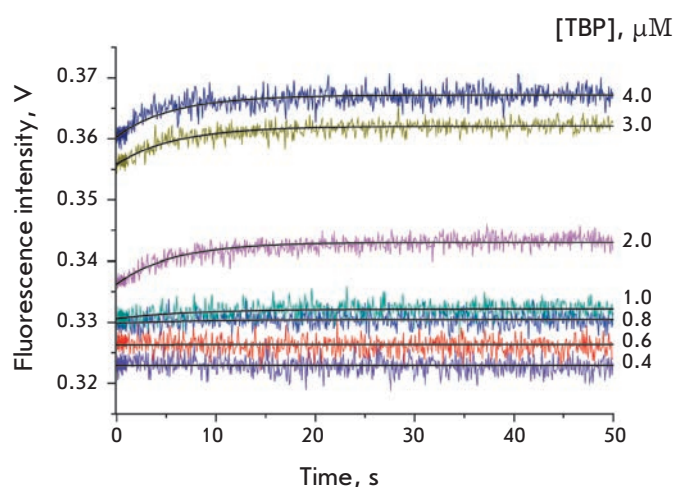


Fig. 3. The kinetics of binding to and bending of the DNA duplex identical to the sequence of the SNP-containing TATA box of the *TPI* gene promoter

It should be noted that by detecting the real-time interaction of human TBP with the Cy3 and Cy5 fluorescently labeled TATA-containing duplexes, it has been demonstrated for the first time that TBP rapidly binds to and simultaneously bends DNA of the *TPI* gene TATA box. This result is consistent with the data obtained previously using full-length human TBP and the AdMLP TATA box with a consensus sequence 5'-CGCTATAAAAGGC-3', the 5'-end of which was attached to the TAMRA fluorophore and the 3'-end was attached to fluorescein [22], which have indicated a one-step mechanism of the binding process and the simultaneous bending of the TATA box by TBP.

It should be noted that these studies have been conducted around the world using different TBP types, full and truncated forms (C-terminal domain), and primarily only the model AdML promoter (less often E4) with the TATA box consensus sequence. The obtained results improved the concept of the TBP/TATA interaction, which is the key interaction in the initiation and regulation of the transcription and synthesis of proteins in eukaryotic cells. ●

The authors are grateful to I.A. Drachkova, T.V. Arshinova, and A.A. Kuznetsova for their assistance in purification of recombinant TBP and performance of experiments.

This work was partially supported by the Program "Molecular and Cell Biology" of the Russian Academy of Sciences (grant № 6.11), the Russian Foundation for Basic Research (grant № 14-04-00485), and Integration Projects of the Presidium of the Russian Academy of Sciences 6.8 and 30.29.

REFERENCES

1. Juven-Gershon T., Kadonaga J.T. // *Dev. Biol.* 2010. V. 339. № 2. P. 225–229.
2. Aso T., Conaway J.W., Conaway R.C. // *J. Biol. Chem.* 1994. V. 269. № 42. P. 26575–26583.
3. Caron C., Rousset R., Beraud C., Moncollin V., Egly J.M., Jalinot P. // *EMBO J.* 1993. V. 12. № 11. P. 4269–4278.
4. Faiger H., Ivanchenko M., Cohen I., Haran T.E. // *Nucl. Acids Res.* 2006. V. 34. № 1. P. 104–119.
5. Hoffman A., Sinn E., Yamamoto T., Wang J., Roy A., Horikoshi M., Roeder R.G. // *Nature.* 1990. V. 346. № 6282. P. 387–390.
6. Hernandez N. // *Genes Dev.* 1993. V. 7. № 7. P. 1291–1308.
7. Wu J., Parkhurst K.M., Powell R.M., Brenowitz M., Parkhurst L.J. // *J. Biol. Chem.* 2001. V. 276. № 18. P. 14614–14622.
8. Cang Y., Auble D.T., Prelich G. // *EMBO J.* 1999. V. 18. № 23. P. 6662–6671.
9. Savinkova L.K., Ponomarenko M.P., Ponomarenko P.M., Drachkova I.A., Lysova M.V., Arshinova T.V., Kolchanov N.A. // *Biochemistry (Mosc)*. 2009. V. 74. № 2. P. 117–29.
10. Brown J.R., Daar I.O., Krug J.R., Maquat L.E. // *Mol. Cell. Biol.* 1985. V. 5. № 7. P. 1694–1706.
11. Watanabe M., Zingg B.C., Mohrenweiser H.W. // *Am. J. Hum. Genet.* 1996. V. 58. № 2. P. 308–316.
12. Rosa R., Prehu M.O., Calvin M.C., Badoual J., Alix D., Girod R. // *Hum. Genet.* 1985. V. 71. № 3. P. 235–240.
13. Wang X., Lu Y., Yang J., Shi Y., Lan M., Liu Z., Zhai H., Fan D. // *J. Cancer Res. Clin. Oncol.* 2008. V. 134. № 9. P. 995–1003.
14. Savinkova L., Drachkova I., Arshinova T., Ponomarenko P., Ponomarenko M., Kolchanov N. // *PLoS One.* 2013. V. 8. № 2. e54626.
15. Drachkova I.A., Savinkova L.K., Arshinova T.V., Ponomarenko M.P., Peltek S.E., Kolchanov N.A. // *Hum. Mut.* 2014. V. 35. № 5. P. 601–608.
16. Peterson M.G., Tanese N., Pugh B.F., Tjian R. // *Science.* 1990. V. 248. № 4963. P. 1625–1630.
17. Pugh B.F. // *Methods in molecular biology: in vitro transcription and translation protocols* / Ed. Tymms M.J. Totowa, N.J.: Humana Press Inc., 1995. V. 37. P. 359–367.
18. Bradford M.M. // *Anal. Biochem.* 1976. V. 72. P. 248–254.
19. Kuzmic P. // *Anal. Biochem.* 1996. V. 237. № 2. P. 260–273.
20. Humphries A., Ationu A., Lalloz M.R., Layton D.M. // *Hum. Genet.* 1999. V. 104. № 6. P. 486–491.
21. Chang M.L., Artymiuk P.J., Wu X., Hollan S., Lammi A., Maquat L.E. // *Am. J. Hum. Genet.* 1993. V. 52. № 6. P. 1260–1269.
22. Masters K.M., Parkhurst K.M., Daugherty M.A., Parkhurst L.J., Lawrence J. // *J. Biol. Chem.* 2003. V. 278. № 34. P. 31685–31690.

Structural Features of the Telomerase RNA Gene in the Naked Mole Rat *Heterocephalus glaber*

S. A. Evfratov¹, E. M. Smekalova¹, A. V. Golovin^{2,3}, N. A. Logvina¹, M. I. Zvereva^{1,3},
O. A. Dontsova^{1,3}

¹ Faculty of Chemistry, Moscow State University, 1-3 Leninskie Gory, Moscow, 119991, Russia

² Faculty of Bioengineering and Bioinformatics, Moscow State University, 1-40 Leninskie Gory, Moscow, 119991, Russia

³ Belozersky Institute of Physicochemical Biology, Moscow State University, 1-40 Leninskie Gory, Moscow, 119991, Russia

*E-mail: evfratov@gmail.com

Received 10.10.2013

Revised manuscript received 14.03.2014

Copyright © 2014 Park-media, Ltd. This is an open access article distributed under the Creative Commons Attribution License, which permits unrestricted use, distribution, and reproduction in any medium, provided the original work is properly cited.

ABSTRACT Telomere length, an important feature of life span control, is dependent on the activity of telomerase (a key enzyme of the telomere-length-maintaining system). Telomerase RNA is a component of telomerase and, thus, is crucial for its activity. The structures of telomerase RNA genes and their promoter regions were compared for the long-living naked mole rat and different organisms. Two rare polymorphisms in *Heterocephalus glaber* telomerase RNA (hgTER) were identified: A→G in the first loop of pseudoknot P2b-p3 (an equivalent of 111nt in hTR) and G→A in the scaRNA domain CR7-p8b (an equivalent of 421nt in hTR). Analysis of TER promoter regions allowed us to identify two new transcription factor binding sites. The first one is the ETS family site, which was found to be a conserved element for all the analyzed TER promoters. The second site is unique for the promoter region of TER of the naked mole rat and is a binding site for the SOX17 transcription factor. The absence of one Sp1 site in the TER promoter region of the naked small rat is an additional specific feature of the promoter area of hgTER. Such variation in the hgTER transcription regulation region and hgTER itself could provide increased telomerase activity in stem cells and an extended lifespan to *H. glaber*.

KEYWORDS *H. glaber*; telomerase RNA; bioinformatics; promoter analysis; comparative genomics.

ABBREVIATIONS TER – telomerase RNA; hTR – human telomerase RNA; TERT – telomerase catalytic subunit; hTERT – human telomerase catalytic subunit; hgTER – *Heterocephalus glaber* telomerase RNA.

INTRODUCTION

Several studies have shown that stem cell function is impaired during aging [1–3]. A decrease in stem cell function may contribute to impaired maintenance and the function of some tissue during aging. The role of telomere shortening was identified to be the mechanism contributing to the accumulation of DNA damage in replicative aging of stem cells [4]. Experiments in mTER^{-/-} mice with telomere shortening have provided the experimental evidence that this process can impair the function of somatic and germline stem cells [5]. Telomerase is a key component of the telomere-length-maintaining system and an important contributor to the reduction of replicative senescence in germ and stem cells [6, 7]. Temporary telomerase reactivation in late-generation TERT-deficient mice extends telomeres, reduces DNA damage signaling and associated

cellular checkpoint responses, and eliminates degenerative phenotypes across multiple organs, including testes, spleen, intestine, and even neurons [7]. Moreover, temporary telomerase expression in aged normal mice significantly increases the lifespan of mice [8].

Telomerase synthesizes new telomere repeats at the G-strand and thus participates in the compensation for telomere loss during replication [9]. Two components are required for telomerase activity *in vitro*: a reverse transcriptase catalytic subunit (TERT) and telomerase RNA (TER) that contains a template for telomere synthesis [10]. TERT was shown to play a role in a number of cellular processes (cell cycle response, oxidative stress, antiapoptotic action, etc. [11]) outside of the telomerase complex. No hTERT was found in most differentiated normal tissues, although a low level of hTERT could be detected in the skin, spleen, stomach

and small intestine and a higher level was detected in testes and the endometrium [12]. In contrast, hTR expression was detected in many normal tissues, including testes, ovary, brain, liver, small intestine, thymus, kidney, and prostate, suggesting that telomerase RNA may also have alternative functions [13]. In some cancer cell lines, the level of TERT expression is critical for telomere elongation; however, in case of stem cells in a living organism it is the high level of TER expression that is more important for telomere elongation. Indeed, an analysis of interspecies crosses of TER- and TERT-deficient mice [14] showed that the increase in the gene copy number of TER, but not TERT, is what is critical in telomere elongation. Ectopic expression of hTER caused telomere elongation in bovine blastocysts, whereas co-expression of hTERT and hTER did not result in further increase in the telomere length [15], providing further evidence of the fact that the level of telomerase RNA is critical for telomerase activity and telomere elongation in the cell within the organism.

The genome and transcriptome of the naked mole rat have recently been sequenced [16, 17]. *Heterocephalus glaber*, the naked mole rat (*H. glaber*), has a very high life expectancy among rodents (> 28 years vs 1.5–7 years in other rodents), high resistance to carcinogenesis and retarded aging [18].

A comparative study of the *H. glaber* genome can help reveal the reasons for the surprisingly long lifespan of this animal. A number of genetic alterations have already been found, which could explain the increase in the DNA repair level, as well as the reduced oxidative damage or reduced replicative senescence [5, 19]. Another reason for the longevity could be the higher level of telomerase activity in *H. glaber* stem cells or telomerase reactivation under a certain type of stimulus. In this study, we have compared the structure of telomerase RNA genes and their promoter regions for the long-living naked mole rat and different organisms with an aim to identify the features that may increase hgTER expression and telomerase activity in stem cells.

MATERIAL AND METHODS

Comparison of TER sequences

To search for the *hgTER* gene of *H. glaber*, we used the whole genome shotgun project entries with IDs: AFSB (GenBank: AFSB00000000.1) and AHKG (GenBank: AHKG00000000.1). We used ClustalW to build an alignment of the sequences of interest with the already well-described telomerase RNA genes. The following reference sequences were used: *Cavia porcellus* TER (GenBank: AF221929.1), *Cavia porcellus* WGS assembly (GenBank: AAKN00000000.2), *Chinchilla chinchilla* TER (GenBank: AF221937.1), *Chinchilla chinchilla*

WGS assembly (GenBank: AGCD00000000.1), *Mus musculus* TER (GenBank: NR_001579.1), *Mus musculus* chromosome 3 (GenBank: NC_000069.6), *Rattus norvegicus* TER (GenBank: NR_001567.1), *Rattus norvegicus* chromosome 2 (GenBank: NC_005101.3), human TER (GenBank: NR_001566.1), human chromosome 3 (GenBank: NC_000003.11), *Danio rerio* TER (GenBank: EF569636.1), and chromosome 25 (GenBank: CU651628.3).

The alignment analysis and the influence of polymorphisms on the secondary structure were performed manually. The sequences of TERs from *Suncus murinus* (GenBank: AF221921), *Geomys breviceps* (GenBank: AF221930), *Microtus ochrogaster* (GenBank: AF221909), *Mus spretus* (GenBank: AY058901), *Mus musculus* (GenBank: AY058900), *Dasyurus hallucatus* (GenBank: AF221919), *Bufo japonicus* (GenBank: AF221913) and *Typhlonectes natans* (GenBank: AF221910) were used to perform a secondary structure analysis.

Comparison of TER promoter areas

We searched for promoter regions using the Jaspar database [20], restricting the search to the Jaspar CORE Vertebrate with a 99–100% relative profile threshold. ConSite with a 85–95% TF score cutoff was used for further analysis of the promoter sequences [21]. Relative scores were used as normalized score values for the quantitative evaluation of hit significances [22]. Hit corrections were done manually where necessary. Visualization of multiple alignments was corrected manually.

RESULTS

Identification of *H. glaber* TER

The full *hgTERC* gene (*Heterocephalus glaber* TER) was identified by local BLAST on the basis of the *H. glaber* genome assembly (WGS record AHKG) and a comparison with multiple alignment data for mammalian TER sequences [23]. The final alignment is available at 93.180.62.254/hgTERC/ESM_1.pdf.

According to phylogenetic data, the closest relatives of *H. glaber* are *Hydrochoerus hydrochaeris*, *Cavia porcellus*, *Chinchilla chinchilla*, and *Myocastor coypus* [18]. TER sequences are known only for *Chinchilla chinchilla* (GenBank: AF221937.1) and *Cavia porcellus* (GenBank: AF221929.1); those were used for further structure comparison. Furthermore, the data for human TER were used for the analysis due to the availability of detailed information about the promoter region and secondary structure of TER.

Comparison of TER promoter areas

A 500 nt (from the expected transcription start site) promoter region was used for the analysis, since the

major regulatory elements were found in this area for human TER (hTER) [24]. The web services JASPAR [20] and ConSite [21] were used to search for transcription factor binding sites in the promoter area of *H. glaber*. These tools provide the possibility to analyze any sequence data; they are relatively simple in operation and allow one to deal with large-position weight matrices with optimal results due to the effective job filtering. We used strict filtering of the results for both tools to find the most reliable sites.

This approach reduced the number of predicted transcription factor binding sites in the hTER promoter area compared to the number of sites determined earlier [24]. The elements in the promoter region of TERs from four different species identified in this study are shown at 93.180.62.254/hgTERC/ESM_2.pdf (the full promoter map is available at 93.180.62.254/hgTERC/ESM_3_old.pdf). The elements found in the promoter region of hgTER are as follows: TATA box in the proximity of the transcription start site, NF-Y site with the conserved CCAAT box, three SP1 sites, ELK4 site, and SOX17 binding site.

The ELK4 transcription factor binding site had never been identified for any TER before; it is located approximately 170 nt upstream from the start of the TER coding region. We have found this promoter element for all tested sequences; *p* values were calculated by MAST. The ELK4 score for the *H. glaber* was 14.059 (the relative score 0.9999; $p = 3.3 \cdot 10^{-6}$); 11.056 (0.9034, $4.1 \cdot 10^{-5}$) for *Cavia porcellus*; 12.053 (0.9311, $2.2 \cdot 10^{-5}$) for *Chinchilla chinchilla*; and 10.398 (0.9396, $5.5 \cdot 10^{-5}$) for humans, thus meaning a very high probability (> 90%) of ELK4 transcription factor binding site occurrence in the TER promoter area, at least from the bioinformatic point of view.

When performing the search, we found that the ELK4 binding site [25] matrix in the JASPAR database was outdated [25–27] and this led to a false identification for most proteins containing the ETS domain, except for families I and II [28]. Since we are dealing with a very small set of sequences and the difference between the new and old matrices is negligible, we used the old position weight matrix (PWM).

Multiple alignments showed that a ETS binding site was present in all four species: human, *Cavia porcellus*, *H. glaber*, and *Chinchilla chinchilla*. The binding sites found have variations in positions 1, 8, and 9 of PWM, which is consistent with the known ETS binding sites [26, 27, 29]. Thus, we suggest that the identified site is a regulatory element for the hgTER promoter.

The SOX17 binding site was detected solely in the *H. glaber* TER promoter region; it is located ~ 430 nt upstream from the transcription start site. The fact that the SOX17 site is present in *H. glaber* but not in other

evolutionary related animals may be an indication of an important difference between these species.

The SOX17 protein contains an HMG_box (Pfam domain high-mobility group box) responsible for the high-affinity binding to non-B-type DNA conformations (kinked or unwound) [30]. The characteristic binding motif in DNA is almost identical for the entire HMG_box family [31, 32]; however, for the transcription factor SOX17 [33, 34] harboring the Sox_C_TAD domain (Pfam: PF12067), the binding sites are largely different from the canonical site – AACAAAT [32, 35].

Based on the common architecture for most TERs, we assumed that hgTER also contains the known secondary structure elements [23]. We mainly focused on the rare TER polymorphisms in the important functional elements of the telomerase RNA secondary structure.

The comparison of hgTER with the TER of *H. glaber*'s closest relatives (guinea pig and chinchilla) and the TER of model organisms (rat, mouse, and humans) revealed a number of differences. Although most changes in *H. glaber* TER were not unique (present in other mammals) and did not affect the functional elements of TER, we managed to find two rare polymorphisms in the functional region of hgTER. The mapped polymorphisms are shown in *Figs. 1a* and *1b*.

The first polymorphism was a A→G replacement in the first loop of pseudoknot P2b-p3 at position 111 (according to the hTER nomenclature). This substitution gives rise to the non-canonical “G–U” pair in the pseudoknot region. Most other TERs have a canonical pair at this position. Moreover, for TERs that have polymorphism A→G111 additional replacement U→C179 takes place that restored the canonical WC pair between bases in 111 and 179 positions (e.g., in *Geomys breviceps* and *Microtus ochrogaster*) [23]. The only example of the same G–U pair was revealed in TERs of the *Dasyurus hallucatus* and *Suncus murinus* [23].

The second polymorphism is the replacement G→A in the stem of the scaRNA domain CR7-p8b at position 421 (according to the hTER nomenclature). This substitution gives rise to the non-canonical “C–A” pair in the p8b stem terminus element at position 421. Most TERs have a canonical base pair at this position. Amphibians (toads and typhlonectes) have G421→A replacement accompanied by C→U transition at position 408, which restores the WC pair [23]. Close relatives – rodents (chinchilla, guinea pig, mice) – have polymorphisms that cause a disturbance in the p8b stem at different positions [23], but this particular substitution at position 421 with the non-canonical pair is unique to *H. glaber*.

DISCUSSION

Telomerase RNA is a crucial telomerase component, and increased expression of telomerase RNA and te-

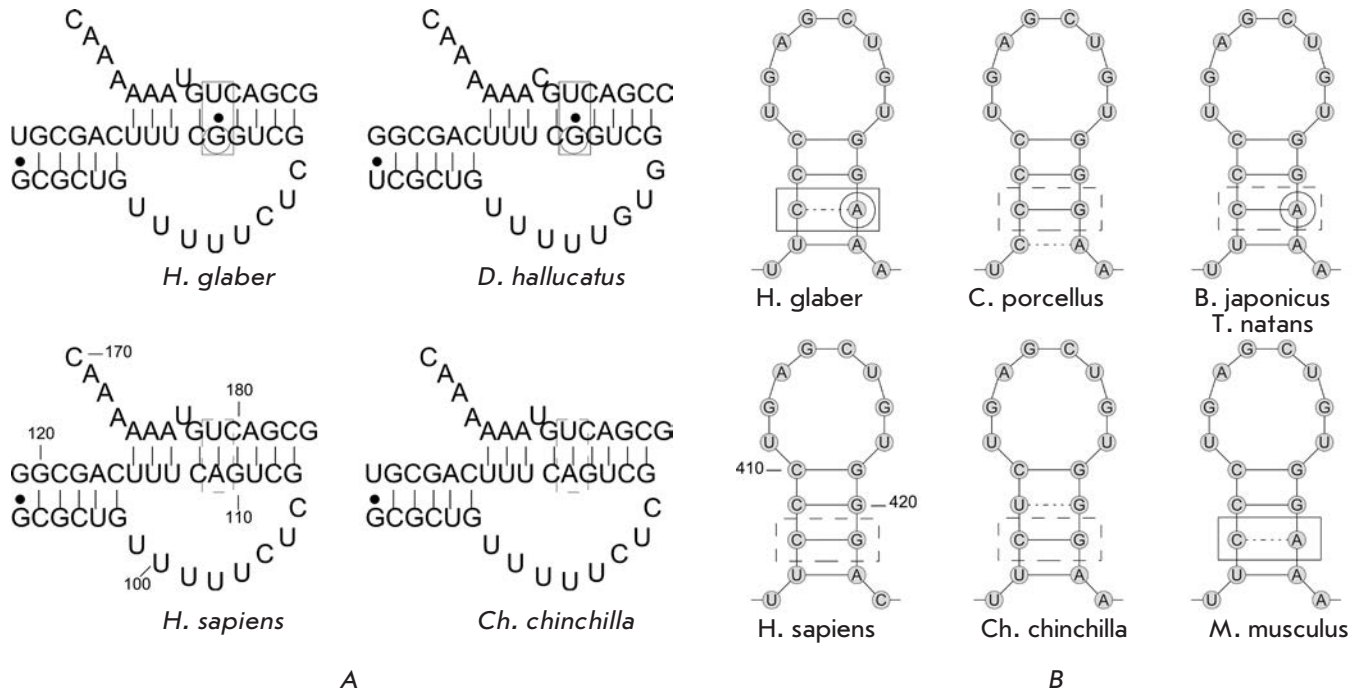


Fig. 1. The P2b-p3 and CR7-p8b areas of pseudoknot with the mapped polymorphisms for different species. The polymorphism is marked with a circle; The Watson-Crick base pairing is marked with a solid line; non-canonical base pairing is marked with a dashed line. A – the P2b-p3 areas of pseudoknot for *H. sapiens*, *Ch. chinchilla*, *H. glaber* and *D. Hallucatus*. B – the CR7-p8b area of the scaRNA TER domain with the mapped polymorphism for *H. sapiens*, *Ch. chinchilla*, *C. porcellus*, *H. glaber*, *M. Musculus*, *Bombina japonica*, and *Typhlonectes natans*

lomease activity in stem cells or other tissues at different stages of an animal's development could be an essential reason for its long lifespan. Comparison of the TER gene promoter region and TER in *H. glaber* with available data on other species allowed us to reveal variations both in the promoter region and telomerase RNA structure.

An analysis of the region 500 nt upstream of hgTER transcription start side allowed us to identify the regulatory elements known for other organisms [24] and two new ones: the ETS site, which is present in all four model organisms, and the SOX17 site presented only in *H. glaber* (Fig. 2). All common elements are located within the ~ 270 nt area, in agreement with the DNase 1 protection data for the human regulatory region [36]. This region contains the TATA box in the proximity of the transcription start site, a NF-Y site with a conserved CCAAT box, SP1 sites, and the newly identified ETS site. In humans, four Sp1 (Sp1.1, Sp1.2, Sp1.3 and Sp1.4) sites were previously identified. An analysis of *H. glaber* and its close relatives revealed that one or more Sp1 sites can be missing in a particular organism. For example, the Sp1.2 site is missing in all rodents (Fig. 2) and the Sp1.3 site is also absent in *Cavia porcellus*.

In case of humans, the two transcription factors Sp1 and Sp3 can bind to the Sp-sites within the promoter. Sp1 stimulates expression, while Sp3 induces dose-dependent repression [36]. The sites adjacent to the CCAAT box from either side (Sp1.1 only for *H. glaber*) are thought to cooperate with NF-Y to mediate positive or negative regulatory effects in humans [37]. The Sp1.3 and Sp1.4 sites adjacent to the transcription start site could also regulate transcription, either positively or negatively, depending on the presence of other proteins that interact with transcription factors [38]. The context of a particular Sp1 site was suggested as essential for the preferential binding of either Sp1 or Sp3 factors, which might influence the TER transcription regulation [38]. Thus, the absence of the Sp1.2 site in rodents may result in differences in the fine regulation of TER transcription via the Sp pathway in rodents, making it more dependent on the particular context of the remaining Sp sites. In case of *H. glaber*, this may have a positive effect on the TER transcription efficiency.

The newly identified ELK4 site is located within the 272 nt area further downstream from the transcription start site. It was found in all the studied species, including humans. ELK4 is a member of the ETS family of

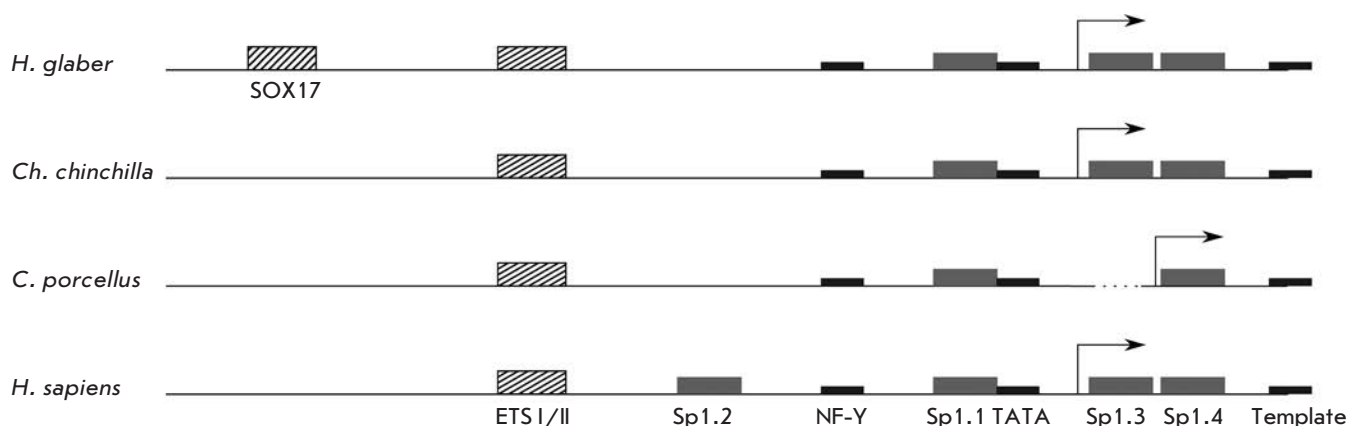


Fig. 2. Schematic annotation of the TER promoter areas for humans, guinea pig, mole rat, and chinchilla. The reference promoter elements are marked as gray rectangles, and the putative elements predicted in this study are marked as hatched rectangles

transcription factors [29]. For *H. glaber*, the sequence of this site is identical to that of ELK4, but it can also be used by the other members of the ETS family [28]. This factor was identified as a novel target for the androgen receptor-activating cascade. The fact that androgen signaling blockade in the case of prostate cancer reduced telomerase activity indirectly proves that ELK4 participates in the regulation of TER transcription [25].

A SOX17 binding site was found only in *H. glaber*. It is located approximately 430 nt upstream of the gene region, and thus outside of the 272 nt promoter area, which was previously shown to be important for hTER transcription. SOX17 belongs to the family of HMG-like SOX proteins. The SOX17 binding site (ACAAT) is identical for the other members of the SOX proteins, and binding of a particular factor depends on the broader context around the conventional site. SOX17 (SRV-box 17) is a transcription factor involved in the regulation of several developmental processes [39, 40], including endoderm formation, vascular development, and fetal hematopoietic stem cell maintenance.

Sox17 is highly restricted in its expression within the hematopoietic system to fetal hematopoietic stem cells (HSCs) [41]. It has recently been shown that Sox17 expression confers self-renewal potential and fetal stem cell characteristics to adult hematopoietic progenitors [42]. Other SOX proteins are involved in the regulation of various cellular processes. A lack of data does not allow one to propose a particular regulation pathway for the SOX binding site, but the presence of this site is an additional possibility for *H. glaber* to regulate the expression of telomerase RNA and to increase the level of telomerase activity, especially in fetal stem cells. This

correlates with earlier studies, where long-living rodent species (such as the *H. glaber* and *Sciurus carolinensis*) have a higher telomerase activity than mice [43].

Telomerase activity depends not only on the transcriptional level of telomerase components; many other processes are involved, including TER maturation, transport, telomerase assembly, interaction between TER and TERT, etc. Mutations in telomerase RNA can influence these processes.

We found two rare polymorphisms in hgTER: A111→G and G421→A. The A111→G transition in hgTER is located in the stem loop of P2b-p3 pseudoknot. The P2b-P3 pseudoknot (Fig. 1a) is highly conserved [23]. The effect of this mutation on the function of telomerase is unknown, but mutations destabilizing the pseudoknot structure affect telomerase activity and lead to aplastic anemia, myelodysplasia, and leukemia in humans [44]. Moreover, mutations that destabilize the pseudoknot structure reduce telomerase activity [45] and lead to dyskeratosis congenita [46]. Polymorphism in this position in other organisms is accompanied by the second mutation that restores the canonical pair. Due to the A→G replacement in *H. glaber*, a non-canonical G–U pair is formed. In contrast to other non-canonical pairs, G–U causes very little distortion to the RNA helix structure [47] and should not have such a severe effect on telomerase as the other ones. The G–U pair in this position is found only in the Asian house shrew and the northern quoll. Life expectancy of the northern quoll is 7 years and about 3 years for shrews [48]. Thus, there is no evident correlation between the existence of the G–U pair in a particular position in the pseudoknot structure and life expectancy.

The polymorphism G→A at position 421 leads to the formation of a C–A non-canonical pair in the p8b stem. Most mammals have the canonical base pair at this position. It should be mentioned that disruption (C→G in C–G) of 408–421 base pairs in humans leads to dyskeratosis congenita [46]. Rodents (chinchilla, guinea pig, mice) have polymorphisms that cause distortion of the p8b stem. The G→A transition in *H. glaber* belongs to the same class of species-dependent variations, but this particular substitution is unique to *H. glaber*. P8b is a part of the CR7–p8b (H/ACA) domain. CR7 is required for 3′-end processing, localization, and the stability of hTER [49]. CR7 contains a conserved Cajal body localization element (CAB box) [50]. The telomerase Cajal body protein 1 (TCAB1) binds to the CAB box [51] and drives hTER to the Cajal body. TCAB1 knockdown prevents telomerase-telomere association and results in telomere shortening [52]. For *H. glaber*, the non-canonical pair “C–A” in the p8b stem loop can improve the interaction between hgTCAB1 and hgTER, make

telomerase traffic more effective and thus result in a more efficient telomere elongation. ●

CONCLUSIONS

Comparison of hgTER and other telomerase RNA genes suggests that both the unique structure of the promoter region and the specific polymorphisms in the functional domains can cause increased expression of the telomerase RNA gene in stem cells, thus reducing replicative senescence and increasing the lifespan. We hope that our finding of a difference in the promoter region of telomerase RNA will inspire other researchers to study these processes using *in vivo* mouse models.

This study was supported by the Ministry of Education and Science of the Russian Federation, project № 829, the Russian Foundation for Basic Research (grants № 11-04-01310-a and 14-04-01092-a), and the Moscow State University development program (PNR5.13).

REFERENCES

- Rando T.A. // *Nature*. 2006. V. 441. P. 1080–1086. doi:10.1038/nature04958.
- Van Zant G., Liang Y. // *Exp. Hematol.* 2003. V. 31(8) P. 659–672. doi: 10.1016/S0301-472X(03)00088-2.
- Rossi D.J., Bryder D., Weissman I.L. // *Exp. Gerontol.* 2007. V. 42. P. 385–390. doi: 10.1016/j.exger.2006.11.019.
- Tümpel S., Rudolph K.L. // *Ann. N.Y. Acad. Sci.* 2012. V. 1266. P. 28–39. doi: 10.1111/j.1749-6632.2012.06547.x.
- Blasco M.A. // *Nat. Chem. Biol.* 2007. V. 3 P. 640–649. doi:10.1038/nchembio.2007.38.
- Nicholls C., Li H., Wang J.Q., Liu J.P. // *Protein Cell.* 2011. V. 2. P. 726–738. doi: 10.1007/s13238-011-1093-3.
- Jaskelioff M., Muller F.L., Paik J.H., Thomas E., Jiang S., Adams A.C., Sahin E., Kost-Alimova M., Protopopov A., Cadiñanos J., et al // *Nature*. 2011. V. 469. P. 102–106. doi: 10.1038/nature09603.
- Bernardes de Jesus B., Vera E., Schneeberger K., Tejera A.M., Ayuso E., Bosch F., Blasco M.A. // *EMBO Mol. Med.* 2012. V. 4. P. 691–704. doi: 10.1002/emmm.201200245.
- Collins K. // *Curr. Opin. Chem. Biol.* 2011. V. 15. P. 643–648. doi: 10.1016/j.cbpa.2011.07.011.
- Kelleher C., Teixeira M.T., Forstemann K., Lingner J. // *Trends Biochem. Sci.* 2002. V. 27. P. 572–579. doi: 10.1016/S0968-0004(02)02206-5.
- Chiodi I., Mondello C. // *Front. Oncol.* 2012. V. 2. P. 133. doi: 10.3389/fonc.2012.00133.
- Hiyama E., Hiyama K., Yokoyama T., Shay W.J. // *Neoplasia*. 2001. V. 3. P. 17–26.
- Smekalova E.M., Shubernetskaya O.S., Zvereva M.I., Gromenko E.V., Rubtsova M.P., Dontsova O.A. // *Biochemistry (Mosc.)* 2012. V. 77. P. 1120–1128. doi: 10.1134/S0006297912100045.
- Chiang Y.J., Hemann M.T., Hathcock K.S., Tessarollo L., Feigenbaum L., Hahn W.C., Hodes R.J. // *Mol. Cell. Biol.* 2004. V. 24. P. 7024–7031. doi:10.1128/MCB.24.16.7024-7031.2004.
- Garrels W., Kues W.B., Herrmann D., Holler S., Baulain U., Niemann H. // *Biol. Reprod.* 2012. V. 87. P. 95. doi: 10.1095/biolreprod.112.100198.
- Kim E.B., Fang X., Fushan A.A., Huang Z., Lobanov A.V., Han L., Marino S.M., Sun X., Turanov A.A., Yang P., et al. // *Nature*. 2011. V. 479. P. 223–227. doi: 10.1038/nature10533.
- Yu C., Li Y., Holmes A., Szafranski K., Faulkes C.G., Coen C.W., Buffenstein R., Platzer M., de Magalhães J.P., Church G.M. // *PLoS One*. 2011. V. 6. e26729. doi: 10.1371/journal.pone.0026729.
- Gorbunova V., Bozzella M.J., Seluanov A. // *Age (Dordr.)*. 2008. V. 30. P. 111–119. doi: 10.1007/s11357-008-9053-4.
- Liang S., Mele J., Wu Y., Buffenstein R. // *Aging Cell*. 2010. V. 9. P. 626–635. doi: 10.1111/j.1474-9726.2010.00588.x.
- Sandelin A., Alkema W., Engström P., Wasserman W.W., Lenhard B. // *Nucl. Acids Res.* 2004. V. 32. D91–D94. doi: 10.1093/nar/gkh012.
- Sandelin A., Wasserman W.W., Lenhard B. // *Nucl. Acids Res.* 2004. V. 32. P. 249–252. doi: 10.1093/nar/gkh372.
- Wasserman W.W., Sandelin A. // *Nat. Rev. Genet.* 2004. V. 5. P. 276–287. doi:10.1038/nrg1315.
- Chen J.L., Blasco M.A., Greider C.W. // *Cell*. 2000. V. 100. P. 503–514. dx.doi.org/10.1016/S0092-8674(00)80687-X.
- Zhao J.Q., Hoare S.F., McFarlane R., Muir S., Parkinson E.K., Black D.M., Keith W.N. // *Oncogene*. 1998. V. 16. P. 1345–1350.
- Makkonen H., Jääskeläinen T., Pitkänen-Arsiola T., Rytinki M., Waltering K.K., Mättö M., Visakorpi T., Palvimo J.J. // *Oncogene*. 2008. V. 27. P. 4865–4876. doi: 10.1038/onc.2008.125.
- Shore P., Sharrocks A.D. // *Nucl. Acids Res.* 1995. V. 23. P. 4698–4706. doi: 10.1093/nar/23.22.4698.
- Mo Y., Vaessen B., Johnston K., Marmorstein R. // *Mol. Cell*. 1998. V. 2. P. 201–212. doi: 10.1016/S1097-2765(00)80130-6.
- Wei G.H., Badis G., Berger M.F., Kivioja T., Palin K., Enge M., Bonke M., Jolma A., Varjosalo M., Gehrke A.R., et al // *EMBO J.* 2010. V. 29. P. 2147–2160. doi: 10.1038/emboj.2010.106.

RESEARCH ARTICLES

29. Sharrocks A.D., Brown A.L., Ling Y., Yates P.R. // *Int. J. Biochem. Cell. Biol.* 1998. V. 29. P. 1371–1387. doi: 10.1016/S1357-2725(97)00086-1.
30. Stros M., Launholt D., Grasser K.D. // *Cell. Mol. Life Sci.* 2007. V. 64. P. 2590–2606. doi: 10.1007/s00018-007-7162-3.
31. Denny P., Swift S., Connor F., Ashworth A. // *EMBO J.* 1992. V. 11. P. 3705–3712.
32. Laudet V., Stehelin D., Clevers H. // *Nucl. Acids Res.* 1993. V. 21. P. 2493–2501. doi: 10.1093/nar/21.10.2493.
33. Dunn T.L., Mynett-Johnson L., Wright E.M., Hosking B.M. // *Gene.* 1995. V. 161. P. 223–225. doi: 10.1016/0378-1119(95)00280-J.
34. Kanai Y., Kanai-Azuma M., Noce T., Saido T.C. // *J. Cell. Biol.* 1996. V. 133. P. 667–681. doi: 10.1083/jcb.133.3.667.
35. Mertin S., McDowall S.G., Harley V.R. // *Nucl. Acids Res.* 1999. V. 27. P. 1359–1364.
36. Zhao J.Q., Glasspool R.M., Hoare S.F., Bilsland A., Szatmari I., Keith W.N. // *Neoplasia.* 2000. V. 2. P. 531–539. doi: 10.1038/sj.neo.7900114.
37. Zhao J., Bilsland A., Hoare S.F., Keith W.N. // *FEBS Lett.* 2003. V. 536. P. 111–119. doi: 10.1016/S0014-5793(03)00038-3.
38. Li L., Davie J.R. // *Ann. Anat.* 2010. V. 192. P. 275–283. doi: 10.1016/j.aanat.2010.07.010.
39. Séguin C.A., Draper J.S., Nagy A., Rossant J. // *J. Cell. Stem Cell.* 2008. V. 3. P. 182–195. doi: 10.1016/j.stem.2008.06.018.
40. Patterson E.S., Addis R.C., Shambloott M.J., Gearhart J.D. // *Physiol. Genomics.* 2008. V. 34. P. 277–284. doi: 10.1152/physiolgenomics.90236.2008.
41. Kim I., Saunders T.L., Morrison S.J. // *Cell.* 2007. V. 130. P. 470–483. doi: 10.1016/j.cell.2007.06.011.
42. He S., Kim I., Lim M.S., Morrison S.J. // *Genes Dev.* 2011. V. 25. P. 1613–1627. doi: 10.1101/gad.2052911.
43. Seluanov A., Chen Z., Hine C., Sasahara T.H. // *Aging Cell.* 2007. V. 6. P. 45–52. doi: 10.1111/j.1474-9726.2006.00262.x.
44. Vulliamy T., Marrone A., Dokal I., Mason P.J. // *Lancet.* 2002. V. 359. P. 2168–2170. doi: 10.1016/S0140-6736(02)09087-6.
45. Chen J.L., Greider C.W. // *Proc. Natl. Acad. Sci. USA.* 2005. V. 102. P. 8080–8085. doi: 10.1073/pnas.0502259102.
46. Vulliamy T., Marrone A., Goldman F., Dearlove A., Bessler M., Mason P.J., Dokal I. // *Nature.* 2001. V. 413. P. 432–435. doi:10.1038/35096585.
47. Leontis N.B., Westhof E. // *RNA.* 1998. V. 4. P. 1134–1153. doi: 10.1017/S1355838298980566.
48. de Magalhães J.P., Costa J. // *J. Evol. Biol.* 2009. V. 22. P. 1770–1774. doi: 10.1111/j.1420-9101.2009.01783.x.
49. Theimer C.A., Jády B.E., Chim N., Richard P., Breece K.E., Kiss T., Feigon J. // *J. Mol. Cell.* 2007. V. 27. P. 869–881. doi: 10.1016/j.molcel.2007.07.017.
50. Jády B.E., Bertrand E., Kiss T. // *J. Cell Biol.* 2004. V. 164. P. 647–652. doi: 10.1083/jcb.200310138.
51. Tycowski K.T., Shu M.D., Kukoyi A., Steitz J.A. // *Mol. Cell.* 2009. V. 34. P. 47–57. doi: 10.1016/j.molcel.2009.02.020.
52. Venteicher A.S., Abreu E.B., Meng Z., McCann K.E., Terns R.M., Veenstra T.D., Terns M.P. // *Artandi SE Sci.* 2009. V. 323. P. 644–648. doi: 10.1126/science.1165357.

High-throughput Method of One-Step DNA Isolation for PCR Diagnostics of *Mycobacterium tuberculosis*

D. V. Kapustin^{1*}, A. I. Prostyakova¹, Ya. I. Alexeev^{2,3}, D. A. Varlamov^{2,3}, V. P. Zubov¹, S. K. Zavriev¹

¹M.M. Shemyakin and Yu.A. Ovchinnikov Institute of Bioorganic Chemistry of the Russian Academy of Sciences, GSP-7, Ul. Miklukho-Maklaya, 16/10, Moscow, Russia, 117997

²ZAO SINTOL, Ul. Timiryazevskaya, 42, Moscow, Russia, 127550

³Russian National Research Institute of Agricultural Biotechnology of the Russian Academy of Agricultural Sciences, Ul. Timiryazevskaya, 42, Moscow, Russia, 127550

* E-mail: kapustin@ibch.ru

Received 09.10.2013

Revised manuscript received 14.03.2014

Copyright © 2014 Park-media, Ltd. This is an open access article distributed under the Creative Commons Attribution License, which permits unrestricted use, distribution, and reproduction in any medium, provided the original work is properly cited.

ABSTRACT The efficiency of one-step and multi-step protocols of DNA isolation from lysed sputum samples containing the *Mycobacterium tuberculosis complex* has been compared. DNA was isolated using spin-cartridges containing a special silica-based sorbent modified with fluoroplast and polyaniline, or using an automated isolation system. One-step isolation using the obtained sorbent has been shown to ensure a significantly lower DNA loss and higher sensitivity in the PCR detection of *Mycobacterium tuberculosis* as compared to a system based on sorption and desorption of nucleic acids during the isolation.

KEYWORDS composite sorbents; DNA isolation; PCR diagnostics; *Mycobacterium tuberculosis complex*; fluoropolymers; polyaniline.

INTRODUCTION

Purified preparations of nucleic acids isolated from different biological sources are increasingly used in biomedical studies (e.g., in sequencing, as immunomodulating or anticancer agents, in designing drug delivery vehicles, etc.), especially in medical diagnosis and bioassay, largely owing to the successful development of PCR technology. The efficiency of sample preparation techniques depends on the development of rapid and reproducible methods for the isolation of DNA that is readily suitable for PCR diagnostics. Various methods for nucleic acid isolation have been described; commercial kits suitable for isolation are available and being used both to solve research problems and in clinical practice. The use of silica particles for DNA sorption in the presence of chaotropic salt was first proposed as early as 1979 [1]. In 1990, the method was improved [2] and some variations are used to this day. Nucleic acid isolation methods using magnetic particles based on silica [3], fibers modified with silica particles [4], affine silica particles [5], etc., are widely used.

Methods of biopolymers separation and isolation are typically based on the differences in the solubilities of nucleic acids, proteins, and polysaccharides. These methods are based on “capturing” the target biopo-

lymer from a mixture with a sorbent and retaining it during the first stage of separation, removing impurities, and eluting the target component from the sorbent surface during the following stages. Thus, the isolation procedures are multi-step, laborious, time-consuming, difficult to automate, and do not always ensure sufficient purity of the isolated DNA for effective PCR assay. The latter generally depends on the presence of PCR inhibitors in the sample (e.g., heme in blood samples, various types of chlorophyll in plant tissue lysates, humic acids in soil samples, etc.).

The one-step extraction scheme is obviously more attractive and promising. In this case, the isolated (and simultaneously purified) biopolymer passes through the sorbent layer without retention on its surface, while the impurities hindering PCR are effectively retained by the sorbent. Several years ago, we developed a one-step procedure for DNA isolation which is based on using the unique sorption properties of certain polymers, namely fluoropolymer (FP) [6] and polyaniline (PANI) [7, 8]. Such polymer coatings formed, for example, on the porous silica surface do not retain DNA but adsorb the proteins and PCR-inhibitory components that are present in typical biological samples (plant or bacterial lysates, smears, plasma, blood, etc.).

We have developed several methods for synthesizing fluoropolymer- and PANI-containing composite sorbents based on various physical and chemical processes [9, 10]. Both the fluoropolymers and PANI being used as surface modifiers of sorbents make possible one-step isolation of nucleic acids from complex biological mixtures. However, each of these polymeric modifiers brings additional significant useful properties. Thus, fluoropolymer-containing sorbents are noted for exceptional chemical resistance, low nonspecific adsorption, and usually they provide the highest yield of DNA. In turn, the PANI-containing sorbents that have excellent wettability and high surface capacity can be successfully used to isolate DNA from “complex” biological mixtures (blood, plant tissue lysates, soil extracts, etc.), as well as to separate nucleic acids depending on their secondary structure.

In this regard, materials modified with both fluoropolymer and PANI nanolayers simultaneously are of particular interest. We have reported the successful application of such material for the one-step isolation of predominantly double-stranded DNA of the human hepatitis B virus and single-stranded DNA of the TTV virus (*Transfusion transmitted virus, Torque teno virus* is the virus that is transmitted during blood transfusion) suitable for PCR assay from human plasma samples [11]. However, the applicability of these sorbents for rapid extraction of human non-viral pathogen DNA from clinical samples remains insufficiently studied. This article discusses the use of a silica sorbent modified with a combination of FP and PANI nanolayers for one-step DNA extraction from inactivated clinical sputum samples containing different amounts of cells of human tuberculosis pathogens known under the common name “*Mycobacterium tuberculosis complex*” (MTC) and including the following mycobacterial species: *M. tuberculosis*, *M. bovis*, *M. bovis BCG*, *M. africanum*, *M. microti*, *M. canettii*, *M. caprae*, *M. pinnipedii*, and *M. mungi*.

The efficiency of one-step DNA extraction using cartridges containing the FP-PANI sorbent was compared with the automated multi-step method of isolation of DNA from MTC that was developed by the ZAO Syntol company (Moscow, Russia) based on a Tecan Freedom EVO ® PCR robotic station (Tecan Trading AG, Switzerland).

EXPERIMENTAL

Aniline (extra-pure grade, Aldrich, Germany) was distilled, and a fraction with n_D^{20} 1.5863 was collected in a temperature range of 182–184°C. Ammonium persulfate (Rotipuran ®, Germany), hydrochloric acid, ethanol (reagent grade, Aldrich, Germany), and water (Milli Q standard) were used.

DNA of tuberculosis mycobacteria was isolated from sputum samples using plastic spin cartridges containing 100 mg of the Si-500-FP-PANI sorbent and a Tecan Freedom EVO ® PCR automated robotic station (Tecan Trading AG, Switzerland) that was adapted to the M-Sorb-Tub-Avtomat kit (ZAO Syntol, Russia) used for automated DNA isolation. Sputum samples were lysed using reagents supplied with the AmpliTub-RV kit (ZAO Syntol, Russia), intended for qualitative and quantitative determination of *Mycobacterium tuberculosis complex* using real-time PCR (lysis reagent B+, diluent, inactivating reagent A).

In this work, we used the following additional equipment: the Tsiklotemp-903 centrifuge for microtubes; a Tsiklotemp-303 thermostat; a Tsiklotemp-901 microcentrifuge shaker for microtubes (all equipment manufactured by ZAO Tsiklotemp, Russia); 20, 200, and 1000 µl variable volume micropipettes; a 1.5-ml test tube holder; 1.5 ml microtubes; and micropipette tips.

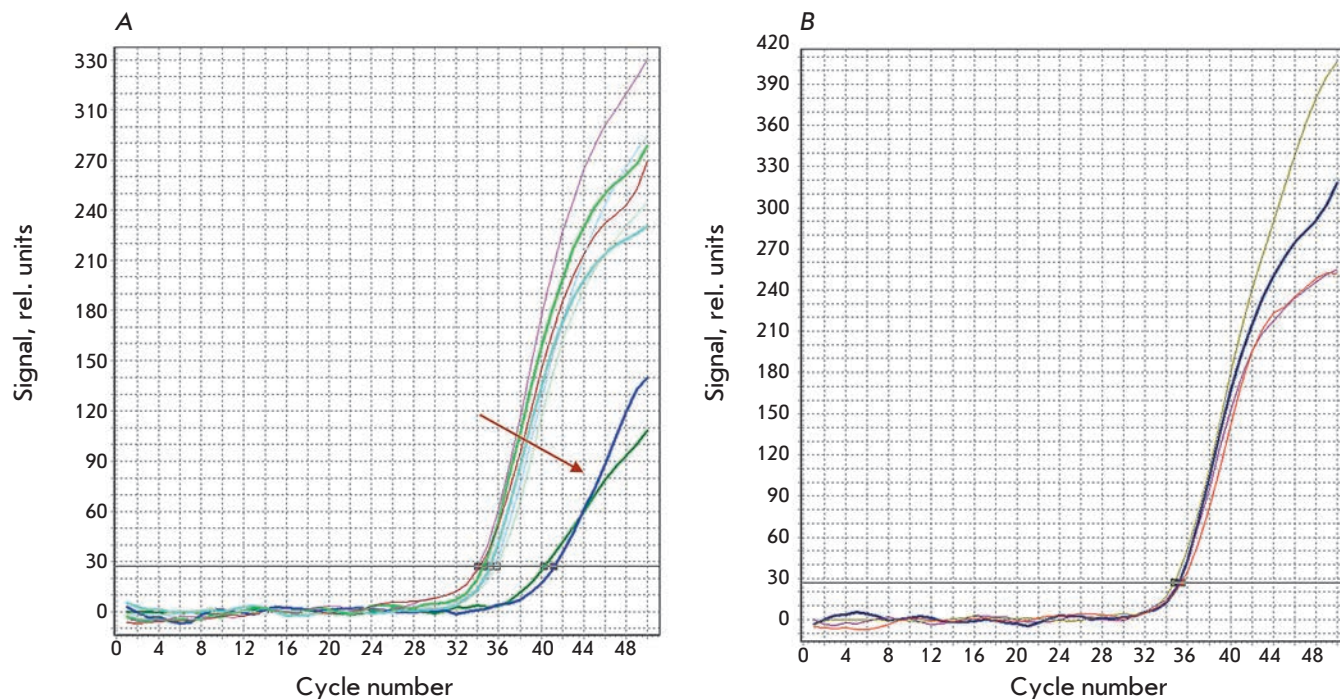
Preparation of the FP-PANI sorbent

Si-500 silica (100 g) was vacuumized in a special reactor for 30–40 min, and then 500 ml of a 0.016% FP solution in acetone was added to the silica. The reactor containing the suspension of silica particles was incubated in an ultrasonic bath at atmospheric pressure for 15 min. The solvent was then removed on a rotary evaporator at 40–45°C. Another portion of the polymer solution in acetone (500 ml) was injected into the reactor, and the manipulations following the injection of the first portion of the polymer solution were repeated. The resulting product was dried in vacuo to a constant weight and used as a matrix during the oxidative polymerization of aniline as described in [11].

Protocol for isolation of mycobacterial DNA using cartridges containing the FP-PANI sorbent

Inactivation. Model and clinical sputum samples were used in the experiments. 500 µl of the inactivating reagent A was added to 500 µl of sputum containing 600 CFU of MTC/ml (in particular, *M. tuberculosis*, *M. bovis*, *M. bovis BCG*, etc.) to inactivate model samples. All clinical samples were pre-inactivated as well: the inactivating reagent A was added to the sputum samples collected in 50-ml test tubes to a final volume of 40 ml. The contents of the test tube were mixed by gently turning the test tube over until complete homogenization, and then they were incubated for 30 min. The tubes were centrifuged (15 min at 3500 rpm). The supernatant was discarded; the precipitate was re-suspended and transferred into 1.5-ml tubes.

Lysis. The tubes with the test material were centrifuged (5 min at 13,000 rpm); the supernatant was discarded, and 100 µl of the lysis reagent B+ was added.



The results of real-time PCR of the mycobacterial DNA isolated from the model sputum lysates using the FP-PANI sorbent and containing 600 CFU/ml. A – the arrow points to the curves obtained using samples that were not purified on the sorbent (original lysates); B – red and brown curves – samples purified using the FP-PANI sorbent; blue curve – the original lysate sample after dilution without further purification using the FP-PANI sorbent

The contents of the tubes were thoroughly mixed in the microcentrifuge shaker and incubated for 10 min at 75°C. The tubes were centrifuged in the microcentrifuge for 15 seconds. The DNA obtained was used for PCR using AmpliTub-RV (for manual DNA extraction) and M-Sorb-Tub-Avtomat (for automated DNA extraction) reagent kits for the detection of a *Mycobacterium tuberculosis* complex.

DNA purification. 400 µl of the diluent was added to the sample tubes and stirred. The contents of the tubes were applied by gentle pipetting on the sorbent cartridges that were inserted into the collector tubes. The cartridges were centrifuged for 1 min at 4,000 rpm and then removed from the collectors.

Real-time PCR. Real-time PCR was performed using an ANK-32 analyzer (Institute for Analytical Instrumentation of the Russian Academy of Sciences, Russia) and the appropriate algorithm developed by ZAO Syntol. The diagnostics method used allows one to detect the presence of specific DNA fragments from the IS6110 gene in the sample, which is present in multiple copies in most MTC strains, but may be absent in the genome of *M. tuberculosis*. At the same time, the method allows one to determine the amount of *regX*, a specific DNA

fragment which is represented by a single copy in the MTC genome.

Conditions for the PCR using the isolated DNA were identical.

RESULTS AND DISCUSSION

Experiments aimed at isolating mycobacterial DNA from a control model and clinical sputum samples were performed at ZAO Syntol (Moscow, Russia). We compared the efficiency of the two methods of DNA isolation from lysed sputum samples: using a FP-PANI sorbent containing cartridges, and using the automated isolation system produced on the basis of Tecan Freedom EVO® PCR robotic station (Tecan Trading AG, Switzerland). In the latter case, the procedure of DNA isolation was based on the adsorption of the nucleic acid molecules of a tuberculosis pathogen on oligonucleotide-coated magnetic particles. The nucleotide sequence of these oligonucleotides was complementary to the target sequence in the pathogenic DNA. As a result, the pathogenic DNA binds complementarily to the matrix surface under the conditions provided by the system. The impurities not bound to the magnetic particles are then removed automatically (including DNA

Table 1. Threshold cycle values and the calculated number of DNA copies in the model samples after real-time PCR

Sample	Threshold cycle, Ct	Calculated number of DNA copies
Original lysate	40.2	0.4
Original lysate	41.03	0.22
Diluted lysate	35.23	13.72
1	35.28	13.19
2	34.27	27.10
3	33.77	38.50
4	33.70	40.41
5	35.69	9.84
6	35.28	13.19
7	35.04	15.69
8	34.66	20.48
9	35.08	15.24
Control dilutions		
10,000,000	16.20	9.948E6
100,000	21.58	2.193E5
1000	29.14	1026.34
100	32.45	97.94

Note. 1–9 – The model sputum samples containing 600 CFU/ml after passing through the cartridge containing the FP-PANI sorbent.

that does not contain the target sequence), and the purified DNA is eluted from the surface of the magnetic particles. In such a way, the multi-step process of DNA isolation is implemented in the automated system. On the contrary, one-step isolation of bacterial DNA takes place when the FP-PANI sorbent is used. The isolated DNA samples were analyzed by real-time PCR. In this way, the efficiency of the amplification of PCR fragments of DNA was assessed after one-step isolation using the FP-PANI sorbent and after multi-step automated isolation. Model sputum samples containing 600 CFU/ml and clinical samples obtained from randomly selected patients were investigated.

The results of model samples testing are shown in the *Figure* and *Table 1*. The *Figure* shows that the efficiency of the amplification of the PCR DNA fragments that were not subjected to further purification on the cartridges with the sorbent (i.e., the original unpurified lysates) was significantly lower (curves shown by an arrow in *Fig. A*, “original lysate” sample in *Table 1*). However, the efficiency of the amplification is improved after dilution of these samples (due to the reduction in the relative concentration of PCR inhibitors in the test sample), and the number of PCR fragments becomes comparable to that of the amplicons obtained using the DNA samples that were purified using the FP-PANI sorbent (*Fig. B*, “diluted lysate” sample in *Table 1*). The control values of the threshold cycle and the relative concentrations of DNA in the samples with a known amount of DNA (10^7 , 10^5 , 10^3 , and 10^2 CFU, respectively) are also shown in *Table 1*. It can be seen that the use of the FP-PANI sorbent does not reduce the sensitivity of PCR detection and allows one to identify about 10

Table 2. Number of PCR fragments of DNA from the *M. tuberculosis complex* after the cartridge and automated isolation of DNA from the clinical samples

Sample	Number of DNA, copies/volume		
	Cartridges, 10 μ l	Automated isolation, 25 μ l	Automated isolation, after dilution
1	4579	3254	325
2	65	Not determined	Not determined
3	5006	3572	357
4	Not determined	Not determined	Not determined
5	733220	23693	2369
6	98	3	< 1
7	12	2	< 1
8	178	32	3

copies of the analyzed DNA in the sample. Therefore, the FP-PANI sorbent provides effective removal of PCR inhibitors and maintains the original amount of DNA in the test sample. Based on these data, we can assume that FP-PANI-containing material is efficient for one-step isolation of DNA from clinical samples and provides purified preparations of nucleic acids that are suitable for PCR analysis.

The amounts of DNA extracted from clinical samples using a FP-PANI sorbent and an automated system were compared to confirm this assumption. The amount of starting material for the automated system was 2 times higher than the amount taken for the isolation on cartridges. However, given that only half of the volume taken is used during the automated isolation, the amount of starting material is comparable in both cases. When using the automated system, the final volume of the DNA solution was fourfold lower, and the amount required for PCR was 2.5 times higher than that in the case of DNA isolation on cartridges. Thus, the amount of DNA for PCR in the automated system is 10 times higher than the amount of DNA for PCR after manual isolation using cartridges.

Table 2 shows the number of PCR fragments of DNA from mycobacteria obtained when analyzing clinical samples by both methods and the amount of DNA determined by automated amplification with allowance for dilution.

It follows from the results shown in Table 2 that the efficiency of automated DNA extraction was 3 to 7% comparable to the extraction using the FP-PANI sorbent.

Therefore, the use of a sorbent modified with a combination of FP and PANI nanolayers substantially reduces DNA loss and provides for a much more sensitive detection of *M. tuberculosis* DNA as compared to the system based on absorption and desorption of nucleic acids during the isolation.

CONCLUSIONS

The methods for isolating nucleic acids from biological mixtures usually involve three different physicochemical processes: extraction, precipitation or adsorption of the target component (nucleic acid) on the sorbent surface, followed by washing of impurities and desorption. These procedures are laborious and often result in a significant loss of the nucleic acid being isolated.

The one-step scheme of nucleic acid isolation using special sorbents seems to be an efficient alternative to multi-step protocols. In this method, the nucleic acid is not retained by the sorbent, while the impurities contained in the original mixture (especially PCR inhibitors) are firmly adsorbed. Due to the unique sorption properties of some synthetic polymers, such as fluoropolymers and PANI, it was possible to develop several composite sorbents that provide one-step isolation of nucleic acids from complex biological mixtures. These sorbents are characterized by a high selectivity when separating nucleic acids and proteins. It is of particular interest to study the sorption properties of a sorbent sequentially modified with FP and PANI nanolayers. This material combines high chemical resistance due to the presence of a fluoropolymer coating and high sorption capacity, determined by the properties of PANI coating.

This paper demonstrates that a sorbent modified with a combination of FP and PANI nanolayers efficiently removes PCR inhibitors and preserves the initial amount of DNA in the sample, as shown by the isolation of *M. tuberculosis* DNA from clinical sputum samples. Due to this fact, high sensitivity in the detection of *M. tuberculosis complex* DNA can be achieved as compared to a system based on absorption and desorption of nucleic acids during isolation. ●

This work was partially supported by a grant from the European Committee DIAGNOSIS (contract № LSHB-CT-037212).

REFERENCES

- Vogelstein B., Gillespie D. // Proc. Natl. Acad. Sci. USA. 1979. V. 76. P. 615–619.
- Boom R., Sol C.J.A., Salimans M.M.M., Jansen C.L., Wertheim-van Dillen P.M.E., van der Noordaa J. // J. Clin. Microbiol. 1990. V. 28. P. 495–503.
- Park M.E., Chang J.H. // Mater. Sci. Eng. C. Biomimetic and Supramolecular Systems. 2007. V. 27. № 5–8. P. 1232–1235.
- Cady N.C., Stelick S., Batt C.A. // Biosens. Bioelectron. 2003. V. 19. P. 59–66.
- Craig J.M., Kraus J., Cremer T. // Hum. Genet. 1997. V. 100. P. 472–476.
- Kapustin D.V., Saburov V.V., Zavada L.L., Evstratov A.V., Barsamyan G.B., Zubov V.P. // Rus. J. Bioorgan. Chem. 1998. V. 24. P. 770–777.
- Kapustin D.V., Yagudaeva E.Yu., Zavada L.L., Zhigis L.S., Zubov V.P., Yaroshevskaya E.M., Plobner L., Leiser R.-M., Brem G. // Rus. J. Bioorgan. Chem. 2003. V. 29. P. 281–285.
- Yagudaeva E.Yu., Muydinov M.R., Kapustin D.V., Zubov V.P. // Russ. Chem. Bull. Int. Ed. 2007. V. 56. № 6. P. 1166–1173.
- Kapustin D., Prostyakova A., Bryk Ya., Yagudaeva E., Zubov V. // Nanocomposites and polymers with analytical methods / Ed. Cuppoletti J. Croatia: Intech 2011. P. 83–106.
- Kapustin D.V., Prostyakova A.I., Ryazantsev D.Yu., Zubov V.P. // Nanomedicine. 2011. V. 6. № 2. P. 241–255.
- Kapustin D., Prostyakova A., Zubov V. // Zing Conferences. Polymer Chemistry Conference. 12–16 November 2012. Cancun. Mexico. Stow Cum Quy, UK, 2012. P. 42.

The *Drosophila agnostic* Locus: Involvement in the Formation of Cognitive Defects in Williams Syndrome

E. A. Nikitina^{1,2*}, A. V. Medvedeva^{1,3}, G. A. Zakharov^{1,3}, E. V. Savvateeva-Popova^{1,3}

¹Pavlov Institute of Physiology RAS, nab. Makarova, 6, 199034, St. Petersburg, Russia

²Herzen State Pedagogical University, nab. r. Moyki, 48, 191186, St. Petersburg, Russia

³Saint-Petersburg State University, Universitetskaya nab., 7-9, 199034, St. Petersburg, Russia

* E-mail: 21074@mail.ru

Received 16.07.2013

Revised manuscript received 10.04.2014

Copyright © 2014 Park-media, Ltd. This is an open access article distributed under the Creative Commons Attribution License, which permits unrestricted use, distribution, and reproduction in any medium, provided the original work is properly cited.

ABSTRACT The molecular basis of the pathological processes that lead to genome disorders is similar both in invertebrates and mammals. Since cognitive impairments in Williams syndrome are caused by LIMK1 hemizygosity, could the spontaneous and mutant variants of the *Drosophila limk1* gene serve as a model for studying two diagnostic features from three distinct cognitive defects of the syndrome? These two symptoms are the disturbance of visuospatial orientation and an unusually strong fixation on the faces of other people during pairwise interaction with a stranger. An experimental approach to the first cognitive manifestation might be an analysis of the locomotor behavior of *Drosophila* larvae involving visuospatial orientation during the exploration of the surrounding environment. An approach to tackle the second manifestation might be an analysis of the most natural ways of contact between a male and a female during courtship (the first stage of this ritual is the orientation of a male towards a female and following the female with constant fixation on the female's image). The present study of locomotor activity and cognitive repertoire in spontaneous and mutant variants of the *Drosophila agnostic* locus allows one to bridge alterations in the structure of the *limk1* gene and behavior.

KEYWORDS Williams syndrome; LIMK1; *Drosophila*; locomotor activity; learning; memory.

ABBREVIATIONS CRSC – conditioned reflex suppression of courtship; LI – learning index; CI – courtship index.

INTRODUCTION

Over the past 20 years, Williams Syndrome has been regarded as one of the most attractive models for establishing a direct relationship between the genes, brain, and behavior [1, 2]. The syndrome results from a 1,500 kb deletion at 7q11.23, whose specific architecture predisposes to unequal recombination. The deletion affects approximately 20 genes; their hemizygosity manifests as a developmental anomaly characterized by cardiovascular problems, “elfin” facial features, and several typical neurological anomalies and cognitive characteristics [3]. LIM-kinase 1 hemizygosity (LIMK1 is the key actin-remodeling enzyme) causes cognitive impairments. They are characterized by a triad of signs: 1) a pronounced defect in visuospatial orientation; 2) a verbal linguistic defect of intermediate severity, which varies depending on the linguistic complexity of a certain culture; and 3) unusually strong gaze fixation on faces.

Experiments on higher animals are extremely expensive; hence, simple animal models are needed to explore for and test drugs capable of correcting these disorders.

Can *Drosophila melanogaster* be used for this purpose? On the one hand, the functions of human disease genes are often identified from the way mutations manifest themselves in the *Drosophila* gene when its sequence is identical to that in the human gene. On the other hand, all the genes that reside in mammals in a single critical region being deleted in Williams syndrome are known in *Drosophila* (let us remind readers that the *frizzled-9* gene was first described in *Drosophila*). Despite the different evolutionary organization of the *Drosophila* genome when these genes localize on different chromosomes, the effect of a certain gene in the emergence of Williams syndrome can be analyzed if it meets the following criteria: 1) mutations of this gene must be known, while their hemizygosity would cause a mutant phenotype in *Drosophila*; 2) the architecture of the *Drosophila* gene locus may predispose to the emergence of chromosomal rearrangements due to unequal recombination; and 3) the gene locus must be characterized by increased recombination frequency, which may result in spontaneous generation of deletions or other rearrangements. This effect must

manifest itself as a polymorphism in wild-type stocks that is specific to this region. The *agnostic* locus carrying the gene encoding LIMK1, which has been detected and characterized by us, meets all these criteria.

The *agnostic* locus was found in the 11 B of the X chromosome using targeted gene screening of temperature-sensitive (*ts*) mutations induced by ethyl methanesulfonate (EMS), which had the potential to inhibit the activity of enzymes of cAMP synthesis and decay [4]. Mutant *agn^{ts3}* fruit flies exhibit an unusually high activity of Ca²⁺/calmodulin-dependent phosphodiesterase 1 [5]. Flies with a heterozygous *Df(1)368* deletion (exposing this locus) and *Df(1)112* deletion (isolated according to the trait of its lethality when combined with *agn^{ts3}*) also die during development at 29°C; i.e., the mutant phenotype manifests itself in hemizygous individuals (similar to that in Williams syndrome). Molecular genetic studies have showed that the *agnostic* gene encodes LIMK1 enzyme containing a repeat of two LIM domains flanked by extensive AT-rich repeats (The National Center for Biotechnology Information, NCBI). Unequal recombination is observed in this region more frequently, causing a strongly pronounced polymorphism in the wild-type stocks *Canton-S* (*CS*), *Berlin*, and *Oregon-R* (*Or-R*) [6–8].

Thus, due to its structure and nucleotide environment, the *agnostic* gene may act as a genetic reserve of polymorphism and can be used as a convenient model for genomic disorders, such as Williams syndrome. If this is true, can this model contribute to the analysis of two diagnostic symptoms of the triad of cognitive impairments in patients with Williams syndrome (disturbance of visuospatial orientation and unusual strong fixation on the faces of other people during pairwise interaction with strangers)?

The former question can be answered by analyzing the locomotor behavior in larvae, which simultaneously includes the exploration of the environment (inevitably involving visuospatial orientation) and larvae feeding (achieved when larvae move over the substrate). The latter problem can also be solved by analyzing the natural contact between an adult male and an adult female during the sexual ritual. The first stage of this ritual is the orientation of a male towards a female and following the female with constant fixation on the female's image

In this study, we showed the changes in the parameters of locomotor activity in larvae and abrupt alterations in tracks during spatial orientation in *Oregon-R* and *agn^{ts3}* males. Imagoes of these stocks have significant learning and memory defects caused by a conditioned reflex suppression of courtship due to abruptly enhanced orientation towards a partner and following the partner.

EXPERIMENTAL

Drosophila stocks

We used stocks exhibiting polymorphism in the *agnostic* locus (region 11B of the X chromosome).

1. Wild-type stock *Canton-S* (*CS*), with temperature-sensitive (*ts*) mutation in the *agnostic* locus (*agn^{ts3}*) maintained in its genetic background.

2. Wild-type stock *Berlin* isolated from the natural Berlin population of *Drosophila melanogaster* and with a significant disturbance in the regulation of the *limk1* gene.

3. Wild-type stock *Oregon-R* (*Or-R*). PCR mapping of the *limk1* gene reveals a deleted fragment between the primers limiting the region containing both LIM domains and a portion of the PDZ domain.

4. *agn^{ts3}*, mutant in the *agnostic* locus containing the *limk1* gene, carrying a 1.7 kb insertion located approximately 1 kb away from the 3'-untranscribed region of the *limk1* gene in the region where the A/T-rich sequence localizes.

Studying the locomotor activity of larvae

The locomotor behavior of *Drosophila* larvae was studied using an original automated construction designed by G.A. Zakharov and T.L. Payalina (Pavlov Institute of Physiology, Russian Academy of Sciences) based on a setup for recording the locomotor behavior of *Drosophila* imagoes which was designed by N.G. Kamyshev *et al.* [9]. Round cameras 20 mm in diameter were used to record the locomotor behavior of larvae. Translocation of a larva was recorded using a Logitech Quick-Cam camera. To perform automated registration of the behavior, we used the original software developed by G.A. Zakharov and N.G. Kamyshev. The experiment duration was 1 h; the temperature in the chambers was 23–24°C.

In order to analyze the rest and motion periods, the total record was subdivided into quanta 1s long. The speed of a larva at this quantum was then calculated. If the resulting speed was lower than the threshold value (0.5 mm/s), it was assumed that the larva was resting during this quantum; otherwise, the larva was assumed to be moving. The neighboring quanta with the identical type of motion were combined, thus forming motion and rest periods.

In order to analyze the dynamics of locomotor activity parameters, the total record time was divided into 300s long intervals. Each rest or motion period was considered to belong to an interval at which it had started. The locomotor frequency (number of initiated locomotions per 100s) and the activity index (share of time spent moving) were also calculated for each interval. At least 25 larvae from each stock were analyzed. The

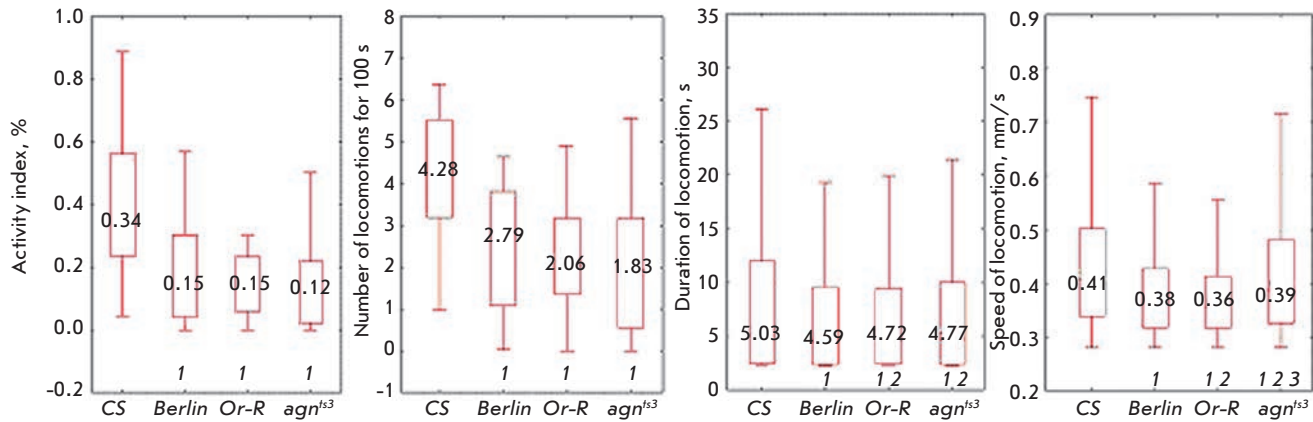


Fig. 1. Total parameters of locomotor activity in larvae. 1 – significant difference from CS, 2 – significant difference from *Berlin*, 3 – *agn^{ts3}* significant difference from *Or-R*. Kruskal–Wallis one-way analysis of variance with the subsequent multiple comparisons of average ranks for all experimental groups, $p < 0.05$

statistical significance of the differences between the experimental groups was determined using a Kruskal–Wallis dispersion analysis, followed by multiple comparisons of the mean ranks for all the experimental groups. Track distribution was compared using the paired t -test for the portions. The statistical significance of all differences was calculated for $p < 0.05$.

Assessment of the learning and memorization ability

In order to develop the conditioned reflex suppression of courtship (CRSC), a 5-day-old sexually inexperienced *Drosophila* male from the tested stock was placed in an experimental organic glass chamber (15 mm in diameter) with a fertilized 5-day-old *Canton-S* female and left for 30 min (training). Learning and memory abilities were tested immediately (0 min) and 3 h (180 min) after the training using new fertilized 5-day-old *Canton-S* females. Sexually inexperienced (naïve) males were used as a control. An ethogram of male's behavior was recorded for 300s the time when certain courtship elements (orientation, vibration, licking, a copulation attempt), as well as those not related to courtship (locomotion, preening, rest), had been started were written down. Recording was started 45s after a fruit fly was placed in the chamber. Specialized software (developed by N.G. Kamyshev) was used to decipher and analyze the data. The courtship index (CI) was calculated for each male; i.e., the time a male spent in courtship shown as a percentage of the total observation time. To qualitatively assess the learning results, we calculated the learning index (LI) using the formula:

$$LI = [CI_I - CI_T] / CI_I \times 100\% = (1 - CI_T / CI_I) \times 100\%,$$

where CI_I and CI_T are the mean courtship indices in independent samples of sexually inexperienced males and males who had been trained. Statistical processing of the results was conducted using a randomization analysis [10–12].

RESULTS AND DISCUSSION

Total differences in locomotor activity parameters

The activity index, shown in *Fig. 1*, is the most general parameter describing the locomotor activity of larvae.

CS has a higher activity index (0.34) compared with the other stocks. One can see it from the median value and from both quartiles. No statistically significant differences between the stocks *agn^{ts3}*, *Berlin*, and *Or-R* with respect to this parameter have been revealed. The activity index can be changed due to alterations in the locomotor frequency and duration. The interlinear differences in locomotion frequency are completely identical to those in the activity index. This means that changes in the activity index can be generally attributed to a decrease in locomotion frequency; however, locomotion duration can differ as well.

CS also differs from the rest of the stocks by this parameter. *CS* is characterized by a higher mean locomotion duration. Furthermore, *Berlin* differs from *Or-R* and *agn^{ts3}*, which was not observed when examining the activity index.

Speed of locomotion is another parameter; it is independent of the previously discussed ones. The highest speed of locomotion was also observed in *CS* larvae. *agn^{ts3}* occupies the second position and is followed by *Berlin* and *Or-R*. Both quartiles have the same distribution.

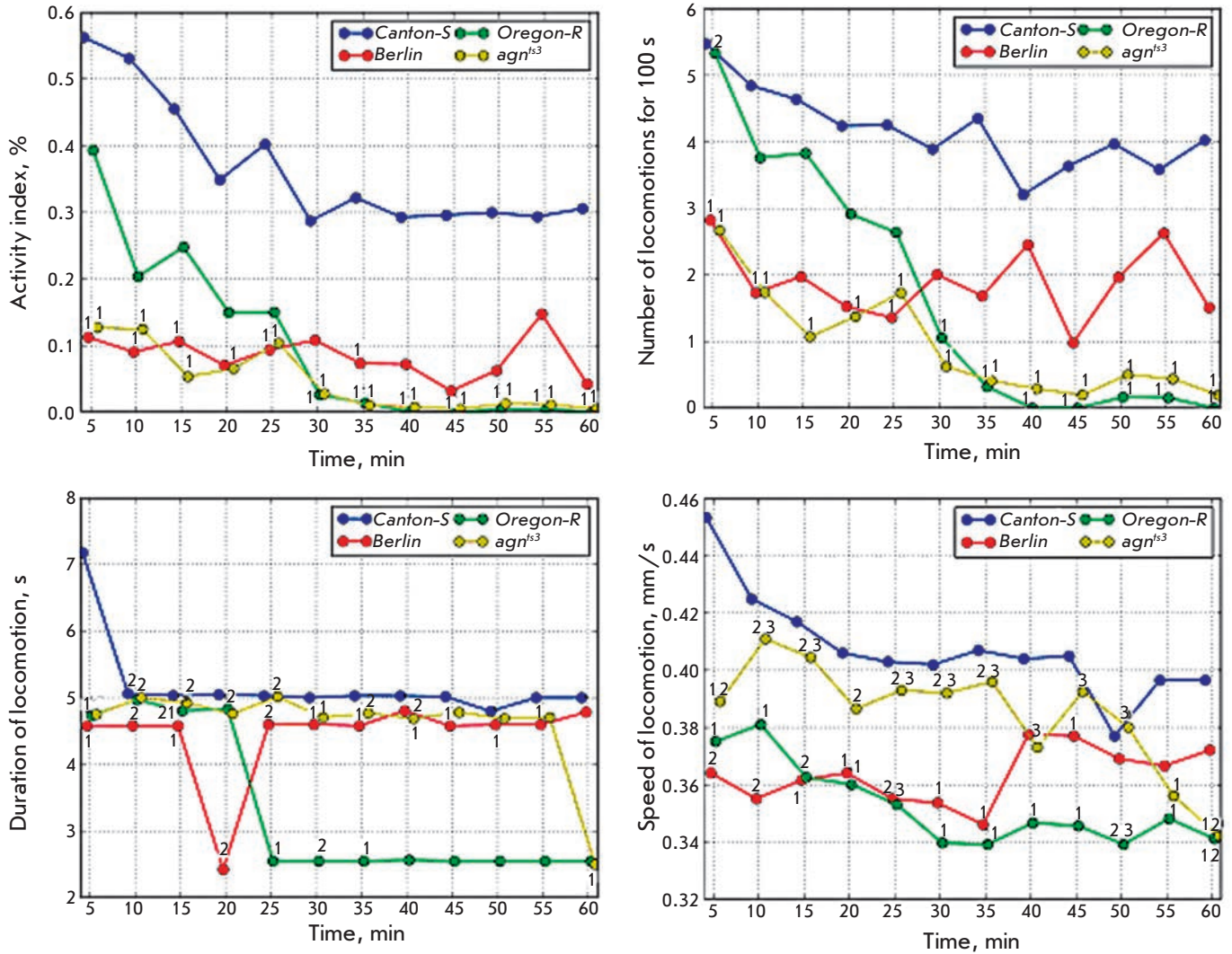


Fig. 2. Temporal dynamics of activity index and speed of locomotion in larvae. Points show the medians of distributions. 1 – significant difference from CS, 2 – significant difference from Berlin, 3 – *agn^{ts3}* significant difference from Or-R. Kruskal–Wallis one-way analysis of variance with the subsequent multiple comparisons of average ranks for all experimental groups, $p < 0.05$

Temporal dynamics of locomotor activity parameters

The temporal dependence of locomotor activity parameters is shown in Fig. 2. CS larvae actively move immediately after they are placed in experimental chambers. The median value of the activity index is ~ 0.55. Activity subsequently gradually decreases. Starting with the 40th minute, the median value of the activity index is 0.3 and further remains unchanged.

Berlin and *agn^{ts3}* larvae under normal conditions are characterized by a considerably lower mobility compared with CS larvae. The median activity index is 0.1–0.15. The differences are significant up to the 25th minute of the experiment and on the 35th minute. Af-

ter that, the differences disappear due to a drop in the activity of CS larvae. Mutant *agn^{ts3}* are characterized by an even lower activity; the differences from CS are statistically significant throughout the entire experiment. *Or-R* originally has a lower mobility compared to that of CS, although it is higher than that in *Berlin* and *agn^{ts3}*. The activity of *Or-R* larvae rapidly drops during the experiment; starting with the 30th minute, it significantly differs from the activity of CS larvae.

Now let us thoroughly discuss the parameters contributing to the alteration of the activity index. The dynamics of the locomotion frequency are similar to the dynamics of the activity index. CS is characterized by

an appreciably high locomotion frequency (the median value is $\sim 5.5 \times 10^{-2}$ Hz), which gradually decreases to reach $\sim 3.6 \times 10^{-2}$ Hz by the end of the experiment. *Or-R* at the beginning of the experiment has the same locomotion frequency as *CS* does (by the 5th minute of the experiment it is statistically higher than that of *Berlin* and *agn^{ts3}*). The locomotion frequency rapidly decreases and becomes lower than that in *CS* by the 30th minute of the experiment. *agn^{ts3}* is characterized by a lower locomotion frequency than *CS* throughout the entire experiment. *Berlin* originally has a lower locomotion frequency than *CS*; however, these differences disappear after the 25th minute.

Thus, *agn^{ts3}* is characterized by the greatest defects compared to the *CS*. There is also a difference in the dynamics of the activities of *Berlin* and *Or-R*. The lower mobility of *Or-R* is related to a rapid decrease in activity during the experiment. *Berlin* originally exhibits a lower activity. However, it decreases slower than that in *CS*; that is why the statistically significant differences disappear in the second half of the experiment.

The dynamics of locomotion duration were rather interesting. During the entire experiment, *CS* flies (except for the first 5 min) have a virtually constant locomotion duration (5 s). *Berlin* is also characterized by a constant locomotion duration (4.5 s; the differences are statistically significant until the 55th minute). The original locomotion duration of *Or-R* is identical to that of *CS* and significantly higher than that of *Berlin*. In the range between the 20th and 25th minute, the locomotion duration decreases abruptly and remains constant (2.5 s). Before the 55th minute, *agn^{ts3}* is characterized by the same locomotion duration as that of *CS*. The differences start being observed only on the 60th minute. In a series of points (5–15, 25, and 35 min), the locomotion duration in *agn^{ts3}* is statistically significantly higher than that in *Berlin*. No significant differences from *Or-R* were detected. In the beginning of the experiment, *CS* larvae have the highest speed of motion (~ 0.45 mm/s), which decreases appreciably rapidly and reaches 0.4 mm/s by the end of the experiment. *Berlin* is originally characterized by a lower speed of motion compared with *CS* (~ 0.36 mm/s). However, in this case the speed of motion does not decrease; instead, it slightly increases by the end of the experiment. Hence, starting with the 40th minute of the experiment, the differences between *Berlin* and *CS* disappear. *Or-R* is characterized by a lower speed of motion compared with *CS* throughout the entire experiment (0.38 mm/s in the beginning and ~ 0.34 mm/s by the end of the experiment). Statistically significant differences from *Berlin* were detected on the 50th and 60th minutes. The total speed of locomotion in *Berlin* and *Or-R* differs statistically significantly throughout the entire experi-

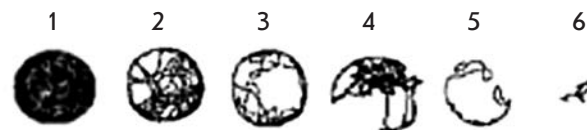


Fig. 3. Examples of track classes. 1 – complete coverage of all space available for movement in the experimental camera; 2 – insignificant defects of coverage; 3 – significant defects of coverage; 4 – distorted movement in space; 5 – strong defects of spatial movements; 6 – dramatic defects of movement in space

ment. *agn^{ts3}* is characterized by a high speed of locomotion. Between the 10th and 50th minutes, no differences with *CS* are observed. Differences with *Berlin* (55–15, 25–35, 60) and *Or-R* (10–50) are observed for a series of points.

Thus, examination of the temporal dynamics of locomotor activity parameters demonstrated that the activity index of larvae and the locomotion frequency coincide for the series *CS* → *Berlin* → *Or-R* → *agn^{ts3}*. The activity index in *Berlin* remains low during the entire experiment, while *Or-R* is characterized by a very rapid drop in the originally high activity index. *Or-R* exhibits the largest difference for the locomotion duration, while *agn^{ts3}* is closer to the wild-type stock. This cross-alteration of locomotion duration and frequency presumably leads to the absence of differences in the activity index between *Berlin*, *Or-R*, and *agn^{ts3}*. The speed of locomotion decreases in the series *CS* → *agn^{ts3}* → *Berlin* → *Or-R*.

Distribution over the shape of movement trajectories (tracks)

The visuospatial orientation ability (i.e., the ability of an animal to orient in the environment when performing exploration and the way an animal stops it with time) can be characterized by analyzing tracks (motion trajectories). All the tracks analyzed were subdivided into six classes. The characteristic shape of each class of tracks is shown in *Fig. 3*.

The distribution of larval tracks over classes has significant interlinear differences. The decrease in the number of class 1 tracks was most noticeable (\sim three-fold) in *Berlin*, *Or-R*, and *agn^{ts3}* as compared to *CS* (*Fig. 4*). The number of class 3 and 6 tracks increases statistically significantly in *Berlin*.

In *Or-R*, only the number of class 4 tracks increases reliably. A decreased number of class 2 tracks and a noticeable increase in the number of class 3 tracks is observed for *agn^{ts3}*.

Thus, each stock has its own defects of locomotor behavior. *Berlin* is characterized by a reduced activ-

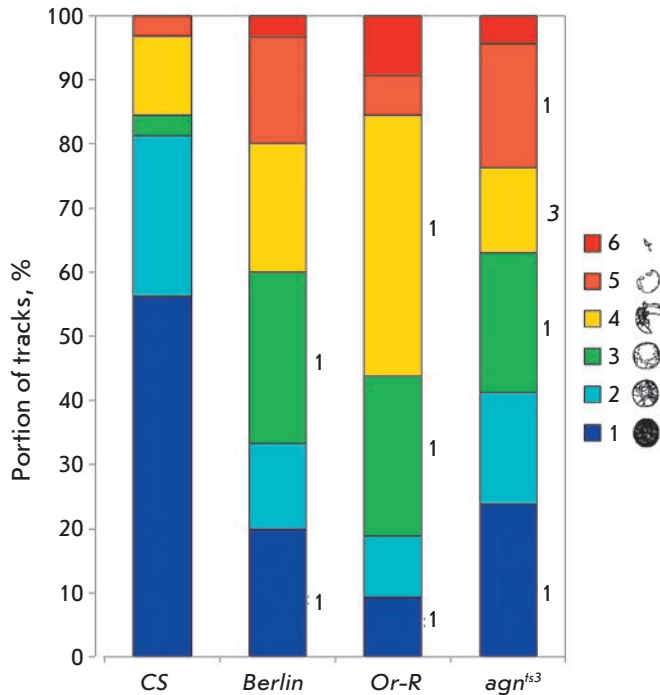


Fig. 4. Comparison of distributions of track classes. * – significant difference from CS, $p < 0.05$; 1 – significant difference from CS, 2 – significant difference from Berlin, 3 – *agn^{ts3}* significant difference from Or-R. Paired Student's *t*-test for shares, $p < 0.05$

ity index and disturbed track distribution. *Or-R* has a spontaneous activity defect: a rapid decrease in the activity index, while the speed of motion is retained. All these disturbances may attest to the significant defects in visuospatial orientation that are observed in *Berlin*, *Or-R*, and *agn^{ts3}*.

Studying the locomotor activity of imago and its contribution to cognitive abilities

Recording the behavior under conditioned reflex suppression of courtship allows one not only to calculate the learning index (LI) with allowance for all the elements of non-sexual (locomotor activity, preening, rest) and sexual behavior (orientation/following, wing vibration, tapping, licking, copulation attempt), but also to analyze the recorded behavioral ethograms individually for each parameter. *Figure 5* demonstrates that, as it was shown earlier, the learning processes and formation of medium-term memory (3 h) are dramatically disturbed both in *agn^{ts3}* mutants [8] and in *Oregon-R* males [13].

If one calculates the learning index with allowance for a random element of sexual behavior, it will be possible to determine why the learning and memorization defects develop. It turned out that suppression of orientation/following makes the key contribution to the total suppression of courtship. In terms of this parameter, *Oregon-R* and *agn^{ts3}* males were unable to learn:

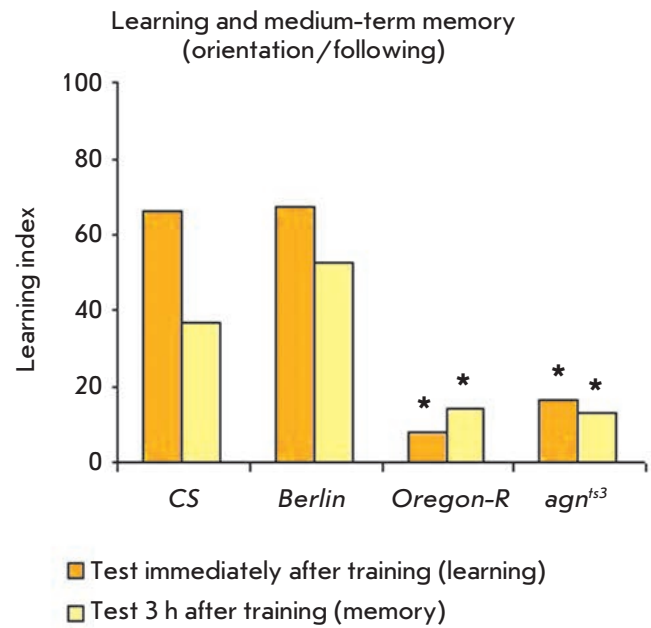
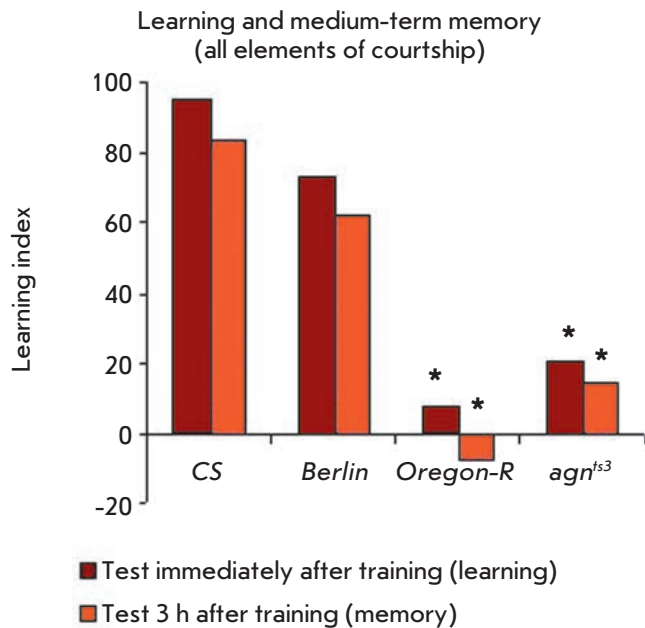


Fig. 5. Contribution of defects in orientation and following to learning and memory disturbances. * – significant difference from CS, $p < 0.05$, two-sided randomization test

the conditioned reflex suppression of courtship was not developed immediately after training. Three hours after the training, the learning index remained at the same level; it also differed statistically significantly from the LI in *Canton-S*. It is clear from Fig. 5 that learning and memory defects in *Oregon-R* and *agn^{ts3}* can be explained by a disturbed orientation/following behavior.

Let us discuss these processes more thoroughly, with a focus on such a parameter of locomotor behavior of imago during intrapair interactions as the locomotor activity of males not related to sexual behavior. Figure 6 shows that the locomotor activity in the control (naive *Oregon-R* and *agn^{ts3}* males) is statistically significantly higher than that in the wild-type *CS* stock. The activity levels were comparable with those in *CS* males immediately and 3 h after training.

As for the activity related to sexual behavior – orientation/following (intrapair interaction between a male and a female) – it is twice as low in *Berlin* and *Oregon-R* males but twice as high as that in wild-type *agn^{ts3}* males. This form of activity is expected to decrease abruptly after training, when conditioned reflex suppression of courtship is observed (an abrupt decrease in the share of activity related to sexual behavior and an abrupt increase in the share of usual locomotor activity). This actually is observed immediately after training in *CS*, *Berlin*, and *Oregon-R* males but not in mutant *agn^{ts3}* males, in whom the activity related to sexual behavior is fourfold higher than that in *CS* males, thus being indicative of a learning defect. Three hours after the training, when the orientation/following parameters may slightly decrease (like in *CS*), orientation/

following in *agn^{ts3}* fruit flies is twice as high as that of *CS*. The contribution of this component to the conventionally calculated courtship indices in the wild-type *CS* stock is 35% (learning) and 42% (memory); in the wild-type *Berlin* stock, 33% (learning) and 34% (memory); in the wild-type *Oregon-R* stock, 50% (learning) and 40% (memory); and in *agn^{ts3}* mutant, 85% (learning) and 83% (memory).

Thus, each stock is characterized by a typical ratio between two activity forms. This seems to provide a good opportunity to test the diagnostic symptom belonging to the triad of cognitive impairments in Williams syndrome: unusually strong gaze fixation on faces (in this case on a target courtship object). Furthermore, this analysis method allows one to take into account the learning component (individual experience). Let us remind the reader that in patients with Williams syndrome, the unusually strong hypersocialization (gaze fixation on strangers' faces) does not lead to tight contacts with peers, school friends, or making friends. In other words, a patient constantly addresses the same stimulus (the face), without properly interpreting the response.

The findings provide grounds for claiming that cognitive defects caused by insufficient suppression of orientation/following of a partner were found in *Oregon-R* and *agn^{ts3}* males. The orientation defects manifest themselves as early as in larvae; male larvae exploring the environment demonstrate abrupt disturbance of motion trajectories in space and temporal dynamics of the activity index, and the locomotion frequency of larvae.

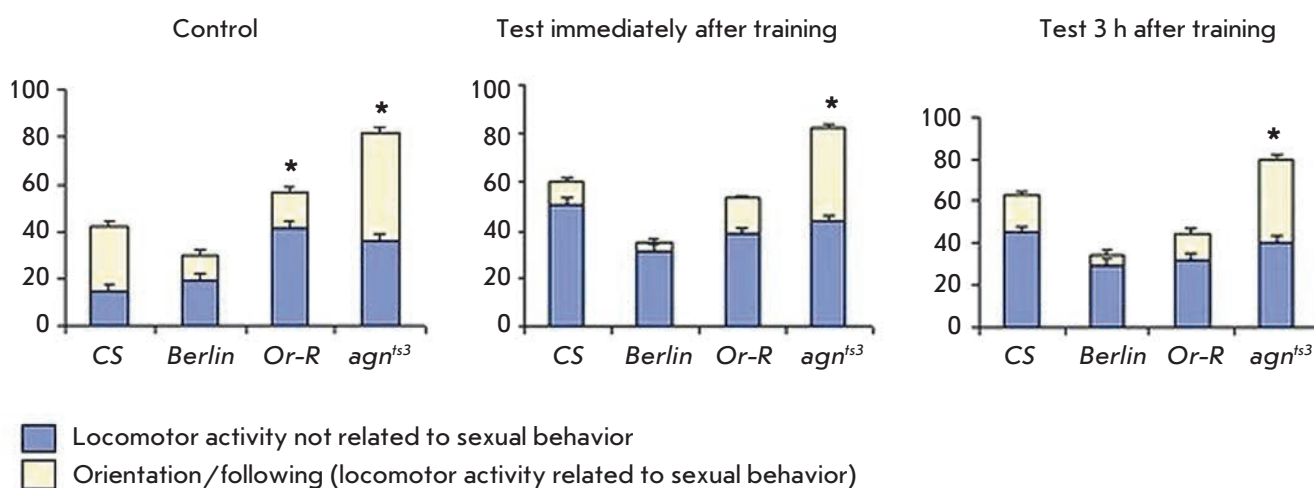


Fig. 6. Portions of locomotor activity connected and not connected to sexual behavior immediately and 3 h after training. * – significant difference from *CS*, $\alpha R \leq 0.05$, one-sided randomization test

CONCLUSIONS

Drosophila melanogaster stocks carrying different variants of the *agnostic* locus with changes in the regulatory and structural regions of the gene encoding LIM kinase 1 (LIMK1) were used to simulate the human deletion Williams syndrome. It is believed that hemizygosity for the *limk1* gene results in disturbance of motor functions, cognitive defects of visuospatial orientation, and strong gaze fixation on a partner [2].

Simulation of this syndrome with the involvement of mutant and spontaneous variants of the *agnostic* locus made it possible to reveal the effect of changes in the *limk1* gene structure on locomotor and cognitive manifestations, including changes in locomotor activity parameters in larvae and abrupt changes in tracks in *Oregon-R* and *agn^{ts3}* males during spatial orientation. Extensive training and memorization defects under conditioned reflex suppression of courtship are observed in imagoes of the same lines due to an abruptly increased orientation towards a partner and following it.

Based on the data obtained by sequencing the *limk1* gene from *Canton-S*, *Berlin*, *Oregon-R*, and *agn^{ts3}* stocks (the International Database of Genetic Data GenBank (<http://www.ncbi.nlm.nih.gov/Genbank/>), numbers Dlimk1_allforGenbank.asn.1 dmel-limk1-CantonS JX987486 Dlimk1_allforGenbank.asn.1 dmel-limk1-agnostict3 JX987487; Dlimk1_allforGenbank.asn.1 dmel-limk1-Oregon-R JX987488; Dlimk1_allforGenbank.asn.1 dmel-limk1-Berlin JX987489; Dlimk1_allforGenbank.asn.1 dmel-limk1-CantonS JX987486; Dlimk1_allforGenbank.asn.1 dmel-limk1-agnostict3 JX987487; Dlimk1_allforGenbank.asn.1 dmel-limk1-Oregon-R JX987488; Dlimk1_allforGenbank.asn.1 dmel-limk1-Berlin

JX987489)), one can assume that the defect of the LIM and PDZ domains in *Oregon-R* stock fruit flies is accompanied by changes in the locomotor behavior and abrupt cognitive impairment. The changes in the LIM and PDZ domains of LIMK1 also reduce both the visuospatial orientation and learning abilities. An insertion of S-transposon in the 3'-untranscribed region of the *limk1* gene in *agn^{ts3}* mutant also results in rather interesting outcomes. Mutant *agn^{ts3}* had defects in orientation ability and a significant impairment of the cognitive sphere, which was accompanied by LIMK1 hyperexpression [8, 14].

It should be mentioned that the results of our study lay the groundwork for developing a method for the rapid assessment of the effect of various pharmacological agents on the locomotor and cognitive ability of *Drosophila*. The proposed methods for recording the behavior of *Drosophila* larvae and imagoes can be used to search for drugs correcting locomotor and cognitive impairments. The celerity and relatively low cost of studies using *Drosophila melanogaster* make it a virtually ideal object for preliminary experimental testing of therapeutic drugs. The drugs that have passed through this stage can be moved to the next stage of testing using vertebrates, which are closer to humans.

The revealed relationship between mutational damage to the *agnostic* gene and defects in the locomotor and cognitive spheres make it possible to use this model to study genome diseases, and Williams syndrome in particular. ●

This work was supported by the Russian Foundation for Basic Research (grant № 12-04-01737-a) and the Presidium of the Russian Academy of Sciences (programs № 7 and 30).

REFERENCES

- Bellugi U., Adolphs R., Cassady C., Chiles M. Towards the neural basis for hypersociability in a genetic syndrome // *Neuroreport*. 1999. V. 10. № 8. P. 1653–1657.
- Järvinen-Pasley A., Bellugi U., Reilly J., Mills D.L., Galaburda A., Reiss A.L., Korenberg J.R. Defining the social phenotype in Williams syndrome: a model for linking gene, the brain, and behavior // *Dev. Psychopathol.* 2008. V. 20. № 1. P. 1–35.
- Pober B.R., Johnson M., Urban Z. Mechanisms and treatment of cardiovascular disease in Williams-Beuren syndrome // *J. Clin. Invest.* 2008. V. 118. № 5. P. 1606–1615.
- Savvateeva E.V., Kamyshev N.G., Rosenblum S.R. Receiving of temperature-sensitive mutations involving cyclic adenosine-3',5'-monophosphate metabolism in *Drosophila melanogaster* // *DAS USSR*. 1978. V. 240. P. 1443–1445.
- Savvateeva E.V., Kamyshev N.G. Behavioral effects of temperature-sensitive mutations affecting metabolism of cAMP in *D. melanogaster* // *Pharmacology, Biochemistry & Behavior*. 1981. V. 14. P. 603–611.
- Savvateeva-Popova E.V., Peresleny A.I., Scharagina L.M., Tokmacheva E.V., Medvedeva A.V., Kamyshev N.G., Popov A.V., Ozersky P.V., Baricheva E.M., Karagodin D., et al. Complex study of *Drosophila* mutants in the *agnostic* locus: a model for connecting chromosomal architecture and cognitive functions // *J. Evol. Biochem. Physiol.* 2002. V. 38. № 6. P. 706–733.
- Savvateeva-Popova E.V., Peresleni A.I., Sharagina L.M., Medvedeva A.V., Korochkina S.E., Grigorieva I.V., Dyuzhikova N.A., Popov A.V., Baricheva E.M., Karagodin D., et al. Architecture of the X Chromosome, Expression of LIM Kinase 1 and Recombination in the *agnostic* Mutants of *Drosophila*: A Model for Human Williams Syndrome // *Rus. J. of Genet.* 2004. V. 40. № 6. P. 605–624.
- Medvedeva A.V., Molotkov D.A., Nikitina E.A., Popov A.V., Karagodin D.A., Baricheva E.M., Savvateeva-Popova E.V. Systemic regulation of genetic and cytogenetic processes by a signal cascade of ac-tin remodeling: locus

RESEARCH ARTICLES

- agnostic in *Drosophila* // Rus. J. of Genet. 2008. V. 44. № 6. P. 771–783.
9. Bragina Y.V., Molotova N.G., Kamysheva E.A., Soboleva S.A., Kamyshev N.G. Identification of *Drosophila* genes showing late maternal effect // VOGiS Herald. 2007. V. 11. № 2. P. 436–444.
10. Kamyshev N.G., Iliadi K.G., Bragina J.V. *Drosophila* conditioned courtship: Two ways of testing memory // Learn. & Mem. 1999. V. 6. № 1. P. 1–20.
11. Kamyshev N.G., Iliadi K.G., Bragina Y.V., Savvateeva-Popova E.V., Tokmacheva E.V., Preat T. Identification of *Drosophila* mutant with memory defects after acquisition of conditioned reflex suppression of courtship // Neurosci. Behav. Physiol. 2000. V. 30. № 3. P. 307–313.
12. Sokal R.R., Rohlf F.J. Biometry. New York: Freeman W.H., 1995. 887 p.
13. Kaminskaya A.N., Nikitina E.A., Payalina T.L., Molotkov D.A., Zakharov G.A., Popov A.V., Savvateeva-Popova E.V. Effect of the LIM Kinase 1 Isoform Ratio on *Drosophila melanogaster* Courtship Behavior: A Complex Approach // Russian Journal of Genetics: Applied Research. 2012. V. 2. № 5. P. 367–377.
14. Medvedeva A.V., Zhuravlev A.V., Savvateeva-Popova E.V. LIMK1, the key enzyme of actin remodeling bridges spatial organization of nucleus and neural transmission: from heterochromatin via non-coding RNAs to complex behavior. In: Horizons in Neuroscience Research. 2010. V. 1. Ch. 4. P. 161–193.

Cell Models for the Investigation of the Role of the Mucin MUC1 Extracellular Domain in Metastasizing

M. S. Syrkina^{1,4*}, M. A. Rubtsov¹, D. M. Potashnikova², Y. D. Kondratenko¹, A. A. Dokrunova³, V. P. Veiko⁴

¹Department of Molecular Biology, M.V. Lomonosov Moscow State University, Leninskie Gory, 1/12, 119899, Moscow, Russia

²Department of Cell Biology and Histology, M.V. Lomonosov Moscow State University, Leninskie Gory, 1/12, 119899, Moscow, Russia

³Bioengineering Department, M.V. Lomonosov Moscow State University, Leninskie Gory, 1/12, 119899, Moscow, Russia

⁴A.N. Bach Institute of Biochemistry, Russian Academy of Science, Leninsky prospekt, 33/2, 119071, Moscow, Russia

*E-mail: krimsy@yandex.ru

Received 02.12.2013

Revised manuscript received 20.03.2014

Copyright © 2014 Park-media, Ltd. This is an open access article distributed under the Creative Commons Attribution License, which permits unrestricted use, distribution, and reproduction in any medium, provided the original work is properly cited.

ABSTRACT The speculations on the role of MUC1, a substance which is overexpressed in glandular cancer cells, on the metastatic potential of such cells are rooted in data that seem to indicate that cell malignization correlates with a change from the apical localization of mucin MUC1 to a peripheral one. Nonetheless, the role of MUC1 in cancer metastasizing remains far from clear. The major hurdle remains the absence of adequate cell models. The aim of the present study was to create cell models that present different fragments of the human mucin MUC1 extracellular domain on their surface. Genetic constructions were generated on the basis of the plasmid vector pEGFP-N3. These constructions contain fusion genes coding for chimeric proteins composed of different combinations of mucin MUC1 functional domains and identification markers (FLAG-epitope, located at the N-terminus, and EGFP, located at the C-terminus of the chimeric proteins). These constructions were used for a stable transformation of HT-29 human cancer cells. The transformants obtained were characterized by flow cytometry. The low expression level of endogenous mucin MUC1 and the high expression level of recombinant proteins were confirmed by real-time PCR. The microscopic examination of the transformed cells confirmed the membrane localization of the fusion proteins. The resulting cell models could be used to investigate the role of the mucin MUC1 domains in cancer cell metastasizing. The obtained cells are used as an applicable model of MUC1-expressing cancers and might be used to study the role of different functional fragments of mucin MUC1 in metastasizing.

KEYWORDS mucin; MUC1; cell models; HT-29; cancer; metastasis.

ABBREVIATIONS PCR – polymerase chain reaction; RT-PCR – polymerase chain reaction with reverse transcription; PBS – phosphate buffered saline; DPBS – Dulbecco's phosphate buffered saline; BSA – bovine serum albumin; GAPDH – glyceraldehyde-3-phosphate dehydrogenase.

Metastasizing, a process characterized by an increased ability of cells to invade and migrate through the endothelium, is considered to be one of the key processes underlying cancer development. The emergence of the ability to metastasize in tumor cells is usually associated with poor prognosis [1]. The molecular mechanisms of the processes that lead to changes in a cell's metastatic potential have been the subject of active investigation for several decades. It

has been established that the molecules that interact with the extracellular matrix [2, 3] or cell adhesion molecules [4, 5] are involved in these processes. One such molecule is human mucin MUC 1. Experimental data indicating that an increased expression of MUC 1 correlates with a reduced aggregating ability of cells in a culture [6] has prompted researchers to postulate that this glycoprotein magnifies the metastatic potential of tumor cells.

Membrane glycoprotein MUC 1 is normally located on the apical surface of the epithelial cells that line the airways and ducts of glands and performs the functions of moisturizer and lubricant. The expression of the MUC1 gene increases in malignant, transformed cells [7–9]; cellular localization [10, 11] and the glycosylation pattern of mucin MUC 1 changes [12].

There are several functional domains in the mucin MUC 1 structure: an extracellular, a transmembrane, and a cytoplasmic one. The data on the influence of the different MUC 1 domains on the metastatic potential of tumor cells are rather contradictory [13–15]. Only the role of the cytoplasmic domain has been established rather unequivocally: the signaling pathways this fragment participates in and the intracellular molecules it interacts with have been identified [16–18]. However, the functional role of the MUC 1 extracellular domain in this process is not entirely clear, although it is known that the changes in the mucin molecule in the course of malignant cell transformation basically affect its extracellular region. A change in the glycosylation pattern of the mucin MUC 1 extracellular domain in tumor cells leads to the formation of tumor-specific antigenic epitopes. It is assumed that the glycosylation pattern of mucin can significantly affect the tumor cell invasiveness. Thus, it has been shown that the carbohydrate components of tumor-associated (but not “normal”) mucin MUC 1 are able to bind the selectins produced by activated endothelium cells [19]. In turn, the selectins mediate the interaction with the receptors on the endothelial cell surface, which apparently promotes the attachment of a metastatic cell to the vessel

wall and subsequent invasion. Furthermore, metastatic cells are characterized by the presence of certain glycosidic epitopes [20, 21]. The glycoside epitopes sialyl Lewisia (sLea) and sialyl Lewisx (sLex) have been identified for MUC 1; their presence is associated with the metastasizing ability of cells. In particular, it has been shown that the sLea content gradually increases during the neoplastic transformation of intestinal cells [22]. Increased amounts of dimeric forms of sLex were also found in subpopulations of lung adenocarcinoma cells demonstrating a considerable ability to form colonies in the lungs of athymic mice [23]. These data indirectly attest to the participation of the mucin MUC 1 extracellular domain in the amplification of the metastatic potential of tumor cells in mammals.

Nevertheless, it remains impossible to study the effect of the MUC 1 extracellular domain on tumor cells metastasizing without adequate cell models. Cell models of aggressive forms of MUC 1-expressing cancers can be used to test both anticancer drugs and diagnostic tools aimed at recognizing the extracellular fragment of mucin MUC 1.

Since expression of mucin MUC 1 is typical of most epithelial tumors, the development of such agents could cover a wide range of cancer diseases.

EXPERIMENTAL

Materials

We used salts purchased from Merck (Germany) and salts of domestic production (special purity grade); components for microbiological media (Difco, USA);

Table 1. Sequences of oligonucleotides used in this work

Name	5'→3' sequence
FLAG_F	AGCTTGACTACAAGGACGATGACGATAAGA
FLAG_R	AGCTTCTTATCGTCATCGTCCTTG TAGTCA
USTR_F	ACGTCTCGAGATGACACCGGGCACCCAGT
TM_F	TGGGGGATCCGTGCCAGGCTGGGGCAT
TM_F(2)	AAGCTTGTGCCAGGCTGGGGCAT
CT_R	ACGTGGATCCCCAAGTTGGCAGAAGTGGC
TM_R	GCTAGGATCCGCACTGACAGACAGCCAAGGC
USTR_R	TGACAAGCTTCCCCAGGTGGCAGCTGAA
GAPDH_F	CAAGGTCATCCATGACAACCTTTG
GAPDH_R	GTCCACCACCCTGTTGCTGTAG

agarose; enzymes and kits for PCR, RT-PCR, real-time PCR, extraction of DNA fragments from agarose gel and isolation of the plasmid DNA, as well as DNA and RNA markers (Thermo Scientific, USA), TR Izol (Sigma, USA), and DEPK (Sigma, USA).

Cell-culturing was performed using a Dulbecco's modified Eagle's medium (DMEM), Versen solution, trypsin solution (PanEco, Russia), fetal calf serum (Hyclone, USA), antibiotics geneticin (G418), penicillin, and streptomycin (Sigma-Aldrich, USA).

Bacterial strains and cell cultures

The *Escherichia coli* JM110 strain (e14-[F 'traD36 pro-AB + lacIq lacZΔM15] hsdR17 (rK-mK +)) came from the collection of the State Research Institute of Genetics and Selection of Industrial Microorganisms ("Genetika"). We used human cell cultures of breast cancer (MCF-7), cervical cancer (HeLa), and colorectal adenocarcinoma (HT-29).

Synthetic oligonucleotides

The oligonucleotides used were synthesized by OOO DNK-Sintez; their sequences are listed in Table 1.

RNA isolation from cell culture

The cells washed with DPBS were pelleted by centrifugation (4 min, 1000 rpm) and re-suspended in 1 ml of the TR Izol reagent. 200 μl of chloroform was added; the pellet was stirred and incubated for 2–3 min at room temperature, then centrifuged (15 min, 13,000 rpm, +4°C), and the upper aqueous phase was collected in a clean tube. An equal volume of isopropanol was added; the mixture was incubated for 10 min at room temperature whereupon nucleic acids were precipitated by centrifugation (10 min, 13,000 rpm, +4°C). The pellet was washed with 75% ethanol, dried, and dissolved in water containing 0.1% DEPK. DNA was removed by digestion with DNase I following the manufacturer's recommendations.

cDNA synthesis

cDNA was synthesized by the reverse transcription technique using a RevertAid First Strand cDNA Synthesis Kit (Thermo Scientific, USA) following the manufacturer's recommendations.

RNA isolated from a MCF-7 cell line and the specific primers USTR_R for cDNA(ustr) and CT_R for cDNA(tmct) were used to obtain cDNA fragments coding for the functional fragments of mucin MUC 1.

RNA isolated from HeLa and HT-29 cells was used to obtain cDNA. cDNA (GAPDH) was obtained using GAPDH_R oligonucleotide. cDNA (MUC 1) was prepared using the oligonucleotide TM_R; cDNA (rMUC 1), using FLAG_R oligonucleotide.

Preparation of DNA fragments encoding mucin MUC 1 functional fragments

The oligonucleotides for producing mucin gene fragments were chosen after the cDNA sequence of human mucin MUC 1 had been analyzed [24].

The *Ustr* fragment was obtained by PCR with cDNA(ustr) and the primers USTR_F and USTR_R; the *tmct* fragment was obtained by PCR with cDNA(tmct) and the primers TM_F and CT_R; the *tm* fragment was obtained by PCR with cDNA(tmct) and the primers TM_F (2) and TM_R. The PCR products were separated by electrophoresis in 1% agarose gel and extracted from the gel using a GeneJET Gel Extraction Kit (Thermo Scientific, USA). The resulting fragments were cloned into the vectors pUC18 – *ustr* at the restriction sites XhoI and HindIII; *tm*, at the restriction sites HindIII and BamHI; and *tmct*, at the restriction site BamHI. The following plasmids were obtained: pUC18-USTR, pUC18-TM, and pUC18-TMCT. Correspondence of the nucleotide sequences of the cloned fragments to the expected ones was confirmed by sequencing.

The *Tr21* fragment was obtained using the technique developed to produce fragments containing different numbers of tandem repeats from the VNTR region of the human MUC1 gene [25], and it was cloned into the vector pUC18 – TR21 (at the restriction sites HindIII and BamHI).

Production of expression vectors containing different fragments of the mucin MUC1 gene

Assembly of the plasmids was performed on the basis of vector pEGFP-N3 (Clontech, USA). The *f* fragment was obtained by annealing the oligonucleotides FLAG_F and FLAG_R.

The vector pUSTR-TR-TMCT-EGFP was obtained by sequential cloning of the fragments *ustr* (at the restriction sites XhoI and HindIII), *tr21* (at the restriction sites HindIII and BamHI), *tmct* (at the restriction site BamHI), and *f* (at the restriction site HindIII). Vector pUSTR-TM-EGFP was obtained by sequential cloning of the fragments *ustr* (at the restriction sites XhoI and HindIII), *tm* (at the restriction sites HindIII and BamHI), and *f* (at the restriction site HindIII). The desired fragments were obtained by restriction of the vectors pUC18-USTR, pUC18-TM, pUC18-TMCT and pUC18-TR21, followed by extraction from the agarose gel. Thus, the pUSTR-TM-EGFP and pUSTR-TR-TMCT-EGFP expression vectors were prepared; they contained genes encoding the USTR-TM-EGFP and USTR-TR-TMCT-EGFP fusion proteins, respectively. A schematic representation of the mutual arrangement of the domains in the structure of the recombinant proteins as compared with the structure of natural mucin is shown in Fig. 1.

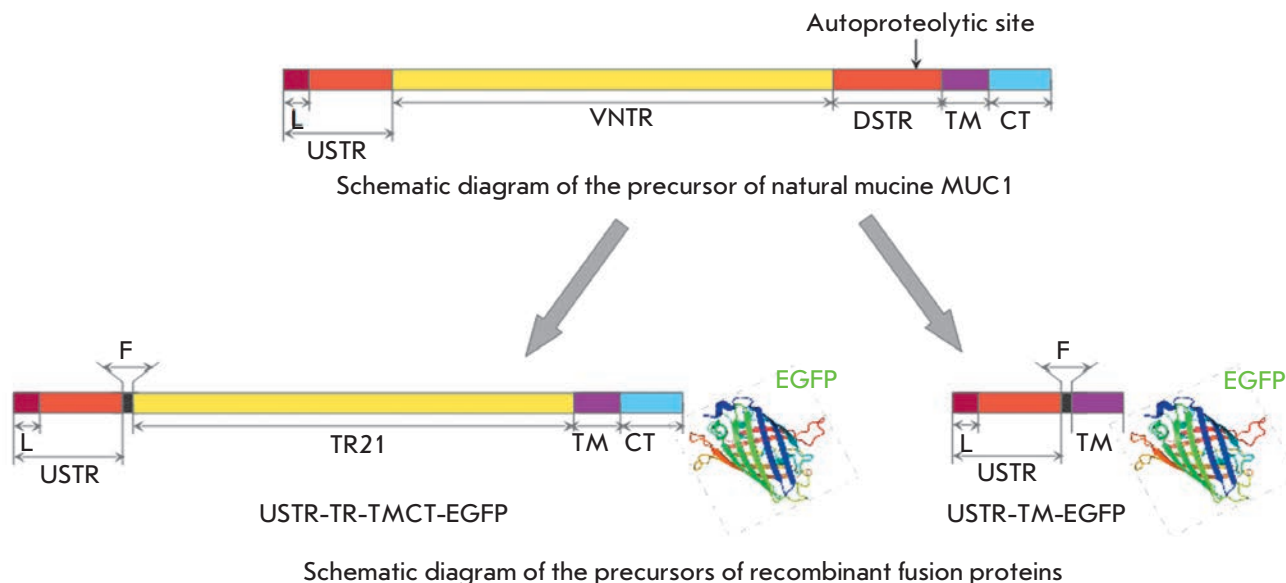


Fig. 1. Arrangement of the major functional domains of endogenous mucin MUC1 and recombinant fusion proteins. L – signal peptide; VNTR – region with a variable number of tandem repeats; TR21 – 21 tandem repeat from VNTR; USTR and DSTR – non-regular repeats located upstream of VNTR and downstream of VNTR, respectively; F – FLAG epitope, TM – transmembrane domain, CT – cytoplasmic domain

Transfection

Vector pEGFP-N3 and the plasmids pUSTR-TM-EGFP and pUSTR-TR-TMCT-EGFP were used for transfection. Transfection of HT-29 cells was performed using a Gene Pulser Xcell Total electroporation system (Bio-Rad, USA). 20 μ l of plasmid DNA (0.4 μ g/ μ l) and 180 μ l of the cell suspension (5×10^6 cells/ml) were placed in a 2-mm electroporation cuvette; the mixture was stirred and subjected to an electric field (500 V/cm, 10 pulses of 1 ms). The cells were then seeded in culture dishes and grown in a complete DMEM medium for 3 days, washed with DPBS, supplied with fresh DMEM containing antibiotic G418 (700 μ g/ml), and cultured for 10–14 days. The most brightly glowing colonies were picked and placed into a 96-well plate. The stably transfected cells were analyzed using a flow cytometer (BD FACS AriaIII, USA).

Flow cytometry

For the flow cytometry analysis, the cells were washed with a DPBS solution three times and re-suspended in DPBD to approximately 1×10^6 cells/ml.

Fluorescence microscopy

The cells were seeded on glass coverslips and analyzed after 24 h using a Nikon Eclipse Ts100 fluorescent microscope (Nikon, Japan) or an LSM510 Meta microscope (Carl Zeiss, Germany).

Real-time PCR

PCR was performed using the Maxima SYBR Green qPCR Master Mix 2X (Thermo Scientific, USA) containing the SYBR Green intercalating agent. The concentrations of primers in the reaction mixtures were 0.03 mmol/l. Dilutions of the cDNA sample (10, 100, 1000 and 10,000-fold) were used to plot a calibration curve. Reactions without cDNA and without reverse transcriptase M-MuLV were used as a control. All experiments were performed in triplicate.

The expression level of endogenous MUC 1 in non-transfected cells was determined using the MUC 1 cDNA and TM_F/CT_R primer pair; the expression level of recombinant mucin MUC 1 was analyzed using the cDNA rMUC 1 and USTR_F/FLAG_R primers.

The results were normalized to the expression level of the GAPDH gene using cDNA (GAPDH) and GAPDH_F/GAPDH_R primers.

Determination of the growth pattern of cells expressing recombinant proteins

The cells of each stable line – HT-29_EGFP, HT-29_USTR-TM-EGFP and HT-29_USTR-TR-TMCT-EGFP – were seeded in culture dishes 3.5 cm in diameter (500,000 cells per dish). After 3 days of growth, the cells were washed with DPBS and their pattern growth was analyzed under a microscope. The number of cells was determined by counting in a Goryaev's chamber.

Table 2. Real-time PCR data showing the content of mRNA of endogenous mucin MUC1 in HT-29 and HeLa cells

mRNA/cell line	Mean ultimate growth	Mean initial count	% with respect to GAPDH
GAPDH / HeLa	25.42	3214.1	100
GAPDH/ HT-29	24.19	11795.4	100
MUC1 / HeLa	25.35	4007.57	125
MUC1 / HT-29	28.24	265.28	2.25



Fig. 2. The primary structure of the mucin MUC1 fragments used to create the constructions. The potential O-glycosylation sites are highlighted in blue; the sequence anchoring the protein in the plasma membrane is highlighted in green. The signal peptide sequence is shown in red

RESULTS AND DISCUSSION

Cell line selection

A number of requirements should be taken into account when choosing a cell line to obtain the desired models.

Since these cell models are supposed to be used to study the properties of a molecule that presumably increases the metastatic potential of cells, a parent cell line demonstrating low initial metastasizing ability should be chosen.

Furthermore, in an ideal case, parent cells should not express endogenous mucin MUC 1 at all to avoid ambiguous results. However, in about 90% of malignancies, there is expression of mucin MUC-1; that is why a tumor cell line with a significantly reduced expression level of endogenous MUC 1 should be chosen.

The glycosylation pattern of mucin is also important when selecting a parent cell line. In 1997,

Burdick *et al.* [20] analyzed the glycosylation pattern of recombinant mucin MUC-1 isolated from four different cell lines. According to the results of glycoprotein hybridization with monoclonal antibodies against the most common tumor-associated glycosidic epitopes occurring in natural mucin, it was shown that only recombinant mucin derived from the HT-29 cell line comprises the sLea and sLex epitopes [20] that are characteristic of cells from aggressive forms of tumors of epithelial origin. According to the published data [2], the HT-29 cell line exhibits a low metastatic potential as well. We compared the expression levels of endogenous mucin in HT-29 and HeLa cells using real-time PCR.

It is known that different isoforms (including the secreted isoform [26]) of mucin MUC-1 can be produced by cells via alternative mRNA splicing. In our case, it was important to estimate the expression level

of the membrane-bound forms of this glycoprotein only; therefore, the TM_F and TM_R primers to the cDNA fragment encoding the transmembrane domain of MUC 1 were used in the PCR reaction. Table 2 shows the results of an evaluation of the *MUC1* gene expression level in the HT-29 and HeLa cell lines.

The results of real-time PCR demonstrate that the amount of MUC 1 mRNA in HT-29 cells is about two orders of magnitude lower than that in HeLa cells. This fact is indicative of the low baseline level of *MUC1* gene expression in HT-29 cells.

Thus, we relied on the published data and our own results and chose the HT-29 cell line to create models of tumor cells that express recombinant proteins comprising certain functional fragments of mucin MUC 1.

Construction of model structures

When studying the role of various functional fragments of MUC 1, researchers usually use DNA encoding natural MUC 1 [27–29]. However, natural MUC 1 is a heterodimer, wherein the extracellular N-terminal subunit is linked to the membrane-bound one by means of stable non-covalent interactions. These interactions might be disturbed, resulting in a “discarding” of the N-terminal subunit from the cell surface [30]. Such a dissociation in the course of studying a protein subunit containing the extracellular domain of mucin might distort the anticipated results. That is why we needed to construct genes of recombinant proteins that have no autoproteolytic sites but contain the desired functional fragments.

The main difference between tumor-associated and normal mucin MUC 1 is that certain glycosidic epitopes are present on the surface of the extracellular domain in the former case: the carbohydrate components of this molecule are supposed to be involved in the interactions with extracellular matrix molecules and, consequently, in metastasizing. Therefore, the recombinant protein to be constructed should contain fragments of the extracellular domain bearing O-glycosylation sites. A large number of the Ser and Thr residues that are supposed to carry oligosaccharides are located in the tandem repeat region (VNTR), where each repeat contains 20 amino acid residues, including five potential O-glycosylation sites. Following the technique developed to construct fragments that encode different amounts of repeats from VNTR of human mucin MUC 1 [25], a fragment encoding 21 tandem repeats was obtained (Fig. 2).

A large number of potential O-glycosylation sites are also characteristic of the areas of degenerate repeats (USTR and DSTR). Since the DSTR region contains an autoproteolytic site, this fragment was not used during the construction. Meanwhile, a DNA fragment coding for the USTR sequence needs to be obtained (see Fig. 2).

Finally, to ensure exposure of the extracellular domain of MUC-1 in the recombinant proteins to the extracellular space, the latter needs to contain at least the transmembrane domain (TM) and the CQC sequence, thus providing membrane localization of the glycoprotein

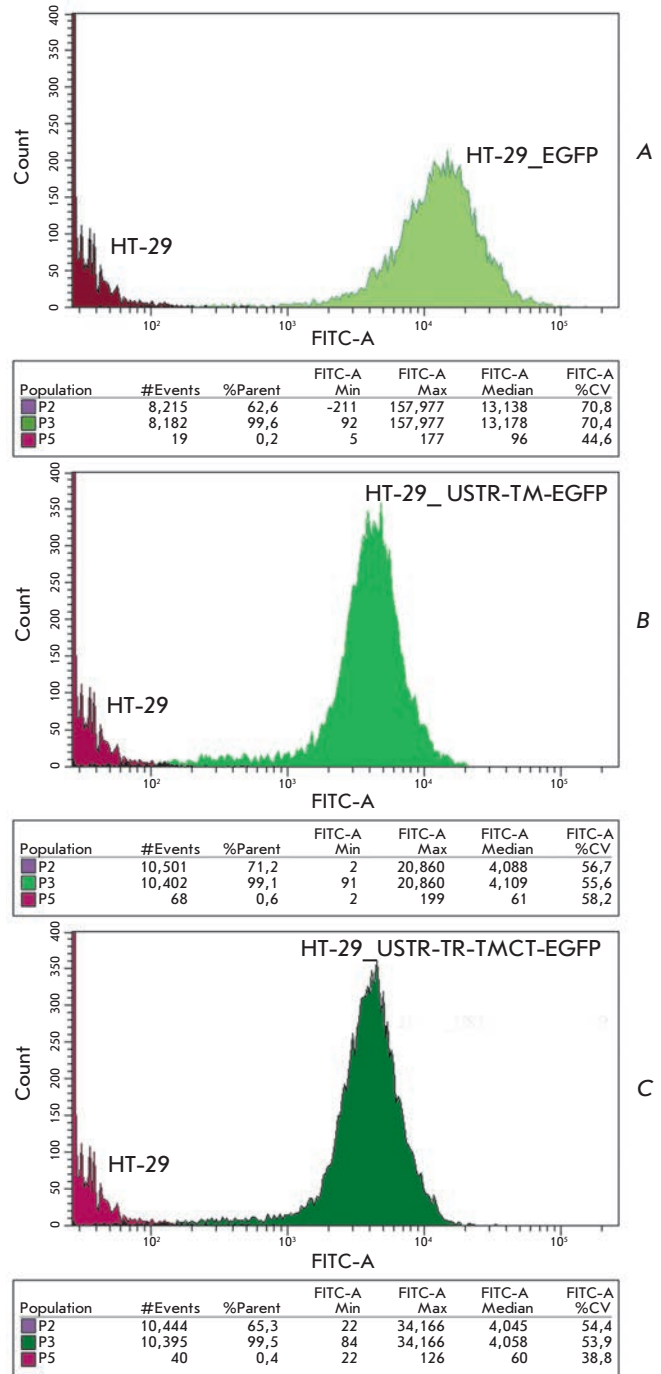


Fig. 3. Fluorescence of HT-29 cells stably transfected with pEGFP-N3 (A), pUSTR-TM-EGFP (B), pUSTR-TR-TMCT-EGFP (C)

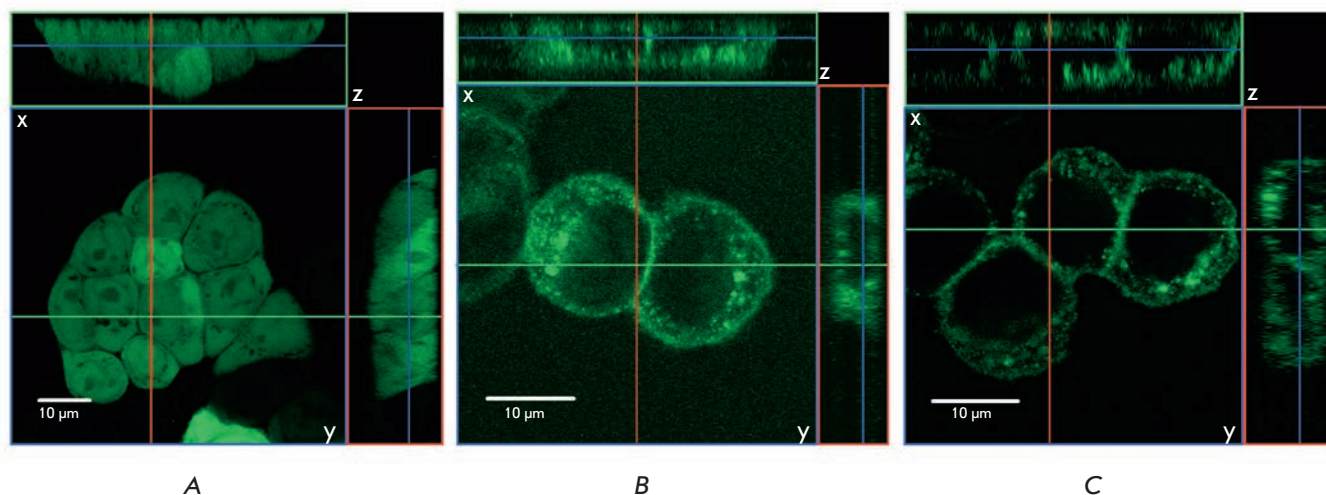


Fig. 4. EGFP fluorescence localization in the stable transfected HT-29 cells. A – HT-29_EGFP, B – HT-29_USTR-TM-EGFP, C – HT-29_USTR-TR-TMCT-EGFP. The upper and side panels of each image demonstrate an optical section of the 3D image in the xz and yz planes, respectively

Table 3. Real-time PCR data showing the content of mRNA of recombinant proteins in stable transfected HT-29 cells

mRNA/cell line	Mean ultimate growth	Mean initial count	% with respect to GAPDH
GAPDH / HT-29_EGFP	14.30	730.65	100
GAPDH / HT-29_USTR-TM-EGFP 1	12.76	1922.36	100
GAPDH / HT-29_USTR-TR-TMCT-EGFP	13.21	1347.97	100
rMUC1 / HT-29_EGFP-N3	22.62	0.94	0.129
rMUC1 / HT-29_USTR-TM-EGFP 1	14.34	373.82	19.446
rMUC1/HT-29_USTR-TR-TMCT-EGFP	14.75	278.03	20.626

tein [31]. The amino acid sequence of the transmembrane domain is shown in Fig. 2.

The nucleotide sequence encoding the cytoplasmic domain (CT, see Fig. 2) was required to construct a gene of full-length mucin lacking only the region encoding the autoproteolytic site and some degenerate repeats.

The fragments encoding the USTR, TM, and CT of mucin MUC 1 were amplified using cDNA of mucin MUC 1 synthesized on the total mRNA derived from MCF-7 breast cancer cells.

Two expression constructs were obtained using the aforementioned fragments; the constructs contained genes of chimeric proteins fused to EGFP at the C-terminus: full-length MUC 1 (pUSTR-TR-TMCT-EGFP)

and that of the lacking tandem repeats and the cytoplasmic domain (pUSTR-TM-EGFP) (Fig. 1).

We inserted the sequence encoding FLAG-epitope between the region of tandem repeats and the fragment encoding degenerate repeats to make it possible to identify the N-terminal region of recombinant proteins using specific antibodies.

Preparation and characterization of cellular models

The expression level of recombinant proteins was assayed by flow cytometry of stable transfected cells by virtue of EGFP fluorescence (Fig. 3).

The expression level of recombinant mucin (rMUC 1) in stable transfected cells was analyzed by real-time PCR and compared to the expression level of the

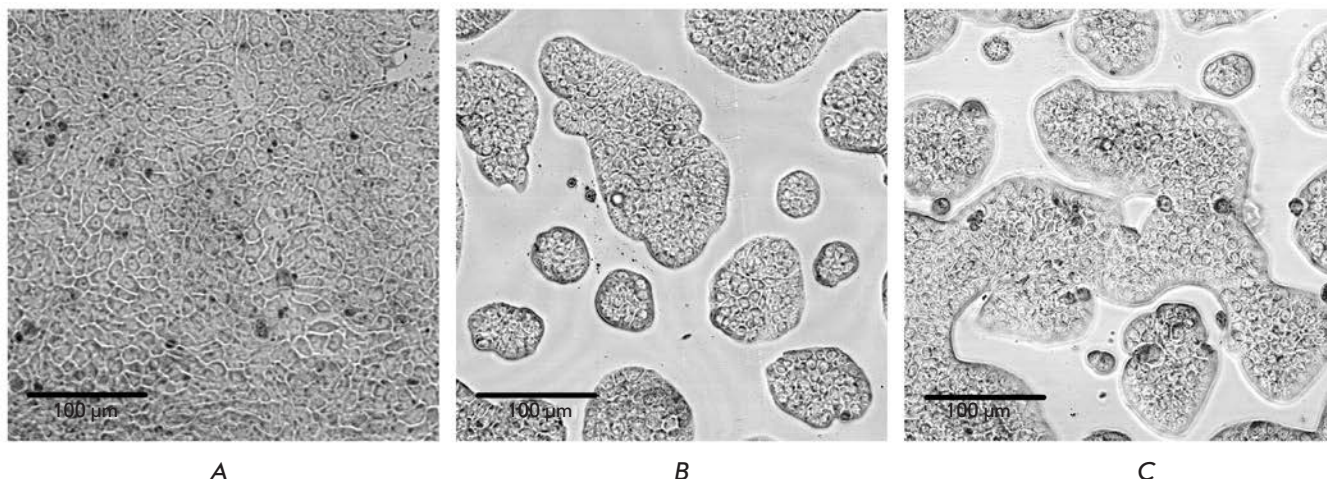


Fig. 5. Effect of the expression of recombinant proteins on the growth pattern of stable, transfected HT-29 cells in culture. A – EGFP-expressing cells, B – USTR-TM-EGFP-expressing cells, C – USTR-TR-TMCT-EGFP-expressing cells

housekeeping GAPDH gene. The results of the measurement of the expression level of recombinant protein genes in stable transfected HT-29 cells are shown in Table 3.

It was shown that the mRNA content in the recombinant proteins USTR-TM-EGFP and USTR-TR-TMCT-EGFP in stable transfected HT-29_USTR-TM-EGFP and HT-29_USTR-TR-TMCT-EGFP cells is approximately 20% of the content of GAPDH mRNA. If we take into account that the mRNA content of endogenous mucin MUC 1 in the HT-29 cell line is 2.25% (Table 2), a conclusion can be drawn that the mRNA of recombinant mucin in stable transfected HT-29 cells is approximately 85% of all the MUC 1 mRNA (both endogenous and recombinant).

An analysis of the localization of recombinant proteins by fluorescence microscopy has shown that the signal in HT-29_EGFP cells in the green part of the spectrum localizes both in the cytoplasm and in the nucleus (*Fig. 4A*), while in HT-29_USTR-TM-EGFP and HT-29_USTR-TR-TMCT-EGFP cells, the signal predominantly localizes in the plasma membrane (*Fig. 4B, C*).

An analysis of the 3D confocal microscopy images demonstrated that proteins containing fragments of mucin fused with EGFP predominantly have a peripheral membrane localization in contrast to the EGFP protein, which was expectedly detected in the cytoplasm and inside the nucleus (*Fig. 4*, top and side panels of each image).

Finally, we found that the resulting cell lines present some differences in their growth patterns. While growing HT-29_EGFP cells form a monolayer (*Fig. 5A*), HT-29_USTR-TM-EGFP and HT-29_US-

TR-TR-TMCT-EGFP cells tend to form individual “islands” (*Fig. 5B, C*). If we take into account the fact that equal amounts of cells (500,000) were seeded in these experiments and that their number also differed insignificantly after 3 days of growth, the assumption about the difference in cell division intensity needs to be rejected. In our opinion, the observed pattern is indicative of the differences in the adhesion properties of the obtained cell lines caused by the presence of recombinant proteins containing mucin 1 MUC fragments on their surface.

CONCLUSIONS

We used HT-29 cell lines to obtain cell models expressing proteins fused with EGFP and constituting fragments of the extracellular domain of human mucin MUC 1 bearing O-glycosylation sites on the outer cell surface. The main difference between the resulting models was either the presence or absence of a domain containing 21 tandem repeats in the structure of recombinant proteins. The models obtained are characterized by a high expression level of recombinant proteins and low expression level of endogenous mucin MUC 1. The model cell lines have different growth patterns compared to EGFP-expressing cells. ●

The authors are grateful to I.A. Vorobiev (Cell Biology and Histology Department, Faculty of Biology, M.V. Lomonosov Moscow State University), A.Yu. Arkhipova, A.A. Ramonova and M.M. Moysenovich (Bioengineering Department, Faculty of Biology, M.V. Lomonosov Moscow State University) for their support and assistance.

This work was supported in part by the Ministry of Science and Education of the Russian Federation (grant № 8800), and by the Russian Foundation for Basic Research (grants № 12-04-33031, 12-04-31338, 12-04-31721, and 13-04-01875). This work was supported in part by the M.V. Lomonosov Moscow State University Program of Development. Some experiments were conducted at the User Facilities

Center of M.V. Lomonosov Moscow State University (BD FACSARIA SORP cell sorter, Carl Zeiss LSM510 Meta confocal microscope) under financial support from the Ministry of Education and Science of the Russian Federation. The funders had no role in the study design, data collection and analysis, decision to publish, or manuscript preparation.

REFERENCES

- Wyld L., Gutteridge E., Pinder S.E., James J.J., Chan S.Y., Cheung K.L., Robertson J.F., Evans A.J. // *Br. J. Cancer*. 2003. V. 89. № 2. P. 284–290.
- Haier J., Nasralla M., Nicolson G.L. // *Br. J. Cancer*. 1999. V. 80. № 12. P. 1867–1874.
- Doerr M.E., Jones J.I. // *J. Biol. Chem.* 1996. V. 271. № 5. P. 2443–2447.
- Varki A. // *Proc. Natl. Acad. Sci. USA*. 1994. V. 91. № 16. P. 7390–7397.
- Qi J., Chen N., Wang J., Siu C.H. // *Mol. Biol. Cell*. 2005. V. 16. № 9. P. 4386–4397.
- Hilkens J., Ligtenberg M.J., Vos H.L., Litvinov S.V. // *Trends Biochem. Sci.* 1992. V. 17. № 9. P. 359–363.
- Dong Y., Walsh M.D., Cummings M.C., Wright R.G., Khoo S.K., Parson P.G., McGuckin M.A. // *J. Pathol.* 1997. V. 183. № 3. P. 311–317.
- Hinoda Y., Ikematsu Y., Horinouchi M., Sato S., Yamamoto K., Nakano T., Fukui M., Suehiro Y., Hamanaka Y., Nishikawa Y., et al. // *J. Gastroenterol.* 2003. V. 38. № 12. P. 1162–1166.
- McGuckin M.A., Walsh M.D., Hohn B.G., Ward B.G., Wright R.G. // *Hum. Pathol.* 1995. V. 26. № 4. P. 432–439.
- Li Y., Ren J., Yu W., Kuwahara H., Yin L., Carraway K.L. 3rd, Kufe D. // *J. Biol. Chem.* 2001. V. 276. № 38. P. 35239–35242.
- Schroeder J.A., Adriance M.C., Thompson M.C., Camenisch T.D., Gendler S.J. // *Oncogene*. 2003. V. 22. № 9. P. 1324–1332.
- Burchell J., Taylor-Papadimitriou J., Boshell M., Gendler S., Duhig T. // *Int. J. Cancer*. 1989. V. 44. № 4. P. 691–696.
- Rahn J.J., Chow J.W., Horne G.J., Mah B.K., Emerman J.T., Hoffman P., Hugh J.C. // *Clin. Exp. Metastasis*. 2005. V. 22. № 6. P. 475–483.
- Bernier A.J., Zhang J., Lillehoj E., Shaw A.R., Gunasekara N., Hugh J.C. // *Mol. Cancer*. 2011. V. 10. № 93. P. 1295–1304.
- Roy L.D., Sahraei M., Subramani D.B., Besmer D., Nath S., Tinder T.L., Bajaj E., Shanmugam K., Lee Y.Y., Hwang S.I., et al. // *Oncogene*. 2011. V. 30. № 12. P. 1449–1459.
- Bafna S., Kaur S., Batra S.K. // *Oncogene*. 2010. V. 29. № 20. P. 2893–2904.
- Ren J., Bharti A., Raina D., Chen W., Ahmad R., Kufe D. // *Oncogene*. 2006. V. 25. № 1. P. 20–31.
- Wei X., Xu H., Kufe D. // *Cancer Cell*. 2005. V. 7. № 2. P. 167–178.
- Nakamori S., Kameyama M., Imaoka S., Furukawa H., Ishikawa O., Sasaki Y., Izumi Y., Irimura T. // *Dis. Colon. Rectum*. 1997. V. 40. № 4. P. 420–431.
- Burdick M.D., Harris A., Reid C.J., Iwamura T., Hollingsworth M.A. // *J. Biol. Chem.* 1997. V. 272. № 39. P. 24198–24202.
- Julien S., Lagadec C., Krzewinski-R ecchi M.A., Courtand G., Le Bourhis X., Delannoy P. // *Breast Cancer Res. Treat.* 2005. V. 90. № 1. P. 77–84.
- Gong E., Hirohashi S., Shimosato Y., Watanabe M., Ino Y., Teshima S., Kodaira S. // *J. Natl. Cancer Inst.* 1985. V. 75. № 3. P. 447–454.
- Inufusa H., Kojima N., Yasutomi M., Hakomori S. // *Clin. Exp. Metastasis*. 1991. V. 9. № 3. P. 245–257.
- Gendler S.J., Lanscater C.A., Taylor-Papadimitriou J., Duhig T., Peat N., Burchell J., Pemberton L., Lalani E.N., Wilson D. // *J. Biol. Chem.* 1990. V. 265. № 25. P. 15286–15293.
- Gul'ko L.B., Pavlova O.V., Diakov N.A., Okorokova N.A., Ratmaova K.I., Logunova N.N., Bobreneva R.A., Makarov V.A., Jurin V.L., Veiko V.P. et al. // *Bioorgan. Khimiya (Bioorgan. Chemistry)*. 2000. V. № 6. P. 423–432.
- Imbert Y., Darling D.S., Jumblatt M.M., Foulks G.N., Couzin E.G., Steele P.S., Young W.W. Jr. // *Exp. Eye Res.* 2006. V. 83. № 3. P. 493–501.
- Ligtenberg M.J., Kruijshaar L., Buijs F., van Meijer M., Litvinov S.V., Hilkens J. // *J. Biol. Chem.* 1992. V. 267. № 9. P. 6171–6177.
- Schroeder J.A., Thompson M.C., Gardner M.M., Gendler S.J. // *J. Biol. Chem.* 2001. V. 276. № 16. P. 13057–13064.
- Rahn J.J., Shen Q., Mah B.K., Hugh J.C. // *J. Biol. Chem.* 2004. V. 279. № 28. P. 29386–29390.
- Julian J., Dharmaraj N., Carson D.D. // *J. Cell. Biochem.* 2009. V. 108. № 4. P. 802–815.
- Pemberton L.F., Rughetti A., Taylor-Papadimitriou J., Gendler S.J. // *J. Biol. Chem.* 1996. V. 271. № 4. P. 2332–2340.

Analysis of the Placental Tissue Transcriptome of Normal and Preeclampsia Complicated Pregnancies

E. A. Trifonova^{1,5}, T. V. Gabidulina², N. I. Ershov³, V. N. Serebrova¹, A. Yu. Vorozhishcheva⁴, V. A. Stepanov^{1,5*}

¹Research Institute of Medical Genetics, Siberian Branch, Russian Academy of Medical Sciences, Nab. Ushayky 10, 634050, Tomsk, Russia

²Siberian State Medical University, Ministry of Health of the Russian Federation, Moskovsky Trakt, 2, 634050, Tomsk, Russia

³Institute of Cytology and Genetics, Siberian Branch, Russian Academy of Sciences, Prosp. Lavrentieva 10, 630090, Novosibirsk, Russia

⁴City Clinical Hospital № 1, Ul. Khitarova, 32, 654000, Novokuznetsk, Russia

⁵Tomsk State University, Lenina Avenue, 36, 634050, Tomsk, Russia

*E-mail: vadim.stepanov@medgenetics.ru

Received 28.08.2013

Revised manuscript received 23.12.2013

Copyright © 2014 Park-media, Ltd. This is an open access article distributed under the Creative Commons Attribution License, which permits unrestricted use, distribution, and reproduction in any medium, provided the original work is properly cited.

ABSTRACT Preeclampsia is one of the most severe gestational complications which is one of the leading causes of maternal and perinatal morbidity and mortality. A growth in the incidence of severe and combined forms of the pathology has been observed in recent years. According to modern concepts, inadequate cytotrophoblast invasion into the spiral arteries of the uterus and development of the ischemia-reperfusion syndrome in the placental tissue play the leading role in the development of preeclampsia, which is characterized by multiple-organ failure. In this regard, our work was aimed at studying the patterns of placental tissue transcriptome that are specific to females with PE and with physiological pregnancy, as well as identifying the potential promising biomarkers and molecular mechanisms of this pathology. We have identified 63 genes whose expression proved to differ significantly in the placental tissue of females with PE and with physiological pregnancy. A cluster of differentially expressed genes (DEG) whose expression level is increased in patients with preeclampsia includes not only the known candidate genes that have been identified in many other genome-wide studies (e.g., *LEP*, *BHLHB2*, *SIGLEC6*, *RDH13*, *BCL6*), but also new genes (*ANKRD37*, *SYDE1*, *CYBA*, *ITGB2*, etc.), which can be considered as new biological markers of preeclampsia and are of further interest. The results of a functional annotation of DEG show that the development of preeclampsia may be related to a stress response, immune processes, the regulation of cell-cell interactions, intracellular signaling cascades, etc. In addition, the features of the differential gene expression depending on preeclampsia severity were revealed. We have found evidence of the important role of the molecular mechanisms responsible for the failure of immunological tolerance and initiation of the pro-inflammatory cascade in the development of severe preeclampsia. The results obtained elaborate the concept of the pathophysiology of preeclampsia and contain the information necessary to work out measures for targeted therapy of this disease.

KEYWORDS microarrays; placenta; genome-wide analysis; preeclampsia; transcriptome; gene expression.

ABBREVIATIONS DEG – differentially expressed genes; MFDs – multifactorial diseases; PE – preeclampsia; GWAS – genome-wide association study; SNP – single nucleotide polymorphism.

INTRODUCTION

The numerous genome-wide association studies (GWAS) conducted so far have provided valuable information on the genetic architecture of multifactorial diseases (MFDs) and revealed hundreds of the risk alleles of single-nucleotide polymorphisms (SNPs) associated with many phenotypes. However, they explain only a relatively small part of the inheritance of complex

traits and have only a very mild impact on the phenotype of associated variants [1]. These results raise the missing heritability problem, which is being intensively discussed today. Another limitation of the GWAS effectiveness related to studies of the hereditary component of predisposition to MFDs is associated with the use of tagSNP. The risk alleles identified in GWAS typically do not belong to the “causal” ones, but are in linkage

disequilibrium (LD) with functionally significant variant alleles [2]; therefore, the biological interpretation of GWAS results is a serious problem.

The current approaches to the identification of the “causal” allelic variants linked to the polymorphisms detected in GWAS are based on the analysis of the coding or transcribed genomic regions [2–4]. However, the vast majority of SNPs identified in GWAS are located in the non-transcribed regions. They are not linked to variants located in exons, and the mechanism of their action is apparently associated with the regulation of gene expression [5, 6]. Therefore, post-genomic methods (which readily provide information on almost all the components coordinating the basic functions of genes, RNA, and proteins at different hierarchical levels) become especially relevant in studying the genetic architecture and molecular mechanisms of MFDs. One such approach, namely the high-performance measurement of gene expression using microarray technology, was used in the present work to characterize the transcriptome patterns in normal pregnancy and preeclampsia (PE), one of the most severe gestational complications.

Preeclampsia, which is associated with the multiple organ dysfunction syndrome, is a specific syndrome that occurs after the 20th week of pregnancy and is characterized by hypertension and proteinuria. PE is diagnosed in 70% of hypertensive disorders in pregnancy, and an increase in the incidence rate of severe and combined forms of this disease has been observed in recent years [7]. Despite the large number of theories related to etiopathogenesis (neurogenic, hormonal, placental, immunological, genetic, etc.), numerous studies of the mechanisms of development of this disease, and the emergence of new therapies, PE remains a leading cause of maternal and perinatal morbidity and mortality. The disease is responsible for up to 70% of stillbirths and miscarriages; the risk of perinatal losses increases almost fivefold in PE [7, 8].

According to the modern concepts, the etiopathogenesis of preeclampsia is closely related to inadequate cytotrophoblast invasion in the uterine spiral arteries and development of the ischemia-reperfusion syndrome, which induces oxidative stress and systemic inflammation [9, 10]. Etiological factors and the mechanisms of this disorder remain unclear and require close attention. In order to identify the likely candidate biomarkers of PE and to study the molecular mechanisms of gestational complications, we analyzed the patterns of the placental transcriptome that are specific to PE and physiological pregnancy, since the placental tissue obviously plays the key role in the development of PE. The strategy of using microarrays in this context seems to be reasonable and powerful enough, as it allows one to thoroughly investigate the possible changes

in gene expression associated with the pathophysiology of preeclampsia at the transcriptome level.

EXPERIMENTAL

Characteristics of the examined groups

A total of 10 patients with PE and 11 patients with physiological pregnancy (the control group) were examined (*Table 1*). The questionnaire included demographic information (ethnicity) and anthropometric parameters (height, weight), lifestyle (smoking habit, psychoactive substance abuse), as well as information about the somatic and obstetric-gynecological history. PE was diagnosed based on leading clinical symptoms of various severity, such as proteinuria, edema, hypertension (systolic blood pressure above 140 mm Hg, diastolic blood pressure above 90 mm Hg) according to the 10th revision of the International Classification of Diseases. PE severity was evaluated according to the criteria of the clinical protocol 2012 “Hypertension during Pregnancy. Preeclampsia. Eclampsia” [11].

The group of PE patients was heterogeneous both in terms of severity (the study included six patients with moderate and four patients with severe PE) and the presence of prior diseases and comorbidities. Four patients were diagnosed with PE in the absence of background diseases; in others the gestational complications developed against the backdrop of extragenital diseases including hypo-/hypertensive type neurocirculatory dystonia, chronic pyelonephritis, chronic cholecystitis, and chronic arterial hypertension. Six females in the control group were also diagnosed with both chronic pyelonephritis and chronic cholecystitis. The age of the gravidas ranged from 18 to 33 years in both groups; the groups were comparable in terms of the average age. Statistically significant differences in the height and weight of infants between the control group and the group of patients were found. The groups also differed in terms of arterial blood pressure and time of birth.

Collection of placental samples

We examined the distal (maternal) portion of the placenta. The tissues were sampled immediately after delivery (sample ischemia time did not exceed 10 min). Placental tissue samples were taken from the central areas close to the umbilical cord at a placental depth of 0.5 cm. The samples were collected from macroscopically normal sections of the placenta (without hemorrhage, calcification, necrosis, or fibrin deposition) without intervening large vessels, washed with saline to remove the residual maternal blood and amniotic fluid, immediately immersed in RNAlater (Ambion, UK), and transferred to be stored at -80°C until the RNA iso-

Table 1. Characteristics of the examined groups

Parameters	PE, N = 10	Control group, N = 11	p-value*
Mean age, years	26 ± 2	28 ± 3	0.241
Mean weight, kg	60 ± 7	62 ± 6	0.324
Body mass index, BMI	23 ± 4	23 ± 3	0.832
The mean maximum systolic blood pressure, mm Hg	162 ± 19	121 ± 3	0.0001
The mean maximum diastolic blood pressure, mm Hg	104 ± 13	80 ± 4	0.0001
Delivery time, weeks	38 ± 1	40 ± 2	0.009
Birth weight, g	2783 ± 560	3549 ± 345	0.004
Length at birth, cm	50 ± 4	53 ± 2	0.021
Premature birth, %	50	0	0.012
Chronic diseases, %	60	50	0.575

* The significance level was determined by comparing the groups using the Mann-Whitney test or Fisher's exact test.

lation procedure. A histological examination revealed chorionic villi and decidua tissue with fibrinoid necrosis foci and small calcifications in all biopsy specimens (Fig. 1).

RNA Isolation

Tissue samples (100–200 mg) were homogenized using TissueLyser (Qiagen) in Trizol; RNA was then isolated using the standard protocol. The concentration of total RNA was determined using Nanodrop ND-1000 based on absorbance at 260 nm in water. The quality of the samples was monitored using an Agilent 2100 Bioanalyzer capillary electrophoresis system (Agilent Technologies Inc., Palo Alto, USA) and spectrophotometric scanning.

Microarray analysis

A genome-wide profile of gene expression in the placental tissue was determined using hybridization on HT-12 BeadChip microarrays (Illumina, USA) containing information about more than 48,000 transcripts. After hybridization, the microarrays were scanned on an Illumina BeadArray Reader device. The raw data were converted into mean values of the signal intensity for each sample (Sample Probe Profile) using the BeadStudio v3 software package (Illumina).

Bioinformatic analysis

The data were analyzed in an R software environment using the limma program package [12]. Nonparametric background correction followed by quantile normalization (neqc function) was performed for the entire data set. The specimens that were identified in all the sam-

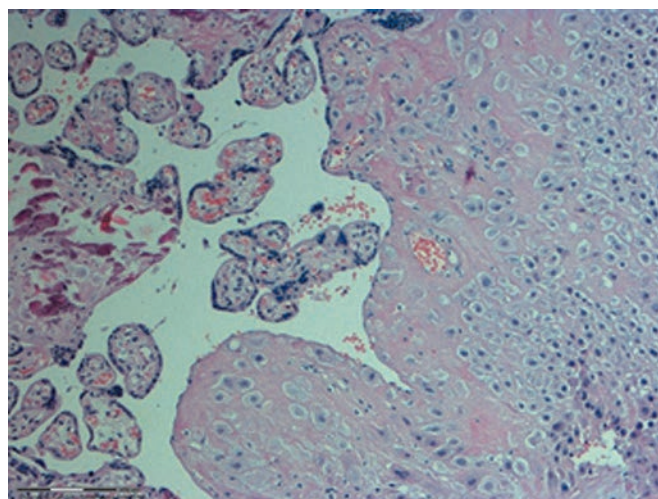


Fig. 1. Micrograph of one of the studied placental biopsy samples. Hematoxylin- and eosin-stained

ples of at least one of the experimental groups (detection p-value <0.01) were further considered. A differential expression analysis was performed using multiple linear regression and moderated t-statistics [12], including the assessment of the quality weights of microarray reading [13] and Benjamin-Hochberg multiple testing correction (FDR) procedure. A 1.5-fold (or greater) change in the level of gene expression (FC – fold change) was considered to be significant at the adjusted significance level of $p \leq 0.1$. Functional annotation and functional cluster analysis of the groups of differentially expressed genes (DEGs) were performed using the DAVID (Database

Table 2. The most significant differentially expressed genes

N ^o	Change in expression level	FC	FDR	Gene	Chromosome	Gene product	Primary functions*
1	↑	1.054	0.0007	<i>LEP</i>	7	Leptin	The gene encodes the protein which is secreted by adipocytes and plays an important role in the regulation of food intake and / or energy consumption to maintain the constancy of the adipose mass. Leptin is also involved in the regulation of immune and inflammatory reactions, and processes of hematopoiesis, stimulation of angiogenesis and inhibition of apoptosis.
2	↓	3.84	0.0001	<i>HS.201441</i>	13	Long non-coding RNA 284	According to the analysis of EST-libraries, tissue-specific expression of <i>HS.201441</i> gene is mainly observed in the placenta and ovaries.
3	↑	2.95	0.0000	<i>BHLHE40</i>	3	Transcription factor including the helix-loop-helix domain	Transcription factor modulating chondrogenesis within the cAMP-signaling pathway. It is involved in the control of cell differentiation.
4	↑	2.93	0.0031	<i>ANKRD37</i>	4	Ankyrin 37 repeat domain	The encoded protein contains four ankyrin repeats, which are mediators of protein-protein interactions and are involved in the regulation of the functioning of key transcription factors, such as NF κ B and TP53. In addition, there is evidence of the important role of <i>ANKRD37</i> in the cellular response to hypoxia [24].
5	↑	2.91	0.0067	<i>SIGLEC6</i>	19	Immunoglobulin-like lectin 6, which binds to the sialic acid	Immunoglobulin-like lectins that bind to sialic acids are a family of type 1 membrane proteins which recognize and bind sialylated glycans. <i>SIGLEC6</i> interacts with the α -2,6-bound sialic acid of cellular membranes of immune cells and regulates cell adhesion, thus participating in the immune response. Furthermore, <i>SIGLEC6</i> is a ligand of leptin [25].
6	↑	2.64	0.0006	<i>ZNF175</i>	19	Zinc finger protein 175	Negative regulation of the expression of various chemokine receptors.
7	↑	2.43	0.0031	<i>CCSAP</i> (C1orf96)	1	Protein localized in centriole, cilia and cleavage spindle (open reading frame 96, chromosome 1)	Presumably plays a role in embryonic development

8	↑	2.43	0.0050	<i>GPT2</i>	16	Alanine aminotransferase 2; glutamate pyruvate transaminase	Catalyzes the reversible transamination between alanine and 2-oxoglutarate to form pyruvate and glutamate participating in amino acid metabolism and gluconeogenesis.
9	↑	2.39	0.0050	<i>RDH13</i>	19	Retinol dehydrogenase 13	Catalyzes oxidation and reduction of retinoids and participates in protecting mitochondria from oxidative stress.
10	↑	2.36	0.0006	<i>BCL6</i>	3	Transcription factor – zinc finger protein 51	Contains N-terminal POZ/BTB-domain and is a sequence-specific transcription repressor. Participates in modulation of STAT-dependent IL-4-induced immune response involving B cells, antibody formation, and lymphangiogenesis.
11	↑	2.33	0.0056	<i>PLIN2</i>	9	Perilipin 2, lipid droplet protein	Perilipin function in basic cells is to stabilize the storage of neutral lipids. Its functions are related to providing PKA-activated lipolysis in activated cells.
12	↑	2.31	0.0174	<i>NR1P1</i>	21	Nuclear factor RIP140	Modulates the transcriptional activity of steroid receptors such as NR3C1, NR3C2, and ESR1 in the nucleus. Can act as a transcriptional activator or repressor, depending on the transcription factors it interacts with [26].
13	↑	2.18	0.0407	<i>HILPDA</i> (C7orf68)	7	Hypoxia-induced protein 2 (open reading frame 68, chromosome 7)	The gene encodes hypoxia-induced factor 2, which promotes the intracellular accumulation of lipids, stimulates the expression of cytokines, including IL-6, MIF, and VEGFA, and enhances growth and proliferation of cells.
14	↑	2.18	0.0006	<i>SYDE1</i>	19	GTPase-activating protein, homolog 1	This protein belongs to the Rho GTPase family, which plays an important role in cell proliferation, apoptosis, gene expression, and regulation of intracellular actin dynamics.
15	↑	2.06	0.0050	<i>CORO2A</i>	9	Coronin 2A	Belongs to actin-binding protein family, which performs important functions related to cell motility, membrane transport, and cell-cell signal transduction. It was shown that coronin 1A mediates Toll-like receptors and is involved in the inflammatory response [27].

* Information from the GeneCards database (<http://www.genecards.org/>) including addendum.

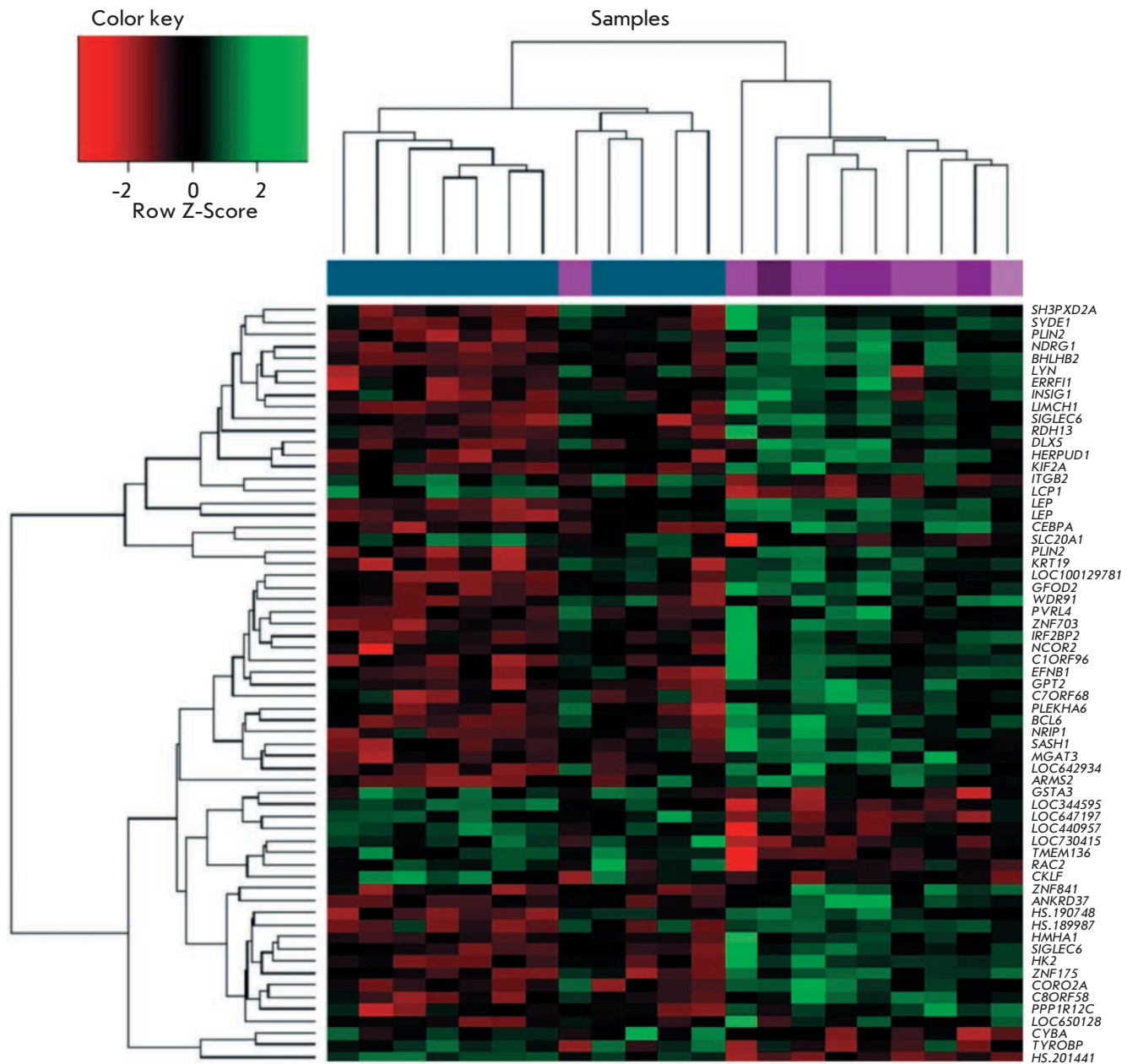


Fig. 2. Heatmap of DEGs (FDR < 0.1; FC \leq 1.5). Each column represents a sample; each row represents DEG. Samples from PE patients are shown in pink; samples from the females of the control group are shown in blue. The color scale of the heatmap indicates the deviation of the normalized expression level in the cell from the mean value for the row

for Annotation, Visualization and Integrated Discovery) web-based tool with the standard values of clustering parameters and enrichment score $EASE \leq 0.01$ [14]. Construction of gene networks was performed using the STRING 9.0 program (Search Tool for the Retrieval of Interacting Genes) [15].

This study was approved by the Ethics Committee at the Research Institute of Medical Genetics, Siberian Branch of the Russian Academy of Medical Sciences.

RESULTS

Our analysis identified 63 genes with significantly different expressions (FDR < 0.1; FC \geq 1.5) in the placental tissue of females with PE and physiological pregnancy (50 DEGs with an increased expression level and 13 DEGs with a decreased expression level). The DEG cluster, whose expression was increased in PE, includes not only known candidate genes that have previously been identified in many genome-wide studies of the ex-

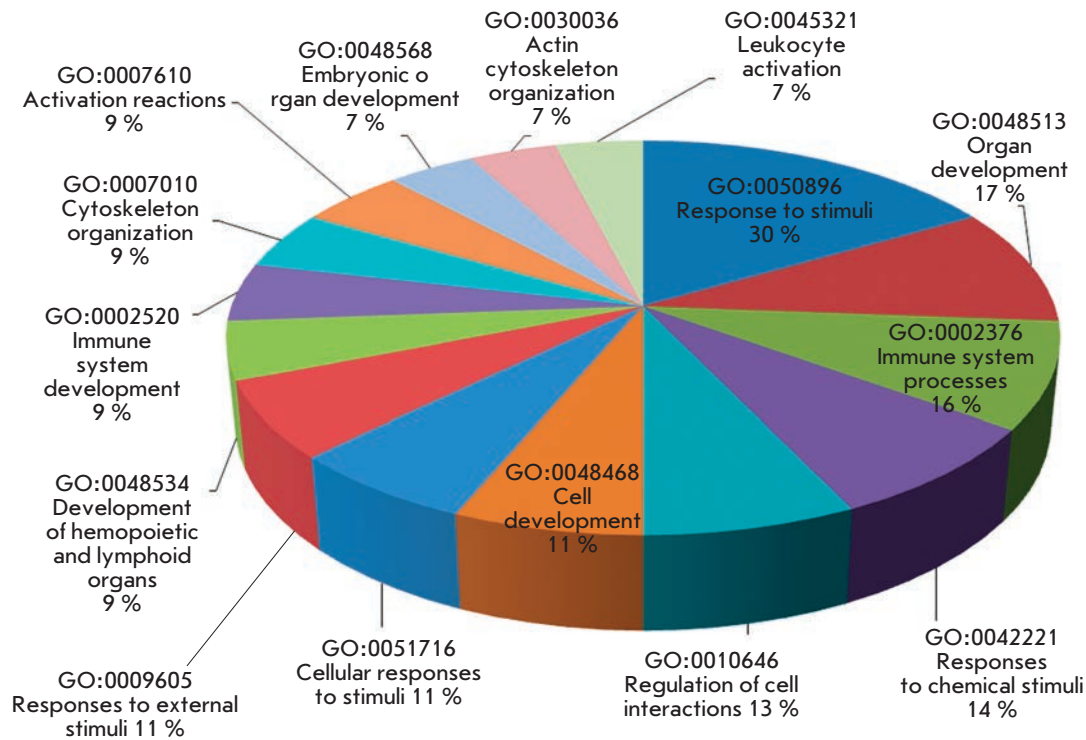


Fig. 3. Main biological processes involving DEGs, which are associated with preeclampsia ($p < 0.05$). The percentage indicates the proportion of identified DEGs associated with this process

pression profiles of the placental genes in preeclampsia (e.g., *LEP*, *BHLHB2*, *SIGLEC6*, *RDH13*, *BCL6*), but also new potential candidate genes (*CORO2A*, *SYDE1*, *PLIN2*, *CEBPA*, *HK2*, *NDRG1*, *ERRF1*, *EFNB1*, *GFOD2*, *NCOR2*, *HMHA1*, *HERPUD1*, *KIF2A*), whose association with the development of PE has been established either in a few studies [16–21], or was done so for the first time in our work. The products of some of these genes, based on current knowledge on their functional features, can be involved in the etiopathogenesis of PE.

Figure 2 shows the heat map with the results of a hierarchical clustering of females according to the expression level of 63 DEGs. It can be seen that all PE patients but one fall into one cluster, while females with physiological pregnancy fall into the other one. One PE sample was assigned to the control group probably due to the significant interindividual variability of the transcription levels of the placental tissue genes. A similar phenomenon was observed in several human cell lines: in particular, in the cell lines of the hepatocyte transcriptome [22, 23].

Table 2 shows the data related to the most significant DEGs ($FC > 2$, $FDR < 0.01$). The presence of several genes whose products are involved in the transcriptional regulation (*BHLHB2*, *ZNF175*, *ANKRD37*, *BCL6*) in this list, as well as a significant increase in the expression level of the *LEP* gene and its receptor gene *SIGLEC6* during the development of PE, is of special interest.

We analyzed DEG using the DAVID online resource to study the biological processes associated with the development of PE (Fig. 3). The major categories of molecular functions of the protein products of these genes include responding to various stimuli, immune processes, regulation of cell communication, intracellular signaling cascades, etc. The analysis of metabolic pathways including DEGs has shown that cytotoxicity pathways associated with NK-cells, transendothelial migration of leukocytes, and signaling pathways mediated by GTPase activators are probably involved in the molecular mechanisms of PE.

Protein-protein interactions of DEG products were analyzed to identify the possible relationships with DEGs (Fig. 4). The associations in the constructed network are mainly based on “text mining” (mentioned in the abstract of one article). The coexpression cluster that includes the *RAC2*, *CYBA*, *TYROBP*, *HMHA1*, *ITGB2*, *LYN* and *LCP1* genes should be mentioned. In addition, *LEP* and its receptor *SIGLEC6* and ephrin with its kinase *LYN* are of certain interest.

Our study also revealed features of differential gene expression depending on PE severity (Table 3). A total of eight DEGs were identified ($FDR < 0.1$; $FC \leq 1.5$), whose expression levels were significantly different in moderate and severe forms of the disease. In our opinion, *HSPA1A* encoding the highly conserved heat shock protein 70 (HSP70) and *BAG3* encoding Bis, a Bcl-2

Fig. 4. Protein–protein interactions between DEG products. The proteins are shown as circles; the color line between these circles indicates the evidential category of protein–protein interaction: yellow – literature data (“text mining”), black – according to the analysis of gene coexpression, purple – the experimental results, blue – evidence from the databases, pink – cumulative evidence

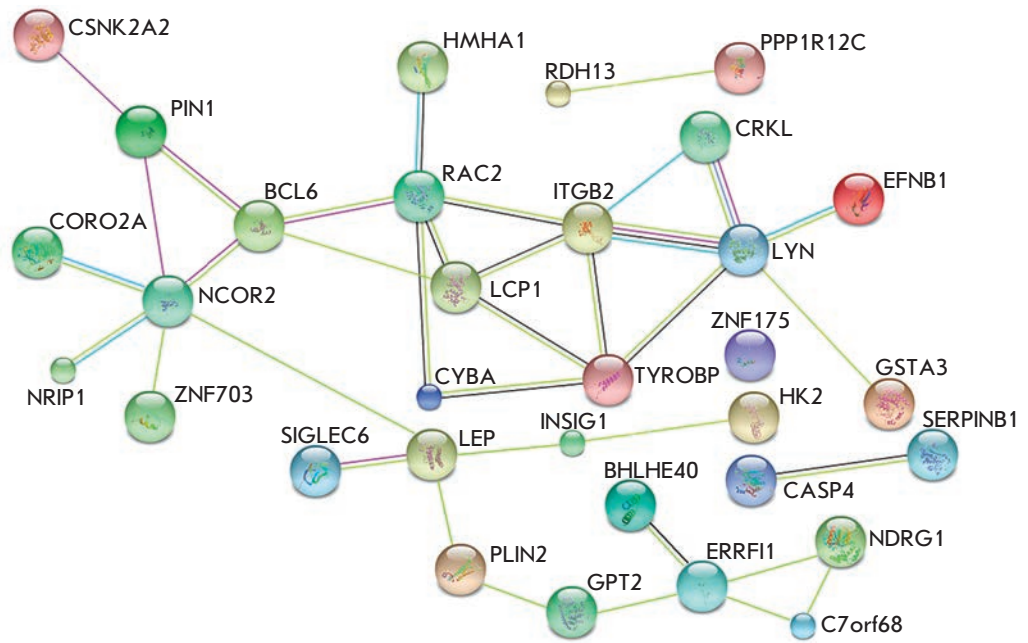


Table 3. List of differentially expressed genes (FDR < 0.1; FC ≤ 1.5) in moderate to severe preeclampsia

Gene	Change in gene expression level	FC	FDR	Gene product
<i>HSPA1A</i>	↑	6.44	0.079549	Heat shock protein 70, HSP70-1A
<i>BAG3</i>	↑	2.14	0.073131	Bcl-2-associated athanogene 3
<i>SNHG8</i>	↑	1.78	0.04105	Small nucleolar RNA 8
<i>LOC729660</i>	↓	2.63	0.010437	No data
<i>LOC728457</i>	↓	2.43	0.010437	No data
<i>APOC1</i>	↓	2.28	0.04433	Apolipoprotein C1
<i>LOC401357</i>	↓	2.27	0.010399	No data
<i>LOC100128326</i>	↓	1.92	0.079549	No data

binding protein, are of the greatest interest. The main function of the Bis protein is inhibiting the chaperone activity of the HSP70/HSC70 complex.

A comparative analysis of gene expression profiles in the placental tissue of females with moderate PE and in the control group revealed 56 transcripts of 52 genes, whose transcription levels differ significantly in these populations. Changes in the expression profile were more pronounced in severe PE: a significant increase in the expression of 55 genes and a decrease in the expression of 35 genes compared to physiological pregnancy were observed (Fig. 5). It should be noted that, along with a small amount of common genes (21 genes) that were differentially expressed in both severe and moderate PE, more than 60 DEGs were specific only to the

severe form of the pathology. The results of a functional annotation of these genes in the DAVID web-resource point to a number of biological processes that are statistically significantly associated with the development of severe PE, such as processing and presentation of peptide or polysaccharide antigens and protein folding (Table 4). An analysis of the metabolic pathways that involve these genes also demonstrates the important role of the mechanisms of processing and presentation of antigens in the molecular pathogenesis of severe PE (according to the KEGG and BIOCARTA databases).

DISCUSSION

The placenta is the key in understanding the physiological processes associated with pregnancy. It is im-

Table 4. Main biological processes that involve differentially expressed genes characteristic of severe preeclampsia

Categories of biological processes	Gene	<i>p</i> *
Processing and presentation of peptides or polysaccharide antigens via class II MHC molecules (GO:0002504)	<i>HLA-DPA1, CD74, HLA-DMA, HLA-DRA</i>	0.0421
Processing and presentation of exogenous peptide antigens (GO:0002478)	<i>HLA-DMA, CD74, HLA-DRA</i>	0.0453
Chaperone-mediated protein folding (GO:0051085)	<i>ERO1L, HLA-DMA, CD74</i>	0.0467
<i>De novo</i> post-translational protein folding (GO:0051084)	<i>ERO1L, HLA-DMA, CD74</i>	0.0478
Reactions of unfolded protein molecules (GO:0006986)	<i>ERO1L, HSPH1, HSPA1A, HERPUD1</i>	0.0489

* Significance level including Benjamin-Hochberg multiple testing correction, which characterized the accuracy of the assignment of this set of genes to a certain biological process.

portant to characterize the genes essential for placental function to understand the mechanisms underlying normal and pathological gestation. The results of this work show that the identified DEGs belong to several biological processes associated with immune responses, cell-cell interactions, and responses to various stimuli. It should be noted that the analysis performed using the module for functional annotation clustering of the DAVID bioinformatical resource made it possible to identify 16 clusters. However, only one of them had an enrichment score of over 2. This cluster includes five genes (*KRT19, RAC2, LIMCH1, BCL6, LCP1*) involved in the biological processes related to the organization of the actin cytoskeleton (GO: 0030036; GO: 0030029; GO: 0007010). Studying the functional role of the actin cytoskeleton is one of the important trends in the study of cellular signaling mechanisms. Numerous experimental data published over the past few years provide evidence of the fact that actin is involved in the regulation of gene expression and mediates it by participating in transcription elongation, assembly of the preinitiation complex, mRNA maturation and export, chromatin reorganization, and other processes [28, 29]. In this context, the increase in the expression level of the *CORO2A* gene seems interesting. The product of this gene, coronin 2A, belongs to the family of actin-binding proteins and mediates the Coro2A/actin-dependent mechanism of derepression of the inflammatory response genes [27].

We found no association between the development of PE and such canonical pathways as abnormal apoptosis and angiogenesis as described in several papers [16, 19, 30, 31]. This is probably attributable to the interethnic variability of the gene expression profiles in the placental tissue due to the population differentiation of the regulatory regions of the genome, or due to the differ-

Severe preeclampsia

Fig. 5. Venn diagram showing the results of the gene expression profiling in moderate and severe preeclampsia and in physiological pregnancy. DEGs – genes that are differently expressed in females with preeclampsia and physiological pregnancy (control group). The arrow shows the increase (↑) or decrease (↓) in gene expression

ent criteria (population size, delivery time, severity of the disease, etc.) used in the formation of the examined groups. The different placental localization of the biopsy samples used in individual studies of the transcriptome in PE is another factor that apparently affects the occurrence of these contradictions. Thus, high-throughput sequencing (RNA-Seq) revealed significant differences in the gene expression profiles in the amnion, chorion, and decidua of the human placenta [32]. Similar findings were previously arrived at when performing a microarray analysis of the transcriptome patterns in different portions of the placenta [33].

Despite the aforementioned differences in the results of the DEG functional annotation, it remains of

interest that changes in the expression levels of some DEGs identified in our work were also described in other studies (Table 5).

Thus, a significant increase in *LEP* gene expression in preeclampsia was observed in almost all genome-wide studies of gene expression profiles in the placental tissue. Leptin, the product of this gene, is one of the new serum markers of PE. It is known that leptin belongs to adipocyte-specific cytokines that regulate energy metabolism and are involved in various metabolic and neuroendocrine processes [39]. The studied group of PE patients did not differ significantly from the control group of patients in terms of weight and body mass index. None of the patients had abnormal weight gain during pregnancy, and therefore it can be assumed that the contribution of leptin to the development of PE is determined by other functions of this protein. Placental leptin is known to be involved in providing the flow of nutrients to the fetoplacental complex and to induce the trophoblast proliferation by inhibiting apoptosis [40, 41]. Thus, an increase in the leptin level in the placenta may be a compensatory mechanism directed against endothelial dysfunction, which is observed in PE. Meanwhile, it was shown that leptin is involved in the activation of the sympathoadrenal system, which contributes to arterial hypertension, the main symptom of PE [42]. In addition, an important immunomodulatory function of leptin was found, which may also contribute to the development of pregnancy failure [43]. Despite the intensive studies devoted to *LEP* gene expression, only some works have focused on the analysis of the hereditary variability of this gene and its role in changing the transcription level and the structure of susceptibility to pregnancy failure. It was shown that carriers of the AA genotype of the rs2167270 locus (G19A) located in the promoter region of the *LEP* gene have elevated levels of expression of this gene in the blood, as well as the risk of PE and hypertension [44]. Association between another polymorphism (G2548A) localized at the *LEP* gene promoter with gestational diabetes [45] was found in the Czech population. Along with this, several studies [37, 46, 47] have revealed significant hypomethylation of this locus, as well as dysregulation of the placental epigenome during the development of PE.

The increase in the expression of the long non-coding RNA 284 gene in the placental tissue of PE patients, which was observed in our work, is of particular interest in the context of the role of epigenetic dysregulation in the formation of this pathology. It has recently been shown that long ncRNAs perform vital regulatory functions in cells. In particular, it is assumed that they can function as a module scaffold in the specific, highly ordered organization of ribonucleoprotein complexes

and induction of epigenetic changes in these loci. Some long ncRNAs can bind chromatin using remodeling enzymes and then participate in the local chromatin modification, e.g. in DNA methylation, by initiating or repressing transcription. This RNA class can participate in the binding of transcription factors and inhibiting gene expression [48].

The association between overexpression of the *BAG3* and *HSPA1A* genes and the development of severe PE seems to be of interest. The protein product of the *BAG3* gene is known to compete with Hip co-chaperone for binding to the ATPase domain of the HSP70/HSC70 complex and thus inhibits the chaperone activity of the heat shock protein 70 (Hsp70), the product of the *HSPA1A* gene, whose expression is significantly elevated in severe PE (more than sixfold as compared to moderate PE and eightfold as compared to the control population). It is known that Hsp70 performs various functions. Improving the resistance of the protein biosynthesis apparatus to damaging influences and chaperone activity are the most significant of them. In addition, there is data indicating that Hsp70 participates in protein transport, conduction of the intracellular signal, and protease-dependent degradation [49]. It should be noted that according to the results of the functional annotation of DEGs, processing and presentation of peptide and polysaccharide antigens and chaperone-mediated protein folding are the principal processes characteristic of severe PE. Since the heat shock protein Hsp70 is capable of forming complexes with non-folded proteins and a wide variety of peptide fragments that are precursors of the antigenic peptides presented on the cell membrane along with other class I and II MHC molecules [50], it is reasonable to assume that the immunological control mechanisms of trophoblast invasion in the uterine wall and the immunological tolerance factors in the mother-fetus system play a key role in the pathogenesis of severe PE. The pathological effect of these factors can lead to gestational complications. Furthermore, many heat shock proteins exhibit immunoregulatory activity, stimulate the maturation of dendritic cells, and induce some proinflammatory cytokines [51]. These properties of these proteins may also contribute to the mechanisms of severe PE.

The statistically significant decrease in the expression of the *APOC1* gene in severe PE, which was revealed in the present study, is probably due to the development of oxidative stress in the blood vessels of the placenta or the recently discovered immunosuppressive properties of the C1 apolipoprotein encoded by this gene [52]. It was previously shown that the serum of PE patients has a high level of triglyceride-rich lipoproteins, which can promote endothelial dysfunction [53,

Table 5. Differentially expressed genes identified in this study whose association with preeclampsia has been previously shown in studies focused on the placental tissue transcriptome

№	Gene	Gene product	FC	Significance level	Ethnic populations	Reference
1	<i>LEP</i>	Leptin	10.94	< 0.0001*	Japanese	[30]
			8.58	0.036*	Chinese	[34]
			40.11	1.35×10^{-9}	Caucasian	[16]
			5.52	0.0020	Caucasian Afro-American Mongoloid Spaniard	[18]
			108.9	< 0.0001	Caucasian	[35]
			4.4	< 0.0001	Korean	[36]
			≥ 1.5	< 0.05	Chinese	[37]
			11.79	< 0.01*	American	[38]
2	<i>BCL6</i>	Transcription factor – zinc finger protein 51	1.78	0.0154	Caucasian Afro-American Mongoloid Spaniard	[18]
			2.02	0.0024	Japanese	[30]
			2.24	3.58×10^{-5}	Caucasian	[16]
			2.60	< 0.01*	American	[38]
			≥ 1.5	< 0.05	Chinese	[37]
3	<i>SIGLEC6</i>	Immunoglobulin-like lectin 6, which binds to sialic acid	-	0.02*	American	[31]
			2.13	0.001	Caucasian	[16]
			2.73	< 0.01*	American	[38]
			≥ 1.5	< 0.05	Chinese	[37]
			4.5	0.019	Caucasian	[35]
4	<i>RDH13</i>	Retinol dehydrogenase13	-	3.86×10^{-8} *	American	[31]
			1.91	< 0.01*	American	[38]
			≥ 1.5	< 0.05	Chinese	[37]
5	<i>NDRG1</i>	Cytoplasmic protein belonging to the hydrolase superfamily	2.02	0.0001	Japanese	[30]
			2.67	1.12×10^{-5}	Caucasian	[16]
6	<i>BHLHE40</i>	Transcription factor with helix-loop-helix domain	1.95	0.0004	Japanese	[30]
			3.08	2.18×10^{-5}	Caucasian	[16]
7	<i>KRT19</i>	Keratin 19	1.75	0.0071	Japanese	[30]
			2.28	1.59×10^{-5}	Caucasian	[16]
8	<i>GPT2</i>	Alanine aminotransferase 2	2.45	3.70×10^{-5}	Caucasian	[16]
9	<i>PPP1R12C</i>	12A regulatory subunit of phosphatase 1	-	2.16×10^{-8} *	American	[31]
10	<i>CEBPA</i>	CCAAT/enhancer-binding protein α	-	2.52×10^{-8} *	American	[31]
11	<i>HK2</i>	Type 2 hexokinase	3.90	3.87×10^{-6}	Caucasian	[16]
12	<i>HMHA1</i>	Minor histocompatibility antigen HA1	-	1.23×10^{-8} *	American	[31]
13	<i>PVRL4</i>	Nectin 4	2.54	3.62×10^{-5}	Caucasian	[16]
14	<i>SASH1</i>	SAM- and SH3-domain-containing protein 1	2.54	1.22×10^{-7}	Caucasian	[16]
15	<i>SH3PXD2A</i>	SH3- and PX-domain-containing protein 2A	≥ 1.5	< 0.05	Chinese	[37]
16	<i>SYDE1</i>	GTPase activating protein, homolog 1	1.55	< 0.01*	American	[38]

* Significance level including multiple testing correction.

54]. Meanwhile, the blood level of E and A1 apolipoproteins is decreased in this pathology [55, 56]. In addition, a protective role of the *APOE* ϵ 2 allele in the Kurd population was demonstrated, which is related to the high antioxidant properties of this allele according to the authors [57]. We failed to find any information about an association between *APOC1* polymorphisms and gestational complications. However, it was shown that the insertion-deletion polymorphism at -317 position of the promoter region of this gene (rs11568822) is associated with Alzheimer's disease, while the rs4803770 marker is associated with the coronary heart disease [58, 59]. Since the *APOC1* gene localizes in the same cluster as the *APOE* gene, it is assumed that these associations are due to the strong linkage disequilibrium between these genes [60]. However, we found no statistically significant changes in the expression level of the *APOE* gene. Therefore, it is reasonable to consider the *APOC1* gene to be an "independent" new candidate gene for PE. However, this assumption needs confirmation.

Thus, the findings indirectly confirm the immunological hypothesis of the development of severe PE, which postulates the key role of immune competent cells (B lymphocytes, monocytes, dendritic and NK cells) in the pathophysiology of this disease. This theory assumes that the etiopathogenesis of PE is triggered by insufficient trophoblast invasion into maternal spiral arteries, which is associated with a decreased expression of HLA antigens and "aggression" against NK cells. This results in reduced placental perfusion and development of hypoxia at the mother/fetus boundary, which, in turn, triggers the activity of pro-inflammatory cytokines, leading to endothelial dysfunction [61]. B cells may also contribute to the development of preeclampsia by producing anti-adrenoceptor antibodies.

CONCLUSIONS

The present work is the first Russian genome-wide study of differential gene expression in the placental tissues in normal and complicated pregnancies. The results indicate that some processes can play an important role

in the molecular pathogenesis of PE: reactions associated with the immune response, cytoskeleton organization, cell-cell interactions, responses to various stimuli, and chaperone-mediated protein folding. Integration of the results of a functional annotation of DEGs, analysis of network interactions of the proteins encoded by these genes, and the study of the transcriptome of the placental tissue make it possible to identify a number of novel genes that could be associated with PE: *LEP*, *SIGLEC6*, *BHLHE40*, *BCL6*, *RDH13*, *HSPH1*, *HSPA1A*, *BAG3*, *KRT19*, *RAC2*, *LIMCH1*, *BCL6* and *LCP1*.

We have also obtained evidence of a significant contribution of oxidative-stress-increasing expression of the genes of the Hsp70 and Hsp105 heat shock proteins, which are involved in the molecular mechanisms associated with impaired immune tolerance and initiation of the pro-inflammatory cascade, to the development of severe PE. Meanwhile, the observed increase in *BAG3* gene expression is probably due to the compensatory mechanisms or anti-apoptotic properties of the protein encoded by this locus. This assumption is supported by a statistically significant increase in the expression of the Hsp70 and Hsp90 heat shock proteins, heat shock factor 1 (HSF1), and Bcl-2 anti-apoptotic factor in endothelial cells of the placenta of PE patients as compared to females with normotensive pregnancy [62]. Moreover, the analysis of the proteome of placental tissue from females with physiological and complicated pregnancies has revealed the significance of stress-inducible proteins, including Hsp70, in the pathogenesis of PE [63].

The findings may be useful for understanding the molecular mechanisms of PE and searching for new candidate genes and biomarkers for this pathology. In addition, they provide information for the development of targeted therapy for this disease. ●

This work was supported by the Federal Target Program "Scientific and Scientific-Pedagogical Personnel of Innovative Russia" (contract number 8118) and the Russian Foundation for Basic Research (grant № 14-04-01467).

REFERENCES

1. Marigorta U.M., Navarro A. // PLoS Genet. 2013. V. 9. № 6. P. e1003566.
2. Manolio T.A., Collins F.S., Cox N.J., Goldstein D.B., Hindorf L.A., Hunter D.J., McCarthy M.I., Ramos E.M., Cardon L.R., Chakravarti A., et al. // Nature. 2009. V. 461. № 7265. P. 747–753.
3. Saccone S.F., Rice J.P., Saccone N.L. // Genet Epidemiol. 2006. V. 30. № 6. P. 459–470.
4. Adzhubei I.A., Schmidt S., Peshkin L., Ramensky V.E., Gerasimova A., Bork P., Kondrashov A.S., Sunyaev S.R. // Nat. Methods. 2010. V. 7. № 4. P. 248–249.
5. Nicolae D.L., Gamazon E., Zhang W., Duan S., Dolan M.E., Cox N.J. // PLoS Genet. 2010. V. 6. № 4. P. e1000888.
6. Zhong H., Yang X., Kaplan L.M., Molony C., Schadt E.E. // Am. J. Hum. Genet. 2010. V. 86. № 4. P. 581–591.
7. Makarov O.V., Volkova E.V., Jokhadze L.S. // Russian Journal of obstetrician-gynecologist. 2012. № 1. P. 35–42.
8. Ailamazyan E.K., Mozgovay E.V. Preeclampsia: theory and practice. M.: MEDpress-Inform, 2008. 272 p.
9. George E.M., Granger J.P. // Expert Rev. Obstet. Gynecol. 2010. V. 5. № 5. P. 557–566.
10. Naljayan M.V., Karumanchi S.A. // Adv. Chronic. Kidney Dis. 2013. V. 20. № 3. P. 265–270.

11. Scientific Center for Obstetrics, Gynecology and Perinatology of Kulakov, the Health Ministry of Russia, Institute for Family Health, The project "Mother and Child". Hypertension in pregnancy. Preeclampsia. Eclampsia. The clinical protocol. , 2012. 51 p.
12. Smyth G.K. // *Stat. Appl. Genet. Mol. Biol.* 2004. V. 3. № 1. P. 1544–6115.
13. Ritchie M.E., Diyagama D., Neilson J., van Laar R., Dobrovic A., Holloway A., Smyth G.K. // *BMC Bioinformatics.* 2006. V. 7. P. e261.
14. Huang da W., Sherman B.T., Tan Q., Kir J., Liu D., Bryant D., Guo Y., Stephens R., Baseler M.W., Lane H.C., Lempicki R.A. // *Nucl. Acids Res.* 2007. V. 35. P. 169–175.
15. Szklarczyk D., Franceschini A., Kuhn M., Simonovic M., Roth A., Minguéz P., Doerks T., Stark M., Muller J., Bork P., et al. // *Nucl. Acids Res.* 2011. V. 39. P. 561–568.
16. Sitras V., Paulssen R.H., Grønås H., Leirvik J., Hanssen T.A., Vårtun A., Acharya G. // *Placenta.* 2009. V. 30. № 5. P. 424–433.
17. Nishizawa H., Pryor-Koishi K., Kato T., Kowa H., Kurahashi H., Udagawa Y. // *Placenta.* 2007. V. 28. № 5. P. 487–497.
18. Enquobahrie D.A., Meller M., Rice K., Psaty B.M., Sis-covick D.S., Williams M.A. // *Am. J. Obstet. Gynecol.* 2008. V. 199. № 5. P. e1–11.
19. Founds S.A., Dorman J.S., Conley Y.P. // *J. Obstet. Gynecol. Neonatal. Nurs.* 2008. V. 37. № 2. P. 146–157.
20. Winn V.D., Gormley M., Paquet A.C., Kjaer-Sorensen K., Kramer A., Rumer K.K., Haimov-Kochman R., Yeh R.F., Overgaard M.T., Varki A., et al. // *Endocrinology.* 2009. V. 150. № 1. P. 452–462.
21. Lapaire O., Grill S., Lalevee S., Kolla V., Hösl I., Hahn S. // *Fetal Diagn. Ther.* 2012. V. 31. № 3. P. 147–153.
22. Rogue A., Lambert C., Spire C., Claude N., Guillouzo A. // *Drug Metab. Dispos.* 2012. V. 40. № 1. P. 151–158.
23. Hulse A.M., Cai J.J. // *Genetics.* 2013. V. 193. № 1. P. 95–108.
24. Benita Y., Kikuchi H., Smith A.D., Zhang M.Q., Chung D.C., Xavier R.J. // *Nucl. Acids Res.* 2009. V. 37. № 14. P. 4587–4602.
25. Lam K.K., Chiu P.C., Lee C.L., Pang R.T., Leung C.O., Koistinen H., Seppala M., Ho P.C., Yeung W.S. // *J. Biol. Chem.* 2011. V. 286. № 43. P. 37118–37127.
26. Nichol D., Christian M., Steel J.H., White R., Parker M.G. // *J. Biol. Chem.* 2006. V. 281. № 43. P. 32140–32147.
27. Huang W., Ghisletti S., Saijo K., Gandhi M., Aouadi M., Tesz G.J., Zhang D.X., Yao J., Czech M.P., Goode B.L., et al. // *Nature.* 2011. V. 470. № 7334. P. 414–418.
28. Gettemans J., van Impe K., Delanote V., Hubert T., Vandekerckhove J., De Corte V. // *Traffic.* 2005. V. 6. № 10. P. 847–857.
29. Percipalle P. // *Nucleus.* 2013. V. 4. № 1. P. 43–52.
30. Nishizawa H., Ota S., Suzuki M., Kato T., Sekiya T., Kurahashi H., Udagawa Y. // *Reprod. Biol. Endocrinol.* 2011. V. 2. № 9. P. 107.
31. Tsai S., Hardison N.E., James A.H., Motsinger-Reif A.A., Bischoff S.R., Thames B.H., Piedrahita J.A. // *Placenta.* 2011. V. 32. № 2. P. 175–182.
32. Kim J., Zhao K., Jiang P., Lu Z.X., Wang J., Murray J.C., Xing Y. // *BMC Genomics.* 2012. V. 27. № 13. P. 115.
33. Sood R., Zehnder J.L., Druzin M.L., Brown P.O. // *Proc. Natl. Acad. Sci. USA.* 2006. V. 103. № 14. P. 5478–5483.
34. Meng T., Chen H., Sun M., Wang H., Zhao G., Wang X. // *OMICS.* 2012. V. 16. № 6. P. 301–311.
35. Várkonyi T., Nagy B., Füle T., Tarca A.L., Karászi K., Schönleber J., Hupuczi P., Mihalik N., Kovalszky I., Rigó J. Jr., et al. // *Placenta.* 2011. V. 32. Suppl. S21. P. 9.
36. Lee G.S., Joe Y.S., Kim S.J., Shin J.C. // *Arch. Gynecol. Obstet.* 2010. V. 282. № 4. P. 363–369.
37. Xiang Y., Cheng Y., Li X., Li Q., Xu J., Zhang J., Liu Y., Xing Q., Wang L., He L., Zhao X. // *PLoS One.* 2013. V. 8. № 3. P. e59753.
38. Winn V.D., Gormley M., Fisher S.J. // *Pregnancy Hypertens.* 2011. V. 1. № 1. P. 100–108.
39. Denver R.J., Bonett R.M., Boorse G.C. // *Neuroendocrinology.* 2011. V. 94. № 1. P. 21–38.
40. Domali E., Messinis I.E. // *J. Matern. Fetal. Neonatal. Med.* 2002. V. 12. № 4. P. 222–230.
41. Laivuori H. // *Front. Biosci.* 2007. V. 12. P. 2372–2382.
42. Aizawa-Abe M. // *J. Clin. Invest.* 2000. V. 105. P. 1243–1252.
43. Fairfax B.P., Vannberg F.O., Radhakrishnan J. // *Hum. Mol. Genet.* 2010. V. 19. № 4. P. 720–730.
44. Sugathadasa B.H., Tennekoon K.H., Karunanayake E.H. // *Hypertens. Pregnancy.* 2010. V. 29. P. 366–374.
45. Vasku J., Dostalova Z., Kankova K. // *J. Obstet. Gynec.* 2008. V. 34. № 5. P. 858–864.
46. Jia R.Z., Zhang X., Hu P., Liu X.M., Hua X.D., Wang X., Ding H.J. // *Int. J. Mol. Med.* 2012. V. 30. № 1. P. 133–141.
47. Hogg K., Blair J.D., von Dadelszen P., Robinson W.P. // *Mol. Cell. Endocrinol.* 2013. V. 367. № 1. P. 64–73.
48. Rinn J.L., Chang H.Y. // *Annu. Rev. Biochem.* 2012. V. 81. P. 145–166.
49. Evdonin A.L., Medvedeva N.D. // *Cytology.* 2009. V. 51. № 2. P. 130–137.
50. Chernikov V.A., Gorohovets N.V., Savateeva L.V., Severin S.E. // *Biomedical Chemistry.* 2012. V. 58. № 6. P. 651–661.
51. Abdulsid A., Hanretty K., Lyall F. // *PLoS One.* 2013. V. 8. № 1. P. e54540.
52. Cudaback E., Li X., Yang Y., Yoo T., Montine K.S., Craft S., Montine T.J., Keene C.D. // *J. Neuroinflammation.* 2012. V. 10. № 9. P. 192.
53. Cekmen M.B., Erbagci A.B., Balat A., Duman C., Maral H., Ergen K., Ozden M., Balat O., Kuskay S. // *Clin. Biochem.* 2003. V. 36. № 7. P. 575–578.
54. Bayhan G., Koçyigit Y., Atamer A., Atamer Y., Akkus Z. // *Gynecol. Endocrinol.* 2005. V. 21. № 1. P. 1–6.
55. Koçyigit Y., Atamer Y., Atamer A., Tuzcu A., Akkus Z. // *Gynecol. Endocrinol.* 2004. V. 19. № 5. P. 267–273.
56. Catarino C., Rebelo I., Belo L., Rocha-Pereira P., Rocha S., Castro E.B., Patrício B., Quintanilha A., Santos-Silva A. // *Acta Obstet. Gynecol. Scand.* 2008. V. 87. № 6. P. 628–634.
57. Ahmadi R., Rahimi Z., Vaisi-Raygani A., Kiani A., Jalilian N., Rahimi Z. // *Hypertens. Pregnancy.* 2012. V. 31. № 4. P. 405–418.
58. Drigalenko E., Poduslo S., Elston R. // *Neurology.* 1998. V. 51. P. 131–135.
59. Ken-Dror G., Talmud P.J., Humphries S.E., Drenos F. // *Mol. Med.* 2010. V. 16. № 9. P. 389–399.
60. Lucatelli J.F., Barros A.C., Silva V.K., Machado Fda S., Constantim P.C., Dias A.A., Hutz M.H., de Andrade F.M. // *Neurochem. Res.* 2011. V. 36. № 8. P. 1533–1539.
61. Laresgoiti-Servitje E. // *J. Leukoc. Biol.* 2013. V. 94. № 2. P. 247–257.
62. Padmini E., Venkatraman U., Srinivasan L. // *Toxicol. Mech. Methods.* 2012. V. 22. № 5. P. 367–374.
63. Gharesi-Fard B., Zolghadri J., Kamali-Sarvestani E. // *Placenta.* 2010. V. 31. № 2. P. 121–125.

Lipid–Protein Nanodiscs Offer New Perspectives for Structural and Functional Studies of Water-Soluble Membrane-Active Peptides

Z. O. Shenkarev^{1,*}, E. N. Lyukmanova¹, A. S. Paramonov¹, P. V. Panteleev¹, S. V. Balandin¹, M. A. Shulepko^{1,2}, K. S. Mineev¹, T. V. Ovchinnikova^{1,3}, M. P. Kirpichnikov^{1,2}, A. S. Arseniev^{1,3}

¹Shemyakin-Ovchinnikov Institute of Bioorganic Chemistry, Russian Academy of Sciences, Miklukho-Maklaya Str., 16/10, 117997, Moscow, Russia

²Lomonosov Moscow State University, GSP-1, Leninskie Gory, 1, Bldg. 12, 119991, Moscow, Russia

³Moscow Institute of Physics and Technology (State University), Institutskii Pereulok, 9, 141700, Dolgoprudny, Moscow Region, Russia

*E-mail: zakhar-shenkarev@yandex.ru

Received 07.10.2013

Revised manuscript received 19.03.2014

Copyright © 2014 Park-media, Ltd. This is an open access article distributed under the Creative Commons Attribution License, which permits unrestricted use, distribution, and reproduction in any medium, provided the original work is properly cited.

ABSTRACT Lipid-protein nanodiscs (LPNs) are nanoscaled fragments of a lipid bilayer stabilized in solution by the apolipoprotein or a special membrane scaffold protein (MSP). In this work, the applicability of LPN-based membrane mimetics in the investigation of water-soluble membrane-active peptides was studied. It was shown that a pore-forming antimicrobial peptide arenicin-2 from marine lugworm (charge of +6) disintegrates LPNs containing both zwitterionic phosphatidylcholine (PC) and anionic phosphatidylglycerol (PG) lipids. In contrast, the spider toxin VSTx1 (charge of +3), a modifier of Kv channel gating, effectively binds to the LPNs containing anionic lipids (POPC/DOPG, 3 : 1) and does not cause their disruption. VSTx1 has a lower affinity to LPNs containing zwitterionic lipids (POPC), and it weakly interacts with the protein component of nanodiscs, MSP (charge of –6). The neurotoxin II (NTII, charge of +4) from cobra venom, an inhibitor of the nicotinic acetylcholine receptor, shows a comparatively low affinity to LPNs containing anionic lipids (POPC/DOPG, 3 : 1 or POPC/DOPS, 4 : 1), and it does not bind to LPNs/POPC. The obtained data show that NTII interacts with the LPN/POPC/DOPS surface in several orientations, and that the exchange process among complexes with different topologies proceeds fast on the NMR timescale. Only one of the possible NTII orientations allows for the previously proposed specific interaction between the toxin and the polar head group of phosphatidylserine from the receptor environment (Lesovoy et al., *Biophys. J.* 2009. V. 97. № 7. P. 2089–2097). These results indicate that LPNs can be used in structural and functional studies of water-soluble membrane-active peptides (probably except pore-forming ones) and in studies of the molecular mechanisms of peptide-membrane interaction.

KEYWORDS antimicrobial peptides; lipid-protein nanodiscs; high-density lipoprotein particles; membrane-active peptides; membrane mimetics; neurotoxins; NMR spectroscopy.

ABBREVIATIONS 5-DSA – 5-doxyl-stearic acid; AMP – antimicrobial membrane-active peptide; Ar2 – arenicin-2 from marine polychaeta lugworm *Arenicola marina*; DLPC – dilauroyl phosphatidylcholine; DLPG – dilauroyl phosphatidylglycerol; DOPG – dioleoyl phosphatidylglycerol; DOPS – dioleoyl phosphatidylserine; LPN – lipid-protein nanodisc; MP – membrane-active peptide; MSP – 44-243 fragment of human apolipoprotein A1 (membrane scaffold protein); NTII – neurotoxin II from *Naja oxiana* cobra venom; POPC – palmitoyloleoyl phosphatidylcholine; POPE – palmitoyloleoyl phosphatidylethanolamine; POPG – palmitoyloleoyl phosphatidylglycerol; R_h – hydrodynamic radius of a particle, Stokes radius; TROSY – transverse relaxation-optimized spectroscopy; TRX – thioredoxin from *Escherichia coli*; VSTx1 – voltage sensor toxin from *Grammostola spatulata* spider venom; η_{XY} – the rate of cross-correlation between dipole-dipole and chemical shift anisotropy relaxation of the ¹⁵N nucleus; τ_r – effective rotational correlation time.

INTRODUCTION

Membrane-active peptides (MPs) are a class of biomolecules that play an important role in the existence of certain organisms and their communities. For example, antimicrobial membrane-active peptides (AMPs), which selectively act on the membranes of various cells, are among the main effectors in the “innate immunity” system, which is the earliest defense system of eukaryotes [1]. Some peptide mediators of the nervous and endocrine systems of mammals and a number of animal toxins, targeted membrane receptors, also exhibit membrane activity and act at several stages, initially binding the membrane surrounding the receptor and only after forming a ligand-receptor complex [2, 3]. In this case, the so-called “membrane catalysis” mechanisms come into play, which greatly increases the efficiency of the ligand-receptor interaction [3].

The structural features of membrane-active peptides complicate their biophysical studies. Due to their hydrophobic properties and significant conformational mobility, many MPs form an “active” spatial structure only in the presence of a biological membrane or a suitable membrane mimetic. These factors hamper MP crystallization and necessitate the use of alternative research methods. One such method is high-resolution NMR spectroscopy, which allows one to study the spatial structure and intramolecular dynamics of MPs directly in solution of membrane mimicking media [4, 5]. The commonly used membrane mimetics have a number of drawbacks, which limit their use in the study of specific peptide-membrane interactions. For example, a large surface curvature and the loose packing of detergent-based media (in the form of micelles or small lipid-containing bicelles) can cause significant distortions in the peptide structure [6] and nonspecific peptide-detergent interactions. Meanwhile, media containing real bilayer membranes in the form of lipid vesicles or lipid/detergent bicelles have sizes that are too large for high-resolution NMR studies of MPs [4, 7].

Lipid-protein nanodiscs (LPNs) or reconstructed nascent high-density lipoprotein particles are nanosized discoid particles (typically 4×10 nm) containing a fragment of the bilayer lipid membrane (~150 lipid molecules), whose hydrophobic part is shielded from the solvent with two molecules of apolipoprotein or its synthetic analogue, the membrane scaffold protein (MSP) [8]. In contrast to the commonly used membrane mimetics, the membrane fragment incorporated in a lipid-protein nanodisc demonstrates increased stability and retains many biophysical properties inherent in real bilayer systems; for example the liquid crystalline to gel phase transition [9]. Recently, several papers demonstrated that LPNs can stand as alternative membrane mimetic media for structural and functional

studies of membrane proteins and hydrophobic (poorly soluble) MPs [10–16]: in particular, using high-resolution NMR spectroscopy [12–15]. The use of LPNs containing various lipids and their mixtures allows one to study different functional aspects of membrane proteins and MPs [15, 16].

The problems related to the application of LPN-based membrane mimetic media in structural and biophysical studies of water-soluble MPs have yet to be studied. It should be noted that this is far from being a trivial matter, since LPNs, unlike vesicles, bicelles, and micelles, contain an additional component, MSP, which is an anionic protein (charge of -6). In this paper, the interaction of water-soluble MPs with LPNs was studied using three model cationic β -structured peptides (Fig. 1), which have different physicochemical properties and represent three classes of membrane-active compounds. The antimicrobial peptide arenicin-2 (Ar2, 21 AA, 2772 Da, charge of $+6$, mean Kyte-Doolittle hydrophobicity index [17] is -0.06^1) from coelomocytes of the polychaete lugworm *Arenicola marina* interacts selectively with membranes containing negatively charged lipid molecules and forms oligomeric pores in them [18]. The VSTx1 toxin (34 AA, 4010 Da, charge of $+3$, hydrophobicity index is -0.27) from *Grammostola spatulata* spider venom uses the “membrane catalysis” mechanism to interact with the voltage-sensitive domains of K^+ -channels localized in the cell membrane, and it lacks pore-forming ability [3]. Neurotoxin II (NTII, 61 AA, 6885 Da, charge of $+4$, hydrophobicity index is -1.10) from *Naja oxiana* cobra venom blocks the activation of the nicotinic acetylcholine receptor through binding to its extracellular domain, but it probably also uses the “membrane catalysis” mechanism when interacting with the polar heads of phosphatidylserine (PS) from the receptor membrane environment [19]. The peptides chosen as study objects are soluble in water at millimolar concentrations; however, they differ greatly from each other in their hydrophobic/hydrophilic properties. Thus, despite its large positive charge, Ar2 is the most hydrophobic among the studied peptides.

EXPERIMENTAL

LPN reconstitution and purification

The recombinant 44–243 fragment of the human apolipoprotein A1 with a N-terminal sequence of six His residues was used as an MSP protein. The purified MSP protein, obtained as described in [20], was mixed at a molar ratio of 1 : 75 with lipids in the presence of

¹ The maximum and minimum values of the Kyte-Doolittle hydrophobicity index [17] are $+4.5$ and -4.5 for poly-Ile and poly-Arg sequences, respectively.

a detergent, sodium cholate (2 : 1 cholate/lipids molar ratio), and the mixture was incubated at 4 °C for 3 h. When using saturated lipids (DLPC, DLPG), the reaction temperature was kept not lower than 25 °C. Spontaneous LPN assembly was initiated by detergent sorption to the Bio-Beads™ resin (Bio-Rad, USA) for 1.5 h. Purification of the nanodiscs was performed on a Ni²⁺ Sepharose 6 Fast Flow resin (GE Healthcare, USA) equilibrated with buffer A (20 mM Tris-HCl, 0.5 M NaCl, 1 mM NaN₃, pH 8.0). After loading the reaction mixture, the resin was washed with a fivefold volume of buffer A. LPNs were eluted with buffer A containing 100 mM imidazole. The MSP concentration was determined spectrophotometrically by absorbance at $\lambda = 280$ nm. The LPN concentration was determined by assuming that each nanodisc contained two MSP molecules.

Gel filtration

Gel filtration with separation of the particles by size was carried out on a Superdex-200 resin using a Tricorn 5/200 column (GE Healthcare, Sweden) in buffer (10 mM Tris-HCl, 0.1 M NaCl, 1 mM EDTA, 1 mM NaN₃, pH 7.4). Thyroglobulin (669 kDa, Stokes radius $R_H = 8.5$ nm), ferritin (440 kDa, $R_H = 6.1$ nm), catalase (232 kDa, $R_H = 5.22$ nm), aldolase (158 kDa, $R_H = 4.81$ nm) BSA (67 kDa, $R_H = 3.55$ nm), and ovalbumin (43 kDa, $R_H = 3.05$ nm) were used as calibration proteins. The flow rate through the column was 0.3 ml/min. Detection was performed at 280 nm. The particle size was determined from the elution volume vs the $\lg R_H$ calibration curve. All the particle size (diameter) values provided below correspond to twice R_H values.

Preparation of a recombinant analogue of Ar2

A recombinant arenicin-2 analogue, whose amino acid sequence is entirely consistent with that of the natural peptide, was obtained in accordance with the protocols [18, 21].

Production and Purification of VSTx1

The standard genetic engineering procedures were used. The *VSTx1* gene was obtained by PCR with six overlapping synthetic oligonucleotides (Evrogen, Moscow, Russia) optimized for rare codons of *Escherichia coli*. The *VSTx1* gene was cloned into the pET-32a(+) vector (Novagen) at the KpnI and BamHI sites in a single reading frame with the thioredoxin (TRX) gene. Then, the sequence encoding the enterokinase cleavage site of the fusion protein was replaced with the sequence encoding the thrombin cleavage site. The resulting plasmid was named pET/TRX-VSTx1.

BL21 (DE3) *E. coli* cells were transformed with the recombinant pET/TRX-VSTx1 vector and plated onto Petri dishes with LB agar (10 g of Bacto Tryptone, 5 g of yeast extract, 10 g of NaCl per 1 liter of the medium, pH 7.4) and ampicillin (100 mg/L). Colonies were transferred from a dish into a TB culture medium (12 g of Bacto Tryptone, 24 g of yeast extract, 4 ml of glycerol, 2.3 g of KH₂PO₄, 5.12 g of K₂HPO₄ in 1 liter of the medium, pH 7.4) containing ampicillin (100 mg/L) and cultured at 37 °C with moderate shaking until the optical density reached 0.6 o.u. The *TRX-VSTx1* gene transcription was induced by adding isopropyl β -D-1-thiogalactopyranoside (IPTG) to a final concentration of 0.025 mM. Cultivation of the cell culture was continued in the TB medium at 37 °C overnight.

The cell culture was centrifuged (20 min, 8000 rpm, 4 °C). The cell pellet from 1 liter of the culture was resuspended in buffer A. Cells were disrupted using an ultrasonic disintegrator (Branson Digital Sonifier) for 10 s with 12-fold repetition. The lysate was centrifuged at 30,000 *g* for 30 min; the supernatant was then collected. The lysate was purified on a metal-affinity resin equilibrated with buffer A. After loading the protein sample, the column was washed with three column volumes of buffer A and three column volumes of buffer A containing 50 mM imidazole. TRX-VSTx1 was eluted with buffer A containing 150 mM imidazole. After purification, specific hydrolysis of the fusion protein with thrombin was carried out. The VSTx1 sample was isolated using subtractive metal affinity chromatography. Reversed phase HPLC (C4 column, 4.6 × 250 mm, A300, Jupiter, Phenomenex) was used for the final purification of the VSTx1 sample. The toxin yield was 1 mg/L of the bacterial culture. Unlike the natural toxin, the recombinant VSTx1 analogue contained the additional N-terminal Gly-Ser residues resulting from the hydrolysis by thrombin. The identity of the recombinant toxin molecular weight to the calculated value was confirmed by mass spectrometry.

Preparation of NTII and its ²H,¹⁵N-labeled variant

The recombinant neurotoxin II sample was obtained according to [22]. The ²H,¹⁵N-labeled NTII sample was prepared as follows: BL21 (DE3) cells, transformed with the pET-22b(+)/STII/NTII vector [22], were plated onto Petri dishes with LB agar and ampicillin (100 mg/L). The colonies from a dish were inoculated into 10 ml of a LB medium and cultured at 37 °C for 1 h. Then, cells were added every hour with 10 ml of a LB medium prepared using deuterated water (²H₂O, 99% of deuterium), until the total volume of the medium reached 110 ml. Under these conditions, cultivation was continued overnight. Afterwards, the cell

pellet was aseptically harvested and re-suspended in 1 liter of a M9 minimal medium (6 g of Na_2HPO_4 , 3 g of KH_2PO_4 , 0.5 g of NaCl , 2 g of $^{15}\text{NH}_4\text{Cl}$, 240 mg of anhydrous MgSO_4 , 11 mg of CaCl_2 , 4 ml of glycerol, 2 mg yeast extract, 200 μl of 5% thiamine chloride per 1 liter of the medium, pH 7.4) prepared with $^2\text{H}_2\text{O}$. Cells were incubated at 37 °C until the culture optical density reached 0.6 o.u. The *stII-ntII* gene transcription was induced with IPTG, which was added to a final concentration of 0.05 mM, and the cell culture was cultured for 1 day. Isolation and purification of ^2H , ^{15}N -NTII was performed according to [22].

NMR Spectroscopy

NMR spectra were acquired at 40–45 °C on AVANCE-700 and AVANCE-III-800 spectrometers (Bruker, Germany) equipped with cryogenically cooled triple-resonance probes at the proton resonance frequencies of 700 and 800 MHz, respectively.

To measure the isotherms of the toxins binding to LPNs and MSP molecules, the VSTx1 and NTII samples (20 mM, 10 mM Tris-Ac, pH 7.0) were titrated with solutions of nanodiscs (70 μM) of various lipid compositions or with a MSP solution (0.7 mM). The 1D ^1H -NMR spectrum was acquired at each point. A data analysis was performed assuming that the intensity of the observed NMR signals of a peptide is proportional to its equilibrium concentration in solution ($[\text{P}]_{\text{free}}$). The binding curves were fitted either to the partition equilibrium equation (1) or to the Langmuir isotherm equation (2), taking into account the dilution of the initial samples upon titration:

$$[\text{P}]_{\text{bound}}/[\text{LPN}/\text{lipid}] = K_p \cdot [\text{P}]_{\text{free}}, \quad (1)$$

$$1/K_n = [\text{P}]_{\text{free}} \cdot (n \cdot [\text{LPN}] - [\text{P}]_{\text{bound}})/[\text{P}]_{\text{bound}}, \quad (2)$$

where $[\text{LPN}/\text{lipid}]$ is the LPN concentration (assuming that one nanodisc contains two MSP molecules) or the lipid concentration (assuming that one nanodisc contains 150 lipid molecules), $[\text{P}]_{\text{bound}}$ is the concentration of a peptide bound to LPN ($[\text{P}]_0 = [\text{P}]_{\text{free}} + [\text{P}]_{\text{bound}}$), K_p is the partition coefficient, n is the number of binding sites for a peptide on the nanodisc surface, and K_n is the affinity constant of the peptide to the binding site on the nanodisc surface.

The interaction of NTII with LPN was studied using a sample containing 45 μM ^2H , ^{15}N -NTII, and 75 μM LPN/POPC/DOPS (4 : 1) (10 mM Tris-Ac, pH 7.0). To identify the peptide HN-groups making contacts with the nanodisc surface, the ^1H signal of choline group of the POPC lipid ($(\text{CH}_3)_3\text{N}^+$, chemical shift is 3.2 ppm) was saturated at a frequency of 125 Hz for 0.1, 0.3, 0.5, 0.8, 1.0, 1.5, and 3.0 s using a relaxation delay of 3 s. The

changes in the intensities of the NTII cross peaks induced by presaturation of POPC choline group were observed in the 2D ^1H , ^{15}N -TROSY spectra. To identify the peptide HN-groups making contacts with the hydrophobic region of the nanodisc membrane, the paramagnetic probe of 5-doxyl-stearic acid (5-DSA) was used. 5-DSA dissolved in a small amount of methanol was added to the sample containing NTII/LPN complexes to a final concentration of 10, 30, and 75 μM . Attenuation of the NTII signal intensity arising due to the paramagnetic enhancement of the ^1H and ^{15}N nuclear relaxation was observed in the 2D ^1H , ^{15}N -TROSY spectra. The rates of the cross-correlation process between the dipole-dipole relaxation and relaxation arising from the chemical shift anisotropy of the ^{15}N nucleus (η_{xy}) were measured for the complexes of NTII with LPN/POPC/DOPS at 40 °C on an AVANCE-III-800 spectrometer, using amplitude modulated 2D ^1H , ^{15}N -TROSY experiments [23]. The rotational correlation time (τ_{R}) for the peptide HN-groups was calculated from the measured η_{xy} values.

RESULTS AND DISCUSSION

Interaction of arenicin-2 with nanodiscs

The cationic AMP, Ar2, contains mainly positively charged and hydrophobic residues and has a β -hairpin structure in water, which is stabilized with one disulfide bond (*Fig. 1*) [21]. Arenicin-2 interacts selectively with membranes containing negatively charged lipid molecules and creates in them oligomeric pores, which are formed with the participation of phospholipids (the so-called “toroidal” pores) [18]. At high concentrations, Ar2 probably causes bilayer micellization [24]. As expected, the β -hairpins of individual peptides within the pore have a transmembrane orientation, so that the N- and C-terminal fragments and β -turn region come into contact with polar areas on the outer and inner sides of the membrane [18].

To study the possibility of obtaining stable Ar2-LPN complexes, nanodiscs containing neutral (POPC) and anionic (DOPG) “long-chain” lipids were used. Earlier, it had been demonstrated using CD spectroscopy that Ar2 does not interact with vesicles formed from POPC and binds with high affinity to DOPG liposomes [18, 21]. To simulate a possible transition of the Ar2 β -hairpin (length \sim 3.5 nm) in the transmembrane state, a mixture of “short-chain” lipids with different charges (DLPC/DLPG = 4 : 1, fatty acid chains with 12 carbon atoms in length, the distance between the phosphate groups on opposite sides of the membrane was \sim 3.4 vs \sim 3.7 nm for long chain lipids [25]) was used. Earlier, LPNs based on the DLPC/DLPG mixture had been used to observe the transitions between the surface-bound and

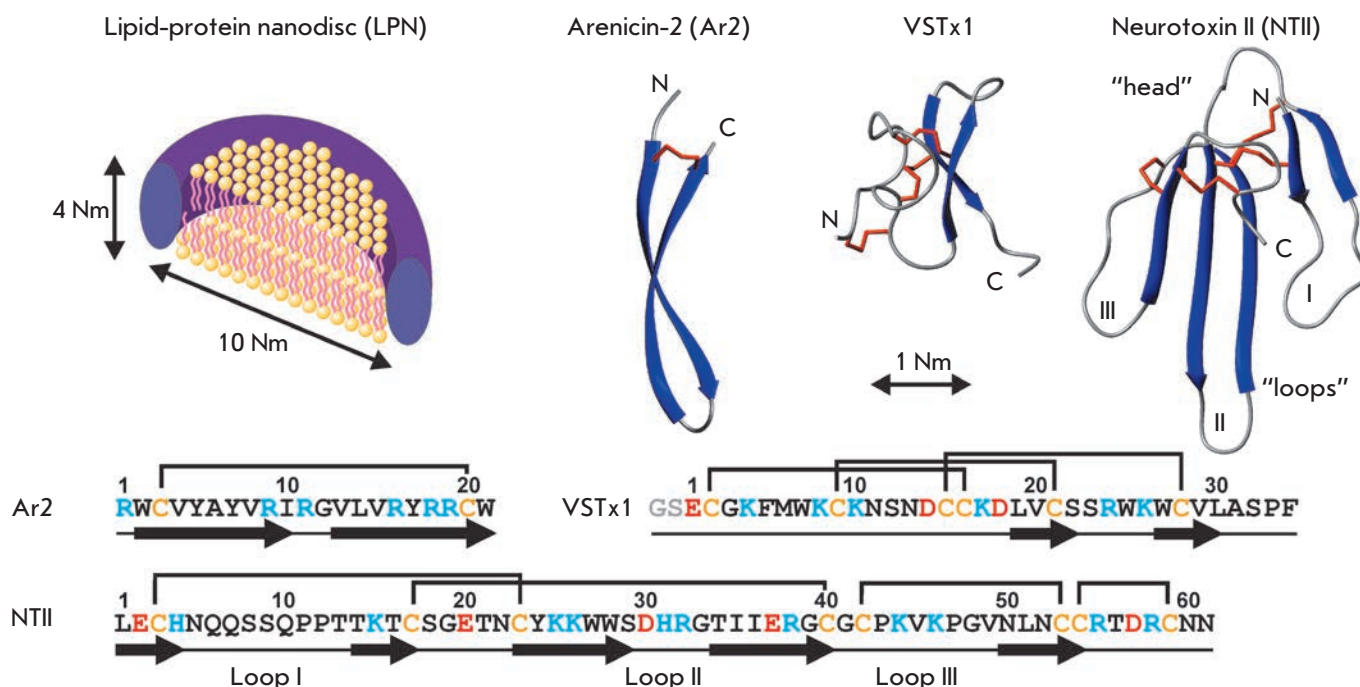


Fig. 1. Schematic representation of a lipid-protein nanodisc and the amino acid sequences and spatial structures of arenicin-2, VSTx1, and NTII (PDB codes 2JNI, 1S6X, and 1NOR, respectively). Two MSP molecules shielding the membrane fragment of the nanodisc from the solvent are drawn as tori. Charged residues and cysteines are highlighted in the peptides sequences with color. A recombinant VSTx1 analogue with additional Gly-Ser residues at the N-terminus was used in this work (shown in gray)

transmembrane state of the channel-forming peptide antibiotic antimioebin I [15].

During that study, an aqueous Ar2 solution was added to nanodisc samples. In all cases, even when small peptide concentrations were added, the LPN solutions were strongly opalescent, while at equimolar concentrations (Ar2/LPN = 1 : 1) and higher the solutions became opaque, which indicates nanodisc disruption and formation of larger particles. An analysis of the sample supernatants by gel filtration confirmed this assumption. Large complexes with characteristic sizes of ~ 15 nm, the residual fraction of LPNs of ~ 10–11 nm in diameter, as well as a small number of particles of ~ 6 nm in diameter were revealed in the samples (Fig. 2A). Comparison with the results of previous studies [20, 26] suggested that the 6 nm particles correspond to MSP aggregates. Apparently, Ar2 causes nanodisc fusion, accompanied by the release of MSP molecules. A similar process is known as high-density lipoprotein remodeling, which can occur both *in vitro* and *in vivo* upon the interaction of lipoprotein particles with lipophilic plasma proteins [27]. Previously, nanodisc fusion had been observed in cell-free protein biosynthesis systems with the cotranslational incorporation of mem-

brane proteins into LPNs containing unsaturated lipids [26]. The spontaneous LPN fusion *in vitro* proceeds very slowly, but it could be considerably accelerated under denaturing conditions [28].

Amphiphilic MSP molecules should introduce a significant positive spontaneous curvature to the lipid bilayer for peripheral stabilization of a membrane fragment. A similar effect on the spontaneous lipid curvature is caused by a multitude of amphiphilic AMPs, whose action is mediated by the formation of “toroidal” pores, which are regions with a large positive curvature [29], or by bilayer micellization. Ar2 does not interact with POPC liposomes [21], so we may assume that the nanodisc fusion observed in the case of LPN/POPC is not directly related to the pore-forming activity of the peptide, but is caused by its attachment to a peripheral region of the LPN membrane. The attached Ar2 molecules displace certain segments of MSP, which leads to the defects in the LPN structure and induces nanodisc fusion. As a result the lipoprotein particles containing large phospholipid domains are formed and the free MSP molecules are released. In the case of LPNs containing anionic lipids, an alternative mechanism for the formation of defects in the LPN structure could be

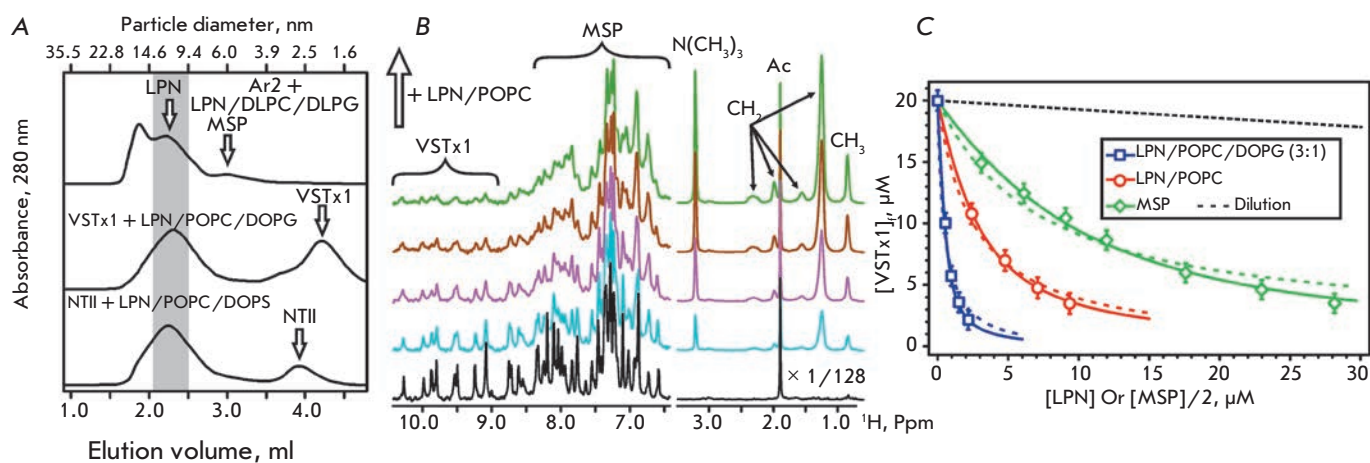


Fig. 2. Gel filtration analysis of LPNs after MP addition and analysis of the interaction of VSTx1 with LPNs and MSP. (A). The positions of the peaks corresponding to nanodiscs, MSP aggregates, NTII, and VSTx1 are shown. (B). Interaction of VSTx1 with LPNs/POPC. The fragments of the 1D ^1H spectra of $20\ \mu\text{M}$ VSTx1 acquired at different LPN concentrations are shown. (C). The binding curves describing VSTx1 interactions with LPN and MSP are approximated by the partition equilibrium equation (eq. 1, dashed lines) and by the Langmuir isotherm (eq. 2, solid lines). Calculated parameters are summarized in the Table

suggested as caused by the ability of Ar2 to interact directly with the nanodisc membrane.

Given that the mechanisms associated with the change in the local curvature of the lipid bilayer (“toroidal” pore formation, bilayer micellization) underlie the action of the overwhelming majority of water-soluble cationic AMPs, we can assume that many of these molecules will have a destructive effect on LPNs. Thus, nanodiscs are probably not suited as a medium for studying these peptides. It should be noted that there are other classes of channel- and pore-forming biomolecules that can be studied in LPN-based media. For example, the literature has described the formation of stable complexes of LPNs with the hydrophobic channel-former antimioebin I (upper limit of solubility in water is $30\ \mu\text{M}$) [12, 15, 20] as well as successful incorporation of integral membrane proteins into the nanodiscs that form ion channels and pores, such as the K^+ channel KcsA [20], nicotinic acetylcholine receptor [30], pore-forming component of the anthrax toxin [11], and a number of proteins with the β -barrel structure [14].

Interaction of the VSTx1 toxin with nanodiscs and MSP

The VSTx1 toxin is a small β -structured peptide stabilized by three disulfide bonds which form a “cysteine knot” (Fig. 1) [31]. VSTx1 weakly interacts with zwitterionic lipid membranes and has considerable affinity for the interface of phospholipid membranes, which contain anionic lipids, and yet has no membrane lytic

activity [31]. According to current data, VSTx1 inhibits the voltage-dependent activation of K^+ channels and uses “membrane catalysis” mechanisms when forming a complex with the voltage-sensing domain of the channel [3]. The toxin activity is significantly dependent on the lipid composition and mechanical state of the lipid membrane surrounding the channel [32].

Previously, a mixture of zwitterionic phosphatidylethanolamine and anionic phosphatidylglycerol lipids (POPE/POPG, 3 : 1) was used to study the interaction of VSTx1 with liposomes [3]. However, the formation of LPNs containing a significant fraction of phosphatidylethanolamine was ineffective, probably because of the high negative spontaneous curvature of the formed bilayer [20, 33]. Therefore, nanodiscs containing zwitterionic phosphatidylcholine and anionic phosphatidylglycerol (POPC and a mixture of POPC/DOPG, 3 : 1) were used to estimate the energetics of VSTx1 interaction with LPN membranes. A MSP sample containing no lipids was used to assess the contribution of the non-specific interactions caused by the presence of a protein component in LPNs. Titration of the VSTx1 sample with a LPN solution or a solution of MSP, which forms relatively large aggregates ($\sim 6\ \text{nm}$ in diameter), led to a gradual decrease in the intensity of the peptide NMR signals (Fig. 2B). This indicated the association of the VSTx1 molecules with the nanodisc surface or MSP. In this case, due to the slow reorientation of nanodiscs and MSP aggregates in the solution, peptide binding resulted in a significant increase in the NMR line width and a decrease in the signal intensity.

Energetic and stoichiometric parameters of VSTx1 and NTII interactions with LPNs and MSP, obtained using the partition equilibrium equation (eq. 1) and Langmuir isotherm (eq. 2)

Peptide	LPN or MSP	Partition equilibrium		Langmuir isotherm	
		$K_p(\text{LPN}, \text{MSP} \times 2)^*$ $\times 10^6 \cdot \text{M}^{-1}$	$K_p(\text{Lipids})^*$ $\times 10^3 \cdot \text{M}^{-1}$	K_n^{**} $\times 10^6 \cdot \text{M}^{-1}$	n^{***}
VSTx1	LPN/POPC	0.39 ± 0.02	2.6 ± 0.2	0.06 ± 0.01	9.6 ± 1.5
	LPN/POPC/DOPG (3 : 1)	2.68 ± 0.24	17.8 ± 1.6	0.13 ± 0.02	34.5 ± 3.9
	MSP $\times 2$	0.10 ± 0.01		0.05 ± 0.02	3.2 ± 0.9
NTII	LPN/POPC/DOPG (3 : 1)	0.32 ± 0.01	2.13 ± 0.07		
	LPN/POPC/DOPS (4 : 1)	0.16 ± 0.01	1.07 ± 0.07		

* K_p – the partition coefficient. The concentration of the “non-aqueous” phase was taken to be equal to either LPN or lipid concentrations. It was assumed that each nanodisc contains two MSP molecules and 150 lipids.

** K_n – the affinity constant of the peptide to the binding site on the LPN surface.

*** n – the number of binding sites on the LPN surface.

Calculations demonstrated that under experimental conditions, we could safely assume that the intensity of the observed NMR signal is directly proportional to the equilibrium concentration of the free peptide in the solution ($[\text{VSTx1}]_f$).

An analysis of the measured binding curves using the partition equilibrium equation (equation 1, *Fig. 2B, Table*) revealed that VSTx1 interacts effectively with LPNs containing anionic lipids (POPC/DOPG mixture), and that it interacts less efficiently with nanodiscs based on zwitterionic lipids (POPC). The calculated partition coefficients ($K_p \sim 17.8 \times 10^3$ and $2.6 \times 10^3 \text{ M}^{-1}$, respectively) were much higher than the values previously observed for vesicles of POPE/POPG (3 : 1) and POPC ($K_p \sim 2 \times 10^3$ and $<0.002 \times 10^3 \text{ M}^{-1}$, respectively) [3, 31]. These differences in the toxin affinity may be due to both the differences in the packing of phospholipid molecules in LPN membranes and vesicles [34] and the use of different buffer systems in the experiments. In papers [3, 31], the toxin binding was studied in buffers containing 150 mM KCl and NaCl, respectively, while a buffer without addition of salt was used in our work. Increased solution ionic strength, leading to partial shielding of electrostatic interactions, probably reduces the VSTx1 affinity to lipid membranes. The observed weak interaction of VSTx1 with MSP (*Fig. 2B, Table*), which is apparently due to the electrostatic interaction between a positively charged toxin molecule and an anionic MSP molecule, can also act as an additional factor enhancing the toxin affinity to LPNs.

An analysis of the binding curves using the Langmuir isotherm (equation 2, *Fig. 2B, Table*) revealed that VSTx1 shows approximately the same affinity to the sites on the nanodisc surface or on a MSP molecule ($K_n \sim 0.05 \times 10^6 - 0.13 \times 10^6 \text{ M}^{-1}$, *Table*); however, the

number of binding sites differs significantly. Thus, a nanodisc containing POPC (~ 150 molecules) can bind up to ~ 10 toxin molecules, and the addition of negatively charged lipids increases the number of binding sites up to ~ 35 (~ 4 lipid molecules per toxin molecule). In turn, each MSP molecule (in the absence of lipids) is able to bind up to 1.6 VSTx1 molecules, which leads to its almost complete charge compensation.

The gel filtration analysis of the VSTx1/LPN complexes revealed no nanodisc disruption upon binding of the toxin. Individual peaks can be seen on the chromatograms (*Fig. 2A*) for particles with a diameter of ~ 10–11 and ~ 2.0 nm, which probably corresponds to nanodiscs and the unbound toxin, which was dissociated from the nanodisc surface (a buffer containing 100 mM NaCl was used for the chromatography).

Interaction of the NTII neurotoxin with nanodiscs

Neurotoxin II (NTII) is a cationic non-hydrophobic peptide which is stabilized by four disulfide bonds and has the so-called “three-loop” β -structure fold characteristic for snake toxins (*Fig. 1*) [35]. NTII is a highly specific inhibitor of the muscle-type nicotinic acetylcholine receptor. It blocks, with its central loop, the ligand binding sites located on the receptor extracellular domain [36]. Unlike VSTx1, NTII has no explicit membrane activity. At the same time, the ^1H , ^{15}N -, and ^{31}P -NMR spectroscopy investigation of NTII in the environment of DOPC/DOPS/cholesterol (3 : 1 : 1) liposomes simulating the membrane environment of the acetylcholine receptor have suggested that the toxin action also includes elements of “membrane catalysis” mechanism [19]. Apparently, the site located in the region of the toxin “head,” near the Glu2, Asp57, and Arg58 residues (*Fig. 3B*), is able to bind, in the 1 : 1 stoichiometry, the charged head-

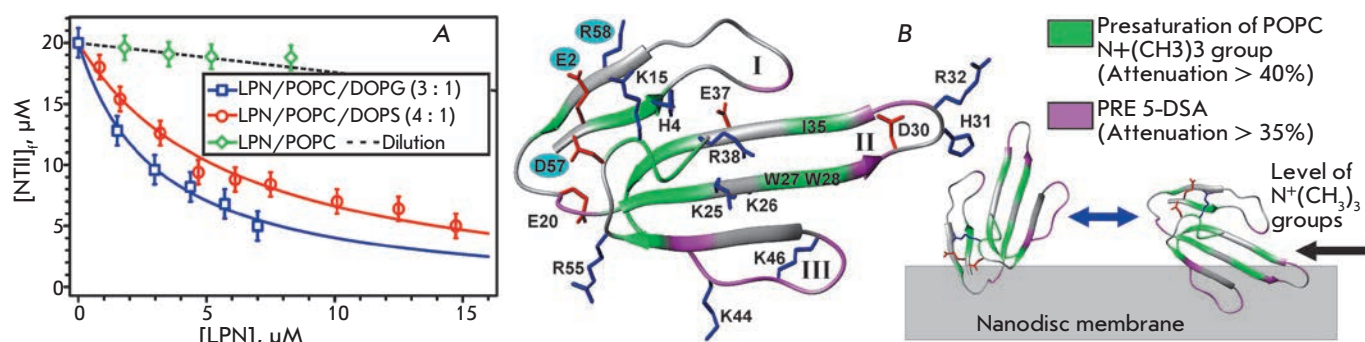


Fig. 3. The binding curves representing NTII interactions with LPNs and the possible topology of the NTII interaction with the surface of the LPN/POPC/DOPS membrane. (A). The binding curves are approximated by the partition equilibrium equation (eq. 1). Calculated parameters are summarized in the Table. (B). The NTII ribbon is colored according to the experimental data (Figs. 4D, E). The residues forming the earlier proposed site of specific interaction with the polar headgroup of phosphatidylserine [19] are marked by blue circles

group of a phosphatidylserine (PS) lipid from the membrane surrounding the receptor. This interaction probably plays a role at the initial stages of NTII action and provides the toxin with the optimal orientation needed for formation of the toxin-receptor complex [19].

The LPNs assembly from a POPC/DOPS/cholesterol (3 : 1 : 1) mixture using the standard protocol for nanodisc formation (see Experimental section) appeared to be ineffective; therefore, LPNs based on a 4 : 1 POPC/DOPS mixture were used for NTII study. Furthermore, nanodiscs based on a POPC and POPC/DOPG (3 : 1) mixture were tested for comparison. Titration of the NTII sample with nanodisc solutions revealed that the toxin does not bind to nanodiscs based on zwitterionic lipids (POPC) and shows a low affinity for LPNs containing anionic lipids (POPC/DOPG and POPC/DOPS) (Fig. 3A, Table). The higher NTII affinity for LPNs based on 3 : 1 POPC/DOPG may be explained by the larger charge of the nanodisc membrane (the relative content of a charged lipid is 25% vs 20% in the 4 : 1 POPC/DOPS membrane). Furthermore, in the membrane containing DOPS, charges of the NH_3^+ - and COOH -groups of serine form a dipole, which may shield the negative charge of the phosphate group. Thus, the apparent charge of the polar head of DOPS will be less than that of DOPG. These findings suggest the lack of significant NTII selectivity for membranes containing different anionic lipids (phosphatidylserine and phosphatidylglycerol).

The lack of detectable binding of NTII to LPN/POPC indicates indirectly the absence of nonspecific toxin interactions with the MSP protein. As in the case of VSTx1, a gel-filtration analysis of the NTII/LPN complexes revealed no disruption of nanodiscs upon toxin binding (Fig. 2A). The chromatograms demonstrate

the peaks corresponding to nanodiscs and the unbound toxin (~ 2.6 nm in diameter).

The topology of the NTII interaction with the POPC/DOPS membrane enclosed into LPN particles was studied using the ^2H , ^{15}N -labeled toxin. NMR experiments were performed under conditions where the toxin was almost completely bound to the nanodisc surface. Despite the significant broadening and attenuation of the signals of the bound peptide (Fig. 4A), the use of the deuterated toxin and TROSY experiments optimized to reduce the transverse relaxation of the ^1H and ^{15}N nuclei allowed us to obtain the ^1H , ^{15}N -correlation spectrum of NTII in a complex with LPN (Fig. 4B). Comparison of the ^1H and ^{15}N chemical shifts of a NTII molecule in an aqueous environment and in a complex with LPN revealed no significant changes in the spatial structure of the toxin upon complex formation. The changes in chemical shifts exceeding 0.03 and 0.2 ppm, respectively, were observed only for one Arg32 residue (data not shown).

The cross-correlation rates of the ^{15}N nuclear relaxation (η_{XY}), measured for the HN-groups of NTII in complex with LPN (Fig. 4B), demonstrated a wide range of values (from 2.5 to 40 Hz, a mean value of 16.3 ± 9.2 Hz, a frequency of 800 MHz, 40 °C), which correspond to rotational correlation times (τ_{R}) in the range from 2 to 31 ns with a mean of ~ 12.5 ns. The calculated mean τ_{R} value corresponds to the reorientation of a globular particle ~5.4 nm in diameter with a mass of ~ 34 kDa, which exceeds significantly the NTII molecule size but is significantly smaller than the nanodisc size. These findings reveal a large anisotropy of interactions within the NTII/LPN complex, which may be explained either by the presence of additional degrees of freedom of a toxin molecule within the complex or by the involvement of

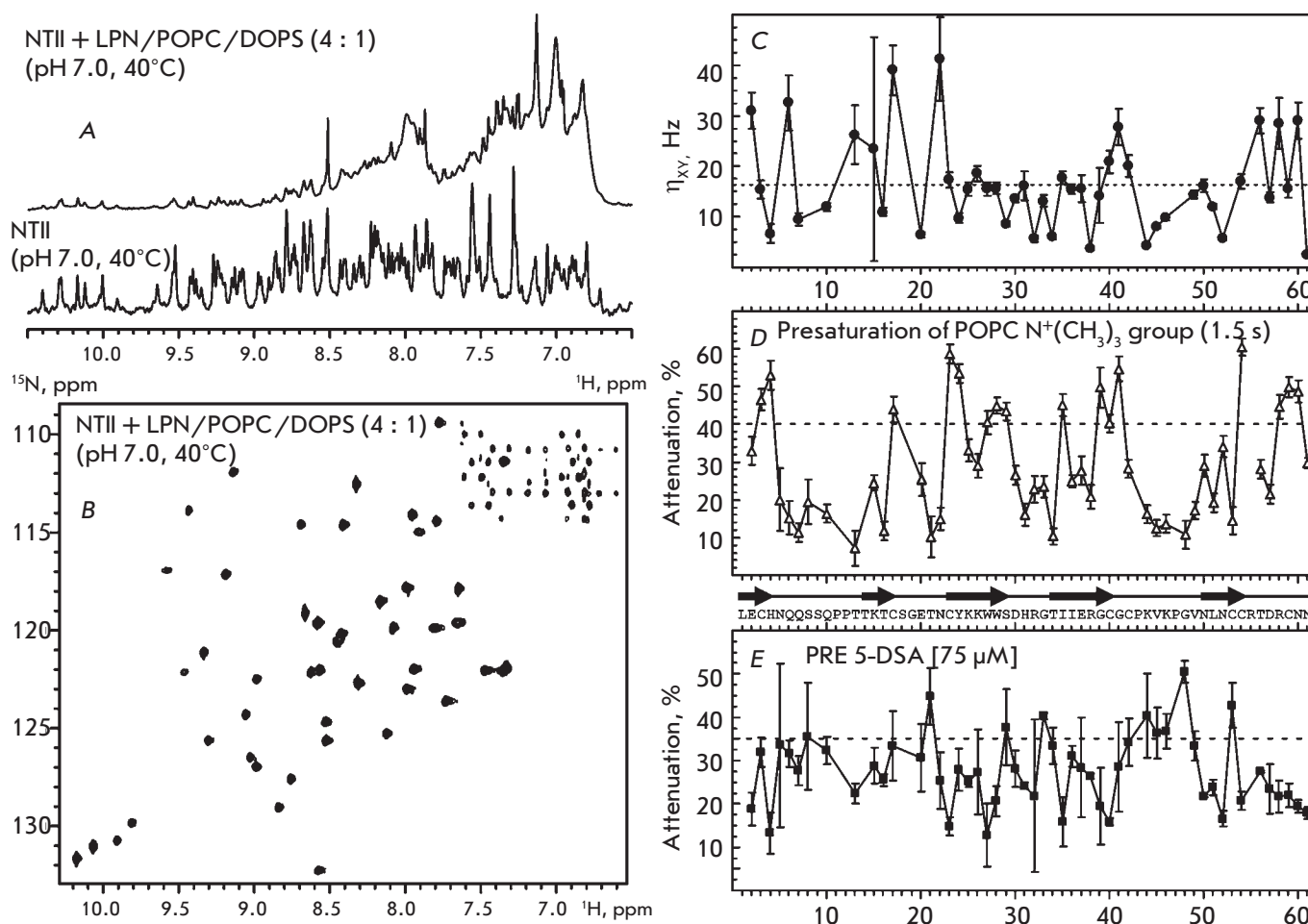


Fig. 4. NMR analysis of NTII interaction with LPN/POPC/DOPS. (A). Comparison of the 1D ^1H spectra of 45 μM ^2H , ^{15}N -NTII in water (bottom spectrum) and in complex with 75 μM LPN/POPC/DOPS (4 : 1) (upper spectrum). (B). 2D ^1H , ^{15}N -TROSY spectrum of 45 μM ^2H , ^{15}N -NTII in complex with 75 μM LPN/POPC/DOPS (4 : 1). (C) ^{15}N cross-correlation relaxation rates (η_{xy}) for NTII in complex with LPN/POPC/DOPS. Mean value is shown with dashed line. (D, E). Attenuation of cross-peak intensities in the ^1H , ^{15}N -TROSY spectrum of NTII in complex with LPN/POPC/DOPS induced by (D) presaturation of the POPC choline group during 1.5 s, or (E) the paramagnetic relaxation enhancement (PRE) from 75 μM 5-DSA

a NTII molecule in a fast (on the NMR scale) exchange process between the bound and unbound states.

The possible orientation of NTII on the nanodisc membrane was determined by measuring the magnetization transfer between the protons of lipids and the toxin HN-groups due to the nuclear Overhauser effect (NOE). The strongest response in the NMR spectra of the peptide was detected upon saturation of the signal of the choline group of POPC. A significant drop in the intensity of the ^1H , ^{15}N -cross peaks was observed for residues located on two NTII regions: 1) in the toxin “head”, near the putative binding site for phosphatidylserine, and 2) in the central (second) loop, at the level of Trp27, Trp28, and Ile35 residues (Figs. 3B, 4D).

The observed intensity decrease indicates the spatial proximity of the corresponding toxin HN-groups to the surface of the LPN bilayer.

Additionally, to determine the topology of NTII on the nanodisc surface we used a lipophilic spin probe 5-DSA. The spin label of 5-DSA embeds in the hydrophobic region of the bilayer close to the polar lipid headgroups. The maximum attenuation of HN-signal intensities, induced by the paramagnetic relaxation enhancement, was observed for the Thr21 residue of the toxin “head” and for residues of the third and second loops (Figs. 3B, 4E). This indicates the presence of a contact between the corresponding HN-groups and the hydrophobic region of the LPN bilayer.

The obtained data are not consistent with a single preferential orientation of a NTII molecule on the nanodisc membrane (Fig. 3B). Probably, the toxin interacts with the nanodisc surface in several (at least two) orientations and participates in the fast (on the NMR scale) exchange processes among complexes with different topologies. However, only one of the possible topologies (Fig. 3B) is “compatible” with the specific interaction of NTII with the polar head of phosphatidylserine at the putative binding site [19]. Thus, nonspecific electrostatic and hydrophobic interactions in the complex of NTII with LPN/POPC/DOPS have energy comparable with specific interactions.

It should be noted that the dynamic equilibrium among complexes with different topologies may play a certain role in the functioning of peripheral membrane proteins and membrane-active peptides. For example, a recent NMR study of a complex of the GTPase Rheb (Ras family) with LPN demonstrated that the protein has two possible orientations relative to the surface of the nanodisc membrane. Meanwhile, the population of these states changes during GTP hydrolysis [37].

CONCLUSIONS

In the present study, the possibility of using LPNs to explore specific peptide/membrane interactions and the mechanisms of “membrane catalysis” in the func-

tioning of membrane-active water-soluble antimicrobial peptides and neuropeptides was investigated. Three model β -structured peptides (arenicin-2, VSTx1, and NTII) were used. It was found that nanodiscs containing phosphatidylcholine and phosphatidylglycerol molecules can disintegrate upon interaction with cationic pore-forming peptides. Probably LPNs are not suited for structural and functional investigation of water-soluble pore-forming peptides. Meanwhile, the media based on LPNs can be used to study the energetics, stoichiometry, and topology of the interaction of membrane-active neurotoxins with a lipid membrane. In the course of such studies, one needs to consider the possibility of non-specific interactions of peptide molecules with the protein component (MSP) and lipid membrane of a nanodisc. ●

This work was supported by the Program of the Presidium of the Russian Academy of Sciences “Molecular and Cell Biology,” the Russian Foundation for Basic Research (grants № 12-04-31485, 12-04-01639, and 14-04-01270), the Ministry of Education and Science (contract number 8789), the fellowship of the President of the Russian Federation (SP-5823.2013.4), and a grant of the President of the Russian Federation (NSh-1766.2014.4).

REFERENCES

- Zaslhoff M. // Nature. 2002. V. 415. № 6870. P. 389–395.
- Thomas L., Scheidt H.A., Bettio A., Beck-Sickinger A.G., Huster D., Zschörnig O. // Eur. Biophys. J. 2009. V. 38. № 5. P. 663–677.
- Lee S.Y., MacKinnon R. // Nature. 2004. V. 430. № 6996. P. 232–235.
- Mäler L. // Mol. Membr. Biol. 2012. V. 29. № 5. P. 155–176.
- Oxenoid K., Chou J.J. // Curr. Opin. Struct. Biol. 2013. Doi: 10.1016/j.sbi.2013.03.010.
- Chou J.J., Kaufman J.D., Stahl S.J., Wingfield P.T., Bax A. // J. Am. Chem. Soc. 2002. V. 124. № 11. P. 2450–2451.
- Warschawski D.E., Arnold A.A., Beaugrand M., Gravel A., Chartrand É., Marcotte I. // Biochim. Biophys. Acta. 2011. V. 1808. № 8. P. 1957–1974.
- Bayburt T.H., Sligar S.G. // FEBS Lett. 2010. V. 584. № 9. P. 1721–1727.
- Denisov I.G., McLean M.A., Shaw A.W., Grinkova Y.V., Sligar S.G. // J Phys Chem B. 2005. V. 109. № 32. P. 15580–15588.
- Frauenfeld J., Gumbart J., Sluis E.O. van der, Funes S., Gartmann M., Beatrix B., Mielke T., Berninghausen O., Becker T., Schulten K., et al. // Nat Struct Mol Biol. 2011. V. 18. № 5. P. 614–621.
- Katayama H., Wang J., Tama F., Chollet L., Gogol E.P., Collier R.J., Fisher M.T. // Proc.Natl.Acad.Sci U.S.A. 2010. V. 107. № 8. P. 3453–3457.
- Lyukmanova E.N., Shenkarev Z.O., Paramonov A.S., Sobol A.G., Ovchinnikova T.V., Chupin V.V., Kirpichnikov M.P., Blommers M.J., Arseniev A.S. // J.Am.Chem.Soc. 2008. V. 130. № 7. P. 2140–2141.
- Shenkarev Z.O., Lyukmanova E.N., Paramonov A.S., Shingarova L.N., Chupin V.V., Kirpichnikov M.P., Blommers M.J.J., Arseniev A.S. // J. Am. Chem. Soc. 2010. V. 132. № 16. P. 5628–5629.
- Hagn F., Etzkorn M., Raschle T., Wagner G. // J. Am. Chem. Soc. 2013. V. 135. № 5. P. 1919–1925.
- Shenkarev Z.O., Paramonov A.S., Lyukmanova E.N., Gizatullina A.K., Zhuravleva A.V., Tagaev A.A., Yakimenko Z.A., Telezhinskaya I.N., Kirpichnikov M.P., Ovchinnikova T.V., et al. // Chem. Biodivers. 2013. V. 10. № 5. P. 838–863.
- Schuler M.A., Denisov I.G., Sligar S.G. // Methods Mol. Biol. 2013. V. 974. P. 415–433.
- Kyte J., Doolittle R.F. // J. Mol. Biol. 1982. V. 157. № 1. P. 105–132.
- Shenkarev Z.O., Balandin S.V., Trunov K.I., Paramonov A.S., Sukhanov S.V., Barsukov L.I., Arseniev A.S., Ovchinnikova T.V. // Biochemistry. 2011. V. 50. № 28. P. 6255–6265.
- Lesovoy D.M., Bocharov E.V., Lyukmanova E.N., Kosinsky Y.A., Shulepko M.A., Dolgikh D.A., Kirpichnikov M.P., Efremov R.G., Arseniev A.S. // Biophys. J. 2009. V. 97. № 7. P. 2089–2097.
- Shenkarev Z.O., Lyukmanova E.N., Solozhenkin O.I., Gagnidze I.E., Nekrasova O.V., Chupin V.V., Tagaev A.A., Yakimenko Z.A., Ovchinnikova T.V., Kirpichnikov M.P., et al. // Biochemistry (Mosc.). 2009. V. 74. № 7. P. 756–765.
- Ovchinnikova T.V., Shenkarev Z.O., Nadezhdin K.D., Balandin S.V., Zhmak M.N., Kudelina I.A., Finkina E.I.,

RESEARCH ARTICLES

- Kokryakov V.N., Arseniev A.S. // *Biochem. Biophys. Res. Commun.* 2007. V. 360. № 1. P. 156–162.
22. Lyukmanova E.N., Shenkarev Z.O., Schulga A.A., Ermo-lyuk Y.S., Mordvintsev D.Y., Utkin Y.N., Shoulepko M.A., Hogg R.C., Bertrand D., Dolgikh D.A., et al. // *J. Biol. Chem.* 2007. V. 282. № 34. P. 24784–24791.
23. Chill J.H., Louis J.M., Baber J.L., Bax A. // *J. Biomol. NMR.* 2006. V. 36. № 2. P. 123–136.
24. Andrä J., Jakovkin I., Grötzinger J., Hecht O., Krasnos-dembskaya A.D., Goldmann T., Gutschmann T., Leippe M. // *Biochem. J.* 2008. V. 410. № 1. P. 113–122.
25. Nagle J.F., Tristram-Nagle S. // *Biochim. Biophys. Acta.* 2000. V. 1469. № 3. P. 159–195.
26. Lyukmanova E.N., Shenkarev Z.O., Khabibullina N.F., Kopeina G.S., Shulepko M.A., Paramonov A.S., Mineev K.S., Tikhonov R.V., Shingarova L.N., Petrovskaya L.E., et al. // *Biochim. Biophys. Acta.* 2012. V. 1818. № 3. P. 349–358.
27. Clay M.A., Pyle D.H., Rye K.-A., Barter P.J. // *J. Biol. Chem.* 2000. V. 275. № 12. P. 9019–9025.
28. Jayaraman S., Gantz D.L., Gursky O. // *Biophys. J.* 2005. V. 88. № 4. P. 2907–2918.
29. Huang H.W. // *Biochim. Biophys. Acta.* 2006. V. 1758. № 9. P. 1292–1302.
30. Sheng J.R., Grimme S., Bhattacharya P., Stowell M.H.B., Artinger M., Prabahakar B.S., Meriggioli M.N. // *Exp. Neurol.* 2010. V. 225. № 2. P. 320–327.
31. Jung H.J., Lee J.Y., Kim S.H., Eu Y.J., Shin S.Y., Milesco M., Swartz K.J., Kim J.I. // *Biochemistry.* 2005. V. 44. № 16. P. 6015–6023.
32. Schmidt D., MacKinnon R. // *Proc. Natl. Acad. Sci. U.S.A.* 2008. V. 105. № 49. P. 19276–19281.
33. Shenkarev Z.O., Lyukmanova E.N., Butenko I.O., Petrovskaya L.E., Paramonov A.S., Shulepko M.A., Nekrasova O.V., Kirpichnikov M.P., Arseniev A.S. // *Biochim. Biophys. Acta.* 2013. V. 1828. № 2. P. 776–784.
34. Nakano M., Fukuda M., Kudo T., Miyazaki M., Wada Y., Matsuzaki N., Endo H., Handa T. // *J. Am. Chem. Soc.* 2009. V. 131. № 23. P. 8308–8312.
35. Golovanov A.P., Lomize A.L., Arseniev A.S., Utkin Y.N., Tsetlin V.I. // *Eur. J. Biochem.* 1993. V. 213. № 3. P. 1213–1223.
36. Teixeira-Clerc F., Ménez A., Kessler P. // *J. Biol. Chem.* 2002. V. 277. № 28. P. 25741–25747.
37. Mazhab-Jafari M.T., Marshall C.B., Stathopoulos P.B., Kobashigawa Y., Stambolic V., Kay L.E., Inagaki F., Ikura M. // *J. Am. Chem. Soc.* 2013. V. 135. № 9. P. 3367–3370.

Construction of a pIX-modified Adenovirus Vector Able to Effectively Bind to Nanoantibodies for Targeting

M. N. Garas^{1*}, S. V. Tillib², O. V. Zubkova¹, V. N. Rogozhin^{1,3}, T. I. Ivanova², L. A. Vasilev², D. Yu. Logunov¹, M. M. Shmarov¹, I. L. Tutykhina¹, I. B. Esmagambetov¹, I. Yu. Gribova¹, A. S. Bandelyuk¹, B. S. Naroditsky¹, A. L. Gintsburg¹

¹N.F. Gamaleya Research Institute of Epidemiology and Microbiology, Ministry of Health of the Russian Federation; Gamaleya Str., 18, Moscow, Russia, 123098

²Institute of Gene Biology, Russian Academy of Sciences; Vavilova Str., 34/5, Moscow, Russia, 119334

³K.I. Skryabin Moscow State Academy of Veterinary Medicine and Biotechnology, Akademik Skraybin Str., 23, Moscow, Russia, 109472

*E-mail: max.garas@yandex.ru

Received 23.10.2013

Revised manuscript received 08.04.2014

Copyright © 2014 Park-media, Ltd. This is an open access article distributed under the Creative Commons Attribution License, which permits unrestricted use, distribution, and reproduction in any medium, provided the original work is properly cited.

ABSTRACT Current targeting strategies for genetic vectors imply the creation of a specific vector for every targeted receptor, which is time-consuming and expensive. Therefore, the development of a universal vector system whose surface can specifically bind molecules to provide efficient targeting is of particular interest. In this study, we propose a new approach in creating targeted vectors based on the genome of human adenovirus serotype 5 carrying the modified gene of the capsid protein pIX (Ad5-EGFP-pIX-ER): recombinant pseudoadenoviral nanoparticles (RPANs). The surfaces of such RPANs are able to bind properly modified chimeric nanoantibodies that specifically recognize a particular target antigen (carcinoembryonic antigen (CEA)) with high affinity. The efficient binding of nanoantibodies (aCEA-RE) to the RPAN capsid surfaces has been demonstrated by ELISA. The ability of the constructed vector to deliver target genes has been confirmed by experiments with the tumor cell lines A549 and Lim1215 expressing CEA. It has been shown that Ad5-EGFP-pIX-ER carrying aCEA-RE on its surface penetrates into the tumor cell lines A549 and Lim1215 via the CAR-independent pathway three times more efficiently than unmodified RPAN and Ad5-EGFP-pIX-ER without nanoantibodies on the capsid surface. Thus, RPAN Ad5-EGFP-pIX-ER is a universal platform that may be useful for targeted gene delivery in specific cells due to “nanoantibody–modified RPAN” binding.

KEYWORDS adenoviral vector; pIX; leucine zipper; nanobody; CEA.

ABBREVIATIONS RPAN – recombinant pseudoadenoviral nanoparticles; CEA – carcinoembryonic antigen; Ad – human adenovirus; Ad5 – Ad serotype 5; CAR – coxsackievirus and adenovirus receptor; a.a. – amino acid residue; pfu – plaque-forming unit.

INTRODUCTION

Recombinant pseudoadenoviral nanoparticles (RPANs), which are derived from the human adenovirus serotype 5 (Ad5) genome with deletion of the region responsible for replication, are considered to be among the most promising tools for targeted gene delivery into mammalian cells. RPANs are extensively used in recombinant vaccines and gene therapy [1, 2]. The fact that RPAN is safe has been confirmed in a number of clinical trials of Ad5-based vaccines and gene therapy products. Since 2008, a quarter of gene therapy clinical trials have utilized the Ad-based RPANs [3]. Furthermore, two Ad5-derived gene therapy prod-

ucts have already been approved in China. There are a number of advantages contributing to the popularity of Ad5-based RNAPs: Ad5-based vectors transduce both dividing and non-dividing cells; adenovirus DNA does not integrate into the host genome but remains extrachromosomal; RPANs can be produced at titer of more than 10¹⁰ pfu/ml, which allows one to use them as live recombinant vaccines; RPANs provide a high expression level of the transferred gene in the targeted cells.

However, some limitations in the use of Ad5-based RPANs exist. For instance, efficiency in the transduction of some mammalian cell types, particularly human tu-

mor cells, can be low. This is due to the fact that the primary receptor for Ad5---coxsackievirus and adenovirus receptor (CAR)---is not expressed in all cell types [4–6]. To provide targeted gene transfer into CAR-deficient and CAR-negative cells, tropism modification strategies that alter the components of the A5-capsid (namely, fiber, hexon, pIX, pIIIa proteins) have been developed. Nowadays, these strategies enable Ad5-based RPAN delivery in various cell types, in particular targeting cervical cancer, glioma, renal cell carcinoma, ovarian cancer, as well as vascular smooth muscle cells [7–12].

Lately, the minor capsid protein IX (pIX) has received considerable attention as a site for protein ligand and integration into adenovirus capsid. There are several advantages to pIX modification: the possibility to integrate relatively large peptide fragments to the C-terminus of pIX; the high structural compatibility of ligands with pIX; and a wide range of applications for Ad-based vectors with modified pIX [13].

It has recently been shown that integration of the RGD-motif (arginine-glycine-aspartic acid) into the pIX structure increases efficiency in the binding of Ad5-based RPANs to cells expressing $\alpha_v\beta_3$ integrins [14]. A single chain T-cell receptor (TCR) directed against the melanoma-associated antigen in complex with HLA I (major histocompatibility complex) introduced to the C-terminus of pIX also enables RPANs to effectively transduce human melanoma cells [15].

Existing approaches to pIX modification imply a costly and time-consuming generation of RPANs for each targeted receptor. Hence, the development of a universal targeted gene delivery platform based on specific binding of certain molecules to the adenovirus capsid surface, which provides effective targeting of RPANs, is of great interest.

To build this platform, the synthetic domain $EE_{12}RR_{345}L$ (ER domain) was introduced into the C-terminus of pIX. The ER domain is capable of high efficiency heterodimerization with the partner domain $RR_{12}EE_{345}L$ (RE domain), yielding a stable structure (leucine zipper). Both synthetic leucine zipper domains were genetically engineered and derived from the appropriate domain of a vitellogenin gene-binding protein (VBP) [16, 17]. Neither of the two 43-amino acid domains forms homodimers even at low temperatures (6 °C and above). However, they heterodimerize under physiological conditions, forming a stable structure “leucine zipper” $EE_{12}RR_{345}L/RR_{12}EE_{345}L$ (or ER/RE) with the melting point at 73 °C and a dissociation constant $K_d = 1.3 \times 10^{-11}$ M [17].

It should be noted that the approach to the modifying of Ad-based RPANs has already been described [18]. A similar one is used in our work but essentially differs in terms of the choice of the modifiable capsid protein,

antibody format, and strategy for vector generation.

We propose integrating the ER domain into pIX as the number of pIX monomers is six times higher than the number of fiber monomers in the Ad5-capsid. Accordingly, more antibodies bind to RPAN in this case, providing more effective penetration of the pIX-modified RPANs into the target cells.

We used single-domain antibodies (nanoantibodies) directed against the carcinoembryonic antigen (CEA) as molecules binding to the modified RPANs and providing targeted gene delivery to specific cells. This choice was determined by a number of the advantages of nanoantibodies; in particular, by the simplicity of genetic manipulations, reduced immune response, favorable pharmacokinetics, good solubility, pH tolerance, and high thermal stability. The nanoantibodies directed against CEA (aCEA-RE) were selected as this receptor, because they are often found in cancer cells. Furthermore, our experience in the generation of nanoantibodies and their applications, including the homotrimer of “isoleucine zipper” [19, 20], as well as in the utilization of RPANs for nanoantibody expression *in vivo* [21, 22] significantly contributed to the choice of nanoantibodies.

The aCEA-RE that were used in our work can effectively recognize the CEA-cell surface antigen expressed in the tumor cell lines A549 and Lim1215 to a high level. We have shown that pIX-modified RPANs (Ad5-EGFP-pIX-ER) carrying aCEA-RE on their surfaces three times more effectively penetrate into the tumor cells lines A549 and Lim1215 via the CAR-independent pathway than unmodified RPANs (Ad5-EGFP) and Ad5-EGFP-pIX-ER (pIX-modified RPANs, which do not have aCEA-RE on their surfaces). We have created the Ad5-EGFP-pIX-ER vector system: a versatile platform for targeted gene delivery, which enables the targeting of particular (tumor) cells by specific binding nanoantibodies directed against a (tumor-specific) surface antigen on the RPAN surface.

EXPERIMENTAL

Plasmid vectors

We used the pBluescript II SK (+) plasmid vector (Fermentas MBI, Lithuania); pGEM-T-Easy plasmid system (Promega, USA); pShuttle-CMV-EGFP shuttle vector containing the cytomegalovirus (CMV) promoter, enhanced green fluorescent protein (EGFP) reporter gene and Ad5 genomic fragments; and pAdEasy-1 plasmid (Stratagene, USA).

RPAN and bacterial strains

Ad5-EGFP RPANs comprising the full-length Ad5 genome, and the green fluorescent protein expression

tion with the ER1F and ER1R or RE1F and RE1R primers (for ER- or RE domains, respectively) resulted in PCR1 product of 97 bps (PCR1). A PCR2 product of 71 bps (PCR2) was obtained by amplification with primers ER2F and NotI-Cend-Zipper-rev (for ER domain) or RE2F and NotI-Cend-Zipper-rev (for RE domain). In the next PCR reaction, we used PCR1 and PCR2 products as primers and obtained a PCR3 product of 154 bps comprising the ER- or RE-domain sequence. The PCR3 products were then inserted into the XhoI - NotI site of the pBluescript II SK (+) plasmid vector, which resulted in pER and pRE plasmids containing nucleotide sequences encoding the full-length heteromeric leucine zipper domains. The correct insertions of the ER- and RE-domain genes were confirmed by sequencing. For convenience of cloning (to introduce the XhoI site at the 5'-end of the DNA sequence), the third nucleotide of the original sequence, G, was substituted for C. The amino acid sequence remained unchanged.

Construction of a plasmid carrying the Ad5 genome with deletion of the E1 region, EGFP cassette, and the sequence of the heteromeric domains of leucine zipper at the C terminus of pIX

To integrate the ER domain into the C-terminus of pIX, a sequence containing the pIX gene with a deleted stop codon; a spacer (a sequence of the longest α -helix of human apolipoprotein E4 (33 a.a.)) [18], a polylinker carrying the restriction sites BamHI, Kpn2I, NotI, HindIII, AscI and SwaI to insert the target ligands, and the *pIVa2* gene (from 1 to 832 bps) were synthesized (ZAO "Evrogen"). The synthetic sequence was cloned into the pBluescript II SK plasmid vector to generate plasmid pBssk-pIX-mod containing the *pIX* gene with sites for modifications.

The nucleotide sequence encoding the ER domain was amplified using the BamHI-zipp-forw (5'-gga-tcc-ctc-gag-atc-gag-gca-gct-ttc-c-3') and SwaI-zipp-rev (5'-att-taa-att-tac-aga-ggt-ccg-taa-cga-gtt-cg-3') primers, which flanked the 5'- and 3'-regions of the leucine zipper and contained the BamHI and SwaI restriction sites, respectively. The aforementioned plasmid, pER, was used as a template.

The PCR product of 146 bps was cloned into the pGEM-T-Easy plasmid vector. The pGEM-T-ER plasmid was digested with the restriction enzymes BamHI and SwaI, and the sequence encoding the leucine zipper was cloned into the pBssk-pIX-mod plasmid using the same restriction sites. The ApaI-HpaI adenovirus genome fragment containing the modified gene *pIX* was then excised from the pBssk-pIX-ER plasmid and cloned into the pShCMV-EGFP vector at the same sites. Thus, we obtained a pShCMV-EGFP-pIX-ER shuttle vector comprising the sequence encoding the

modified pIX with the leucine zipper at the C-terminus, and the *EGFP* reporter gene cassette. This plasmid was linearized by restriction digestion with PmeI and co-transformed together with the pAdEasy-1 plasmid into *E. coli* BJ5183 cells as described in the AdEasy adenoviral vector system (Stratagene, USA). The pAd5-EGFP-pIX-ER plasmid was obtained as a result of homologous recombination. It contained the full-length Ad5 genome with deletion of the E1 region, the expression cassette with the *EGFP* reporter gene, and the fragment encoding the leucine zipper at the C-terminus of pIX.

Production, accumulation, and purification of the pIX-modified RPANs

The RPANs were produced via transfection of a HEK293 cell line with the pAd5-EGFP-pIX-ER plasmid, which was previously linearized at the PacI restriction site. The transfection was performed with a Metafectene Pro agent (Biontix, Germany). Ad5-EGFP-pIX-ER was accumulated in the HEK293 cell culture. The RPANs were purified and concentrated by cesium chloride density gradient ultracentrifugation of the infected cells lysates. The concentration of the purified RPAN was determined spectrophotometrically ($\lambda = 260$ nm) using the conversion factor: 1 OD = 1.12×10^{12} viral particles/ml. Ad5-EGFP-pIX-ER titer was determined using plaque formation assay in the HEK293 cells culture.

Antibodies

We used commercial anti-CAR polyclonal antibodies (R&D systems, USA, cat. # AF3336), murine sera containing anti-Ad antibodies obtained after immunization of mice with RPANs, equine secondary antibodies (GE Healthcare, UK), and monoclonal anti-HA antibodies (CHGT-45P-Z, ICL, Inc., USA).

Generation of aCEA with an additional terminal RE domain

Generation of single domain mini-antibodies (nanoantibodies) recognizing the carcinoembryonic antigen (aCEA) was performed as previously described [24–28].

Bactrian camel *Camelus bactrianus* was immunized sequentially (five times) by subcutaneous injection of an antigen mixed with an equal volume of a complete (for the first injection) or incomplete (for the following injections) Freund's adjuvant. The antigen, human CEA, was purchased from Xema Medica, Russia (catalog number R224). 0.26 mg of human CEA was used for each injection. The second injection (immunization) was performed three weeks after the initial one, and the following three immunizations were performed every two weeks. Blood (150 ml) was collected five

days after the last injection. Then, we isolated RNA from B lymphocytes, synthesized cDNA, carried out two-step PCR and cloning of the amplified sequences encoding nanoantibodies into a pHEN4 phagemid vector. Selection of cDNA clones encoding nanoantibodies was performed through phage display [24–28]. In this procedure, we used M13KO7 helper phage (New England Biolabs, USA) and human CEA as an antigen immobilized on the bottom of the wells of a 96-well ELISA plate. The same human CEA was used for injections. cDNA from the selected clones was then re-cloned into a new expression vector. Before re-cloning, we added sequences encoding HA and (His)₆ tags at the 3'-end of the cDNA to increase the efficiency of nanoantibody detection and purification after expression. The specificity and relative affinity of the initially selected nanoantibodies were determined by ELISA via their binding to the immobilized human CEA protein, and, subsequently, to fixed cells overexpressing CEA on the cell surface. Based on the conducted assays, we chose the most effective nanoantibody, anti-CEA/aCEA1. (The antibody sequence, details of its production and analysis are described in the recent patent application # 2,012,113,421, Russian Federation: Tillib, S.V. The single-domain nanoantibody, aCEA1, specifically binding the CEA protein.) To ensure stable binding of aCEA1 to the modified pIX Ad5 (pIX-ER), the former was modified as described in [20] but a different ligand was used. A RE domain capable of effective dimerization with the ER domain to form a leucine zipper was integrated into aCEA1 instead of the homotrimeric domain (ILZ). Constituents of the modified aCEA1, aCEA-RE, with amino acid sequences, partial for some of them, are shown in *Fig. 2B*. The aCEA-RE accumulating in bacterial periplasm was purified as described previously [20] and detected as an individual band after separation by SDS-PAGE in a 14% gel (*Fig. 3A*).

ELISA for detection of leucine zipper interactions of recombinant nanoantibodies and pIX RPANs

A 96-well plate was coated with 2 µg/well of aCEA-RE in a 40 mM potassium carbonate buffer (pH 9.6) at +4° C for 12 h. The plate was then washed three times with 0.05% Tween-20 and three times with distilled water. After Ad5-EGFP-pIX-ER was added at a concentration of 1 µg/ml in the working solution, the plate was incubated in a shaker for 1 h at +37° C. Ad-EGFP was used as a control. Different dilutions of murine sera in the working solution (1: 800 to 1: 204 800) containing anti-Ad-antibodies were added to the plate and incubated in a shaker at +37° C for 1 h. Following plate washing, horseradish peroxidase (HRP) conjugated anti-species antibodies of working dilution (1: 10000) in phosphate buffered saline (PBS), pH 7.4, with 0.05%

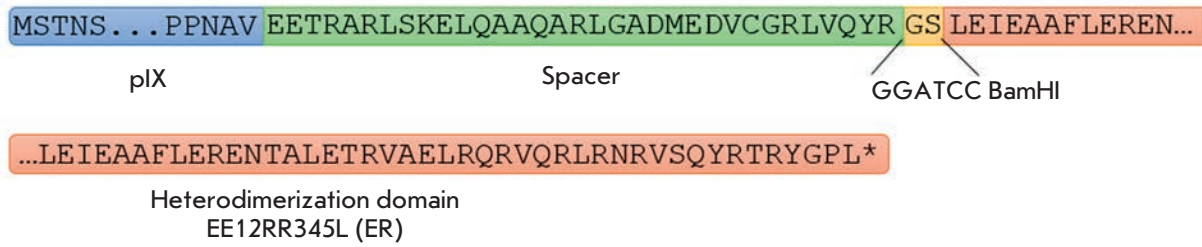
Tween-20 were added. TMB substrate was used to visualize the HRP enzymatic reaction; 4 M H₂SO₄, to stop it. The optical density of the colored product of the HRP reaction was measured on an iEMS Reader MF (Termo labsystems) at 450 nm.

Immunohistochemical assay to detect binding of aCEA-RE nanoantibodies to CEA expressed on the surface of tumor cells and to the purified CEA protein

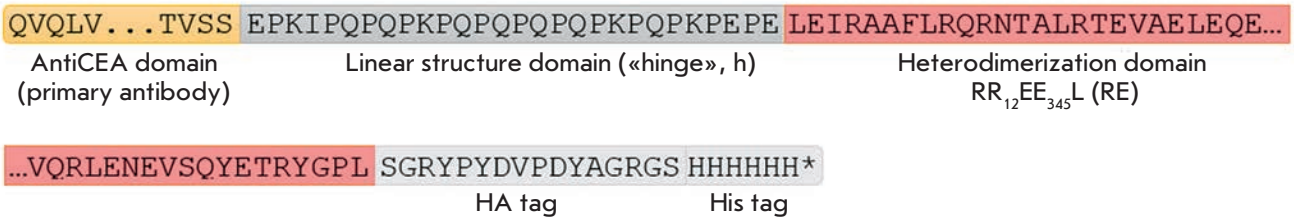
The ability of aCEA-RE to bind to the human CEA protein immobilized on the surface of microplate wells was examined by the standard ELISA protocol. Microplate wells with immobilized bovine serum albumin (BSA) were used as a control. Anti-HA monoclonal antibodies conjugated to horseradish peroxidase, which were directed against HA-tag at the C-terminus of the aCEA-RE antibodies, were used as secondary antibodies. The activity of horseradish peroxidase was determined using the ABTS chromogenic substrate (2,2'-azinobis(3-ethylbenzothiazoline-6-sulfonic acid)). The optical density was measured at 405 nm using a microplate fluorometer. Control wells (with immobilized BSA) contained no antigen and were blocked and processed together with the experimental wells (with antigen).

The possibility of using aCEA-RE antibody to detect the CEA protein expressed on the tumor cell surface was examined by ELISA on immobilized/fixed cells. The following cell lines were used: A549, H1299, H460, H292, Lim1215, SW480, and HCT-116. The HEK293 cell line (derived from human embryonic kidney cells) served as a negative control as the CEA protein is not detected in this cell line according to published reports. Chinese hamster ovary (CHO) cells were another negative control. The cells were seeded into a 96-well plate at a density of 10⁴ cells per well. A day after seeding, the cells were washed with PBS three times and fixed in 3.7 % formaldehyde diluted in a buffer for 10 min. Fixation was stopped by adding a glycine solution to a concentration of 125 mM. The fixed cells were washed with PBS three times and covered with a blocking buffer, 1% BSA in 1×PBS, for 2 h. The cells were rinsed with 1×PBS and covered with a solution (1×PBS, 0.1 % BSA) containing aCEA-RE nanoantibodies at a concentration of 100 ng/ml. Anti-HA monoclonal antibodies conjugated to horseradish peroxidase were used as secondary antibodies directed against the C-terminal HA-tag of the tested aCEA-RE nanoantibody. Horseradish peroxidase activity was determined using a ABTS chromogenic substrate. The optical density was measured at 405 nm using a microplate fluorometer. Control wells (with immobilized HEK293 and CHO cells) were blocked and processed together with the experimental wells.

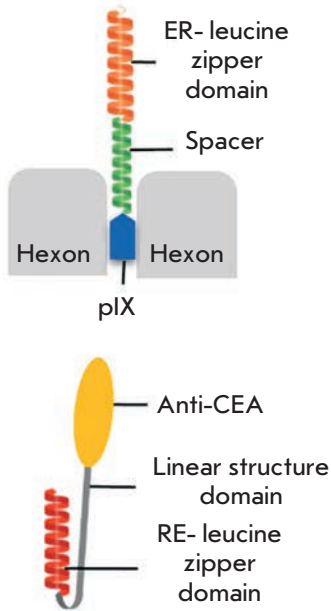
A



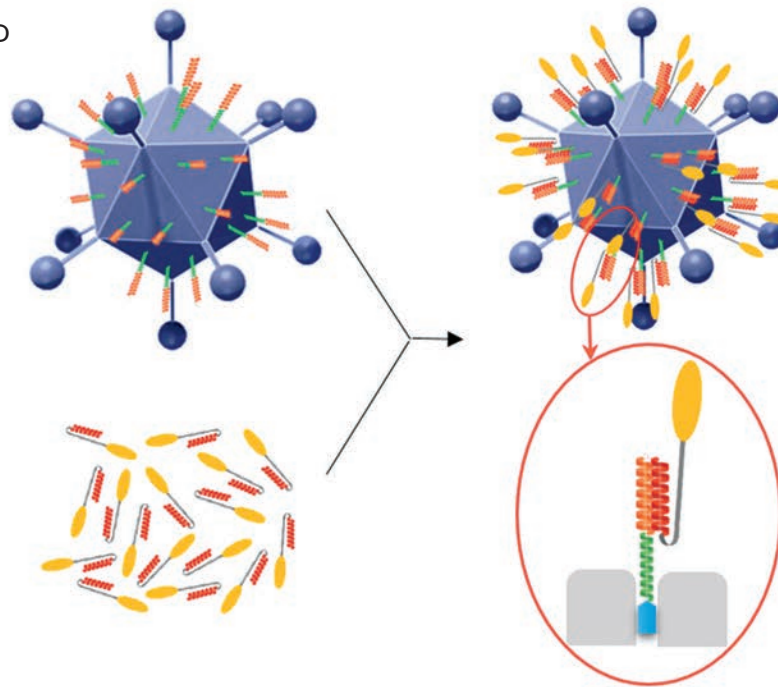
B



C



D



Ad5-EGFP-pIX-ER/aCEA-RE complex

Fig. 2. Schematic representation of the recombinant nanoantibody, the structure of the pIX protein modified by the integration of a spacer and the ER-leucine zipper domain, and the formation of a Ad5-EGFP-pIX-ER/aCEA-RE complex with altered tropism. Schemes of the amino acid sequences of the domains of the recombinant pIX (A) and the chimeric nanoantibody aCEA-RE (B). C – positions of the complementary leucine zipper domains; one domain is integrated into the C-terminus of the pIX of Ad5 and protrudes above the capsid surface due to the spacer; another domain is “attached” to the N-terminus of aCEA. D – Formation of the Ad5-EGFP-pIX-ER/aCEA-RE complex through heterodimerization of ER- and RE-leucine zipper domains

Thermal stability assay for pIX-modified RPANs

HEK293 cells were seeded into 24-well plates at a density of 10^5 cells per well. After 24 h, the monolayer HEK293 culture was infected with pIX-modified RPAN (10^3 viral particles per cell in 200 μ l of the medium). Before infection, the pIX-modified RPAN were incubated at +37° C and +42° C for 5, 15 and 30 min. The number of fluorescent cells was determined by flow cytometry (Backman Coulter Cytomix FC-500, USA) 24 h after infection.

Transduction of eukaryotic cells with blocked CAR-receptors by RPANs

A549 and Lim1215 cells were seeded into a 48-well plate at a density of 2×10^4 cells per well, covered with 10 mg/ml of anti-CAR antibodies and incubated at +37° C for 30 min. The antibodies were removed, the cells were washed and transduced by RPANs (500 viral particles per cell). The RPANs were first pre-incubated with aCEA-RE (240 antibodies per viral particle) for 30

min at +4° C under constant stirring; unbound RPANs were removed. The relative number of fluorescent cells was determined by flow cytometry (Backman Coulter Cytomix FC-500, USA) 24 h after transduction.

RESULTS AND DISCUSSION

Construction of recombinant pseudoadenoviral vectors with the modified IX protein

In 2009, J.N. Glasgow *et al.* conducted a study. They “attached” a leucine zipper domain to the C-terminus of Ad5-fiber to enable specific binding of A5-capsid to single-chain antibodies carrying a complementary leucine zipper domain. Thus, RPANs changed their tropism, providing targeted gene delivery [18]. Our aim was to construct a Ad5-based RPAN bearing a leucine zipper domain at the C-terminus of pIX. We hypothesized that this modification of pIX would provide a more efficient delivery of target genes. Ad5-capsid comprises 240 pIX and 36 fiber monomers. Hence, substantially more anti-

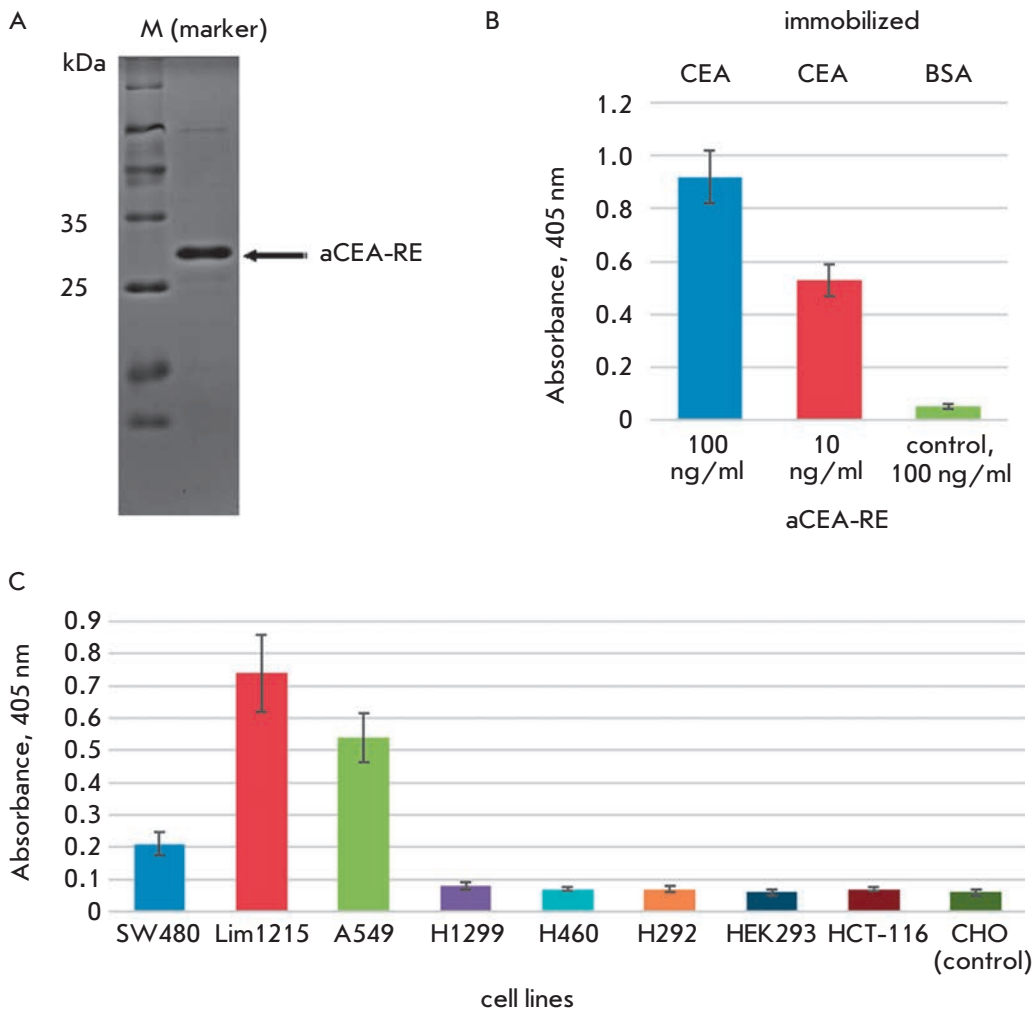


Fig. 3. ELISA to detect binding of aCEA-RE to the CEA protein. **A** – SDS-PAGE of purified aCEA-RE in a 14% SDS-polyacrylamide gel. **B** – ELISA for detection of aCEA-RE binding to immobilized CEA. The concentrations of aCEA-RE in assay were 100 ng/ml and 10 ng/ml. Wells with immobilized bovine serum albumin were used as a negative control. **C** – ELISA for detection of the aCEA-RE binding to CEA exposed on the tumor cell surface

bodies would bind pIX-modified RPANs than fiber-modified RPANs. However, peptide integration into the capsid may cause conformational changes leading to disturbance of RPAN assembly as the C-terminus of pIX is situated between capsid hexons [29]. Therefore, we introduced a spacer of the longest human apolipoprotein E4 α -helix sequence between the C-terminus of pIX and the leucine zipper domain. Such a spacer is the most effective one; it does not significantly affect Ad-assembly as it places the leucine zipper domain above the capsid surface, thus improving the efficiency of Ad5-based RPAN binding to recombinant nanoantibodies, which was demonstrated by J. Vellinga *et al.* [30]. The constructed Ad5-based RPAN with the pIX-modification is schematically shown in *Fig. 2*.

The recombinant vector Ad5-EGFP-pIX-ER encoding the modified pIX protein with a spacer sequence and ER domain of the leucine zipper at the C-terminus was obtained by homologous recombination in *E. coli*.

Characterization of the Ad5-EGFP-pIX-ER RPAN

The Ad5-EGFP-pIX-ER RPAN was characterized by the following parameters: concentrations of viral particles and plaque-forming units, thermostability.

The concentration of Ad5-EGFP-pIX-ER was 6.5×10^{12} viral particles/ml, 4.0×10^{10} pfu/ml, while the concentration of the control vector, Ad5-EGFP, was 6.3×10^{12} viral particles/ml, 6.0×10^{10} pfu/ml. These results suggest that the modification introduced into the adenovirus capsid did not affect the efficiency of virion assembly and the vector quality, which is defined by the ratio of viral particles to plaque-forming units (162.5 and 105 for Ad5-EGFP-pIX-ER and Ad5-EGFP, respectively).

One of the problems associated with Ad-capsid protein modifications is destabilization of RPANs. The primary function of a pIX protein is to stabilize interactions between adjacent hexons [31]. Accordingly, modifications of pIX proteins destabilize the capsid structure [32]. Therefore, we examined the structural integrity of virions by comparing the thermal stability of Ad5-EGFP-pIX-ER, the modified vector, and Ad5-EGFP, the unmodified vector, to see whether the ER-leucine zipper domain integrated into the pIX protein affects the structural integrity of the virion.

The Ad5-EGFP-pIX-ER and Ad5-EGFP RPANs were incubated at 37 and 42 °C for 5, 15 and 30 min; the number of infected cells was determined using a thermal stability assay (*Fig. 4*).

The Ad5-EGFP-pIX-ER and Ad5-EGFP infectivities did not change when the RPANs were heated up to +37 °C for 5, 15, and 30 min. Upon heating at +42 °C for more than 5 min, the transduction efficiency for Ad5-EGFP-pIX-ER reduced by 32% and approached

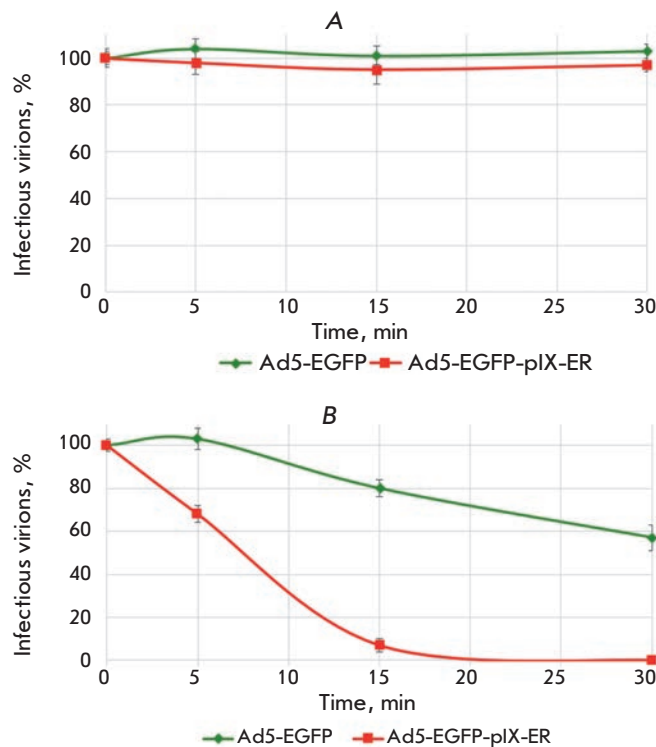


Fig. 4. Thermal stability of Ad5-EGFP-pIX-ER. Ad5-EGFP-pIX-ER and Ad5-EGFP were incubated at +37 °C (A) and +42 °C (B) for 5, 15, and 30 min. HEK-293 cells were then infected with 10^3 viral particles per cell. The number of fluorescent cells was determined by flow cytometry 24 h post infection

0% if the heating time exceeded 15 min; whereas the Ad5-EGFP infectivity remained the same after 5 min and decreased by 20 and 43% after 15 and 30 min, respectively, under identical conditions. Our data show that the integration of a leucine zipper ER domain into the pIX protein structure reduces the thermostability of Ad5-EGFP-pIX-ER, compared with that of RPANs containing wild-type pIX and are consistent with the published data [33, 34].

The efficiency in binding the leucine zipper ER domain of the pIX-modified RPANs to the complementary leucine zipper RE domain of recombinant nanoantibodies

The ability of the leucine zipper ER domain, which was introduced into the pIX protein, to bind to the complementary leucine zipper RE domain of recombinant anti-CEA was defined by ELISA.

Wells of a 96-well plate of high adsorption capacity were coated with aCEA-RE. After incubation, unbound antibodies were removed by washing; Ad5-EGFP-pIX-

ER RPANs were added to the wells. RPANs that did not bind to nanoantibodies were washed away; the formation of an Ad5-EGFP-pIX-ER/aCEA-RE complex was detected using anti-Ad-antibodies (Fig. 5).

Thus, we have shown that hydrophobic interactions of the ER- and RE domains of Ad5-EGFP-pIX-ER and nanoantibodies, respectively, to form a leucine zipper provide specific binding of recombinant nanoantibodies to RPANs.

Selection of cell lines exposing CEA for efficient binding to the aCEA-RE nanoantibody on their surface

At the next stage of our study, we examined the ability of aCEA-RE nanoantibodies to specifically bind not only to purified CEA, but also to CEA exposed on the cell surface.

Figure 3B shows the ELISA results indicating that the aCEA-RE nanoantibody specifically binds to the immobilized human CEA protein at concentrations of 100 and 10 ng/ml. Wells with immobilized bovine serum albumin were used as a control. Signal intensity (optical density at $\lambda = 405$ nm) shows the efficiency of nanoantibody binding.

If nanoantibodies recognize the isolated CEA protein, this does not mean that the epitope is accessible for recognition by the nanoantibody when the protein is localized on the cell surface. The possibility to use aCEA-RE nanoantibodies for detecting CEA overexpressed on a tumor cell surface was examined by comparative ELISA for the cell lines SW480, Lim1215, A549, H1299, H460, H292, and HCT-116. The HEK293 and CHO cell

lines were used as negative control. The ELISA results are shown in Fig. 3B.

Identically to the case of isolated CEA protein, aCEA-RE nanoantibody effectively works at a concentration of 100 ng/ml. Specific recognition of A549 and Lim1215 cells occurs due to the high-level expression of CEA residing on the surface of these cells. In contrast, the CEA protein is almost not expressed in control HEK293 cells, which is reflected by the background optical density in the corresponding cells. Similarly, the background signal is observed for the control CHO cells.

As a result, it was shown that the recombinant aCEA-RE nanoantibody is able to specifically interact with two cell lines: A549 and Lim1215. These cell lines were used in further experiments to study the transduction efficiency. At this point, we can solely speculate why only two of the seven tested cell lines specifically interact with the nanoantibody.

This may be caused, for instance, by the different accessibilities of the CEA epitope recognizable by the nanoantibody on the tested cell line surfaces, or by the potential loss of CEA from some cell line surfaces due to uncontrolled prolonged cultivation.

Ad5-EGFP-pIX-ER in complex with aCEA-RE efficiently transduce tumor cells via the CAR-independent pathway

At this stage, we examined the effectiveness of penetration of the Ad5-EGFP-pIX-ER/aCEA-RE complex into tumor cells. Due to the fact that the A549 and Lim1215 cell surfaces comprise a large number of CAR receptors [35], native Ad5 receptors, it was necessary to block them. To do so, A549 and Lim1215 cell lines

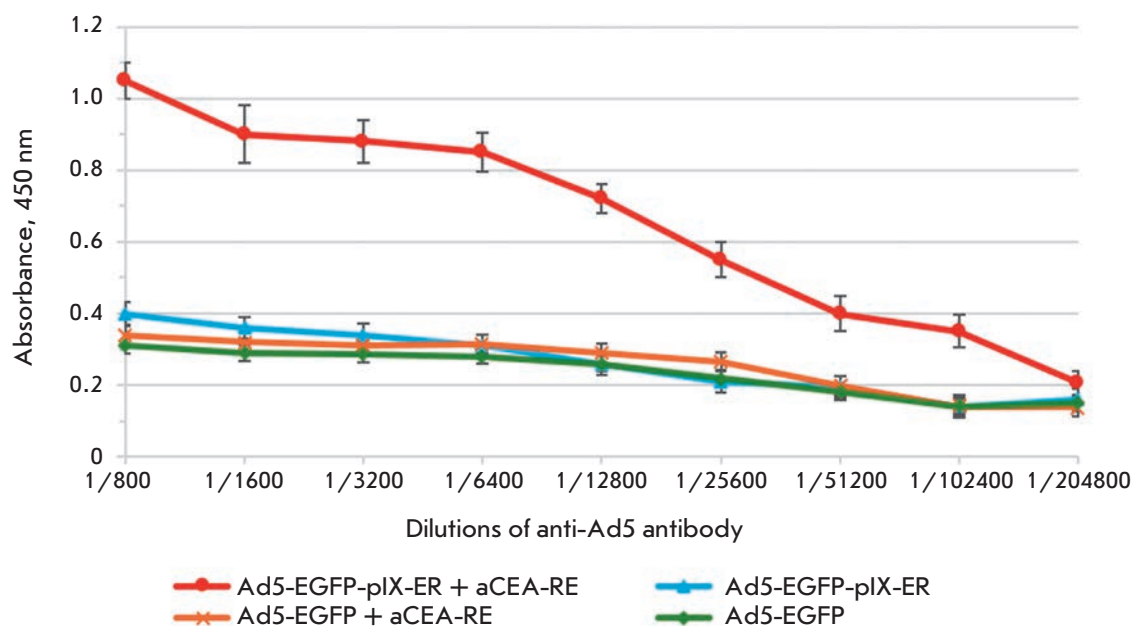


Fig. 5. Detection of the Ad5-EGFP-pIX-ER binding to aCEA-RE nanoantibodies by ELISA

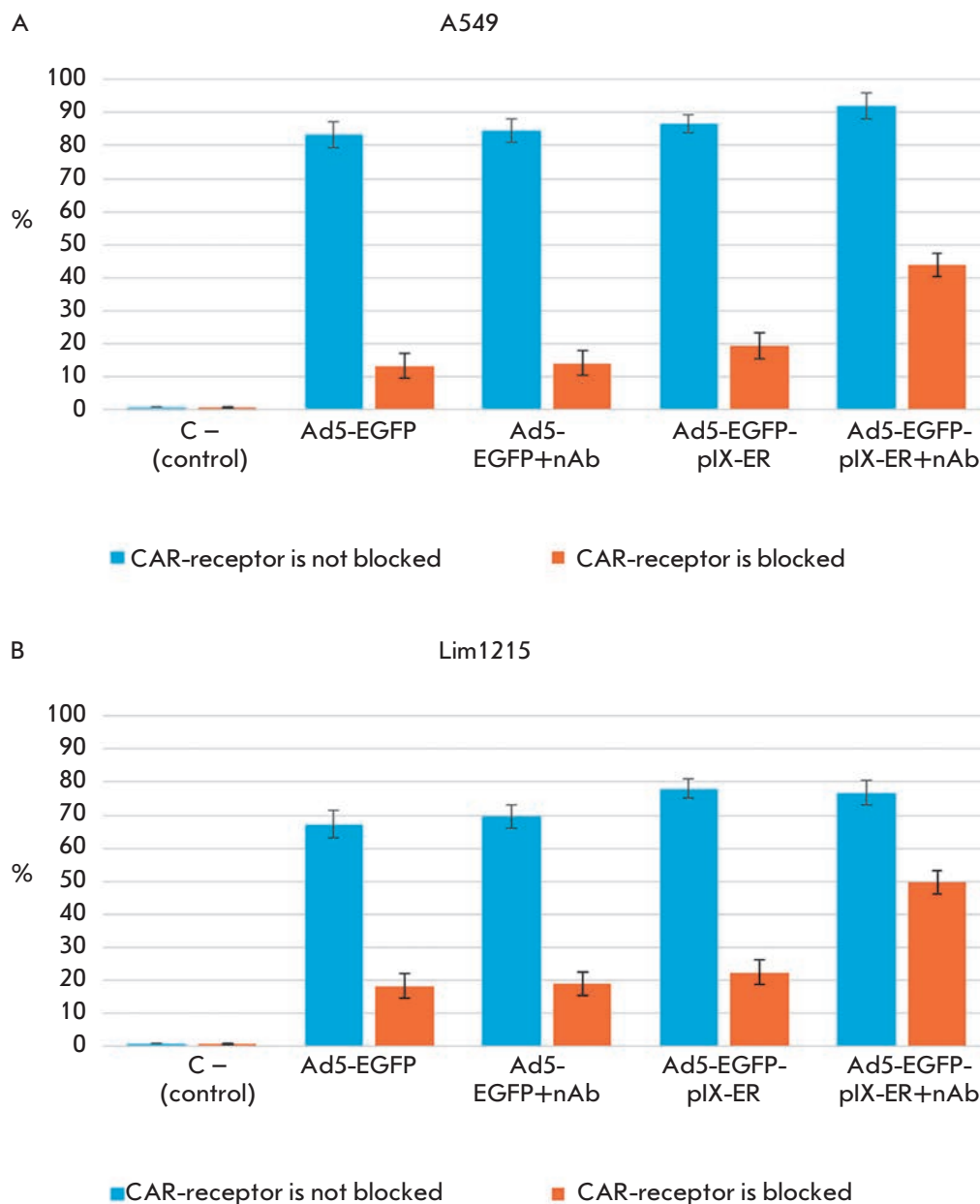


Fig. 6. Transduction of tumor cells with Ad5-EGFP-pIX-ER. Cells of the A549 (A) and Lim1215 (B) cell lines were incubated with anti-CAR antibodies at a concentration of 10 mg/ml at +37° C for 30 min. Then, they were infected with Ad5-EGFP-pIX-ER and Ad5-EGFP pre-incubated with CEA-RE at a ratio of 1 VP to 240 antibodies at +4° C for 30 min. The used vector dose was 500 VPs per cell. The number of transduced cells was determined by flow cytometry

were incubated with 10 mg/ml of anti-CAR-antibodies, and then they were transduced by Ad5-EGFP-pIX-ER “pre-loaded” with anti-CEA. Ad5-EGFP-pIX-ER (without anti-CEA), Ad5-EGFP and Ad5-EGFP “loaded” with anti-CEA were used as a control (*Fig. 6*).

It was shown that Ad5-EGFP-pIX-ER carrying aCEA-RE on the capsid surface threefold more efficiently transduce A549 and Lim1215 cells than RPN without bound nanoantibodies under conditions when CAR receptors are blocked. Noteworthy, only 40–60 % of A549 cells in the culture express CEA [36]. Therefore, it can be assumed that the efficiency in the penetration of modified RPNs into tumor cells will be sig-

nificantly higher when nanoantibodies directed against other tumor-associated receptors or other tumor cell lines are used.

CONCLUSIONS

We have constructed Ad5-based RPNs with modified pIX proteins carrying leucine zipper domains on the capsid surface. The ability of such Ad5-based RPNs to adsorb nanoantibodies containing complementary leucine zipper domains on their surface has been proved. It has been shown that RPN with leucine zipper domains “loaded” with aCEA-REs three times more effectively penetrates into the tumor cells

of the A549 and Lim1215 cell lines via the CAR independent pathway than unmodified Ad5-EGFP and Ad5-EGFP-pIX-ER without surface-adsorbed nanoantibodies.

Thus, the results of our work suggest that the vector Ad5-EGFP-pIX-ER can be used as a universal platform that provides targeted gene delivery to particular (tumor) cells by specific binding of nanoantibodies directed against a certain (tumor) surface antigen to the RPAN surface. Any other properly modified pro-

tein that specifically recognizes a target of interest can be used instead of nanoantibodies. ●

This research was conducted under the Federal Target Program “Scientific and Scientific-Pedagogical Personnel of Innovative Russia” in 2009–2013 (Agreement #8779), and also partially supported by the RAS Presidium program for fundamental studies #24 “Fundamental Basis of Nanostructure Technologies and Nanomaterials” (grant S.V.T.).

REFERENCES

- Bonnekoh B., Greenhalgh D.A., Chen S.H., Block A., Rich S.S., Krieg T., Woo S.L., Roop D.R. // *J Invest Dermatol.* 1998. V. 110. № 6. P. 867–871.
- Benihoud K., Yeh P., Perricaudet M. // *Curr Opin Biotechnol.* 1999. V. 10. № 5. P. 440–447.
- The Journal of Gene Medicine. Clinical Trials Database. <http://www.abedia.com/wiley/vectors.php>
- Zhang Y., Bergelson J.M. // *J. Virol.* 2005. V. 79. № 19. P. 12125–12131.
- Vindrieux D., Le Corre L., Hsieh T.J., Metivier R., Escobar P., Caicedo A., Brigitte M., Lazennec G. // *Endocr. Relat. Cancer.* 2011. V. 18. № 3. P. 311–321.
- Sakurai F., Mizuguchi H., Yamaguchi T., Hayakawa T. // *Mol. Ther.* 2003. V. 8. № 5. P. 813–821.
- Breidenbach M., Rein D.T., Everts M., Glasgow J.N., Wang M., Passineau M.J. // *Gene Therapy.* 2005. V. 12. № 5. P. 187–193.
- Korokhov N., Mikheeva G., Krendelshchikov A., Belousova N., Simonenko V., Krendelshchikova V., Pereboev A., Kotov A., Kotova O. et al. // *J. Virol.* 2003. V. 77. № 24. P. 12931–12940.
- Terao S., Acharya B., Suzuki T., Aoi T., Naoe M., Hamada K., Mizuguchi H., Gotoh A. // *Anticancer Res.* 2009. V. 29. № 8. P. 2997–3001.
- Hiwasa K., Nagaya H., Terao S., Acharya B., Hamada K., Mizuguchi H., Gotoh A. // *Anticancer Res.* 2012. V. 32. № 8. P. 3137–3140.
- Hongju W., Han T., Belousova N., Krasnykh V., Kashentseva E., Dmitriev I., Kataram M., Mahasreshti P. J. and Curiel D. T. // *J. Virol.* 2005. V. 79. № 6. P. 3382–3390.
- Vigne E., Mahfouz I., Dedieu J.F., Brie A., Perricaudet M., Yeh P. // *J. Virol.* 1999. V. 73. № 6. P. 5156–5161.
- Dmitriev I.P., Kashentseva E.A., Curiel D.T. // *J. Virol.* 2002. V. 76. № 14. P. 6893–6899.
- Vellinga J., Van der Heijdt S., Hoeben R.C. // *J Gen Virol.* 2005. V. 86. № 6. P. 1581–1588.
- Davison E., Diaz R.M., Hart I.R., Santis G., Marshall J.F. // *J. Virol.* 1997. V. 71. № 80. P. 6204–6207.
- Iyer S.V., Davis D.L., Seal S.N., Burch J.B. // *Mol Cell Biol.* 1991. V. 11. № 10. P. 4863–4875.
- Moll J.R., Ruvini S.B., Pastan I., Vinson C. // *Protein Science.* 2001. V. 10. P. 649–655.
- Glasgow J.N., Mikheeva G., Krasnykh V., Curiel D.T. // *PLoS One.* 2009. V. 4. № 12. P. 8355.
- Tillib S.V. // *Molecular biology.* 2011. V.45. P. 77–85.
- Tillib S., Ivanova T.I., Vasilev L.A., Rutovskaya M.V., Saakyan S.A., Gribova I.Y., Tutykhina I.L., Sedova E.S., Lysenko A.A., Shmarov M.M., Logunov D.Y., Naroditsky B.S., Gintsburg A.L. // *Antiviral Research.* 2013. V. 97. P. 245–254.
- Gribova I.Y., Tillib S.V., Tutykhina I.L., Shmarov M.M., Logunov D.Y., Verkhovskaia L.V., Naroditsky B.S., Gintsburg A.L. // *Acta Naturae.* 2011. V. 3. P. 66–72.
- Tutykhina I., Sedova E., Gribova I., Ivanova T.I., Vasilev L.A., Rutovskaya M.V., Lysenko A., Shmarov M., Logunov D., Naroditsky B., Tillib S., Gintsburg A // *Antiviral Research.* 2013. V. 97. P. 717–720.
- Shmarov M.M., Cherenova L.V., Shashkova E.V., Logunov D.U., Verkhovskaia L.V., Kapitonov A.V., Neugodova G.L., Doronin K.K., Naroditskii B.S. // *Mol. Gen. Mikrobiol. Virusol.* 2002. V. 2. P. 30–35.
- Hamers-Casterman C., Atarhouch T., Muyldermans S., et al. // *Nature.* 1993. V. 363. P. 446–448.
- Nguyen V.K., Desmyter A., Muyldermans S. // *Adv. Immunol.* 2001. V. 79. P. 261–296.
- Saerens D., Kinne J., Bosmans E., Wernery U., Muyldermans S., Conrath K. J // *Biol Chem.* 2004. V. 279. P. 51965–51972.
- Rothbauer U., Zolghadr K., Tillib S., et al. // *Nature Methods.* 2006. V. 3. P. 887–889.
- Tillib S., Ivanova T.I., Vasilev L.A. // *Acta Naturae.* 2010. V. 2 (3). P. 100–108.
- Ghosh-Choudhury G., Haj-Ahmad Y., Graham F.L. // *EMBO J.* 1987. V. 6. № 6. P. 1733–1739.
- Vellinga J., Rabelink M.J., Cramer S.J., van den Wollenberg D.J., Van der Meulen H., Leppard K.N., Fallaux F.J., Hoeben R.C. // *J. Virol.* 2004. V. 78. № 7. P. 3470–3479.
- Boulanger P., Lemay P., Blair G.E., Russell W.C. // *J. Gen. Virol.* 1979. V. 44. № 3. P. 783–800.
- Mathis J.M., Bhatia S., Khandelwal A., Kovetski I., Lokitz S.J., Odaka Y., Takalkar A.M., Terry T., Curiel D.T. // *PLoS One.* 2011. V. 6. № 2. P. 16792.
- Campos S.K., Parrott M.B., Barry M.A. // *Mol. Ther.* 2004. V. 9. № 6. P. 942–954.
- Tang Y., Le L.P., Matthews Q.L., Han T., Wu H., Curiel D.T. // *Virology.* 2008. V. 377. № 2. P. 391–400.
- Davison E., Kirby I., Whitehouse J., Hart I., Marshall J.F., Santis G. // *J Gene Med.* 2001. V. 3. № 6. P. 550–559.
- Simpson H.D., Barras F. // *J. Bacteriol.* 1999. V. 181. № 15. P. 4611–4616.

Optimization of the Protocol for the Isolation and Refolding of the Extracellular Domain of HER2 Expressed in *Escherichia coli*

V. V. Dolgikh¹, I. V. Senderskiy¹, G. V. Tetz¹, V. V. Tetz^{1*}

Department of Microbiology, Virology and Immunology, First Pavlov State Medical University of Saint Petersburg, L'va Tolstogo Str., 6-8, 197022, St. Petersburg, Russia

*E-mail: vtetzv@yahoo.com

Received 07.06.2013

Revised manuscript received 10.02.2014

Copyright © 2014 Park-media, Ltd. This is an open access article distributed under the Creative Commons Attribution License, which permits unrestricted use, distribution, and reproduction in any medium, provided the original work is properly cited.

ABSTRACT Receptor 2 of the human epidermal growth factor (HER2/neu, c-erbB2) is a 185 kDa proto-oncogene protein characterized by an overexpression in some oncological diseases, including 30% of mammary glands cancers, as well as tumors in the ovary, stomach and other organs of the human body. Since HER2- tumor status testing is the essential part of a successful cancer treatment, the expression and purification of substantial amounts of the extracellular domain (ECD) of HER2 is an important task. The production of ECD HER2 in *Escherichia coli* has several advantages over the use of eukaryotic expression systems, but the bulk of the recombinant product in bacteria accumulates as insoluble protein inclusion bodies. In this study, we obtained ECD HER2 in *Escherichia coli* as insoluble inclusion bodies and elaborated a simple, efficient, and fast protocol for the solubilization, refolding, and isolation of the protein in soluble form.

KEYWORDS epidermal growth factor receptor; extracellular domain; bacterial expression; refolding.

ABBREVIATIONS ECD HER2 – extracellular domain of receptor 2 of the human epidermal growth factor; SDS-PAGE – protein electrophoresis in polyacrylamide gel in the presence of sodium dodecyl sulfate as an anionic detergent.

INTRODUCTION

Receptor 2 of the human epidermal growth factor (HER2/neu, c-erbB2) is a 185 kDa proto-oncogene protein consisting of three main domains: an extracellular, a transmembrane and an intracellular one. The intracellular domain exhibits tyrosine kinase activity [1]. In normal cells, the protein forms heterodimers with some other representatives of the family of human epidermal growth factors and takes part in the regulation of cell proliferation and differentiation [2]. The bulk of oncological diseases, including 30% of mammary gland cancers, as well as tumors in the ovary, stomach, and other organs are accompanied by a hyperexpression of protein HER2. Herewith, the high level of protein expression is a characteristic feature of cancer recurrence cases with a bad prognosis [2]. A sufficiently effective therapy based on the target drug Herceptin (Trastuzumab) is used to treat HER2-positive diseases. New target-based drugs have recently been discovered: Pertuzumab, which inhibits the dimerization of HER2 with other receptors and immunotoxin Trastuzumab emtansine, which is a conjugate of Herceptin and cytotoxic agent mertansine. Therefore, the immunodiagnostics

of the HER2 status of a tumor is significantly important to a successful treatment. Attention has been paid to revealing HER2 protein in the serum of patients, together with immunochemical and immunohistological analyses of the material taken at biopsy. It was found that N-terminal part of the molecule presented by the extracellular domain (ECD) of the protein circulates in human blood [3] and that the antibodies specific to this part of the molecule were secreted in the examined patients [4]. A correlation between disease severity and level of ECD HER2 in serum of patients was evaluated [5]. It was shown later that the dependence is not definitive and that further investigation is warranted for confirmation [6, 7].

The aforesaid data demonstrate the necessity to have at the ready considerable amounts of purified ECD HER2 that is required for production of diagnostic antibodies and the analysis of the antibodies titer in serum of patients; moreover, it is important for the development of next-generation target drugs [8].

Production of ECD HER2 in *Escherichia coli* has a number of advantages over the use of eukaryotic expression systems. First of all, the former procedure pro-

vides a recombinant product in better yield and lower cost [9]. An additional protocol for production of the relatively inexpensive protein is the expression of ECD HER2 in yeast *Pichia pastoris*. The process is characterized by protein mannosylation to a high extent, which is not intrinsic in native molecules synthesized in the human body [10]. It should be noted that ECD HER2 has seven sites for N-glycosylation; therefore, expression of the protein in *Escherichia coli* does not allow one to prepare a protein with the appropriate posttranslational modification. However, the protein produced by the bacteria is of indubitable interest for the elaboration of test systems and screening of suitable antibodies. Accumulation of the recombinant product in the form of insoluble inclusion bodies is also an essential disadvantage in the expression of ECD HER2 in cells of *Escherichia coli*.

Thus, heterology expression sequence encoding ECD HER2 (together with the signal peptide) on pGEX-6P-1 and pQE30 vectors allowed one to prepare recombinant proteins bound to the N-terminal groups of glutathione S-transferase (GST-ECD HER2) and a sequence consisting of six histidine residues, respectively [9]. In both cases, almost all the expression product accumulated in bacterial cells in the form of insoluble inclusion bodies. The authors tried different schemes for refolding with a varied pH, temperature, incubation time, concentrations of urea, EDTA (ethylenediaminetetraacetic acid), L-arginine, oxidized, and reduced glytathione. All these modifications had only insignificant impact on the efficiency of GST-ECD HER2 refolding. Thus, the efficiency was 63–92% of the best achieved value for some of the protocols applied. The authors emphasized that only two of the seven analyzed factors, namely, pH and incubation time, influenced the efficiency of protein refolding. This fact allowed us to propose that recombinant ECD HER2 in a form of protein inclusion bodies accumulated in bacteria may be converted to soluble species via the simple procedures of dilution, concentration, and dialysis.

In our previous study, we repeated the expression of ECD HER2 in *Escherichia coli* using pRSET vector (Life Technologies) under the control of a highly active promoter, bacteriophage T7 [11]. In the construct used, the N-terminal signal peptide responsible for the secretion of HER2 and cut in a eukaryotic cell in the course of its translocation into the endoplasmic reticulum lumen, was removed. In this case, the vector construction implies the addition of the N-terminal peptide with a polyhistidine sequence to the recombinant protein. In this study, the recombinant protein obtained in a form of insoluble protein inclusion bodies was used to demonstrate the possibility of its solubilization and refolding by the most simple and fast protocol, without

the use of complex reagents. We also demonstrated the crucial role of SH-reagents for effective dissolution of the protein inclusion bodies formed by ECD HER2.

EXPERIMENTAL

The procedures for cloning the sequence encoding human ECD HER2 in vector pRSET, as well as the effective production of the recombinant protein in strain C41 *E. coli*, isolation, washing off and storage of protein inclusion bodies were described earlier [11].

The approaches used to solubilize and restore the native conformation of the recombinant protein are listed in the Results and Discussion section.

The protein was purified by metal-chelate affinity chromatography on a column with a HIS-Select[®] resin (Sigma-Aldrich) equilibrated by a solution containing 50 mM Tris-HCl (pH 8), 0.3 M NaCl, and 10 mM imidazole. For this purpose, a solution of the protein containing the same components was passed through the column. The bound components were washed with the equilibration buffer solution and eluted in the presence of 0.3 M imidazole. The resulting fractions were combined, concentrated using Centricon centrifugal concentrators (Millipore) that allowed passage of molecules of up to 30 kDa through them, and stored at –20 °C in the presence of a 50% glycerol solution. The protein concentration in the samples was determined by the Bradford method [12].

Gel electrophoresis of the proteins in a 12% polyacrylamide gel in the presence of an anionic detergent, sodium dodecyl sulfate (SDS-PAGE), was performed in a Mini-PROTEAN[®] chamber (Bio-Rad). For immunoblotting, the proteins after SDS-PAGE were transferred on a nitro-cellulose membrane using a Mini-Trans-Blot[®] insert according to the manufacturer's instructions. The membranes were blocked for 1 h in the presence of TTBS (50 mM Tris-HCl (pH 7.4), 150 mM NaCl and 0.05% Tween 20 solution) and a 1% BSA solution; they were then incubated overnight at 4 °C with anti-polyHis-antibodies (Sigma-Aldrich) conjugated to horseradish peroxidase (the antibodies were diluted 3,000-fold by the same solution). After washing off in TTBS and then in TBS (TTBS without Tween 20), the membrane was incubated in a freshly prepared solution for developing the peroxidase reaction containing TBS, 15% methanol, 0.05% 4-chloro-1-naphthol (Sigma-Aldrich), and 0.02% H₂O₂.

RESULTS AND DISCUSSION

At the first stage of our study, the recombinant protein ECD HER2 produced in bacteria was isolated as insoluble protein inclusion bodies according to the earlier described procedure [11]. In order to solubilize the protein inclusion bodies, the scheme used for GST-ECD HER2

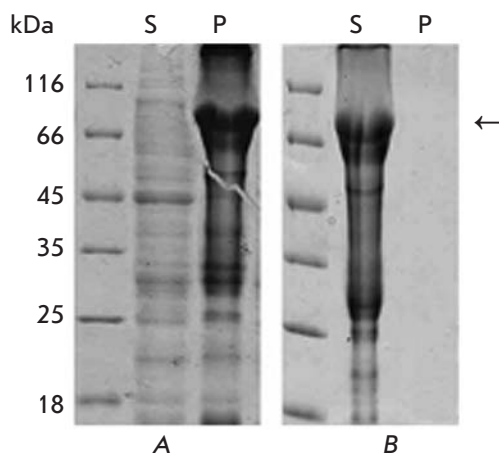


Fig. 1. Analysis of the precipitates (P) and supernatants (S) after extraction of the recombinant ECD HER2 from the protein inclusion bodies. Solutions applied: A – 50 mM Tris-HCl (pH 8), 8 M urea; B – 50 mM Tris-HCl (pH 8), 8 M urea, 1% 2-mercaptoethanol. The proteins were separated by SDS-PAGE in a 12% gel and stained with a Coomassie R-250 dye. The bands corresponding to the investigated protein are shown with an arrow

[9] was repeated, strictly following the reported protocol. The protein inclusion bodies were re-suspended in a solution containing 10 mM Tris-HCl, 0.1 M NaH_2PO_4 , 8 M urea, and 5 mM dithiothreitol (pH 8) and were incubated for 30 min at room temperature. After centrifugation of the solubilized material at 14,000 g for 10 min pellet was re-suspended in the same solution until the volume of supernatant was reached. The content of the recombinant protein in the pellet and the supernatant was compared by SDS-PAGE. The experiments showed that approximately half of the recombinant protein remained insoluble after the described scheme was used. Moreover, the achieved result was observed only when a freshly prepared solution was used. When stored for ~ 2 months at 4 °C, the efficiency of the solu-

tion for solubilization of the protein significantly decreased. It was proposed that the main reason for the decrease in the solubilizing property of the solution might be due to the oxidation of dithiothreitol, which is a relatively unstable reagent containing reduced SH-groups.

To confirm the important role of SH-reagents in protein solubilization, we analyzed the solubility of the recombinant product in the presence of 8 M urea without addition of SH-containing reagents, as well as in the presence of 8 M urea with 1% 2-mercaptoethanol added. With this aim in mind, the protein inclusion bodies were solubilized in a solution containing 50 mM Tris-HCl (pH 8), together with the aforementioned components, and the solution was incubated for 30 min at room temperature. Identically to the previous experiment, the solubilized material was separated by centrifugation and the resulting pellets were re-suspended in the same solutions until they reached the volume of the supernatant in order to compare the content of the recombinant protein in the samples. The experiment showed that the ECD HER2 accumulated in bacteria was practically insoluble in the solution containing 8 M urea without 2-mercaptoethanol (*Fig. 1A*). When 2-mercaptoethanol was added to the solubilizing solution, total dissolution of the recombinant protein was registered (*Fig. 1B*). This result confirmed the crucial role of SH-containing compounds in the solubilization of ECD HER2 expressed in bacteria and proved that the increased content of dithiothreitol or 2-mercaptoethanol in the solution for the solubilization of protein inclusion bodies can increase the yield of the soluble form of ECD HER2. A quantitative determination of the protein content in the supernatant demonstrated that the protocol used allowed us to obtain about 70 mg of the protein extracted from the protein inclusion bodies, which were isolated from 1 L of bacteria.

The material extracted in the presence of 8 M urea and 1% solution of 2-mercaptoethanol was used to as-

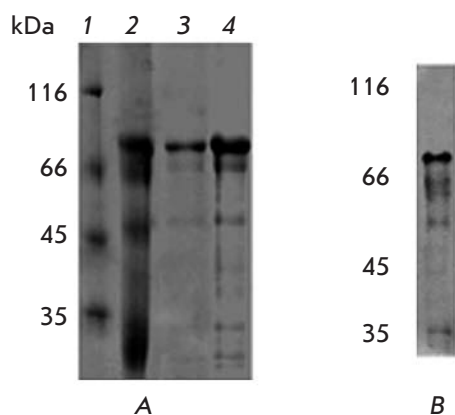


Fig. 2. Analysis of the soluble form of ECD HER2 by SDS-PAGE and immunoblotting technique. A – The protein extracted in the presence of 8 M urea and 1% 2-mercaptoethanol (track 2) was diluted 250-fold with the equilibration buffer resin HIS-Select® and purified on a column using metal chelate affinity chromatography (lanes 3 and 4, different amounts of the protein were applied). The proteins were separated by SDS-PAGE in a 12% gel and stained with a Coomassie R-250 dye. Track 1 is plotted on the molecular weight markers. B – Immunoblotting analysis of the protein extracted from the protein inclusion bodies demonstrated the presence of minor bands of a smaller size recognized by anti-polyhistidine antibodies, which attested to an insignificant hydrolysis of the recombinant protein

sess the possibility of using the simplest scheme for refolding when producing recombinant ECD HER2 in the soluble form. For this purpose, the supernatant from the previous experiment containing 18 mg/ml of the solubilized protein was diluted 250-fold under vigorous stirring. The solution for dilution was the same as that applied to equilibrate a HIS-Select® Ni-containing resin (Sigma-Aldrich) during metal chelate affinity chromatography (50 mM Tris-HCl (pH 8.0), 0.3 M NaCl and 10 mM imidazole). The protein diluted in 50 ml of solution was immediately passed through a column with 400 µl of the resin; the column was thoroughly washed with the equilibration buffer, and the recombinant ECD HER2 was eluted in the presence of a 0.3 M imidazole solution. The protein content measured in the starting extract solution and the resulting fractions showed that 15 % of the protein loaded into the column was bound to the resin and eluted (0.54 of 3.6 mg).

The analysis of the fractions obtained by SDS-PAGE proved that the protocol applied allowed us to prepare the soluble recombinant protein in a sufficiently pure form (Fig. 2A, lanes 3 and 4). The resulting fractions contained almost no ballast proteins with a molecular weight higher than that of ECD HER2. Some minor components with a lower molecular weight might result from an insignificant extent of the hydrolysis of recombinant protein during its isolation, since some of them react with anti-polyhistidine antibodies (Fig. 2B). Since the protein purified by metal chelate affinity chromatography most often contains some impurities, optimization of the chromatography conditions and the use of additional purification methods may be helpful for obtaining products completely free of impurities. ●

This work was supported by the Russian Foundation for Basic Research (grant № 12-08-01086-a).

REFERENCES

- Coussens L., Yang-Feng T.L., Liao Y.C., Chen E., Gray A., McGrath J., Seeburg P.H., Libermann T.A., Schlessinger J., Francke U., et al. Tyrosine kinase receptor with extensive homology to EGF receptor shares chromosomal location with neu oncogene. // *Science*. 1985. V. 230. P. 1132–1139.
- Marmor M.D., Skaria K.B., Yarden Y. Signal transduction and oncogenesis by ErbB/HER receptors. // *Int. J. Radiat. Oncol. Biol. Phys.* 2004. V. 58. P. 903–913.
- Tan M., Yu D. Molecular mechanisms of erbB2-mediated breast cancer chemoresistance. // *Adv. Exp. Med. Biol.* 2007. V. 608. P. 119–29.
- Santin A.D., Bellone S., Roman J.J., McKenney J.K., Pecorelli S. Trastuzumab treatment in patients with advanced or recurrent endometrial carcinoma overexpressing HER2/neu. // *Int. J. Gynaecol. Obstet.* 2008. V. 102. № 2. P. 128–31.
- Menard S., Balsari A., Casalini P., Tagliabue E., Campiglio M., Bufalino R., Cascinelli N. HER-2-positive breast carcinomas as a particular subset with peculiar clinical behaviors. // *Clin. Cancer Res.* 2002. V. 8. P. 520–525.
- Sandri M.T., Johansson H., Colleoni M., Zorzino L., Passerini R., Orlando L., Viale G., Serum levels of HER2 ECD can determine the response rate to low dose oral cyclophosphamide and methotrexate in patients with advanced stage breast carcinoma. // *Anticancer Res.* 2004. V. 24. P.1261–1266.
- Disis M.L., SchiVman K., Guthrie K., Salazar L.G., Knutson K.L., Goodell V., dela Rosa C., Cheever M.A. Effect of dose on immune response in patients vaccinated with an her-2/neu intracellular domain protein-based vaccine. // *J. Clin. Oncol.* 1996. V. 22. № 10. P. 1916–1925.
- Pichon M.F., Hacene K., Guepratte S., Neumann R. Serum HER-2 extracellular domain (ECD) before the first metastasis in 128 breast cancer patients. // *Clin. Lab.* 2004. V. 50. № 3-4. P. 163–170.
- Leary A.F., Hanna W.M., van de Vijver M.J., Penault-Llorca F., Rüschoff J., Osamura R.Y., Bilous M., Dowsett M. Value and limitations of measuring HER-2 extracellular domain in the serum of breast cancer patients. // *J Clin Oncol.* 2009. V. 27. № 10 P.1694–1705.
- Lennon S., Barton C., Banken L., Gianni L., Marty M., Baselga J., Leyland-Jones B. Utility of serum HER2 extracellular domain assessment in clinical decision making: pooled analysis of four trials of trastuzumab in metastatic breast cancer. // *J. Clin Oncol.* 2009. V. 27. № 10. P. 1685–1693.
- Belimezi M.M., Papanastassiou D., Merkouri E., Baxevanis C.N., Mamalaki A. Growth inhibition of breast cancer cell lines overexpressing Her2/neu by a novel internalized fully human Fab antibody fragment. // *Cancer Immunol. Immunother.* 2006. V. 55. № 9 P. 1091–1099.
- Liu X., He Z., Zhou M., Yang F., Lv H., Yu Y., Chen Z. Purification and characterization of recombinant extracellular domain of human HER2 from *Escherichia coli*. // *Protein Expr. Purif.* 2007. V. 53. № 2. P. 247–254.
- Dimitriadis A., Gontinou C., Baxevanis C.N., Mamalaki A. The mannosylated extracellular domain of Her2/neu produced in *P. pastoris* induces protective antitumor immunity. // *BMC Cancer.* 2009. V. 9. P. 386.
- Waugh D.S. Making the most of affinity tags. // *Trends Biotechnol.* 2005.V. 23 № 6 P.316–320.
- Nallamsetty S., Waugh D. Solubility-enhancing proteins MBP and NusA play a passive role in the folding of their fusion partners. // *Protein Expr. Purif.* 2006. V. 45. № 1. P.175–182.
- Nallamsetty S., Waugh D.S. A generic protocol for the expression and purification of recombinant proteins in *Escherichia coli* using a combinatorial His₆-maltose binding protein fusion tag. // *Nat. Protoc.* 2007. V. 2. № 2. P.383–391.
- Dolgikh V.V., Senderskiy I.V., Tetz G.V., Tetz V.V. Extracellular domain of HER2 heterologous expression in bacteria. Accepted for publication by *Uchenye zapiski Sankt-Peterburgskogo Gosudarstvennogo Meditsinskogo Universiteta im. acad. I.P. Pavlova* (Proceedings of St. Petersburg State Pavlov Medical University) in September 2013 (in Russian).
- Vogelstein B., Gillespie D. // *Proc. Natl. Acad. Sci. USA.* 1979. Vol. 76. № 2. P. 615–619.
- Miroux B., Walker J.E. // *J. Mol. Biol.* 1996. V. 260. P. 289–298.
- Laemmli U.K. // *Nature.* 1970. V. 227 P. 680–685.
- Cleland W.W. // *Biochemistry.* 1964. V. 3. P. 480–482.

The Effect of Melaxen on the Activity of Caspases and the Glutathione Antioxidant System in Toxic Liver Injury

S. S. Popov^{1*}, K. K. Shulgin², A. N. Pashkov¹, A. A. Agarkov²

¹N.N. Burdenko Voronezh State Medical Academy, Ministry of Health of the Russian Federation, Studencheskaya Str. 10, Voronezh, Russia, 394036

²Voronezh State University, Ministry of Education and Science of the Russian Federation, Universitetskaya Str. 1, Voronezh, Russia, 394006

*E-mail: biomed-popova@yandex.ru

Received 25.06.2013

Revised manuscript received 10.02.2014

Copyright © 2014 Park-media, Ltd. This is an open access article distributed under the Creative Commons Attribution License, which permits unrestricted use, distribution, and reproduction in any medium, provided the original work is properly cited.

ABSTRACT A comparative study of the activity of caspase-1 and caspase-3, the glutathione antioxidant system and NADPH-generating enzymes (glucose-6-phosphate dehydrogenase and NADP-isocitrate dehydrogenase) and a study of DNA fragmentation in the blood serum of patients with chronic alcoholic hepatitis during basic treatment and combination therapy including melaxen have been carried out. It was found that the blood serum level of reduced glutathione, which decreases in pathology, increased more significantly in patients receiving melaxen as compared to the group of patients receiving the standard treatment. More significant changes in the activity of caspase-1 and caspase-3, glutathione reductase, glutathione peroxidase, glutathione-S-transferase, glucose-6-phosphate dehydrogenase and NADP-isocitrate dehydrogenase toward the control values were observed during the combination therapy. The correction in the melatonin level under the influence of melaxen apparently had a positive effect on the free-radical homeostasis in patients, which resulted in more pronounced changes in the investigated parameters towards the normal values as compared to the basic treatment.

KEYWORDS chronic alcoholic hepatitis; glutathione peroxidase; glutathione reductase; reduced glutathione; glutathione-S-transferase; caspases; melaxen.

ABBREVIATIONS LPO – lipid peroxidation; ROS – reactive oxygen species; GSH – reduced glutathione; GR/GP system – glutathione reductase / glutathione peroxidase system; CAH – chronic alcoholic hepatitis; FRO – free-radical oxidation; GP – glutathione peroxidase; GR – glutathione reductase; GST – glutathione-S-transferase; G6PD – glucose-6-phosphate dehydrogenase; AOS – antioxidant system; NADP-IDH – NADP-isocitrate dehydrogenase.

INTRODUCTION

Toxic liver injury usually develops after 5–10 years of alcohol abuse and is characterized by necrosis, along with an inflammatory reaction. The characteristic features of liver damage in patients include the prevalence of steatosis and other abnormalities in the perivascular (centrilobular) acinar zone. The mechanism of this zonal selectivity is associated with a relative oxygen deficiency. Low oxygen tension increases the redox potential shift caused by ethanol. Ethanol increases the lactate/pyruvate ratio and decreases the pyruvate level more significantly in the venous blood of the liver than in the entire body. Hypoxia leads to an increase in the NADH level, dysfunction of some enzymes, formation of oxygen radicals, and activation of lipid peroxidation (LPO) [1]. It is known that alcohol-induced cytochrome-P450-monooxygenase (CYP2E1) catalyzes the oxidation of

ethanol, which contributes to the growth of tolerance to alcohol, as well as its transformation into highly toxic metabolites, including reactive oxygen species (ROS). Depletion of the reduced glutathione (GSH) level, which occurs under these circumstances, induces oxidative stress and damage to liver cells. Disturbance of the redox homeostasis in toxic liver injury can cause the activation of programmed cell death (apoptosis), which is characterized by the activation of the cascade of intracellular cysteine proteases known as caspases [2]. It is believed that activation of caspases is a key step in the intermediate and terminal stages of this process [3]. Thus, caspase-3, which belongs to the ced-3 family, is directly involved in apoptosis and is capable of activating other caspases. Then the process of programmed cell death becomes irreversible. We cannot exclude the participation of caspase-1, which belongs to the ICE

family and is involved in the processing of cytokines [3], in apoptotic cell death. For example, caspase-1 expression was observed in the atrophic acinar cells of the pancreas in patients with chronic pancreatitis. This fact is indicative of their death. Moreover, caspase-1 promotes caspase-3 activation [3].

It is known that GSH and the enzymes associated with its transformations play an important role in protecting the body against both ROS and toxic substances. GSH belongs to the most important group of toxicity control agents. It is capable of reacting with free radicals, in particular, neutralizing singlet oxygen and hydroxyl radicals, and inhibiting LPO processes [4]. The glutathione reductase/glutathione peroxidase (GR [EC 1.6.4.2.]; GP [EC 1.11.1.9.]) system performs the detoxification of H₂O₂ and hydroperoxides using GSH, due to the action of glutathione peroxidase. The rate of GSH formation in the coupled reaction catalyzed by glutathione reductase mainly depends on the NADPH level [5]. The pentose phosphate pathway with glucose-6-phosphate dehydrogenase (G6PDG [EC 1.1.1.49.]) being its key enzyme catalyzing the conversion of glucose-6-phosphate to 6-phosphogluconolactone is one of the major suppliers of NADPH to the GR/GP-system [6]. The reaction catalyzed by NADP-isocitrate dehydrogenase (NADP-IDG [EC 1.1.1.42.]), which includes the oxidative decarboxylation of isocitrate to 2-oxoglutarate [7], can be an alternative source of NADPH. The glutathione antioxidant system (AOS) also includes glutathione-S-transferases (GST), the multifunctional proteins that use GSH for the metabolism of many hydrophobic substances and perform the detoxification of xenobiotics [8]. GST protects DNA, mitochondria, and other vital cell components against toxic substances and, thus, significantly increases the resistance of cells and the organism as a whole [9].

Melatonin, a hormone of the diffuse neuroendocrine system, which regulates several physiological functions, belongs to antioxidants. Melatonin is involved in the formation of circadian rhythms, suppression of some pituitary functions, and regulation of immune responses. According to its chemical structure, melatonin (N-acetyl-5-methoxytryptamine) is a derivative of serotonin, the biogenic amine which is in turn synthesized from tryptophan amino acid [10, 11]. There is evidence that melatonin can act as an interceptor of the hydroxyl radical, singlet oxygen, and nitric oxide [12]. Furthermore, melatonin facilitates the expression of the genes that are responsible for the synthesis of Cu-Zn-dependent superoxide dismutase [13]. It is believed that melatonin mainly protects DNA against free radicals, although it has a significant protective effect on other macromolecules. Owing to its lipophilic properties, melatonin can easily penetrate into all organs and

tissues, where its antioxidant activity can be implemented [14]. We have previously found that exogenous melatonin inhibits the development of oxidative stress in rats with toxic hepatitis [15], type 2 diabetes mellitus [16], and hyperthyroidism [17]. In this study, we have used melaxen, a synthetic drug containing melatonin, in the treatment of patients with toxic liver damage caused by excessive alcohol consumption.

This study was aimed at a comparative evaluation of the activity of caspase-1, caspase-3, GR, GP, GST, NADPH-generating enzymes (G6PDG and NADP-IDG), the GSH content, and the degree of DNA fragmentation in the blood of patients in the acute stage of chronic alcoholic hepatitis (CAH) during basic treatment and combination therapy including melaxen.

EXPERIMENTAL

The clinical study included 52 patients with toxic liver injury caused by chronic alcohol abuse. All patients were males aged 22–69 years, mean age 41.4 ± 7.2 years. All of them suffered from the alcohol dependence syndrome. The average duration of the disease was 2.2 ± 0.5 months. Alcoholic hepatitis was diagnosed based on clinical symptoms, biochemical blood tests, and hepatic ultrasound findings. The most common comorbidities included chronic gastritis – 32 patients (50%) and hypertension – 24 patients (30.5%).

The control group included 65 apparently healthy subjects with normal clinical and biochemical blood tests.

Viral hepatitis, cancer, diabetes mellitus, acute myocardial infarction, and cerebrovascular accident were the exclusion criteria.

The patients were divided into two groups. The first group (28 patients) received a basic treatment including complete alcohol withdrawal, diet number 5, 0.9% NaCl solution and vitamin B1 solution (10 ml) intravenously, riboxinum solution (10 ml) intravenously, vitamin B6 solution (4 ml) intramuscularly, and relanium solution (4 ml) intravenously. Hepatoprotectors: carsil (equivalent to 35 mg of silymarin) two tablets three times a day at mealtimes, Essliver Forte (essential phospholipids 300 mg) two tablets three times a day for 10 days. The second group (24 patients) in addition to the basic treatment received melaxen (Unifarm, Inc., USA) one tablet containing 3 mg of melatonin once a day 30–40 minutes before bedtime for 10 days.

The activities of caspase-1 and caspase-3 were determined using the Caspase 1 Assay Kit, Colorimetric and Caspase 3 Assay Kit, and Colorimetric (Sigma). A cocktail of protease inhibitors (0.08 mM aprotinin, 1.5 mM pepstatin A, and 2 mM leupeptin) was added to the measurement environment at a ratio of 100:1 (all reagents produced by Sigma, USA).

Effects of basic therapy and combination therapy including melaxen on liver function parameters in patients with the acute stage of chronic alcoholic hepatitis

Group		Liver function parameters		
		γ -GTP, $\mu\text{kat/L}$	ALT, nmol/(s·L)	AST, nmol/(s·L)
Control group, normal values ($n = 65$)		0.88 ± 0.04	95.9 ± 13.7	52.5 ± 7.3
Group 1, basic therapy ($n = 28$)	Before treatment	$3.34 \pm 0.14^*$	$241.6 \pm 19.3^*$	$151.6 \pm 10.8^*$
	After treatment	$1.63 \pm 0.06^{**}$	$161.8 \pm 16.2^{**}$	$108.9 \pm 11.1^{**}$
Group 2, combination therapy including melaxen ($n = 24$)	Before treatment	$3.33 \pm 0.12^*$	$256.1 \pm 14.6^*$	$152.2 \pm 10.4^*$
	After treatment	$1.19 \pm 0.04^{**}$	$145.1 \pm 11.3^{**}$	$96.3 \pm 13.7^{**}$

Note. The difference between the parameter and its reference value (*) or the value in the group of patients after treatment (**) is statistically significant at $p < 0.05$. Reference values of enzyme activity in males: γ -GTP – (0.25–1.77) $\mu\text{kat/L}$; ALT – normal (28–189) nmol/(s·L); AST – (28–127) nmol/(s·L).

The colorimetric analysis of caspase activity is based on hydrolysis of the Acetyl-Tyr-Val-Ala-Asp-p-nitroanilide (Ac-YVAD-pNA) peptide substrate (for caspase-1) and acetyl-Asp-Glu-Val-Asp-p-nitroanilide (Ac-DEVD-pNA) peptide substrate (for caspase-3) to form a p-nitroanilide residue that has an absorption maximum at 405 nm (the molar absorption factor = $10.5 \text{ M}^{-1} \text{ cm}^{-1}$). Caspase activity was expressed in pmoles of the product formed during 1 min per 1 mg of protein.

DNA was isolated from blood leukocytes using the phenol-chloroform method [18]. DNA fragmentation was detected by electrophoresis in an agarose gel in a TAE (Tris-acetate-EDTA) buffer containing ethidium bromide [19]. A MassRuler kit comprising markers from 1,500 to 10,000 bp (Fermentas, Lithuania) was used as a molecular weight marker.

The activities of glutathione AOS enzymes and NADPH-generating enzymes were determined spectrophotometrically at 340 nm on a Hitachi U-1900 spectrophotometer (Japan). The amount of the enzyme catalyzing the transformation of 1 micromole of the substrate during 1 min at 25°C was taken as the activity unit. The activity was calculated per 1 ml of blood serum. GR activity was determined in a medium containing a 50 mM potassium phosphate buffer (pH 7.4), 1 mM EDTA, 0.16 mM NADPH, and 0.8 mM oxidized glutathione. GP activity was determined in a medium containing a 50 mM potassium phosphate buffer (pH 7.4), 1 mM EDTA, 0.12 mM NADPH, 0.85 mM GSH, 0.37 mM H_2O_2 , and 1 unit/ml GR. GST activity was determined using the method based on the assessment of the rate of glutathione-S-2,4-dinitrobenzene formation in the reaction of GSH with 1-chloro-2,4-dinitrobenzene. GST activity was measured in the following medium: a 0.1 M potassium phosphate buffer (pH 7.4), 1

mM EDTA, 1 mM 1-chloro-2,4-dinitrobenzene, and 5 mM GSH. G6PDG activity was determined spectrophotometrically in the following medium (mM): a 0.05 Tris-HCl buffer (pH 7.8), 3.2 glucose-6-phosphate, and 0.25 NADP. NADP-IDG activity was determined in a 50 mM Tris-HCl buffer (pH 7.8) containing 1.5 mM isocitrate, 0.25 mM NADP, and 1.5 mM MnCl_2 . GSH concentration was determined using a reaction with 5,5-dithiobis(2-nitrobenzoic) acid, which results in the formation of thionitrophenyl anion (TNPA) with the absorption maximum at 412 nm [20]. Total protein was determined by a standardized biuret test [21]. The activity of γ -glutamyl transpeptidase (γ -GTP) was evaluated according to the rate of the glutamyl residue transfer reaction from γ -L-(+)-glutamyl-4-nitroanilide to glycylglycine (Biotest, PLIVA – Lachema Diagnostika). The activities of the marker enzymes of hepatocyte damage (ALT, AST) were determined along with the standard parameters of the biochemical blood test on a Klima 15MC biochemical analyzer (Spain).

The Caspase 1 Assay Kit, Colorimetric and Caspase 3 Assay Kit, Colorimetric, isocitrate, glutathione reductase preparation, Tris-Acetate-EDTA, ethidium bromide (Sigma, USA), NADP, NADPN, Tris-HCl buffer, EDTA (Reanal, Hungary), oxidized and reduced glutathione, and glucose-6-phosphate (ICN, USA) were used in this study. The rest of the reagents used were reagent grade or analytical-reagent grade chemicals produced in the Russian Federation.

Statistical processing of the material included the standard analysis of variance methods (calculation of mean values (M), error of the mean values (m), Student's t-test) and the non-parametric Wilcoxon test using the STATISTICA 6.0 software. The differences were considered to be statistically significant at $p \leq 0.05$.

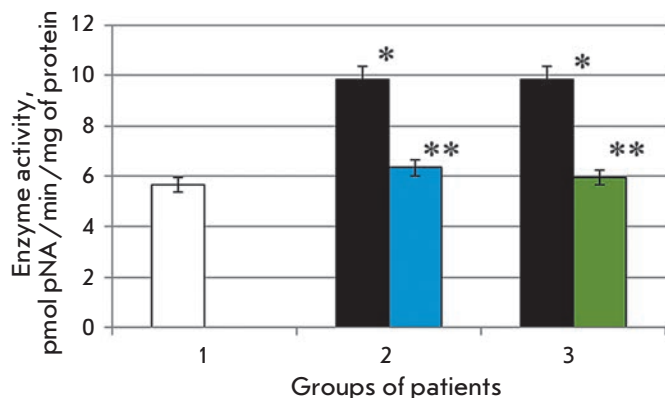


Fig. 1. Activity of caspase-1 in the blood serum in the normal state (1) in patients with chronic alcoholic hepatitis after standard therapy (2), in the case of the combination therapy including melaxen (3): before (blue) and after treatment (green)

Note: The accuracy of the values ($p \leq 0.05$ (*)) – compared with the normal value (**)) – compared with the pathology.

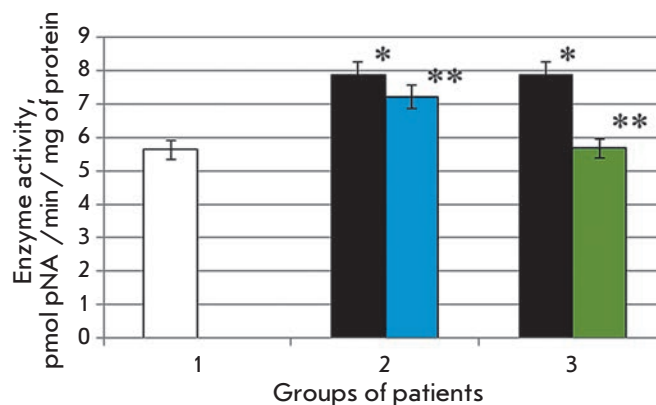


Fig. 2. Activity of caspase-3 in the blood serum in the normal state (1) in patients with chronic alcoholic hepatitis after standard therapy (2), in the case of the combination therapy including melaxen (3): before (blue) and after treatment (green)

Note: The accuracy of the values ($p \leq 0.05$ (*)) – compared with the normal value (**)) – compared with the pathology.

RESULTS

γ -GTP activity was on average 3.8-fold higher ($p < 0.05$) in patients of the first and second groups as compared to the control group (Table). ALT and AST activities also increased in both groups on average 2.5- and 2.9-fold ($p < 0.05$), respectively. Standard treatment resulted in a 2.1-fold decrease in the γ -GTP activity ($p < 0.05$), and 1.5- and 1.4-fold decrease in the ALT and AST activities, respectively. The activity of hepatocyte damage marker enzymes changed more significantly in the second group of patients receiving the combination therapy including melaxen. Thus, the γ -GTP activity decreased 2.8-fold ($p < 0.05$), ALT activity decreased 1.8-fold ($p < 0.05$), and AST activity decreased 1.6-fold ($p < 0.05$).

The study revealed that the development of CAH in patients was associated with 1.7- and 1.4-fold increases in the caspase-1 and caspase-3 activities ($p < 0.05$), respectively (Fig. 1, 2), which is indicative of intensification of apoptotic processes. Basic therapy resulted in changes in the caspase activity toward normal values. Thus, caspase-1 activity decreased 1.6-fold, and caspase-3 activity decreased 1.1-fold ($p < 0.05$) compared to the results obtained before treatment (Fig. 1, 2). A more pronounced decrease in the activities of both caspase-1 (1.7-fold) and caspase-3 (1.4-fold) ($p < 0.05$) (Fig. 1, 2) was observed in the group of patients who received melaxen along with the conventional treatment, which apparently was associated with the correction of the melatonin level under the action of this drug.

The data on the changes in the caspase activity in CAH patients are consistent with the results of the assessment of the fragmentation degree of blood leukocyte DNA in patients. According to the results of an electrophoretic analysis, DNA was represented by a single fragment at the beginning of the track (Fig. 3) in the blood samples from the control group donors. DNA isolated from the leukocytes of CAH patients was fragmented compared to DNA from the control samples. The degree of DNA fragmentation decreased after the standard treatment. DNA fragmentation was barely visualized in most blood samples from patients receiving melaxen along with the basic therapy.

The serum GSH level in the first group of CAH patients decreased on average 2.1-fold ($p < 0.05$) compared to the control level (Fig. 4) before the administration of hepatoprotectors. It is known that alcohol induces oxidative stress and damages the liver cells [22]. Obviously, activation of free-radical oxidation associated with this process reduces the GSH level. We observed a 1.7-fold increase in GSH concentration ($p < 0.05$) after basic treatment as compared to the values obtained before treatment.

The GSH level was 2.1 times lower ($p < 0.05$) in the second group of patients than that in the control group. Concentration of this metabolite increased after the combination therapy including melaxen and became equal to that of the control group (2.1-fold) (Fig. 4).

Our study revealed that the GP and GR activities in the serum of CAH patients of the first group decreased

Fig. 3. Electrophoregram of DNA from the blood leukocytes of the patients: control group (2), patients with CAH before treatment (3), after the conventional therapy (4), and after combined therapy including melaxen. Lane 1 shows DNA marker

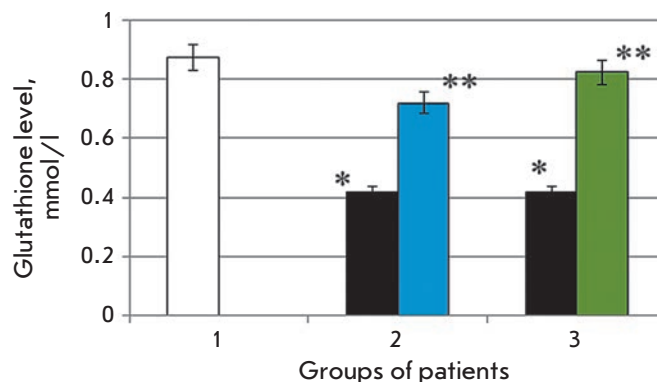
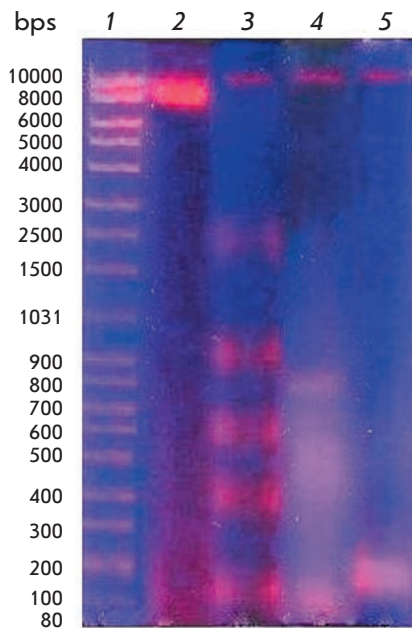


Fig. 4. The reduced glutathione level in the blood serum of the control group patients (1), patients with chronic alcoholic hepatitis after standard therapy (2), in the case of combination therapy including melaxen (3): before treatment (blue), after treatment (green)

Note. The accuracy of the values ($p \leq 0.05$ *) – compared with the normal value (**) – compared with the pathology.

on average 1.6-fold ($p < 0.05$) and 1.2-fold ($p < 0.05$), respectively, before the administration of the basic treatment as compared to the control level (Fig. 5, 6). The decrease in GR activity in CAH patients apparently can contribute to the decrease in the GSH level. After the standard treatment, the GP and GR activities increased on average 1.8-fold ($p < 0.05$) and 2.0-fold ($p < 0.05$), respectively, as compared to the values prior to the basic therapy.

In the second group of CAH patients, the GP and GR activities decreased prior to the therapy within the same range as in the first group. The GP and GR activities increased 2.9- and 2.8-fold, respectively, after combination therapy including melaxen. Thus, the most significant increase in GP/GR- system activity was observed in this group of patients (Fig. 5, 6).

The GST activity decreased 1.6-fold ($p < 0.05$) in the first group of CAH patients prior to the administration of hepatoprotectors as compared to the control level. Obviously, the decrease in the GST activity was caused by a significant consumption of reduced glutathione in response to excessive formation of ROS due to oxidative stress induced by CAH. This hypothesis is consistent with the observed increase in the GST activity along with the increase in the GSH level after treatment. Thus, the enzyme activity increased 1.5-fold ($p < 0.05$) after the basic therapy including the administration of hepatoprotectors.

In the second group of CAH patients, the GST activity prior to the therapy varied within the same range as in the first group. The GST activity increased 1.8-fold

($p < 0.05$) after the combination treatment including the administration of hepatoprotectors and melaxen as compared to the results before the treatment. Thus, the administration of melaxen resulted in a more significant increase in the GST activity as compared to the first group of patients (Fig. 7).

Changes in the activities of NADPH-generating enzymes in CAH patients and after treatment were revealed. It was found that the serum activity of NADP-IDG decreased on average 1.7-fold in the groups of CAH patients as compared to the control group. NADP-IDG activity increased on average 1.4-fold after the basic treatment as compared to the values before treatment. In the case of combination therapy including melaxen, enzymatic activity increased more significantly and was 1.8 times higher than the activity before treatment (Fig. 8).

G6PDG activity decreased on average 1.4-fold ($p < 0.05$) in CAH patients. The activity increased 1.4-fold after the standard therapy as compared to the results before treatment (Fig. 9). The combination therapy including melaxen on average led to a 1.7-fold increase in G6PDG activity in the second group of patients with the acute stage of CAH (Fig. 9).

The decrease in the activities of NADPH-generating enzymes apparently could be one of the reasons for the decrease in the GR activity in CAH patients.

It should be noted that in several studies on animal models, the activity levels of antioxidant enzymes, including glutathione AOS, NADPN-generating enzymes, as well as the parameters showing the intensity

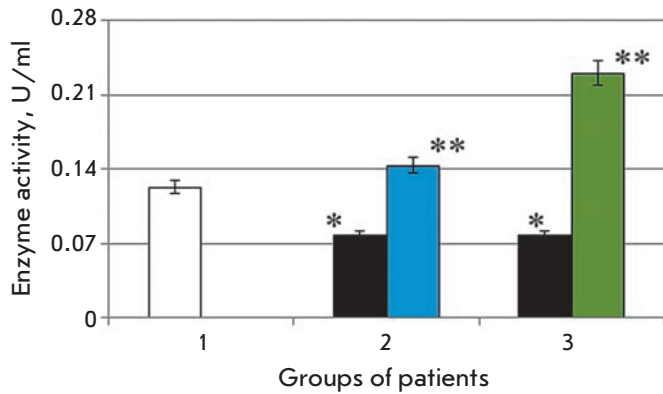


Fig. 5. Glutathione peroxidase activity in terms of E per ml (A) and specific enzyme activity (B) in patients with chronic alcoholic hepatitis after the standard therapy (2), in the case of the combination therapy including melaxen (3) before treatment (blue), after treatment (green)
Note. The accuracy of the values ($p \leq 0.05$ *) – compared with the normal value (**) – compared with the pathology.

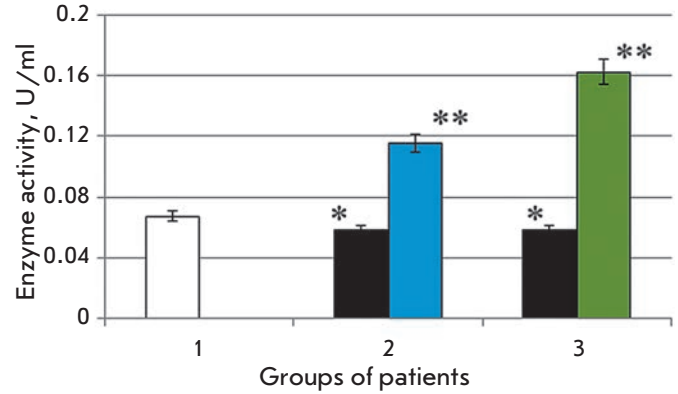


Fig. 6. Glutathione reductase activity in terms of E per ml (A), and specific enzyme activity (B) in patients with chronic alcoholic hepatitis after the standard therapy (2), in the case of the combination therapy including melaxen (3) before treatment (blue), after treatment (green)
Note. The accuracy of the values ($p \leq 0.05$ *) – compared with the normal value (**) – compared with the pathology.

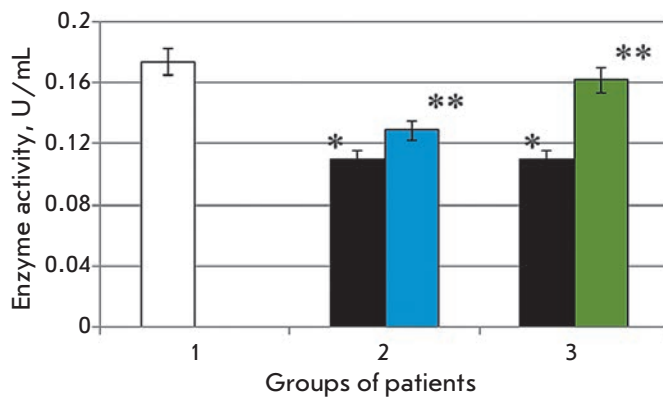


Fig. 7. Glutathione transferase activity in terms of E per ml (A), and specific enzyme activity (B) in patients with chronic alcoholic hepatitis after the standard therapy (2), in the case of the combination therapy including melaxen (3) before treatment (blue), after treatment (green)
Note. The accuracy of the values ($p \leq 0.05$ *) – compared with the normal value (**) – compared with the pathology.

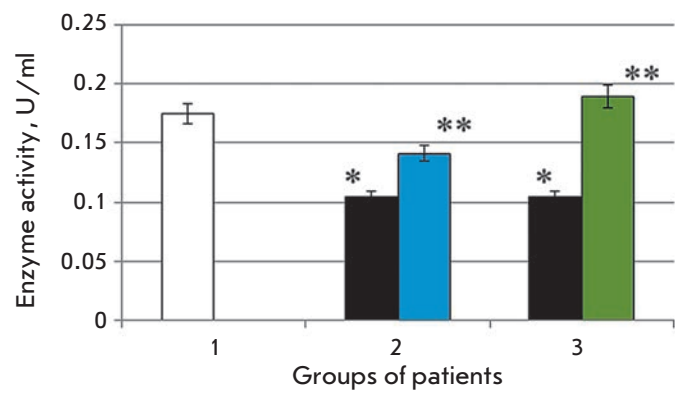


Fig. 8. NADP-isocitrate dehydrogenase activity in terms of E per ml (A) and specific enzyme activity (B) in patients with chronic alcoholic hepatitis after the standard therapy (2), in the case of the combination therapy including melaxen (3) before treatment (blue), after treatment (green)
Note. The accuracy of the values ($p \leq 0.05$ *) – compared with the normal value (**) – compared with the pathology.

of free-radical processes (biochemiluminescence parameters, DC level), correlated with those in the liver, and with the status of liver damage, as assessed by the activity of marker enzymes (ALT, AST) [23–27].

DISCUSSION

Biochemical parameters of liver functions (Table) confirm that CAH is associated with the metabolic disorders in hepatocytes and their damage is accompa-

nied by cell cytolysis and the release of ALT, AST and γ -GTP in blood. The decrease in the values of the investigated parameters confirms the hepatoprotective effect of the basic treatment. More pronounced changes in parameters in the second group of patients suggests that inclusion of melaxen to the basic therapy, which corrects melatonin levels in the body, enhanced the hepatoprotective effect apparently due to the antioxidant and immunostimulatory effect of this hormone.

The increase in caspase activity in the serum of CAH patients (*Fig. 1 and 2*) was apparently associated with excessive generation of ROS in this pathology. Thus, the development of hepatocyte apoptosis was observed in the experimental models of alcohol-induced liver diseases [28]. Furthermore, the experimental hepatitis induced by concanavalin A was associated with the increased activity of caspase-3 that was in particular due to liver-infiltrating lymphocytes, which are subjected to activation-induced apoptosis [29]. The reduced activity of both caspases after the basic therapy was apparently due to the fact that current treatment reduced the rate of ROS generation and inhibition of apoptotic processes. More significant changes in the activities of caspase-1 and caspase-3 in patients who received the combination therapy including melaxen were probably due to the correction in the melatonin level during the administration of this drug. It is known that melatonin reduces oxidative damage to lipids, DNA and mitochondria [30], and it increases the expression of anti-apoptotic genes that belong to the Bcl-2 group, protecting lipids from peroxidation and cells from subsequent apoptosis [31].

The results in determining DNA fragmentation in the blood leukocytes of CAH patients are consistent with the data on change in the caspase activity in CAH, during the standard treatment, and melaxen intake along with basic therapy. DNA extracted from the blood samples of CAH patients was significantly fragmented. According to some researchers, such fragments are produced due to the action of apoptosis-specific nucleases in the terminal phase of apoptosis [32]. DNA degradation at first produces large fragments of approximately 300 kbps, and later – 30–50 kbps. The next step produces fragments of 180 bps or their multiples by the internucleosomal degradation of the DNA due to the action of CAD (caspase-activated DNase) calcium-sensitive endonuclease. It is these fragments that are detected by electrophoresis as the “apoptotic ladder.” It is known that such DNA fragmentation can be related to proteolytic cleavage by caspases and DNA topoisomerase II, which participates in DNA supercoiling. Furthermore, H1 histone, which protects DNA from endonuclease action at the internucleosomal level, is the substrate of caspases during apoptosis [33]. The electrophoretic analysis of DNA extracted from the blood of CAH patients revealed a band at the molecular-weight range corresponding to degraded DNA that is characteristic of necrosis [34]. A decrease in DNA fragmentation was observed after the conventional therapy, indicating a positive effect of the treatment. Inclusion of melaxen in the basic therapy significantly reduced the degree of DNA fragmentation, which may be indicative of an anti-apoptotic action of this drug.

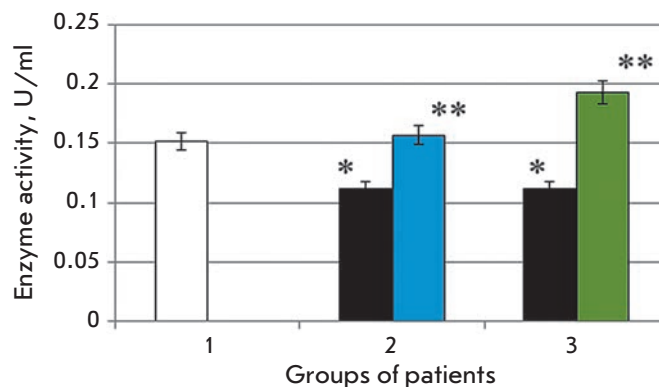


Fig. 9. The activity of glucose-6-phosphate dehydrogenase in terms of E per ml (A) and specific enzyme activity (B) in patients with chronic alcoholic hepatitis after the standard therapy (2), in the case of the combination therapy including melaxen (3) before treatment (blue), after treatment (green)

Note. The accuracy of the values ($p \leq 0.05$ (*) – compared with the normal value (**) – compared with the pathology.

A decrease in the serum GSH level in CAH patients of more than 2-fold with respect to the control (*Fig. 4*) is apparently due to the imbalance between the rate of free-radical processes and the antioxidant system activity. It is known that reduced glutathione plays a key role in the low-molecular-weight thiol antioxidant system. It effectively inactivates ROS and is the most sensitive component in the overall scheme of non-specific resistance of the body under oxidative stress conditions [35]. In addition, glutathione is involved in the conversion of antioxidants, such as ascorbic acid, α -tocopherol, thioctic acid, ubiquinone, in maintaining the optimal structural and functional state of biological membranes and regulating the synthesis of heat shock proteins [36]. As noted above, the microsomal enzymes of the monooxygenase system, in particular SUR2E1, not only oxidize alcohol, but also can transform xenobiotics into toxic metabolites. Concomitant activation of free-radical oxidation apparently leads to the depletion of the GSH level, which demonstrates that the ability of the liver to neutralize toxic compounds is impaired.

After the basic treatment, the GSH concentration was 1.7 times higher than that before treatment, which is apparently due to the decrease in the intensity of free-radical oxidation (FRO), and, as a result, a decrease in the consumption of this metabolite owing to the positive treatment effect. The combination treatment including melaxen facilitated the recovery of the glutathione concentration to its normal level, which is obviously associated with the powerful antioxidant effect of melatonin and its positive effect on the glutathione system (*Fig. 4*).

Research into the functioning of glutathione antioxidant system enzymes has shown that chronic alcohol intoxication is associated with a decrease in the serum activity of selenium GP and GR, which is also indicative of the decreased antioxidant status of patients. The decrease in the GP activity is probably due to the decrease in selenium concentration in chronic alcohol intoxication. It is known that the activity of selenium GP depends on the selenium level. An insufficient selenium level results in the inhibition of enzyme activity. A reduced activity of the enzyme associated with a deficiency of selenium is due to the decrease in the amount of GP mRNA [37]. Selenium is required for the synthesis of selenocysteine, which is part of the active center of the enzyme and plays an important role in catalysis [38]. GP functioning is closely related to the functioning of GR. Since the reaction catalyzed by GR yields a quickly mobilizable source of GSH, it is likely that a decrease in the GR activity can significantly contribute to the decrease in the concentration of this thiol in CAH patients.

The increased activity of the GP/GR-system after the standard treatment of CAH patients was apparently associated with the positive effect of the basic therapy on the antioxidant status of the patients. GP and GR activities increased even more significantly after the combination therapy including melaxen (*Fig. 5, 6*). The antioxidant activity of melatonin apparently can be associated with the activation of antioxidant enzymes and/or stimulation of their synthesis [39].

The significant decrease in GST activity that was revealed in the serum of CAH patients compared to the normal activity could obviously be associated with a significant consumption of the reduced glutathione in response to an excessive formation of ROS during the development of the oxidative stress induced by the pathological condition. It is known that GST uses the reduced glutathione for conjugation with hydrophobic substances, their reduction or isomerization. GSH is an essential component in the reaction of neutralization of the toxic products of lipid peroxidation, reduction of lipid hydroperoxides, and the biotransformation of xenobiotics catalyzed by multifunctional GST [14]. In this regard, the decreased GSH levels in CAH could well lead to a reduced activity of GST. This hypothesis is consistent with the increasing GST activity, along with the increasing GSH level after treatment. The increase in GST activity was likely associated with the positive effect of the treatment on the antioxidant status of patients, including the decrease in GSH consumption. Notably, the administration of melaxen facilitated a more significant increase in the GST activity as compared to the first group of patients (*Fig. 7*).

It was found that CAH is also associated with an altered activity of NADPH-generating enzymes (NADP-IDG and G6PDG). NADP-IDG activity decreased to a greater extent than G6PDG activity. A less significant decrease in G6PDG activity is probably attributable to the role of the pentose phosphate pathway as a supplier of reducing equivalents for fatty acid biosynthesis, which is activated in the liver cells under conditions of its fatty degeneration in chronic alcohol intoxication. It is known that it is G6PDG, being the key enzyme of the pentose phosphate pathway, that is responsible for the bulk of the NADPN required for the synthesis of fatty acids [40]. The decrease in the activity of NADPN-generating enzymes could be due to the negative effect of ROS, which is excessively generated in the pathological state. There is evidence of inhibition of the activity of some glycolysis enzymes in patients with chronic alcohol intoxication, which is accompanied by an increase in the hepatic glucose and lactate levels [41]. The decrease in the activity of the enzymes involved in the transformation of tricarboxylic acids, and NADP-IDG in particular, can apparently occur under these conditions (*Fig. 8*).

A more significant increase in the activity of NADP-IDG and G6PDG in the blood of patients who received drug capable of melatonin level correction as compared to those receiving the standard treatment could be due to the induction of enzyme synthesis under the action of this hormone. It is known that melatonin can increase the expression of some of the enzymes involved in the antioxidant defense of the body [42].

It should be noted that the decrease in the activity of NADPN-generating enzymes could be one of the reasons for the decrease in the GR activity in CAH patients. Moreover, a significant increase in GR activity after the basic treatment and an even more significant recovery of enzyme activity during the administration of melaxen were associated with an increase in the G6PDG and NADP-IDG activities under these conditions. The increased reference level of the activity of the GR and NADPN-generating enzymes that was observed under these conditions could be due to the strong effect of antioxidant therapy, which facilitates AOS mobilization under oxidative stress conditions and becomes systemic in chronic alcohol intoxication. It is likely that melatonin (its level is corrected under the action of melaxen) can act as an adaptogen regulating the activity of the glutathione system, as well as enzymes capable of generating NADPN, in accordance with the exposure of the body to disease-producing factors.

CONCLUSION

Inclusion of melaxen to the CAH therapy enhances the hepatoprotective and membrane-stabilizing effects.

This fact has been confirmed by the parameters that characterize the functioning of the liver; in particular, aminotransferases and γ -GTP. This is apparently due to the antioxidant properties of melatonin, which is included as a component of melaxen. A combination therapy using melaxen led to a more significant decrease in the development of apoptotic processes in CAH patients, as evidenced by a more significant decrease in the activity of caspase-1 and caspase-3, and the DNA fragmentation degree, than that in patients who re-

ceived the conventional therapy. Correction of the melatonin level in the body leads to significant recovery in the GSH level, activity of glutathione group enzymes of AOS (GR, GP, GST, as well as G6PDG and NADP-IDG NADPN-generating enzymes) as compared to such parameters during the basic treatment. The findings suggest the effective protective action of melaxen in toxic liver injury, which has a favorable impact on the state of free-radical homeostasis and significantly reduces the severity of cytolytic hepatocyte injury. ●

REFERENCES

- Boyer J.L., Blum H.E., Maier K.P., Sauerbruch T., Stalder G.A. Liver cirrhosis and its development. Dordrecht: Kluwer Acad. Publ. and Falk Foundation, 2001. 357 p.
- Kuzmina E.I., Nelyubin A.S., Shchennikova M.K. // *Interuniversity miscellany: Biochemistry and Biophysics of Microorganisms*. 1983. P. 179–183.
- Sukhanova G.A., Akbasheva O.E. Apoptosis. Tomsk: Publishing House of the TPU. 2009. 172 p.
- Zenkov N., Lapkin V.Z., Menshchikova E.B. Oxidative stress. Biochemical and pathophysiological aspects. Moscow: Nauka / Interperiodica, 2001. 343 p.
- Su F., Hu X., Jia W., Gong C., Song E., Hamar P. // *J. Surg. Res.* 2003. V. 113. № 1. P. 102–108.
- Gupte R.S., Ata H., Rawat D., Abe M., Taylor M.S., Ochi R., Gupte S.A. // *Antioxid. Redox Signal.* 2011. V. 14. № 4. P. 543–558.
- Ufer C., Wang C.C. // *Front. Mol. Neurosci.* 2011. V. 4. A. 12. Doi: 10.3389/fnmol.2011.00012.
- Wang Z., Jin L., Węgrzyn G., Węgrzyn A. // *BMC Biochem.* 2009. V. 10. A. 6. Doi: 10.1186/1471-2091-10-6.
- Sun H.-D., Ru Y.-W., Zhang D.-J., Yin S.-Y., Yin L., Xie Y.-Y., Guan Y.-F., Liu S.-Q. // *World J. Gastroenterol.* 2012. V. 18. № 26. P. 3435–3442.
- Anisimov V.N. Melatonin: the role in the body, clinical application. St. Petersburg: System. 2007. 40 p.
- Reiter R.J., Tan D.X., Leon J., Kilic U., Kilic E. // *Exp. Biol. Med.* 2005. V. 230. P. 104–117.
- Baraboi V.A. // *Ukrainian biochem. journal.* 2000. V. 73. № 3. P. 5–11.
- Anisimov V.N., Kvetnoy I.M., Komarov F.I., Malinowska N.K., Rapoport S.I. Melatonin in the physiology and pathology of the gastrointestinal tract. Moscow: Soviet Sport, 2000. 184 p.
- Popova T.N., Pashkov A.N., Semenikhina A.V., Popov S.S., Rakhmanov T.I. Free-radical processes in biological systems. *Starii Oskol. Kirillica*, 2008. 192 p.
- Popov S.S., Pashkov A.N., Popova T.N., Semenikhina A.V., Rakhmanov T.I. // *Exp. Clin. Pharmacol.* 2007. V. 70. № 1. P. 48–51.
- Agarkov A.A., Popova T.N., Matasova L.V. // *Biomed. Chem.* 2013. V. 59. № 4. P. 434–442.
- Popov S.S., Pashkov A.N., Popova T.N., Zoloedov V.I., Rakhmanov T.I. // *Bul. Exper. Biol. and Med.* 2007. V. 144. № 8. P. 170–173.
- Maniatis T., Fritsch E., Sambrook J. *Methods of genetic engineering. Molecular cloning*. Moscow. World, 1984. 478 p.
- Kalinina T.S., Bannova A.V., Dygalo N. // *Bul. Exper. Biol. and Med.* 2002. V. 134. P. 641–644.
- Karpishchenko A.I. *Medical laboratory technology. Guidelines for clinical laboratory diagnostics*. Moscow. GEOTAR-Media, 2013. V. 2. 792 p.
- Matasova L.V., Rakhmanov T.I., Safonova O.A., Popova T.N. *Laboratory works and tasks at biochemistry*. Voronezh: VSU, 2006. 79 p.
- Ivashkin V.T., Mayevskaya M.V. *Alcoholic and viral liver diseases*. Moscow. Litterra, 2007. 160 p.
- Agarkov A.A., Popova T.N., Matasova L.V. // *Pharmaceutical Chemistry Journal*. 2011. V. 45. № 7. P. 7–10.
- Safonova O.A., Popova T.N., L. Saidi // *Biomed. Chemistry*. 2010. V. 56. № 4. P. 490–498.
- Popova T.N., Panchenko L.F., Semenikhina A.V., Rakhmanov T.I. Allekrad H. // *Questions of Biol. Med. Pharm. Chemistry*. 2010. № 2. P. 66–69.
- Popov S.S., Pashkov A.N., Popova T.N., Zoloedov V.I., Semenikhina A.V., Rakhmanov T.I. // *Biomed. Chemistry*. 2008. V. 54. № 1. P. 114–121.
- Popov S.S., Pashkov A.N., Popova T.N., Zoloedov V.I., Rakhmanov T.I., Semenikhina A.V. // *Problems of Endocrinology*. 2008. V. 54. № 3. P. 47–50.
- Natori S., Rust C., Stadheim L.M., Srinivasan A., Burgart L.J., Gores G.J. // *J. Hepatol.* 2001. V. 34. № 2. P. 248–253.
- Biburger M., Tiegs G. // *J. Immun.* 2005. V. 175. P. 1540–1550.
- Watanabe K., Wakatsuki A., Shinohara K., Ikenoue N., Yokota K., Fukaya T. // *J. Pineal Res.* 2004. V. 37. № 4. P. 276–280.
- Baydas G., Koz S.T., Tuzcu M., Etem E., Nedzvetsky V.S. // *J. Pineal Res.* 2007. V. 43. № 3. P. 225–231.
- Muller K. // *Eur. J. Pharmacol.* 1992. V. 226. № 6. P. 209–214.
- Earnshaw W.C. // *Curr. Opin. Cell Biol.* 1995. V. 7. № 3. P. 337–343.
- Yarilin A.A. // *Patol. Physiol. Exp. therapy*. 1998. V. 2. P. 38–48.
- Exner R., Wessner B., Manhart N., Roth E. // *Wien Klin Wochenschr.* 2000. V. 112. № 14. P. 610–616.
- Evans J.L., Goldfine I.D., Maddux B.A., Grodsky G.M. // *Endocrine Rev.* 2002. V. 23. № 5. P. 599–622.
- Sunde R.A., Evenson J.K., Thompson K.M., Sachdev S.W. // *J. Nutr.* 2005. V. 135. № 9. P. 2144–2150.
- Zubkov L.L. // *Kazan science*. 2010. № 3. P. 241–244.
- Beni S.M., Kohen R., Reiter R.J., Tan D. X., Shohami E. // *FASEB J.* 2004. V. 18. P. 149–151.
- Stover N.A., Dixon T.A., Cavalcanti A.R.O. // *PLoS One*. 2011. V. 6. № 8. e22269.
- Lelevich S.V. // *Biomed. Chemistry*. 2009. V. 55. № 6. P. 727–733.
- El-Abhar H.S., Shaalan M., Barakat M., El-Denshary E.S. // *J. Pineal Res.* 2002. V. 33. P. 87–94.

GENERAL RULES

Acta Naturae publishes experimental articles and reviews, as well as articles on topical issues, short reviews, and reports on the subjects of basic and applied life sciences and biotechnology.

The journal is published by the Park Media publishing house in both Russian and English.

The journal *Acta Naturae* is on the list of the leading periodicals of the Higher Attestation Commission of the Russian Ministry of Education and Science

The editors of *Acta Naturae* ask of the authors that they follow certain guidelines listed below. Articles which fail to conform to these guidelines will be rejected without review. The editors will not consider articles whose results have already been published or are being considered by other publications.

The maximum length of a review, together with tables and references, cannot exceed 60,000 symbols (approximately 40 pages, A4 format, 1.5 spacing, Times New Roman font, size 12) and cannot contain more than 16 figures.

Experimental articles should not exceed 30,000 symbols (20 pages in A4 format, including tables and references). They should contain no more than ten figures. Lengthier articles can only be accepted with the preliminary consent of the editors.

A short report must include the study's rationale, experimental material, and conclusions. A short report should not exceed 12,000 symbols (8 pages in A4 format including no more than 12 references). It should contain no more than four figures.

The manuscript should be sent to the editors in electronic form: the text should be in Windows Microsoft Word 2003 format, and the figures should be in TIFF format with each image in a separate file. In a separate file there should be a translation in English of: the article's title, the names and initials of the authors, the full name of the scientific organization and its departmental affiliation, the abstract, the references, and figure captions.

MANUSCRIPT FORMATTING

The manuscript should be formatted in the following manner:

- Article title. Bold font. The title should not be too long or too short and must be informative. The title should not exceed 100 characters. It should reflect the major result, the essence, and uniqueness of the work, names and initials of the authors.
- The corresponding author, who will also be working with the proofs, should be marked with a footnote *.
- Full name of the scientific organization and its departmental affiliation. If there are two or more scientific organizations involved, they should be linked by digital superscripts with the authors' names. Abstract. The structure of the abstract should be very clear and must reflect the following: it should introduce the reader to the main issue and describe the experimental approach, the possibility of practical use, and the possibility of further research in the field. The average length of an abstract is 20 lines

(1,500 characters).

- Keywords (3 – 6). These should include the field of research, methods, experimental subject, and the specifics of the work. List of abbreviations.

- INTRODUCTION
- EXPERIMENTAL PROCEDURES
- RESULTS AND DISCUSSION
- CONCLUSION

The organizations that funded the work should be listed at the end of this section with grant numbers in parenthesis.

- REFERENCES

The in-text references should be in brackets, such as [1].

RECOMMENDATIONS ON THE TYPING AND FORMATTING OF THE TEXT

- We recommend the use of Microsoft Word 2003 for Windows text editing software.
- The Times New Roman font should be used. Standard font size is 12.
- The space between the lines is 1.5.
- Using more than one whole space between words is not recommended.
- We do not accept articles with automatic referencing; automatic word hyphenation; or automatic prohibition of hyphenation, listing, automatic indentation, etc.
- We recommend that tables be created using Word software options (Table → Insert Table) or MS Excel. Tables that were created manually (using lots of spaces without boxes) cannot be accepted.
- Initials and last names should always be separated by a whole space; for example, A. A. Ivanov.
- Throughout the text, all dates should appear in the “day.month.year” format, for example 02.05.1991, 26.12.1874, etc.
- There should be no periods after the title of the article, the authors' names, headings and subheadings, figure captions, units (s – second, g – gram, min – minute, h – hour, d – day, deg – degree).
- Periods should be used after footnotes (including those in tables), table comments, abstracts, and abbreviations (mon. – months, y. – years, m. temp. – melting temperature); however, they should not be used in subscripted indexes (T_m – melting temperature; $T_{p.t.}$ – temperature of phase transition). One exception is mln – million, which should be used without a period.
- Decimal numbers should always contain a period and not a comma (0.25 and not 0,25).
- The hyphen (“-”) is surrounded by two whole spaces, while the “minus,” “interval,” or “chemical bond” symbols do not require a space.
- The only symbol used for multiplication is “×”; the “×” symbol can only be used if it has a number to its right. The “·” symbol is used for denoting complex compounds in chemical formulas and also noncovalent complexes (such as DNA·RNA, etc.).
- Formulas must use the letter of the Latin and Greek alphabets.

GUIDELINES FOR AUTHORS

- Latin genera and species' names should be in italics, while the taxa of higher orders should be in regular font.
- Gene names (except for yeast genes) should be italicized, while names of proteins should be in regular font.
- Names of nucleotides (A, T, G, C, U), amino acids (Arg, Ile, Val, etc.), and phosphonucleotides (ATP, AMP, etc.) should be written with Latin letters in regular font.
- Numeration of bases in nucleic acids and amino acid residues should not be hyphenated (T34, Ala89).
- When choosing units of measurement, SI units are to be used.
- Molecular mass should be in Daltons (Da, KDa, MDa).
- The number of nucleotide pairs should be abbreviated (bp, kbp).
- The number of amino acids should be abbreviated to aa.
- Biochemical terms, such as the names of enzymes, should conform to IUPAC standards.
- The number of term and name abbreviations in the text should be kept to a minimum.
- Repeating the same data in the text, tables, and graphs is not allowed.

GUIDENESS FOR ILLUSTRATIONS

- Figures should be supplied in separate files. Only TIFF is accepted.
- Figures should have a resolution of no less than 300 dpi for color and half-tone images and no less than 500 dpi.
- Files should not have any additional layers.

REVIEW AND PREPARATION OF THE MANUSCRIPT FOR PRINT AND PUBLICATION

Articles are published on a first-come, first-served basis. The publication order is established by the date of acceptance of the article. The members of the editorial board have the right to recommend the expedited publishing of articles which are deemed to be a priority and have received good reviews.

Articles which have been received by the editorial board are assessed by the board members and then sent for external review, if needed. The choice of reviewers is up to the editorial board. The manuscript is sent on to reviewers who are experts in this field of research, and the editorial board makes its decisions based on the reviews of these experts. The article may be accepted as is, sent back for improvements, or rejected.

The editorial board can decide to reject an article if it does not conform to the guidelines set above.

A manuscript which has been sent back to the authors for improvements requested by the editors and/or reviewers is reviewed again, after which the editorial board makes another decision on whether the article can be accepted for publication. The published article has the submission and publication acceptance dates set at the beginning.

The return of an article to the authors for improvement does not mean that the article has been accepted for publication. After the revised text has been received, a decision is made by the editorial board. The author must return the improved text, together with the original text and responses to all comments. The date of acceptance is the day on which the final version of the article was received by the publisher.

A revised manuscript must be sent back to the publisher a week after the authors have received the comments; if not, the article is considered a resubmission.

E-mail is used at all the stages of communication between the author, editors, publishers, and reviewers, so it is of vital importance that the authors monitor the address that they list in the article and inform the publisher of any changes in due time.

After the layout for the relevant issue of the journal is ready, the publisher sends out PDF files to the authors for a final review.

Changes other than simple corrections in the text, figures, or tables are not allowed at the final review stage. If this is necessary, the issue is resolved by the editorial board.

FORMAT OF REFERENCES

The journal uses a numeric reference system, which means that references are denoted as numbers in the text (in brackets) which refer to the number in the reference list.

For books: the last name and initials of the author, full title of the book, location of publisher, publisher, year in which the work was published, and the volume or issue and the number of pages in the book.

For periodicals: the last name and initials of the author, title of the journal, year in which the work was published, volume, issue, first and last page of the article. Must specify the name of the first 10 authors. Ross M.T., Grafham D.V., Coffey A.J., Scherer S., McLay K., Muzny D., Platzer M., Howell G.R., Burrows C., Bird C.P., et al. // Nature. 2005. V. 434. № 7031. P. 325–337.

References to books which have Russian translations should be accompanied with references to the original material listing the required data.

References to doctoral thesis abstracts must include the last name and initials of the author, the title of the thesis, the location in which the work was performed, and the year of completion.

References to patents must include the last names and initials of the authors, the type of the patent document (the author's rights or patent), the patent number, the name of the country that issued the document, the international invention classification index, and the year of patent issue.

The list of references should be on a separate page. The tables should be on a separate page, and figure captions should also be on a separate page.

The following e-mail addresses can be used to contact the editorial staff: vera.knorre@gmail.com, actanaturae@gmail.com, tel.: (495) 727-38-60, (495) 930-87-07